Spring 5-15-2022

Antigen Presentation in Central Nervous System Antitumor Immunity

Jay Aaron Bowman-Kirigin
Washington University in St. Louis

WASHINGTON UNIVERSITY IN ST. LOUIS

Division of Biology and Biomedical Sciences

Immunology Graduate Program

Dissertation Examination Committee
Gavin Dunn, Principal Investigator and Co-Chair
David DeNardo, Co-Chair
Kenneth Murphy
Gwendalyn Randolph
Joshua Rubin
Robert Schreiber

Antigen Presentation in Central Nervous System Antitumor Immunity

by
Jay Bowman-Kirigin

A dissertation presented to
The Graduate School
of Washington University in
partial fulfillment of the
requirements for the degree
of Doctor of Philosophy

May 2022

St. Louis, Missouri

Table of Contents

List of Figures

CHAPTER TWO

CHAPTER THREE

CHAPTER FOUR

CHAPTER FIVE

CHAPTER SIX

List of Tables

Acknowledgements

I am remarkably fortunate to have countless people who supported me and made contributions to my thesis work. My acknowledgements below are nowhere near exhaustive, and if I left anybody out, please accept my sincere apologies.

First and foremost, I'd like to thank my thesis advisor, Dr. Gavin Dunn. Gavin (or Dr. Dunn as I call him when I want to annoy him) is a fantastic mentor who goes above and beyond for his trainees. Joining Gavin's lab was the second best choice I made during my MD/PhD training (to know my first, read to the end of this section). I am humbled to be the his first graduate trainee, and I definitively know that I will not be the last. One of the most awe inspiring days in medical school thus far was when I shadowed him in the operating room—he precisely and delicately resected a massive parietal lobe glioblastoma that afflicted his patient, and it was clear that his patient was in good hands with the good doctor. The image of the pulsating brain that rippled with every heartbeat will remain etched in my memory.

It brings me peace of mind to know that Gavin is in my corner. One of the joys of working in his lab has been the transition from more hands-on mentorship and guidance in the beginnig of my PhD, to a longer-leashed, hands-off approach, which affords me the opportunity to pilot the ship and drive my own project. I am so fortunate that Gavin has provided the type of training environment that facilitates learning, collaboration, and scientific excellence. There is no heirarchy when we walk through the door (or enter the zoom meeting these days) into lab meeting—all ideas, regardless of from whom they

originate, are evaluated with equal consideration and rigor. This type of approach helps maximize the scientific potential for trainees of this lab—I know it did for me.

Secondly, I would like to thank my thesis committee: Dr. David DeNardo (the OG chair), Dr. Gwendalyn Randolph, Dr. Kenneth Murphy, Dr. Robert Schreiber, and Dr. Joshua Rubin. You have been wonderful. Like I said before, I don't mean to sound like an annoying kiss-ass, but I very much appreciate having each one of you on my committee. Your contributions, whether they were imparting scientific wisdom, sharing resources, or co-mentoring me for my F30 (special shout out to Josh), have been instrumental in advancing my project leaps and bounds. Thank you for being a part of my graduate and scientific education.

Thirdly, I'd like to thank members of the Dunn Lab, past and present. We are a young, plucky lab on the up and up. You have been my comrades in the scientific trenches, and you make going to work every day infinitely more enjoyable. I would not have been able to do this without you. To Max Schaettler, fellow MD/PhD graduate student, HHMI medical student Dr. Connor Liu, Dr. Tanner Johanns, Dale Kobayashi, Alex Livingstone, Dr. Paul Zolkind, Dr. Yujie Fu, Andrew Coxon, Mac Egan, Dr. Rupen Desai, Dr. Jimmy Manyanga, Anthony Wang, Ngima Sherpa, and Pujan Patel, working with all of you has been a pleasure—you made things so much more fun and interesting.

I would also like to thank my undergraduate science professors at Westminster College as well. Dr. Chris Cline, Dr. Paul Hooker, Dr. Peter Conwell, and Dr. Robyn Hyde all taught me the foundational critical thinking skills in physics and chemistry that I have

continued to use throughout graduate training in immunology. I was so lucky to have been in your classes so you could impart your wisdom upon me.

My post-baccalaureate experience is probably what pushed me to pursue MD/PhD training. Dr. Dean Y. Li, also a WashU MSTP alumnus, cardiologist, PI (formerly) at the University of Utah, and now Vice President of Merck Research Laboratories was gracious enough give me a job in his lab at the University of Utah between my undergraduate and graduate training. I probably would not have applied to WashU had I not worked in his lab. Thanks Dean, as well as Dr. Shannon Odelberg, Dr. Kirk Thomas, Dr. Chris Gibson, Dr. Chadwick Davis, Dr. Nikos Diakos, and the other lab members who worked there and made my post-bac exciting, fun, and inspiring.

I would also like to thank Dr. Bernd Zinselmeyer and Brian Saunders for all their help with 2-photon microscopy. You were such wonderful collaborators and our remarkable experiments with 2-photon microscopy would not have been possible without you. Those images you helped us make are always the stars of any presentation I give—without a doubt people want to see more of those pictures every single time!

Thank you also to the those who have helped me in the Washington University Immune Monitoring Lab (especially Dr. Diane Bender, Hailey Freres, Dr. Likui Yang, and Tammi Vickery) with assays, tetramers, and making sure the flow cytometer was always in tip-top shape. You helped me generate some of our most foundational data.

I would also like to thank all the staff of the Washington University Department of Pathology and Immunology Flow Cytometry & Fluorescence Activated Cell Sorting Core. Dorian Brinja, Dr. Erika Lantelme, and Pascaline Akitani always kept those touchy

cell sorters and flow cytometers working so smoothly and helped me do some excellent cell sorting in the process.

To all the other WashU staff and faculty, you help make this place so great. Our animals are in better hands because of you, our equipment works better because of you, and we can always rely on you to help us with our scientific needs. Thank you.

I would also like to thank the Washington University Medical Scientist Training Program. Dr. Wayne Yokoyama, Dr. Clarissa Craft, Brian Sullivan, Linda Perniciaro, Christy Durbin, and Liz Bayer, you have been so kind and so helpful. Thank you for taking a chance on me, for giving me the opportunity to embark upon my journey of training to be a physician-scientist, and for doing everything you could to make MD/PhD training as smooth and seamless as possible.

I would also like to thank an illustrator who works with our lab: Matthew Holt. He made some of the best and most intricate drawings for our paper, which were also employed for countless presentations as well as this document. I always get compliments on these illustrations—we are lucky to have him.

A particular group that deserves special mention are the scores of patients and patient families who made this research possible. Glioblastoma is an inexorably lethal disease, and we conduct our research under the hope that one day, patients afflicted by this terrible disease might suffer less and live longer than they currently do. Their bravery to face this disease inspires me. Their tumor specimens were the backbone of some of our most foundational discoveries: that antigen uptake takes place in human brain tumors just like

in mice and is uniquely restricted to antigen presenting cells. I will be forever indebted to them for their contributions. I can't thank them enough.

Finally, I would like to thank my friends and family. Whether you're my St. Louis friends or my Utah friends, you made MD/PhD training thus far so much more bearable. Artie & Sonya, Doug, and Sage, I can't believe how many barbecues we've had, how may ribs we cooked, how much skiing we've done, and how many waves we've caught.

By far the very best choice I made during MD/PhD training was to ask my lovely wife and mother to our furry children, Mindy, out on a date when we were first-year medical students. I started to fall in love with her at the same time I became captivated by immunology—we attended the first-year immunology review sessions together and I was enchanted. I'll never know if it was the subject matter or her company, but somehow, I decided to join the immunology graduate program after this. I still love immunology so perhaps it was meant to be—that in addition to marrying her, I would continue to study and enjoy immunology. Nevertheless, my introduction to immunology with her at my side certainly must've helped. Her radiant smile illuminates any room she enters and her wickedly clever sense of humor regularly leaves me in stitches. I am the luckiest guy on earth to be her husband. She is and has always been immensely supportive through all my training endeavors, all while finishing her MD, and pursuing her own medical training as a family medicine doctor. Although my work trying to understand the GBM immunity cycle might hopefully extend a patient's life someday, the work she does as a primary care doctor out on the front lines is immensely impactful and will improve more lives and bestow upon society more person-life-years than I could ever hope to.

To my mom and late dad, I am incredibly lucky to be your child. My dad, himself an electrical engineer, instilled in me a love of science. I so desperately wish he could see what I am doing today. I remember when he taught me what multiplication meant when we were on the playground, or how he explained relativity's consequence of time dilation in a way that I could understand. My mom instilled in me a love of humanity and taught me the importance of service and caring for those who need help. She is both a registered nurse and attorney—I know I will be a good doctor if I can fight for my patients as hard as she fights for her clients. Both of you are a constant source of inspiration to me. MD/PhD training combines my love of science and of humanity in a way that I think perfectly marries what you two taught me, and I know I would not be here without you.

Jay Bowman-Kirigin

Washington University in St. Louis

May 2022

ABSTRACT OF DISSERTATION

Antigen presentation in central nervous system antitumor immunity

by

Jay Bowman-Kirigin

Doctor of Philosophy in Biology and Biomedical Sciences

Immunology

Washington University in St. Louis, 2022

Gavin Dunn, Principal Investigator and Co-Chairperson

David DeNardo, Co-Chairperson

Glioblastoma multiforme (GBM) patients face limited treatment options and poor outcomes. The median survival is less than two years, and there are no FDA approved immune therapies. Although GBM itself is an immune-suppressive, heterogeneous tumor, the lack of FDA approved immune therapies might be in part because the cancer immunity cycle is less well understood for GBM than for other tumor types. My studies focused on developing mouse models of malignant glioma that more faithfully recapitulate human GBM from an immunologic perspective, and on defining the role of the conventional dendritic cell 1 subset (cDC1) and lymphatic drainage in central nervous system (CNS) antitumor immunity.

While genetically engineered mouse models of glioma have been described, they are for various reasons unsuitable to study the immune system's reaction against the tumor, due to their use of outbred mice, immunologically immature mice, human oncogenes to drive

transformation, or highly inflammatory initiation events. Furthermore, the most commonly deleted tumor suppressors in GBM are underrepresented in existing models. Thus, we engineered the tumor suppressor genes $p16^{INK4a}$ and $p19^{ARF}$ (*INK4a/ARF*; *CDKN2A/B* in humans) and phosphate and tensin homolog (*PTEN*) to be loxP-flanked on a pure C57BL/6 background. We used lentiviral transduction of Cre and the murine oncogene platelet derived growth factor beta (*PDGFβ*) to conditionally delete these tumor suppressors and transform target cells in brains of immunologically mature mice, which resulted in brain tumor formation.

With the standard treatment, GBM invariably recurs, with 20%-30% of cases hypermutated. It is often the loss of mutS homolog 6 (MSH6), a mismatch repair protein, that confers resistance to temozolomide (standard-treatment) and leads to treatment-induced hypermutations. We developed the tools to model this phenomenon in a preclinically. We isolated astrocytes from the B6 $INK4a/ARF^{fl/fl}$ x $PTEN^{fl/fl}$ mice and transformed them with the Cre/mPDGFβ lentivirus constructs. We used CRISPR to delete the mismatch repair protein MSH6 in these ex-vivo transformed astrocytes. We characterized their resistance to temozolomide and successfully induced hypermutation with long term temozolomide treatment and inhibition.

Within the immunologically distinct location of the CNS the type of antigen presenting cell (APC) responsible for priming T cell responses against brain tumors remains undefined. In other non-CNS tumors, the conventional dendritic cell 1 (cDC1) subset cross-presents tumor-derived and cell-associated tumor antigen to generate antitumor $CD8^+$ and $CD4^+$ T cell responses. However, the homeostatic brain parenchyma is largely devoid of cDC1—their steady state location is restricted to the choroid plexus and the dura. Using

orthotopic, syngeneic transplant models of murine glioblastoma, we investigated the roles of cDC1 and other antigen presenting cells in antitumor immunity of the CNS. We used the cDC1-deficient interferon regulatory factory 8-deficient (*IRF8+32*$^{-/-}$) mice to determine that cDC1 are required to mediated αPD-L1 induced survival benefit as well as to generate neoantigen-specific CD8^{+} T cell responses against the brain tumors. Furthermore, using a fluorescent tracking system, we observed that dendritic cells (including the cDC1 subset) isolated from the tumor, the lymphatic vessel-containing dura, and the cervical lymph nodes harbored tumor-derived antigen. We extended these findings to humans. We identified several subsets of conventional dendritic cells, including the CD141^{+} cDC1 equivalent, in the immune cell infiltrate of a variety of human brain tumor types (including GBM), as well as in the tumor-adjacent dura. We determined tumor-infiltrating dendritic cells, including the CD141^{+} subset (equivalent to the mouse cDC1), contained the tumor-specific fluorescent metabolite of 5-aminolevulinic acid (5-ALA), protoporphyrin IX (PPIX), which is used for fluorescence guided resection of malignant glioma. The PPIX signal was absent in both tumor-infiltrating T cells and equivalent dendritic cell subsets isolated from intraoperatively harvested peripheral blood, which indicates that this phenomenon was specific to antigen presenting cells that had infiltrated the tumor. To our knowledge, this is the first observation in humans of antigen presenting cells ingesting tumor-derived material.

Together, these data provide evidence that cDC1 play a significant role in CNS antitumor immunity in mice and humans. Collectively, these studies have yielded improved tools to study the immunity cycle in GBM and have shed light on some of the elements regarding the nature and mechanism of antigen presentation in CNS antitumor immunity.

CHAPTER ONE

Introduction to glioblastoma, cancer immunology, and CNS immunity

1.1 Glioblastoma patients face a poor prognosis

Glioblastoma GBM is the most common primary malignancy of the central nervous system (CNS), with about 13,000 new cases per year [1]. Patients stricken with this disease have universally poor outcomes. With the standard treatment, the median survival is 15-20 months [2, 3]. Despite immense resources dedicated toward investigating better therapies to improve disease outcomes, the standard therapy has remained largely the same since 2005, and is based on a landmark New England Journal of Medicine paper in which the authors described improved outcomes based on addition of temozolomide therapy to gross total resection and radiotherapy [2]. Unfortunately for patients, temozolomide treatment only provides benefit for the subset of patients with low methylguanine-methyltransferase expression in their tumors [4], which occurs in just one-third to one-half of cases [5, 6].

Following initial treatment and gross total resection of the tumor, GBM invariably occurs, with a five-year survival of just 6.8% [1]. One of the major challenges for treating GBM is that despite maximal resection, the malignant cells always extend beyond the margin of the tumor to distant parts of the brain, where they seed themselves to drive recurrence. Evidence for this phenomenon was demonstrated by GBM cases which recurred despite efforts to resect tumors with an immense margin of healthy brain tissue surrounding the tumor. This included GBM recurrence despite complete hemispherectomies performed in

the 1920s by Walter Dandy attempting to treat GBM [7]. The severity of this disease combined with the absence of treatments which lead to long term survival warrant further investigation into different treatment types.

1.2 Immune editing

The ability of the immune system to restrain cancer had been an idea of varying popularity but was definitively demonstrated in a landmark study by Shankaran and colleagues (of Robert Schreiber's lab) in which they described how immunocompromised Rag2-deficient hosts, which lack T cells and B cells, grew greater numbers of spontaneous tumors than their wild-type counterparts. They further described that carcinogen-induced tumors from immune deficient animals were rejected when transplanted in immune competent syngeneic hosts, whereas carcinogen-induced tumors that originated from immune competent counterparts were less immunogenic and grew progressively when transplanted into immune competent hosts [8]. These findings demonstrated the principle that tumors which originated from immune competent hosts had already been "edited" by the immune system, which consisted of removing more immunogenic cells and leaving behind less immunogenic cells so that the resultant tumor was less immunogenic. In contrast, "un-edited" tumors that originated from immune deficient mice had never been exposed the immune system to eliminate the more immunogenic targets, which made these "un-edited" tumors able to be rejected when transplanted into wild-type immune competent hosts. By demonstrating these findings, the paper showed conclusively that the immune system restrained tumor growth and settled this question regarding whether the immune system could recognize and respond to malignancies.

It is now widely accepted that tumors that present clinically exist because they have escaped control of the immune system [9]. The immunoediting model is based on the following premise: malignant cells harbor mutations that result in the expression of mutated proteins, which can be seen as “foreign” by the immune system since the immune system was not tolerized against these “new” antigens, termed “neoantigens.” As a tumor grows, it gives rise to mutant proteins. Tumor-infiltrating conventional dendritic cells can phagocytize and capture these mutant proteins, activate, migrate to a draining lymph node, and present the processed mutant proteins to prime naïve T cells against the neoantigens contained within the mutant protein. Once primed and clonally expanded, these neoantigen-specific effector T cells home from lymph node to tumor, where malignant cancer cells may present peptides derived from their own mutated proteins on major histocompatibility complex I (MHCI). In the tumor, malignant can be destroyed by neoantigen-specific effector $CD8^+$ T cells as any foreign invader would be. Moreover, the immune response is further bolstered by effector $CD4^+$ T cells, which can secrete cytokines in response to neoantigens presented on major histocompatibility complex II (MHCII) by professional antigen presenting cells. These stimulated $CD4^+$ T cells can subsequently orchestrate and direct the immune response against the tumor. Occasionally, malignant cells arise that can evade complete destruction by surveilling immune cells, and persist in equilibrium with the immune system, but still lack the capacity to escape completely beyond the immune system’s control. The immune system and the cancer cells persist in this tug of war, unbeknownst to the host, until selective pressure from the immune system eliminates the more immunogenic tumor cells. Due to this selective pressure, the remaining less immunogenic malignant cells grow out. At this

point, wherein the malignant cells have completely escaped beyond the control of the immune system, the tumor becomes clinically apparent [9-12]. While this process has been described for mouse fibrosarcoma and a variety of other tumor types, it remains unknown how exactly this process occurs with glioblastoma.

1.3 Brief history of cancer immunology, with particular focus on dendritic cells

The idea that the immune system could potentially be an aid in cancer eradication is not new but has experienced periods varying popularity. The idea of using the immune system to defeat cancer dates to the use of Coley's toxins in the 1890s. Dr. Coley documented several observations in which sarcoma or carcinoma patients became infected with "accidental erysipelas" (presumably from group A streptococcus) following surgery to resect their tumors. In some of these instances, the postoperative erysipelas infection was followed by tumor regression [13]. Dr. Coley began to experiment with the use streptococcus inoculations in his own patients with limited success (some of his patients unfortunately died due to the bacterial infections themselves). In this treatment, Dr. Coley used streptococcal bacterial toxins as an adjuvant to non-specifically activate the immune system, which led to tumor regression in some of his patients who were lucky enough to have a tumor that could be recognized and rejected by the immune system, and who were also fortunate enough not to die from the streptococcus infection itself. Despite these observations, the actual mechanism of tumor regression was poorly understood at the time. Moreover, despite his success, he was doubted by his contemporaries, which may have delayed the commonplace acceptance of similar ideas.

The 1908 Nobel Prize in Physiology or Medicine was awarded to Paul Erlich and Élie Metchnikoff for their discovery of immune surveillance with their observation that foreign substances would in certain instances be phagocytosed and neutralized when implanted into a host organism. Erlich believed that this defense system was also present within the blood and further postulated that the immune system could recognize and protect against cancer. Five decades later in 1959, Lloyd Old and colleagues began to shed more light upon the relationship between cancer and the immune system. In their experiments, they set out "to alter the growth and lethality of various experimental tumors by agents known to possess the common property of stimulating the phagocytic capacity of the reticuloendothelial system." Specifically, they described how immunization with the Bacillus Calmette-Guérin vaccine could lead to regression of transplantable sarcoma model by activating the immune system [14]. In further experiments in 1962, Old and colleagues determined that carcinogen induced tumors possessed antigens—recipient mice could be inoculated with low levels of carcinogen-induced cancer cells, and then would later resist much larger inoculations of those same cells, which would ordinarily result in tumor outgrowth when transplanted into a naïve host [15]. Around the same time, as described in a widely regarded review written by Dunn and colleagues, these discoveries regarding cancer immunity were threaded together to form the hypothesis of "cancer immunosurveillance" that had been partially postulated by Sir Macfarlane Burnet and Lewis Thomas. In this hypothesis, one of the evolutionary tasks of the immune system was to detect and respond to neoplasms [10, 16, 17].

Despite these important observations that the immune system could seemingly detect, respond to, and selectively amplify immune responses against malignancy, the

mechanism by which the immune system carried out this detection and selective amplification remained a mystery. It was believed that there was a missing “accessory cell” that connected innate immunity, which non-selectively phagocytized invaders to form the first line of defense, to adaptive immunity, which amplified humoral or cellular responses against a specific threat or antigen.

In what later panned out to be a remarkably important discovery in 1973 (but perhaps unappreciated at the time), Ralph Steinman and Zanvil Cohn first isolated conventional dendritic cells (cDC) from lymphoid organs of mice. They characterized these cells based on their abundant dendrites and distinguished them from other cells based on their low baseline phagocytic activity, restriction to lymphoid organs, and low frequency (~1% of the total cells in all lymphoid organs measured). While they simply described basic features of this new cell type without characterizing its relevance to the immune system, Steinman presciently quipped that this new cell type might retain “antigens on its cell surface through the mediation of specific antibody” [18]. Although the significance of this newly discovered dendritic cell was unknown at the time, further experiments in 1980 by Michel Nussenzweig (in collaboration with Steinman and Cohn) showed that in contrast to purified macrophages, a second and much more common antigen presenting cell, purified dendritic cells could stimulate cytotoxic $CD8^+$ T cells to activate and proliferate [19]. These discoveries suggested that dendritic cells might possess some unique capacity to function as the bridge between innate and adaptive immunity by performing the role of the sentinel “accessory cell.” In a nutshell, this meant they could bring antigens that they had phagocytized in the periphery into contact with T cells harbored by lymphoid organs

in order to drive amplification of T cells that could in turn recognize antigens derived from the invading pathogens in order to respond to and eradicate the pathogen.

These discoveries also augured that cDC might be critical to the early detection of neoplasms through their sentinel-like immune surveillance functions and ability to initiate an adaptive immune response, however mice that were deficient in cDC (or particular cDC subsets) would be needed to prove this *in vivo*. Decades later in 2008, experiments by Kai Hildner of Kenneth Murphy's lab punctuated that point and definitively established a role for dendritic cells in immune surveillance against cancer. They developed a mouse in which the conventional dendritic cell 1 subset (cDC1) failed to develop by targeting and selectively deleting the gene for Basic Leucine Zipper ATF-Like Transcription Factor 3 (BATF3), a transcription factor required for cDC1 development. They used this mouse to establish that cDC1 were critical to mount an effective antitumor immune response *in vivo*. They employed a regressor fibrosarcoma tumor developed in Bob Schreiber's lab. Under ordinary conditions, wild-type mice spontaneously reject this tumor. In contrast, the tumor grows progressively in *Rag2*$^{-/-}$ mice, which lack T cells and B cells. Hildner and colleagues established that cDC1 were also required for tumor rejection by demonstrating that the tumor also grew progressively in their cDC1-deficient *BATF3*$^{-/-}$ mouse [20].

The role of dendritic cells (mostly cDC1, but also cDC2 in select studies) in tumor immunology has been expanded and defined further. The importance of cDC for antitumor immunity has been demonstrated in a variety of tumor types. Several functions of cDC have been well described, including the ability of cDC to phagocytize tumor-associated material and traffic that material to lymph nodes [21-24], to cross present antigen (cDC1 specifically) to prime $CD8^+$ T cells and drive tumor rejection [25], as well as to present

cell-associated antigen (cDC1 specifically) to prime $CD4^+$ T cells [26]. Moreover, experiments have demonstrated additional important roles of cDC1 in antitumor immunity, including: the requirement of cDC1 for type 1 interferon signaling [27, 28], the additional role of cDC1 in antitumor immunity independent of cross presentation [29], the requirement of cDC1 in establishing the immune microenvironment [30], and their susceptibility to subversion from the tumor by manner of cDC1-exclusion as a mechanism of tumor escape [30, 31]. Despite these discoveries establishing the importance of cDC1 in antitumor immunity more broadly, the role of the cDC1 in CNS antitumor immunity remains unknown. cDC have been understudied in the CNS likely for variety of reasons, perhaps because they are absent in the steady state brain parenchyma, because the CNS lacks conventional lymphatics, and/or because the CNS immune response is unique, all of which will be discussed below.

1.4 CNS immune privilege dogma

Historically, the CNS has been widely regarded as an immune privileged anatomic location, meaning that foreign tissues transplanted there would not stimulate an immune response that led to rejection of the transplanted tissue by the host's immune system, in contrast to other regions outside the CNS, where transplanted foreign tissues would be attacked. This understanding was largely based on experiments which demonstrated that immune responses were delayed or weakened in the brain parenchyma compared to an equivalent perturbation in the periphery.

Examples of this include experiments by Shirai in 1921 in which he observed that a xenografted rat fibrosarcoma grew well in the mouse brain, but was rejected when implanted subcutaneously or intramuscularly into mice [32]. In 1923 Murphy and Strum

added a twist to these findings by showing that while xenografted fibrosarcoma cells grew well when transplanted into a mouse brain, that co-transplantation of the same xenograft fibrosarcoma cells into both the mouse's spleen and brain stimulated rejection of the transplanted fibrosarcoma from the brain [33]. In 1948 Medwar extended the principle that immune responses in the brain could occur under specific circumstances in an elegant set of experiments in which he demonstrated that rabbit skin allografted into a recipient rabbit's brain parenchyma only rejected if that rabbit had been simultaneously allografted elsewhere on the body [34]. The observations with xenograft fibrosarcoma and allogeneic skin that (1) peripheral immunization was required to stimulate a brain parenchymal immune response, and (2) that immune responses primed solely in the brain parenchyma were weak or absent compared to an immune response primed by the same stimulus in the periphery, have been repeated using bacteria (Bacillus Calmette–Guérin) [35], influenza viruses [36], and adenovirus vectors [37], as summarized nicely by Galea et al [38]. Interestingly, these observations of attenuated immunity resulting from a stimulus being implanted into the brain parenchyma required the stimulus to be introduced solely and specifically to the brain parenchyma—when xenografted tumors, BCG vaccine, or influenza were introduced to the ventricles, they all elicited strong immune responses in the brain [33, 35, 36]. Furthermore, when H-2 incompatible neocortical allograft tissue was transplanted into cerebral ventricles of mice alone, rejection occurred without external stimulus and was further hastened by simultaneous transplant of allograft tissue into the skin [39]. Similarly, neural tissue that was either xenografted or derived from the same species but differed at both major and minor histocompatibility loci was likewise rejected when transplanted into the third ventricles of mice or rats [40]. Rejection of engrafted tissue from the brain

parenchyma may be context dependent as well: experiments in the early 1990s showed data that seemed to contradict previous observations. Finsen and colleagues were able to document certain instances in which mouse neural tissue xenografted into the hippocampus of rat brains stimulated inflammation including extravasation of T cells, macrophages, and IgG into the xenografted tissue, which was followed by rejection in most cases when they extended the observation period and looked beyond the day 35 timepoint [41].

These experiments, taken at face value, might lead one to conclude that the brain parenchyma is an immunologically privileged anatomic location in which only absent or weakened immune responses can occur. However, upon closer inspection, these observations offer a more nuanced view of CNS immunology and collectively show that given the correct initiating event, the CNS immune response has potential to be immensely potent. In many of these experiments, other than the initiating inflammatory stimuli of transplanting the tissue or pathogen into the brain parenchyma, there lacked a constant source of inflammation that propagated enough to drive recruitment of immune cells into the brain parenchyma. Moreover, the inability of the CNS immune system to spontaneously reject tumors from the brain is not a universal phenomenon as suggested by Shirai's 1921 fibrosarcoma brain tumor experiments [32]. We have made several observations to the contrary and indeed our field of work would not exist if this were the case. Furthermore, several conditions involving the immune system in the CNS, such as demyelinating disease, infectious encephalitis, and the previously documented immune responses against CNS tumors illustrate the potential for potent immune responses within the CNS under the right conditions.

1.5 The blood brain barrier

The uniquely regulated and generally impermissive blood-brain barrier (BBB) has posed a second roadblock to disputing the belief firmly held by some that the brain is hermetically sealed from the immune system. As summarized by Engelhardt et al. [42], the blood brain barrier is formed by specialized endothelial cells conjoined by tight junctions that form a much tighter barrier compared to endothelial cells in systemic circulation [43]. Additionally, the BBB endothelial cells themselves have low pinocytotic activity [44] so as to limit transcellular or paracellular efflux from the blood into the brain parenchyma. There is a second boundary, as reviewed by Abbot et al. [45], which is formed by astrocyte foot processes and pericytes that comprise the glia limitans and which surrounds cerebral vasculature. This further restricts entry of substances from the blood to the brain parenchyma. However, the integrity of the blood brain barrier is not uniform—circumventricular regions of the brain lack a functional blood brain barrier [46], and perhaps more importantly, the blood brain barrier suffers dysregulation and loss of integrity during inflammatory conditions [44, 45] and in the setting of brain tumors. In an elegant set of experiments, Don Long used electron micrographs of brain tumor tissue sections to demonstrate that brain tumors are vascularized by endothelial cells with dysmorphic cell-cell junctions. He identified that expected fusions between endothelial cells were often absent, with large spaces opening in place of junctions. Secondly, he observed an absence of the glia limitans, which would ordinarily be formed by pericytes and astrocyte foot processes. These breaches in the endothelial barrier allowed for passage of tracers or other substances from the blood in his experiments [47], and could presumably serve as a conduit for immune cells, which will be discussed below. Moreover, Elegant

experiments by Rong Wang and colleagues demonstrated that subpopulations of endothelial cells isolated from glioma tumors harbored the same mutations as the tumor, which suggests that stem-like cells originating from the tumors themselves can differentiate into endothelial cells allowing for additional blood flow into the tumor [48].

While the blood brain barrier restricts passage of most cells and solutes from blood to brain in the steady state, inflammation itself and the dysregulated vasculature associated with brain tumors can drive open the barrier in specific places, allowing surveilling immune cells to enter. The consequence of this is that brain tumors are not sequestered from the immune system, and the logical conclusion is that there are abundant opportunities for interaction between the immune system and the brain tumor itself. Moreover, evidence exists for steady state immune surveillance of the brain, which will be discussed below.

1.6 Immune surveillance and antigen presentation in the CNS

While the brain is not immune privileged in the sense that the immune response is completely absent from the brain, it is appropriate to state that the immune response is different from other regions of the body. The innate immune cell type response for immune surveillance and antigen presentation in the CNS remains an unsettled debate. The only steady state leukocyte in the brain parenchyma is the microglia [49]. A specialized macrophage called the border associated macrophage exists along the basement membranes of blood vessels [49]. Even though these two cell types can present antigen, they are not known to be able to migrate outside the CNS to lymph nodes, a role ordinarily carried out by conventional dendritic cells. While conventional dendritic cells do possess the machinery necessary to be able to capture antigen and migrate to lymph nodes to stimulate T cell responses, the steady state brain parenchyma is relatively devoid of them.

Early studies performed in 1981 which investigated various rat tissues for the presence of the recently discovered dendritic cell found that with one exception, all the tissues they investigated, including heart, liver, thyroid, pancreas, skin, kidney, ureter, and bladder harbored dendritic cells. The striking exception to their observations was the brain [50]. However, studies fifteen years later determined that the CNS was not truly devoid of dendritic cells, and rather that their location was restricted to the choroid plexus, which supplies CSF to the ventricles, and the meninges, which comprises the fibrous sheath covering the brain [51]. However despite the observations demonstrating that the brain parenchyma is devoid of dendritic cells in the steady state, dendritic cells have been shown to infiltrate the brain parenchyma in considerable numbers once inflammation begins [51]. it is further conceivable that a dysregulated blood-brain barrier as is the case in glioma would permit entry of surveilling dendritic cells regardless of inflammation status. Needless to say, despite these previous observations regarding various antigen presenting cell subset characteristics and behavior, the type of antigen presenting cell that conducts immune surveillance and primes T cell responses in the brain remains an open question.

Evidence does exist for steady state antigen sampling in the brain. Harris and colleagues of Zsuzsanna Fabry's group showed that sampling of brain-derived antigens does indeed occur in a set of remarkably clever experiments [52]. They engineered a mouse to express the MHCI and MHCII restricted ovalbumin epitopes selectively in oligodendrocytes (a CNS-restricted cell type which functions to myelinate neurons), or in gut epithelial cells. They found that adoptively transferred OTI $CD8^+$ T cells, which recognize the MHCI-restricted ovalbumin epitope, divided equivalently in the spleens of either the

oligodendrocyte-OVA or gut epithelium-OVA mice, which showed that antigen sampling in the steady state occurred equally when that antigen either was confined to the gut or to the CNS. They determined that while antigen sampling occurred as evidenced by the division of OTI cells following their adoptive transfer into the oligodendrocyte-OVA mice, that the OTI cells did not physically enter the brain parenchyma in the steady state, and additionally that the mice bore no evidence of disease. Notably, this phenomenon was largely restricted to OTI cells. In contrast, OTII $CD4^+$ T cells, which recognize the MHCII epitope in ovalbumin, did not divide when adoptively transferred, although the oligodendrocytes did express full length ovalbumin, which included the ovalbumin specific MHCII antigen. While neither of these adoptively transferred transgenic T cells entered the brain parenchyma in the steady state, the opposite happened in the inflamed state. They found that OTI cells did enter the brain parenchyma in the inflamed condition of experimental autoimmune encephalitis (EAE), however the presence of OTO cells did not exacerbate disease to a greater degree than in the EAE-only group which had no additional adoptively transferred OT-I $CD8^+$ T cells. These data collectively show that even in the steady state, immune surveillance in the form of afferent immunity still takes place in the CNS. While this set of experiments did provide strong supporting evidence that steady state antigen sampling does indeed exist for CNS-derived antigens, it stopped short of determining which cell type was responsible for initiating this surveillance.

Interestingly, Zozulya and colleagues (also of Fabry's group) found that monocyte-derived dendritic cells (cultured by treating hematopoietic stem cells with GM-CSF (sometimes additionally with IL-4)) could cross a brain-endothelial cell monolayer *in vitro* [53]. The endothelial tight junctions became reorganized when dendritic cells crossed, and the

transcytosis could be inhibited by blocking matrix metalloproteases that were expressed by dendritic cells. This process occurred without affecting endothelial barrier integrity, which they assessed by measuring electrical resistance across the endothelial monolayer. This experiment provided evidence that this type of dendritic cell possesses the machinery necessary to cross the blood-brain barrier, and suggests that dendritic cells could be the cell type responsible for steady state antigen sampling, although this paper stopped short of describing this phenomenon *in vivo*, Furthermore, the authors did not use true conventional dendritic cells which are grown using Flt3L culture instead of GM-CSF, and more closely represent the dendritic cells which arise *in vivo*.

A third interesting study by Fabry's group led by Karman and colleagues showed that injection of a traceable fluorescent ovalbumin antigen into the brain parenchyma of mice led to recruitment of dendritic cells, which processed the ovalbumin [54]. They further identified that intracerebrally injected monocyte-derived dendritic cells migrated to cervical lymph nodes in the neck and could stimulate a systemic immune response, which caused T cells to home back to the brain. They also described that antigen-specific T cell homing to the brain required dendritic cells to be injected intracerebrally and could not be re-created by peripherally injecting antigen-loaded dendritic cells. Collectively, these data highlighted the role of dendritic cells in initiating an immune response in the CNS, but their studies used exogenously derived monocyte-derived dendritic cells for most experiments, therefore they didn't fully answer how endogenous antigen presentation takes place by the dendritic cells that arise naturally *in vivo*.

Perhaps the most intriguing study regarding which cell type is responsible for CNS antigen presentation was conducted by Mundt and colleagues, of Burkhard Becher's

group. In an elegant set of experiments, they used temporal and conditional deletion of MHCII from different antigen presenting cell types known to exist in the brain in either the steady state or inflamed state and measured the effect of their perturbations on EAE [55]. They deleted MHCII from microglia by crossing the microglial-specific *Sall1*^{CreERT2} mouse to an *MHCII*$^{fl/fl}$ mouse. They identified that MHCII on microglia was dispensable for EAE. They administered tamoxifen at different time points to a *Cx3xr1*^{CreERT2} mouse (expressed in all brain APCs) which had been crossed to a *MHCII*$^{fl/fl}$ mouse. Constant tamoxifen treatment deleted MHCII from all brain APCs (microglia, border associated macrophages, and cDC). One-time early administration of tamoxifen deleted MHCII from only long-lived microglia and border associated macrophages, which turn over slowly. However, one-time treatment permitted MHCII expression to be restored on conventional dendritic cells, which are replaced quickly by HSCs. Only the early one-time treatment regimen, in which MHCII expression was restored in cDC, resulted in disease. In contrast, long term treatment, which deletes MHCII from all APC subsets (microglia, macrophages, cDC) prevented disease. This suggests that that border associated macrophages (in addition to microglia), but not cDC, were dispensable for disease progression. This clever set of experiments provided strong evidence that conventional dendritic cells are required for disease progression in EAE and that they may be the type of APC responsible for immune surveillance and T cell priming in the CNS, at least in this disease model of autoimmunity.

Finally, in a shrewd set of experiments by David Giles and colleagues of Benjamin Segal's lab, they demonstrated in an EAE model that cDC accumulated in considerable numbers in the CNS and possessed superior ability to prime MOG-specific $CD4^+$ T cells (which recognize the antigen used to trigger EAE) compared to endogenously arising $Ly6C^+$

monocyte-derived dendritic cells (moDC) (not to be confused with GM-CSF cultured monocyte-derived dendritic cells). They also showed that cDC were more pro-inflammatory than moDC (from LPS stimulation, cDC made more IL-12p40 compared to moDC, and moDC made more of the immune-suppressive cytokine IL-10 compared to cDC), and that depletion of cDC using a ZBTB46-DTR mouse, which depletes all conventional dendritic cells, resulted in attenuated disease severity compared to wild-type mice [56].

While the steady state brain is relatively devoid of conventional dendritic cells, these studies showed that homeostatic CNS antigen sampling still takes place, that cultured dendritic cells possess the ability to cross the endothelial portion of the blood brain barrier *in vitro*, that dendritic cells process antigen injected into the brain, and that when exogenously introduced into the brain, exogenously cultured monocyte-derived dendritic cells can migrate to cervical lymph nodes. Moreover, by using multiple different experimental approaches, researchers have also demonstrated that conventional dendritic cells are required for disease progression in EAE. These studies drive home the point that the brain is far from immune privileged, and that CNS immune surveillance likely occurs at all times. These studies are also highly suggestive that dendritic cells play a role in immune surveillance against CNS tumors.

1.7 CNS lymphatic drainage

Two unique features of the CNS, which have also contributed to the CNS immune privilege dogma, are the lack of conventional lymphatic tissues within the brain parenchyma and the absence of secondary lymphoid tissue in close anatomic proximity to the CNS. Without definitively describing the presence of dura lymphatics, investigators

have known for quite some time that there exist mechanisms to clear debris and solutes from the brain, and secondly that the cervical lymph nodes in the neck likely hold importance in lymphatic drainage and priming an immune response in the CNS in autoimmune conditions.

Of historical note, CNS-associated lymphatics are first known to be described by Italian physician and anatomist Paolo Mascagni (1755-1815). In 1787, he published a book that described the lymphatic vessels of the human body, which included descriptions of meningeal lymphatic vessels. This book was published in Latin, and not translated until recently [57]. His work was also later overshadowed by anatomist Gustaf Retzius (1842-1919) who described the absence of meningeal lymphatic vessels, contrary to Mascagni's work [57]. Perhaps these two reasons—the lack of translation of Mascagni's work, and the contrary descriptions by later anatomists, might be partly responsible for why dura lymphatics were overlooked until much more recently. Moreover, later anatomists quipped that Mascagni "was probably so impressed with the lymphatic system that he saw lymph vessels even where they did not exist — in the brain" [57, 58]. In the 20th century, studies have produced evidence of dura lymphatics in a variety of species ranging from dogs to rats to humans as described by Sandrone et al. [57], but they did not completely describe the drainage route, nor did they describe the precise anatomic structures of lymphatic vessels associated with the CNS, although the logical conclusion was that some sort of CNS lymphatic drainage mechanism likely existed.

Some of these early studies which stopped short of completely describing CNS lymphatics consisted of injecting tracers into various anatomic locations in the CNS. In 1992 Zhang and colleagues showed drainage of that intracranially injected carbon

particles which had entered the subarachnoid space superficial to the vertex of the hemispheres drained along paravascular pathways to the cribriform plate, and into the superficial cervical lymph nodes [59]. In 1993 Kida and colleagues described that India ink injected into the cisterna magna caused deep cervical lymph nodes to be “selectively blackened within 30 min” followed 6 hours later by selective blackening of lumbar para-aortic lymph nodes. They also described that intracerebrally injected carbon particles accumulated around arterial structures and localized to “discrete channels which passed through the cribriform plate and into lymphatics in the nasal submucosa.” [60] While these studies partially described routes by which debris was cleared and implicated some sort of lymphatic system which carries out this process, they stopped short of describing the complete structure, and importantly, how the immune system was involved.

Some of the first experiments to test hypotheses regarding the immune involvement of the cervical lymph nodes in CNS immunology where those involving EAE models. In the late 1990s Phillips and colleagues showed that cervical lymphadenectomy reduced disease severity in EAE in Lewis Rats, which was one of the first studies establish a connection between cervical lymph nodes and the CNS immune response [61]. In the late 2000s further studies extended these results: Furtado and colleagues demonstrated that activated myelin basic protein-specific $CD4^+$ T cells first appeared in the cervical lymph nodes before appearing in the brain, and that lymphadenectomy reduced disease burden in a mouse spontaneous EAE model [62]. In a similar study of chronic relapsing EAE, Furtado and colleagues resected the superficial cervical, the deep cervical, and the lumbar lymph nodes, and determined that resecting these particular lymph nodes could ameliorate disease compared to sham treated mice. They also demonstrated that reactive

T cells against the immunizing peptide first appeared in the superficial cervical lymph nodes, and that epitope spreading to other EAE antigens occurred in the deep cervical lymph nodes, the lumbar lymph nodes, and the spleen [63]. While these studies provided strong circumstantial evidence that regions of the brain likely were equipped with lymphatic drainage, and that the cervical lymph nodes in the neck were a key player, they did not definitively demonstrate the presence of lymphatic vessels in or around the anatomic structures surrounding the brain, nor did they precisely describe how antigen presenting cells migrate from brain parenchyma to the cervical lymph nodes.

In two landmark studies published in 2015, Louveau and colleagues (from Jonathan Kipnis's group), along with Aspleund and colleagues (from Kari Alitalo's group) described *bona fide* lymphatic vessels harbored by the dura which drained solutes and macromolecules from the CNS to the deep cervical lymph nodes, as well as to the superficial cervical lymph nodes [64, 65]. The general lymphatic drainage route model that they described was of dura lymphatics traversing along the venous sinuses (also harbored by the dura) as they exit the skull and enter the neck, with lymphatic vessels hugging the venous sinuses along the entire path, eventually converging on deep cervical lymph nodes that lie upon the internal jugular vein the neck. Louveau and colleagues specifically described that when Evan's Blue Dye was injected into the ventricles of mice, the deep cervical lymph nodes contained Evan's Blue within 30 minutes of ventricular injection. They also reported that the superficial cervical lymph nodes contained Evan's Blue at later time points following ventricular injection. Complimenting those findings, Aspleund and colleagues reported that molecular tracers injected into the brain parenchyma drain to the deep cervical lymph nodes, and that this process could be

inhibited by ligating the lymphatic vessels that run along the internal jugular vein in the neck. Interestingly, the Aspleund and colleagues did not observe lymphatic drainage from the CNS to occur in the superficial cervical lymph nodes, however this might have been because they were using a different tracer or were injecting the tracer into a different anatomic location within the brain.

In 2018 Da Mesquita and colleagues (also from Kipnis's group) extended their earlier findings and determined that ablation of meningeal lymphatics diminished solute clearance and accelerated Alzheimer's disease in mice compared to control mice, and conversely, that improving dura lymphatic function by administering VEGF-C increased antigen clearance from ventricles and alleviated cognitive deficits compared to control mice [66]. In another study by Louveau and colleagues which further described the role of dura lymphatics, they demonstrated that ablation of dura lymphatics reduced disease burden in EAE and also prevented CCR7-dependent trafficking to the cervical lymph nodes of both cisterna magna-injected, as well as dura-associated T cells. They also demonstrated that ablation of lymphatics along the cribriform plate prevented T cells from migrating specifically to the superficial cervical lymph nodes compared to control mice [67].

Most importantly, dura lymphatics have been described in humans and non-human primates in studies using MRI. In a shrewd set of experiments. Absinta and colleagues described lymphatic vessels by discerning differential MRI signal between two different contrast agents: one that easily extravasates across a permeable capillary endothelial barrier, and one that does not and remains in the blood [68]. This allowed them to discern between blood vessels and other vessels that collect waste products (i.e., lymphatic vessels). They found that the contrast agent which easily diffused across capillaries

became concentrated in two distinct lumens traversing along each side of the superior sagittal sinus, whereas the blood-confined contrast agent that remained in the blood vessels was restricted to the superior sagittal sinus. The anatomic location and structure of these lymphatic vessels in the CNS mirrored that which had been demonstrated to exist in mice: lymphatic vessels traverse along the superior sagittal sinus and exist in close proximity to the cribriform plate across many different mammalian species.

Finally, of particular relevance to our work, studies have demonstrated dura lymphatics to be important for CNS antitumor immunity. In a landmark study just recently published in 2020, Song and colleagues (from Akiko Iwasaki's lab) showed in a preclinical model of glioblastoma that expansion of dura lymphatics using VEGF-C agonism provoked a more potent antitumor immune response by strengthening $CD8^+$ T cell responses against the tumor, and additionally extended survival compared to control mice with unexpanded dura lymphatics. Importantly, the researchers determined that the benefit of VEGF-C agonism could be abrogated by ligating the lymphatic vessels that drain from the CNS to the deep cervical lymph node [69].

While brain tumors present clinically because they have escaped beyond the control of the immune system, it seems unlikely that this process arose because of the failure of immune surveillance to detect and respond to malignant cells that arose in the first place. Experiments which have demonstrated active CNS immune surveillance and potent immune responses suggest instead that the immune system exerts selective pressure on the tumor from its nascence, eliminating more immunogenic malignant cells early on, which leaves behind less immunogenic malignant cells which can then escape beyond control of the immune system to form the clinically apparent brain tumor. These studies

which collectively demonstrate potent CNS immune responses under varying circumstances and conditions suggest that the CNS immune response could potentially be augmented in a clever way to develop more effective therapies against glioblastoma.

1.8 GBM itself is immune-suppressive and heterogeneous

Beyond the unique nature CNS immune surveillance, several factors underlie the challenge with harnessing the immune system to treat GBM, among them are that GBM itself is generally an immune-suppressive tumor. A wide variety of immunologic defects has been associated with GBM, including systemic effects, and defects within the tumor itself. These factors pose unique challenges toward developing immune therapies against GBM and warrant further discussion.

GBM has been demonstrated to cause severe lymphopenia in a large fraction of patients. In a recent study, Pakawat Chongsathidkiet and colleagues of Peter Fecci's group explored this phenomenon. They identified that a significant fraction of treatment naïve GBM patients present with lymphopenia and decreased average blood $CD4^+$ and $CD8^+$ T cell concentrations, as well as decreased average splenic volume compared to healthy controls. They determined that lymphopenia results from sequestration of T cells in the bone marrow, mediated by loss of S1P receptor on the T cells. S1P receptor normally functions as a chemokine receptor that recently primed T cells use to egress from the lymph node in which they were primed into the blood [70], where S1P ligand concentrations are the highest. They also demonstrated in a preclinical model that artificially increasing the SP1 receptor concentration on host cells using a S1P receptor knock-in mouse could improve survival in the brain tumor setting when combined with 41BB agonism, compared to S1P knock-in alone, or wild-type mice treated with 41BB agonist. Lastly, they identified

that the effect of lymphopenia was specific to having a malignancy of the brain using preclinical models—the same tumor injected peripherally did not cause the same degree of lymphopenia [71, 72]. This study identified potential causes of systemic lymphopenia in GBM patients. The implications are important to consider when assessing possible immune therapies for GBM.

Beyond causing systemic lymphopenia, GBM suppress the immune system locally as well using a variety of mechanisms. One mechanism is the production of indoleamine 2,3 dioxygenase 1 (IDO1) by the tumor. IDO1 enzymatically catabolizes tryptophan as part of the first (and rate limiting step) of kynurenine synthesis. In turn, kynurenine has immune-suppressive effects. While only being expressed at low levels in steady state brain parenchyma, IDO1 can be induced by inflammatory conditions [73], and strikingly, IDO1 is expressed by expressed by 90% of IDH1-wt GBM tumors. Moreover, IDO expression can be induced in GBM cell lines with baseline undetectable IDO1 by exposing those cell lines to pro-inflammatory cytokines [74]. The downstream tryptophan metabolite kynurenine, upregulated by IDO1 production, has been shown to cause selective apoptosis of murine T_H1 but not T_H2 thymocytes *in vitro* [75], deletion of specific thymocyte subsets *in vivo* [75], and conversion of T_H17 cells into T regulatory cells [76], all of which could polarize the immune response into one ineffective against tumors. Pivotal studies by Derek Wainwright have additionally defined the role of IDO1 in GBM *in vivo* using preclinical models. Wainwright and colleagues first showed that whereas IDO1 expression caused recruitment of the immune-suppressive T-regulatory cell (T_{reg}) to the tumor, suppression of IDO1 in brain tumors led to decreased infiltration of T_{reg} cells into the tumor, and increased survival compared to control mice. Furthermore, they

demonstrated that this beneficial effect of IDO1-suppression in the tumor was immune-mediated and required the presence T cells in order to occur. They demonstrated that the survival benefit of IDO1 suppression was lost in *Rag1*$^{-/-}$ mice, which lack T and B cells [77]. In follow up studies, they identified that drug inhibition of IDO1 in mice augmented the effects of checkpoint blockade and improved survival in a T cell-mediated process, and that this effect was somewhat inhibited by temozolomide administration. They also showed that paradoxically, a small amount of systemic IDO1 expression was required for maximal response to checkpoint blockade, and that inhibiting IDO1 in the tumor, rather than systemically deleting IDO1 in the host, provided greatest benefit [78, 79].

In addition to IDO expression, GBM tumors have high levels of immune-suppressive cytokines. GBM cells themselves can produce TGF-β [80-82], and the tumor microenvironment is known to have high levels of IL-10, although IL-10 is unlikely produced by the tumor cells themselves [82], and is instead produced by tumor-associated CD68 expressing macrophages/microglia [83, 84]. TGF-β and IL-10 normally produced by T_{reg} cells to inhibit the B7-1,B7-2-CD28 APC-T cell co-stimulation pathway, to polarize the immune system away from T_H1 responses, and to limit IL-2 production and subsequent T cell proliferation [85], which would ordinarily strengthen antitumor immunity.

Beyond the immune-suppressive mechanisms by the tumor discussed above, GBM tumors have high levels of PD-L1 expression, which normally functions to suppress the immune system. In a survey of glioblastoma tumor samples, Anna Berghoff and colleagues (of Wolfgang Wick's group) identified that 88% of primary GBM specimens, and 72% of recurrent specimens have high levels of PD-L1 expression, and that 73% of tumors had sparse to moderate tumor infiltrating lymphocyte (TIL) density [86]. Notably, the

presence of TIL or PD-L1 expression did not appear to correlate with outcome. In a clever study, Andrew Parsa, and colleagues of Russell Pieper's lab, discovered a previously unknown connection between tumor suppressor loss and upregulated PD-L1 expression. They identified that deletion of phosphate and tensin homolog (*PTEN*; a tumor suppressor lost or deleted in 41% of GBMs [6]) caused increased PD-L1 expression in tumor cells and reduced the cytotoxic activity of tumor antigen-specific $CD8^+$ T cells [87]. Moreover, the microenvironment of GBM can induce PD-L1 expression on monocytes/macrophages as well. Bloch and colleagues (of Andrew Parsa's group, after he had started his own lab) discovered that glioma conditioned media could induce PD-L1 expression on monocytes isolated from healthy donor peripheral blood mononuclear cells. This included both conditioned media from gliomas resected from patients, as well as conditioned media from glioma cell lines, although they did not identify the soluble factor responsible for this process. They noted that IL-10 induced PD-L1 expression on the monocytes, but to a lesser degree than caused by tumor-conditioned media itself, which suggests that another factor was likely responsible [88].

In addition to upregulation of these immune-suppressive factors described above, GBMs are infiltrated by the immunosuppressive myeloid derived suppressor cells (MDSCs)[89]. Moreover, GBM patients tend to have high levels of circulating levels of MDSCs compared to healthy controls [90]. An excellent review by Dmitry Gabrilovich and Srinivas Nagaraj summarizes the characteristics and function of MDSCs [91], which will be briefly described. Although MDSCs share similar markers to neutrophils and monocytes when examined by flow cytometry, MDSCs have unique immune-suppressive functions and have a more immature phenotype compared to their mature myeloid counterparts. They

exert their immunosuppressive effects primarily through secretion of arginase, and their production of nitric oxide and reactive oxygen species. Among the consequences of depleted arginine and increased ROS are suppressed T cell activation and division [91].

Beyond the above-mentioned mechanisms of immune suppression, GBM is a heterogeneous tumor [92, 93], which itself is an immune-suppressive mechanism. Mutations are often not commonly shared between different regions of the tumor—determining the mutations present in the tumor requires sampling the whole tumor. For instance, EGFRvIII, a common oncogene in GBM, has been demonstrated to be expressed only by a fraction of the tumor cells within EGFRvIII-positive GBM specimens [93, 94]. There are several implications of this: first, there are more elements a prospective treatment would need to target. For instance, a T cell (or any drug inhibitor) which might be effective against one tumor cell, or against a subclone, might not be effective at all against a different cell or subclone within the same tumor. Second, increased intratumoral heterogeneity itself has been demonstrated to reduce tumor immunogenicity. In a clever set of experiments, Yochai Wolf and colleagues of Yarenda Samuels's lab demonstrated that the B2905 melanoma cell line could be transformed into a more heterogeneous, less immunogenic, more aggressive tumor when subjected to UVB irradiation before implantation into immune competent wild-type mice, but that single cell clones isolated from that same heterogeneous tumor cell line rejected when implanted into wild-type mice [95]. Moreover, they determined that the growth differences between the parental, UVB-irradiated, or single-cell clone tumors were diminished when those cell clines were injected into immune-compromised NSG mice. These findings demonstrated that intratumoral heterogeneity itself is a mechanism of immune evasion. As such, the high

degree of intratumoral heterogeneity within GBM will pose additional challenges to any immune therapy—clever and potentially combinatorial methods of treatment will be required to overcome this.

These studies collectively show that multiple causes contribute to the immune system's failure at eradicating GBM. There are immune-suppressive effects GBM that act locally, such as IDO1 depletion of tryptophan/production of kynurenine, PD-L1 expression, MDSC induced depletion of arginine and production of ROS, and production of the immune-suppressive cytokines IL-10 and TGFβ. There are also immune-suppressive effects of GBM that act globally, including tumor-induced lymphopenia, and increased peripheral circulating MDSCs. Intratumoral heterogeneity poses additional hurdles. These factors collectively indicate that the immunosuppressive mechanisms of GBM are complicated and multi-factorial. Anyone hoping to develop successful immune therapy should take care to select an immune therapy that not only bolsters the immune system, but which also successfully addresses and inhibits the immune-suppressive factors present in GBM.

1.9 Background on immunotherapy and its current role in GBM

Immunotherapy has led to success in the treatment of once-thought incurable advanced-stage cancers. Beyond Coley's toxins of the late 19th century, the idea of bolstering the immune system as a means of cancer treatment largely remained an unturned stone. This changed in the 1980s, when Steve Rosenberg successfully used recombinant IL-2, the essential growth factor required for T cell division, to exogenously expand a patient's own T cells and then transplant them back into the patient to drive antitumor immunity and treat advanced melanoma. The identification of the potential utility of bolstering T cell

responses to combat cancer by using recombinant IL-2 played a large role “in the introduction of immunotherapy into the mainstream of cancer treatment” as reported by Dr. Rosenberg himself [96].

Beyond establishing that T cells were important, pivotal work was done to establish various regulatory cell surface proteins that modulated the activity of T cells. CTLA-4 was first identified as an inhibitory protein expressed by activated T cells and T regulatory cells. In a pivotal study in 1995, Matthew Krummel and Jim Allison discovered that CTLA-4 had opposing effects compared to CD28 on T cell stimulation, and that crosslinking CTLA-4 with CD28 and the T cell receptor could almost completely suppress T cell proliferation and IL-2 secretion, compared with crosslinking CD28 and the T cell receptor alone [97]. The potent inhibitory effects of CTLA-4 on lymphoproliferation were further demonstrated by Tivol and colleagues in (of Arlene Sharpe’s lab) in parallel. They generated CTLA-4 knockout mice and demonstrated that compared to wild-type mice, *CTLA-4*$^{-/-}$ mice rapidly developed “lymphoproliferative disease with multiorgan lymphocytic infiltration and tissue destruction.” [98] In further work by the Allison lab that established the link between CTLA-4 modulation and antitumor immunity, Dana Leach along with Matthew Krummel used CTLA-4 blocking antibodies to drive rejection of a variety of experimental tumors in mice, including with therapeutic (not just prophylactic) antibody administration of the CTLA-4 blocking antibody [99].

Around the same time, Yasumasha Ishida and colleagues (out of Tasuku Honjo’s lab) used subtractive hybridization to identify *PD-1* as a gene that was commonly expressed between a murine T cell hybridoma and a murine hematopoietic progenitor cell line when they underwent apoptosis [100]. In further studies, Agata and colleagues (also of Honjo’s

lab) identified PD-1 as a cell surface protein that was upregulated on T cells as a result of activation, and established the role of PD-1 as a negative feedback loop of T cell activation, rather than a signaling mechanism for apoptosis [101]. Hiroyuki Nishimura of Honjo's lab extended the role of PD-1 and did similar experiments to those which established that CTLA-4 controlled autoimmunity. They established that compared to wild-type mice, *PD-1*$^{-/-}$ mice suffered severe autoimmunity in the form of dilated cardiomyopathy, which was abrogated by crossing a *PD-1*$^{-/-}$ mouse with the immune-deficient *Rag2*$^{-/-}$ mouse [102]. Yosiko Iwai (of Nagahiro Minato's lab) established the link of PD-1 to cancer immunology by blocking PD-L1/PD-1 signaling to drive rejection of experimental tumors in mice, much as Leach had done with CTLA-4 blockade a few years before [103].

These discoveries demonstrated the concept that immune checkpoint molecules could be inhibited to unleash the immune system and restrain cancer growth. While CTLA-4 blockade is less commonly used clinically due to its severe autoimmune side effects, it has shown success, along with PD-1/PD-L1 blockade in treating melanoma and non-small cell lung carcinoma (NSCLC) [104]. These treatments have also showed promise in treating melanoma or NSCLC-originating metastases to the brain [105-108].

Despite these advances for immunotherapy with select cancer types, immunotherapy has been somewhat of a white whale for GBM. With the exception of a very small number cases, including that of select cases of hypermutated GBM [109, 110], PD-1/PD-L1 blockade is not an effective therapy to treat GBM. Two phase III clinical trials testing PD-1/PD-L1 blockade in unmethylated methyl guanine methyl transferase (MGMT) GBM (Checkmate 498 Trial, NCT02617589), and the same target in methylated MGMT GBM (Checkmate

548 Trial, NCT02667587) failed to demonstrate benefit from PD-1/PD-L1 blockade in treating GBM [111].

However, there have been specific settings in which checkpoint blockade has shown some benefit to the broadest group of GBM patients: that is, when administered as a neoadjuvant (before surgery). In a phase II trial that compared neoadjuvant to adjuvant (or post-surgery) pembrolizumab (anti PD-1) to treat GBM, researchers demonstrated survival benefit from pembrolizumab administered as a neoadjuvant compared to adjuvant pembrolizumab alone. They also identified that neoadjuvant treatment led to increased $CD8^+$ T cell infiltrate, increased interferon gamma signature, and decreased cell-division signature within the tumor at the time of tumor resection, compared to post-surgery pembrolizumab adjuvant alone [112]. The limited success of checkpoint blockade as a neoadjuvant rather than as an adjuvant therapy (administered after tumor resection) demonstrated that pre-operatively boosting T cell function could be therapeutically beneficial. The authors of the neoadjuvant study suggest that neoadjuvant treatment leads to positioning already primed, functional $CD8^+$ T cells within the tumor at the time of surgery, which leads to more complete destruction of residual tumor. In contrast, post-surgery adjuvant therapy alone allows for dysfunctional T cells to exert greater effects at the time of resection, which might result in less effective killing of residual tumor cells, as suggested by the lack of clinical benefit when checkpoint blockade is delayed until after surgery. However, the mechanism of neoadjuvant therapy underlying the benefit has not been fully characterized.

In addition to trials that tested checkpoint blockade to treat GBM, there are a few examples of clinical trials that tested the benefit from targeting neoantigens themselves

to treat GBM. EGFRvIII is one of the most common neoantigens in GBM. It is expressed at varying levels (measured by mRNA expression) in 10-20% of GBM patients [6]. It consists of a deletion of exons 2 through 7 of EGFR [6] and results in a junctional protein that harbors an immunogenic antigen. This antigen can generate an antibody response [113], which makes it an attractive target for chimeric antigen receptor (CAR) T cells. The antigen also contains MHCI and MHCII binding peptides capable of generating a T cell response [114, 115]. The Rindopepimut vaccine against EGFRvIII in GBM patients showed early promise in a phase II trial [116], but failed at the phase III stage [117]. Preliminary therapies using chimeric antigen receptor T cells (CAR-T) against EGFRvIII [118] have demonstrated evidence of EGFRvIII antigen loss by the tumor [119], which suggests immune editing may have taken place. Notwithstanding these results, CAR-T cells did not perform better than the standard of care in these clinical trials [120].

There have also been efforts to develop a dendritic cell vaccine. The DC-Vax trial from Northwest Biotherapeutics trial has entered phase III, with results incoming, however early data suggests that this vaccine formulation doesn't perform radically better than standard of care. The vaccine consists of harvesting $CD14^+$ monocytes from the patient, differentiating them into dendritic cells using a combination of GM-CSF and IL-4, maturing them with TNF-α, IL-1β, and IL-6, exposing them to tumor lysate, and injecting them subcutaneously into the GBM patient [121]. The phase III trial currently in progress reports a median survival of 23.1 months and a group of long-term survivors in their intent to treat cohort compared to the placebo group, but the trial is still underway [122].

Despite these challenges, there is ample evidence that immune responses are indeed present (albeit deranged) within GBM. The promising results associated with the

neoadjuvant trial suggest that the key to unlocking effective immune therapies might require thinking outside the box and employing a multi-pronged combinatorial approach which utilizes various treatments and targets different aspects of the immune system as well as the tumor itself.

1.10 Conclusion

GBM is a complex tumor located within a unique immunologic environment where the immune response differs compared to other regions of the body. This anatomic location uniquely has a lack of parenchyma lymphatics, absence of proximal lymph nodes, lack of infiltrating immune cells at baseline, and a restrictive endothelial cell barrier. GBM also poses the additional challenge of being an immune-suppressive, heterogeneous tumor. Despite this, considerable evidence exists that immune responses in the CNS have potential to be strong (as evidenced by demyelinating disease and encephalitis). It is also clear that despite their apparent absence in the steady state brain, conventional dendritic cells almost certainly play a key role in immune responses in the brain based on the studies discussed above, however the role of dendritic cells in CNS antitumor immunity is not well described. Although no silver bullet yet exists to treat GBM, and successful treatment of GBM will require addressing the hurdles of immune suppression and tumor heterogeneity, our hope is that investigating the cancer immunity cycle in GBM as it occurs endogenously, with particular focus on dendritic cells, lymphatic drainage, and antigen presentation might offer insight and clues into developing better treatments. Herein, I will discuss the body of work I performed during my PhD studies that encompasses developing immunologically faithful and better representative preclinical models of GBM, and finally, I will describe how we think dendritic cells, lymphatic

drainage, and antigen presentation work in preclinical models of GBM. Finally, I will discuss the relevance of conventional dendritic cells to GBM in humans and share the discoveries we have made in clinical samples.

CHAPTER TWO

Immunologically faithful autochthonous genetically engineered mouse models of malignant glioma

2.1 Introduction

Autochthonous genetically engineered mouse models (GEMMs) of cancer are a powerful tool to recapitulate malignancy in a manner that more faithfully represents human cancer than other preclinical mouse models of cancer. These models typically function by leveraging a nearly silent initiation event to cause one or a few cells in a specific tissue to transform into malignant cells which coevolve with the immune system for their entire lifespan to give rise to the tumor. In contrast, orthotopic models require transplanting a bolus of malignant cells into the brain, many of which probably fail to engraft and die, which itself is likely an inflammatory event.

Glioblastoma is a low to moderate mutational burden tumor, with 50-100 somatic mutations [6], and tumors typically do not respond to checkpoint blockade except in rare cases [111]. In contrast, orthotopic glioma models harbor thousands of somatic mutations [123]. Two out of the three of the most commonly used models (GL261 and CT2A) are carcinogen-induced and all three (those two as well SMA650) can be successfully treated by checkpoint blockade alone [124, 125] or by combined checkpoint blockade and vaccination in the more aggressive model CT2A [126]. In contrast to orthotopic models, GEMMs allow for precise targeting of genes to cause transformation, which has potential to result in a lower mutational burden tumor that has a mutational landscape more like human GBM

and as such has a greater chance of more faithfully recapitulating the tumor-immune system interactions than orthotopic preclinical models.

There are a variety of methods to cause the genetic mutations required for GEMM glioma models. Typically, GEMMs are engineered such that the host organism is permissive to a transforming event that will cause the target cells or tissue to have gain of function of oncogenes, and loss of growth restraint by tumor suppressors, both of which are required to engender malignant potential in the transformed target cells [127]. In contrast to GEMMs in which germline mutations of tumor suppressor genes drive non-specific tumor formation, or alternatively GEMMs in which mice that harbor tissue-specific Cre are crossed to mice with loxP-flanked tumor suppressors to drive tissue-specific tumor formation, viral delivery of the transforming agent has the added benefit of allowing for precise spatial and temporal control of tumor formation. The usual method is to deliver an oncogene, as well as Cre, which excises loxP-flanked tumor suppressors in target cells if the mouse is genetically engineered as such.

The agents of delivery typically used for GBM GEMMs are retrovirus, adenovirus, the RCAS-tVA system, and Lentivirus. Retrovirus allows for stable integration of transferred genes, however it only infects actively dividing cells [128]. Although retrovirus has been used successfully to induce GBM in preclinical models [129], we chose not to bias our GBM model toward only originating from actively dividing precursors, as the cell of origin for GBM is not entirely settled [130].

Adenovirus has been used in preclinical models of glioma [131], and can transduce both actively dividing and non-dividing cells [132], although the virus's genes do not integrate into the target cell's genome and expression of the virally delivered genes is transient [133, 134].

This means that any potential oncogene delivered by the adenovirus would be lost shortly after initiation of transformation and continuous expression of the oncogenes required to drive transformation of target cells would not be possible. Thus, adenovirus can only usefully delete loxP-flanked genes given that this scenario only requires transient Cre expression. Adenovirus-driven GEMMs require the mouse to be engineered such that Cre both causes tumor suppressor deletion and oncogene gain of function. As such, in addition to requiring loxP-flanked tumor suppressors, the mouse must also be engineered with a transgene insert consisting of loxP-stop-loxP-oncogene or a similar construct such that Cre expression also causes oncogene gain of function. The consequence of this is that the transformation-driving oncogene is hard to substitute easily and doesn't allow for the flexibility provided by other virally-driven GEMMs.

The RCAS/tv-a glioma model system uses expression of the TVA retroviral receptor under control of a specific promoter (typically under different promoters to target astrocytes, neural stem cells, or oligodendrocyte precursor cells), which binds the RCAS virus to permit entry into the target cell to drive transformation [135-137]. The promoter-specific tv-a mouse is typically crossed to a mouse with the desired loxP-flanked tumor suppressors. In this system, the RCAS retrovirus transduces only cells which express the TVA receptor to deliver the oncogene and Cre. This means targeting is precise to a specific target cell type, however the drawbacks of this system are that it restricts the cell of transformation to only those cells which express the desired tv-a promoter. The second drawback is that to achieve sufficient viral titers to transduce target cells, DF-1 chicken fibroblasts that produce the RCAS virus must be physically implanted into the brains of the tv-a mouse [136]. Injecting a foreign cell type into a mouse brain has potential to be

highly inflammatory and might provoke an outsize immune response that subjects the tumor to more immune editing early in its lifecycle or other such undesired consequences more so than in other GEMMs, which in contrast only require implanting the virus itself.

Lentivirus has also been used successfully for GEMM glioma models [138, 139]. We selected lentivirus because it offers flexibility to substitute oncogenes easily, because it can infect dividing and non-dividing cells (especially relevant given the unknown cell of origin in GBM), because it stably integrates (and thus would drive continuous oncogene expression), and because it does not require xenografting foreign cells into the brains of recipient mice to achieve viral titers sufficient for transformation.

While similar genetically engineered autochthonous models of glioma have been used before, to our knowledge, these systems have used outbred mice, immune compromised mice, human oncogenes to drive tumor formation, or highly immunogenic initiation events. These factors make the other models less than ideal for studying the pure interaction between tumor and the immune system. With outbred mice, the investigator can never conclude with certainty that an observed immune reaction is due to the presence of a tumor-derived neoantigen, whether it's due to the mixing of different genetic backgrounds, or whether it's due to unique genetic differences with immunologic consequences that may arise by nature of the strain being outbred. With GEMMs that use immune compromised mice, any antitumor immune response is attenuated or absent, and certainly does not simulate how antitumor immunity could occur in humans.

We modeled our GEMM glioma to target two of the most commonly lost tumor suppressors in GBM. We engineered mice with *INK4a/ARF*$^{fl/fl}$ and *PTEN*$^{fl/fl}$ mutations on a pure C57BL/6 background. These tumor suppressors are mutated or lost in 60% and

34% of GBM cases respectively [6]. We selected murine platelet derived growth factor beta (PDGFβ) as our transforming oncogene as, PDGFβ aberrancy is observed in 13% of GBM tumors [6], and has led to transformation in previous models when the human PDGFβ construct was used [129, 139, 140]. Our model is appropriate for immunologic studies because it faithfully recapitulates the mutations expressed in a larger proportion of GBM tumors, uses inbred mice, uses lentivirus instead of retrovirus, and employs murine PDGFβ instead of human PDGFβ used in previous models (to which the mouse is not immunologically tolerant). These unique features make our model more suitable for studying antitumor immunity in GBM

2.2 Results

2.2.1 GEMM glioma concept: lentivirus specifically and precisely alters target cells

For tumor induction, we selected the Lenti-LucOS lentiviral backbones created by the Tyler Jacks Lab. These have used in a preclinical model of mouse fibrosarcoma [141], and hence would likely be suitable for target cell transformation in our model. Under the control of a ubiquitin promoter, the lentivirus normally drives expression of luciferase fused with the H-2K^b restricted antigens SIINFEKL and SIYRYYGL, as well as the I-A^d antigen from ovalbumin (termed “OS” cassette). In a second open reading frame, the lentivirus drives expression of Cre under the control of a PGK promoter. We substituted luciferase in the construct with murine PDGFβ followed by a stop codon to prevent expression of the antigens in the downstream OS cassette (termed Lenti-PDGFβ). The ubiquitin-driven and PGK-driven open reading frames (ORFs) in this lentivirus backbone make the lentivirus suitable for expression of lentivirally delivered genes in most target cells given their ubiquitous expression.

We engineered mice to individually possess *INK4a/ARF*$^{fl/fl}$ or *PTEN*$^{fl/fl}$ mutations on pure C57BL/6 backgrounds, intercrossed them, and bred them to homozygosity at both alleles for the loxP mutations flanking these genes. These mutations permit selective deletion of *INK4a/ARF* and *PTEN* in target cells that express Cre. The underlying concept behind the model is to use lentivirus to transform target cells by simultaneously forcing PDGFβ oncogene overexpression and inducing Cre production required to delete the above-mentioned tumor suppressors. These collective mutation events lead to transformation of target cells (Figure 2-1A) such that they have potential to form tumors (Figure 2-1B).

2.2.2 Lenti-PDGFβ lentivirus drives gene deletion and PDGFβ overexpression

We assessed the function of the Lenti-PDGFβ lentivirus *in vitro*. To do so, we measured PDGFβ expression and Cre-mediated deletion of loxP-flanked genes in target cells by a variety of methods. We first tested Cre function using Cre-reporter line. To generate the Cre-reporter line, we transduced 3T3 cells with the pMSCV-loxP-dsRed-loxP-eGFP-Puro-WPRE retrovirus [142]. At baseline, these cells fluoresce red. Cre expression mediates excision of the loxP-flanked dsRed gene responsible for red fluorescence, and eGFP expression commences (Figure 2-1C). When the 3T3 Cre-reporter cells were untransduced by a Cre expressing lentivirus, they fluoresced red. In contrast, when transduced with Lenti-PDGFβ, they expressed GFP just 24 hours post-transduction (Figure 2-1D). When observed at later time points, RFP expression extinguished in target cells, and they only expressed GFP (data not shown).

Figure 2-1

A

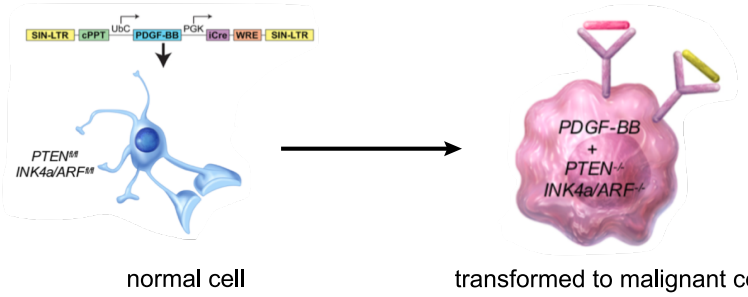

B

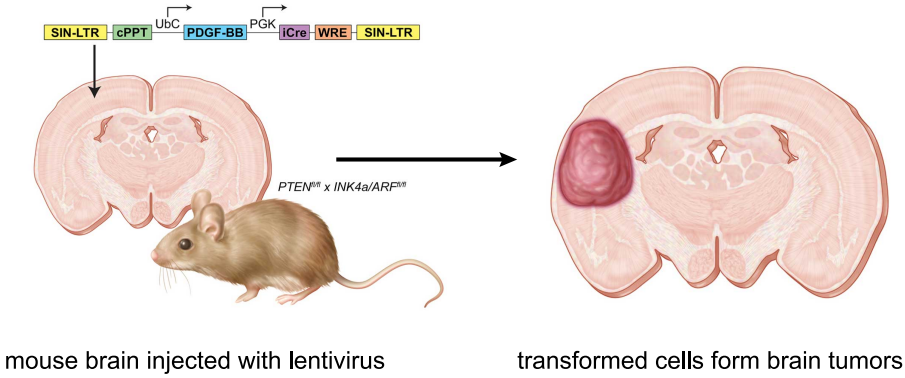

C

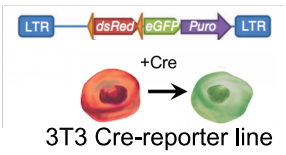

D

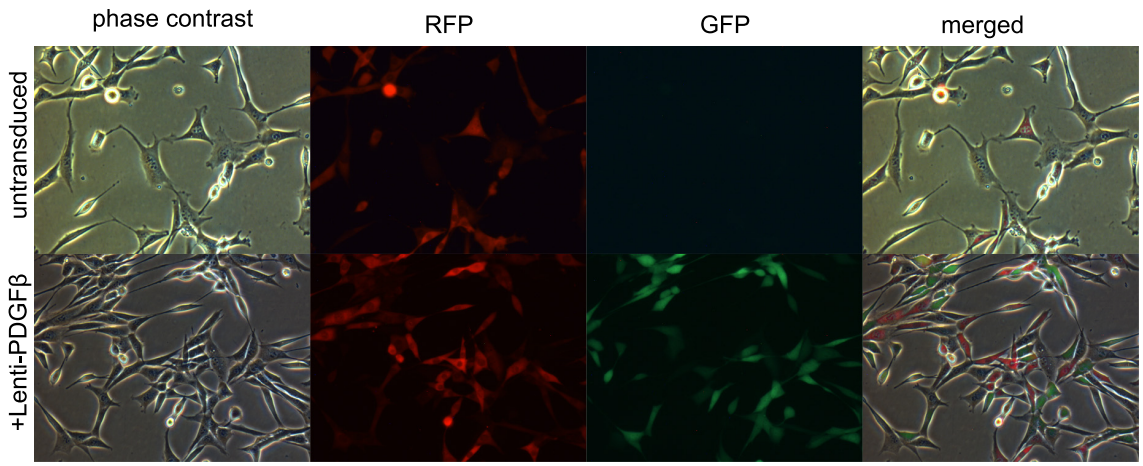

Figure 2-1. Autochthonous tumor model. A. Overview of lentiviral transforming event in autochthonous tumor model. B. Concept of tumor growth *in vivo*. C. 3T3 Cre-reporter line. D. Fluorescent microscopy of 3T3 Cre-reporter cells transduced with Lenti-PDGFβ.

To determine the ability of the lentiviral constructs to drive PDGFβ expression in target cells, we extracted mRNA from 3T3 Cre-reporter cells described above that had been untransduced with additional constructs, transduced with Lenti-Cre empty (carries Cre only), Lenti-PDGFβ, or Lenti-PDGFβ-OS, (which also expresses ovalbumin MHCI and MHCII antigens, as well as SIY antigen). Compared to untransduced or to Lenti-Cre empty transduced controls, Lenti-PDGFβ and Lenti-PDGFβ-OS transduced cells expressed high levels of murine *PDGFβ* mRNA (Figure 2-2A).

To determine the ability of the Lenti-PDGFβ lentivirus to drive deletion of loxP-flanked tumor suppressors in *INK4a/ARF*$^{fl/fl}$ x *PTEN*$^{fl/fl}$ target cells, we isolated astrocytes from this mouse strain and transduced them with lentivirus. We extracted their DNA and performed PCR to determine whether the *INK4a*/*ARF* genes had been deleted. Compared to wild-type tail or *INK4a/ARF*$^{fl/fl}$ x *PTEN*$^{fl/fl}$ tail DNA, *INK4a/ARF*$^{fl/fl}$ x *PTEN*$^{fl/fl}$ astrocytes that had been transduced with Lenti-PDGFβ harbored deletion of *INK4a/ARF* genes measured by PCR (Figure 2-2B). We performed a similar test of genetic deletion in murine embryonic fibroblasts (MEFs) that had been isolated from the founder *PTEN*$^{fl/fl}$ mouse line. Compared to untransduced *PTEN*$^{fl/fl}$-MEFs, those transduced by Lenti-PDGFβ lost expression of PTEN as measured by western blot (Figure 2-2C).

To determine the capacity of Lenti-PDGFβ to drive secretion of PDGF-BB from cells which carried the backbone lentiviral sequence, we transiently transfected 293Ts with Lenti-PDGFβ and measured PDGF-BB concentrations in the conditioned growth media, as well as in the total cell lysates. Compared to Lenti-Cre empty or untransfected 293Ts, those transfected by Lenti-PDGFβ or Lenti-PDGFβ-OS secreted high levels of PDGF-BB into the growth media at 24 and 48-hours post-transfection and expressed high levels of

intracellular PDGF-BB as well (Figure 2-2D). Collectively, these data demonstrate that the lentivirus possesses functional Cre, drives excision of loxP-flanked tumor suppressors in target cells, forces murine PDGFβ overexpression, and has the capacity to cause murine PDGF-BB secretion, all of which would be required to transform target cells *in vivo*.

2.2.3 Lenti-PDGFβ lentivirus drives brain tumor formation in vivo

Having assessed that Lenti-PDGFβ lentivirus functioned as hypothesized *in vitro*, we next assessed the ability of the lentivirus to cause brain tumor formation *in vivo*. We hypothesized that tumor formation would require both tumor suppressor deletion and oncogene and gain of function, and that tumor suppressor deletion alone would be insufficient. To test this hypothesis, we injected either highly concentrated Lenti-Cre empty lentivirus (expresses Cre only), or highly concentrated Lenti-PDGFβ lentivirus (expresses Cre and mPDGFβ) into the striata of *INK4a/ARF*$^{fl/fl}$ x *PTEN*$^{fl/fl}$ mice. Compared to Lenti-Cre empty lentivirus injected mice, those injected with Lenti-PDGFβ lentivirus formed malignant glioma brain tumors and had a median survival of 140 days. In contrast, 100 percent those with Lenti-Cre empty survived for the entire observation period (Figure 2-2E). Histology of the tumors revealed hallmarks of malignancy: anaplasia and mitotic figures, however, the tumors possessed histological features of gliosarcoma (Figure 2-2F). Out of nine tumors measured examined by histology, 8 were gliosarcomas and 1 was an oligodendroglioma. Gliosarcomas stained strongly for type III collagen and were negative for glial fibrillary acidic protein (GFAP), a marker of cells of astrocytic origin (data not shown).

Figure 2-2

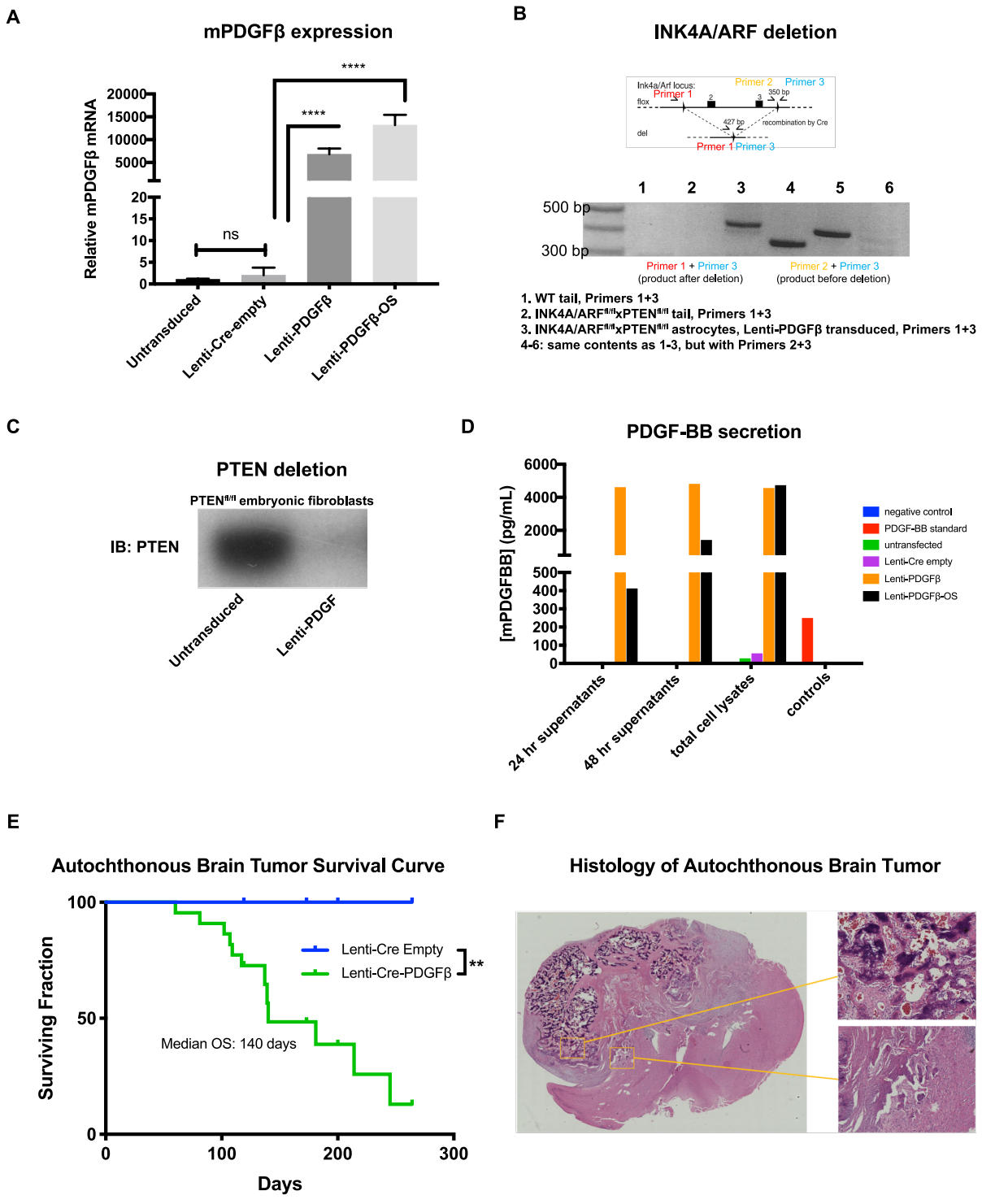

Figure 2-2. Lentivirus function and brain tumor induction in autochthonous tumor model. A. Murine PDGFβ mRNA expression in 3T3 Cre-reporter cells transduced with various lentivirus constructs. B. Genomic loss of *INK4a/ARF* or C. Loss of PTEN protein expression following transduction by Lenti-PDGF. D. Lentivirus-driven PDGF-BB secretion. E. Survival curve following intracranial lentiviral injection and subsequent brain tumor formation. F. Histology of autochthonous Lenti-PDGFβ-induced brain tumor.

Notably, several of the mice in each of the cohorts intracranially injected with Lenti-PDGFβ lentivirus also had neck masses, which appeared to harbor malignant cells after they were cultured ex-vivo. We also observed an interesting phenomenon in some of the mice that did not suffer brain tumors, particular to later cohorts: they became sick with ascites and died. When dissected, these mice did not have brain tumors, but notably appeared to have liver cirrhosis upon gross inspection. Collectively, the data show that while Lenti-PDGFβ could drive brain tumor formation, the histology was not that of glioblastoma multiforme, and instead had histologic characteristics of gliosarcoma.

Having determined that the Lenti-PDGFβ lentivirus led to gliosarcoma formation when injected into the striatum, we selected a different lentivirus backbone with different open reading frame promoters to selectively target glial cells. We chose three different lentiviruses to drive expression in different types of target cells, provided by the Washington University Hope Center. In these lentiviral backbones, ORF expression is driven by the GFAP promoter to target astrocytes and their progenitors, the myelin basic protein (MBP) promoter to target oligodendrocytes and their progenitors [143], or the CMV promoter to broadly target cells in throughout the white matter [143], including astrocytes and oligodendrocytes. We cloned Cre-P2A-mPDGFβ into each of these lentivirus backbones and verified their function *in vitro* as we had done before with the other lentiviral constructs. We determined that the three Cre-PDGFβ lentivirus constructs, driven by either MBP, GFAP, or CMV, could drive genomic deletion of *INK4a/ARF*, loss of PTEN protein expression, and mPDGFβ overexpression by qPCR. Having verified their function *in vitro*, we injected concentrated lentivirus into the brains of *INK4a/ARF*$^{fl/fl}$ X *PTEN*$^{fl/fl}$ mice with the assistance of the Hope Center. We also targeted a different region

of the brain—the subventricular zone, which has higher concentrations of neural stem cells (including astrocyte and oligodendrocyte progenitors) [144], which we envisioned would be more permissive to transformation and which has been targeted to efficiently generate glioblastoma in other GEMMs [135, 145-147]. We targeted the subventricular zone with four different lentivirus constructs: CMV-Cre empty, CMV-Cre-PDGFβ, GFAP-Cre-PDGFβ, and MBP-Cre-PDGFβ. We injected four mice per construct and monitored their health continuously. Notably, none of the mice developed brain tumors, but nearly all of them developed the same ascites as the mice injected with the Lenti-PDGFβ constructs in previous experiments. They also had cirrhotic appearing livers when dissected. This suggests that both types of lentivirus constructs used had peripheral effects.

2.3 Conclusion and Discussion

In summary, we have created a genetically engineered mouse model of malignant glioma that relies on both loss of function of tumor suppressors and gain of function of oncogenes to completely drive transformation. Notably, our model has features that make it more appropriate for immunologic study. First, the mice we used were both immunologically competent and inbred. To our knowledge, most genetically engineered mouse models of glioma use outbred mice. Secondly, to our knowledge our model is the first to use murine PDGFβ—models that report using PDGFβ as the oncogene to drive transformation have used human PDGFβ, to which the mouse immune system is not tolerant.

Although these features make this model more suitable for immunologic study and did lead to brain tumor formation in some instances, unfortunately the histology was not that of glioblastoma, and instead was that of gliosarcoma. Notably, gliosarcoma is one of the rare malignant tumors of the CNS that is known to metastasize extraneurally [148]. The

metastatic neck masses we observed in some of the mice are additional features beyond histology that suggest our model was that of gliosarcoma. The next and easiest logical step would be to use different oncogenes to drive tumor formation. EGFR is mutated in 57% of GBM, whereas PDGF signaling is overexpressed in 10% of GBMs [6]. Moreover, EGFRvIII, the most common EGFR modification, is highly expressed in 11% of GBMs, and expressed above background in 19% of GBMs [6]. Thus, EGFRvIII could be cloned into both the Lenti-LucOS backbone, as well as the MBP/GFAP/CMV promoter lentiviral backbones. Once its function was verified, this virus could be injected intracranially into mice in an attempt to develop a glioblastoma GEMM.

As an attempt to generate a tumor that had histologic characteristics of glioblastoma rather than gliosarcoma, we targeted specific cell types using lentivirus with ORFs driven by the GFAP and MBP promoters, which are specific to glial cells. Unfortunately, no tumors were observed following injection of any of these lentiviruses. When the mice died, they had ascites and appeared to have liver cirrhosis. The absence of tumor formation could be due to injecting lower titers of lentivirus, a different concentration method (we used the Hope Center for the second generation of lentiviruses, whereas we used the University of Iowa Viral Vector Core for the original Lenti-PDGFβ lentivirus constructs), or potentially insufficient expression of PDGFβ by the second-generation lentiviral backbones.

Notably, *PTEN*$^{fl/fl}$ mice have been used in models of steatohepatitis and hepatocellular carcinoma [149]. Given our observations of cirrhotic livers in multiple experiments, we may have inadvertently introduced the virus into systemic circulation, which could have been sequestered by the liver, wherein any Cre expression whatsoever would cause deletion

of tumor suppressors there, bringing about disruptive genetic changes that had potential to alter cell behavior and change the normal function and morphology of the liver.

In summary, we have generated a new GEMM of malignant glioma. We were able to induce successful tumor formation with the Lenti-PDGFβ lentivirus, but not with the Hope Center-originating CMV/GFAP/MBP promoter-driven lentiviruses which we used in an effort generate tumors with GBM histology. The model will require additional work to become a fully competent GEMM of GBM.

CHAPTER THREE

Ex-vivo derived models of recurrent hypermutated glioma

3.1 Introduction

The standard treatment for glioblastoma is maximal safe resection, followed by radiotherapy and temozolomide [2], the latter of which unfortunately is only effective in the roughly one-third to one-half of patients whose tumors express low levels of the DNA repair protein methylguanine methyltransferase (MGMT) [5, 6, 150, 151]. MGMT ordinarily functions to repair methylation damage to DNA, and as such acts to immediately reverse temozolomide-induced DNA damage under normal conditions [152]. In GBM, low MGMT expression is often due to *MGMT* promoter methylation, which silences *MGMT* gene transcription. GBM invariably recurs, and of recurrent cases, approximately 20-30% are hypermutated [153, 154]. GBM itself usually presents as a low to modest mutational burden tumor and harbors a median of 2.2 coding mutations per megabase, which amounts to fewer than 100 total mutations across the entire tumor [6]. We hypothesize that additional mutations, which might ordinarily be a marker of poor prognosis, could serve as additional targets for the immune system.

GBM is not responsive to PD-1/PD-L1 checkpoint blockade under normal circumstances. This was determined by two phase III clinical trials which demonstrated that GBM patients with tumors that had either unmethylated (Checkmate 498 Trial, NCT02617589) or methylated *MGMT* promoters (Checkmate 548 Trial, NCT02667587) experienced no survival benefit from adjuvant PD-1/PD-L1 treatment [111]. However, there are certain

cases in which checkpoint blockade could potentially be an effective tool to treat GBM, distinct from the neoadjuvant setting, which demonstrated survival benefit in a phase II clinical trial as discussed previously [112]. Although the relationship between mutational burden and responsiveness to checkpoint blockade therapy is highly complex, there are several promising case reports in which patients with patients with hypermutated GBM experienced demonstrable benefit from checkpoint blockade therapy [109, 110].

Genomic hypermutation in GBM is often conferred by mutations or deficiencies in the mismatch repair pathway [155, 156]. Ordinarily, MGMT is one of the proteins responsible for repairing the DNA damage caused by temozolomide [152], which exerts its cytotoxic activity by methylating the guanine bases in DNA to cause mispairings and subsequent DNA damage. Because the action of temozolomide would be immediately reversed by MGMT under normal conditions, temozolomide treatment requires low tumor MGMT expression to be an effective therapy [5, 6, 150, 151].

In addition to low MGMT expression, there is a second requirement for temozolomide sensitivity: intact mismatch repair machinery [152]. Ordinarily, when temozolomide methylates the guanine bases in DNA, MGMT reverses this damage. If this first DNA repair step fails (presumably due to low MGMT expression), the methylated guanine is mis-paired with thymine instead of cytosine during replication. When this happens, the mutS homolog 2/mutS homolog 6 (MSH2/MSH6) heterodimer complex recognizes the mis-paired guanine-thymine pairing, and the MSH2/MSH6 complex recruits the additional components of the mismatch repair pathway, mutL homolog 1 (MLH1) and post-meiotic segregation 1 homolog 2, mismatch repair system component (PMS2), to orchestrate removal of the mis-paired thymine and replacement by cytosine, repairing the damage

[157]. When this step happens without reversing the original methylation of guanine that resulted from temozolomide exposure (a function which would normally be performed by MGMT), the cell again mis-pairs methyl-guanine with thymine instead of its correct pair, cytosine. A repeated repair attempt follows, and fails, and the cell can become trapped in a futile cycle of repeated and failed repair attempts because it can't repair the original damage caused by temozolomide. This can lead to cell cycle arrest and temozolomide induced cell death [152, 157].

In contrast to this scenario, when any one of the mismatch repair proteins is defective or missing (often MSH6 in GBM), the cell cannot detect the temozolomide-caused DNA damage, proceeds forward through cell division, and incorporates the mispairings into the daughter cells' genomes. These temozolomide-induced mutations accumulate over successive cell divisions, and lead to the state of hypermutation within the tumor [155, 156]. In addition to hypermutation, a second consequence of defective mismatch repair is loss of sensitivity to temozolomide—in this setting, DNA damage, no longer detected by the cell, does not activate the mismatch repair machinery to attempt the repair the mispairings, which would normally result in restraining cell division and causing cell death [158]. Instead, it's as if cells carry on dividing as though they have no damage to their DNA, because they cannot sense the presence of mispairings without functional MSH6.

The standard of care for all GBM includes temozolomide treatment. This is because the correlation between *MGMT* promoter methylation and MGMT expression is imperfect—some tumors with unmethylated *MGMT* promoters suggestive of high MGMT expression might still actually have low MGMT expression for other unknown reasons independent of *MGMT* promoter methylation status. Therefore, because of the dearth of available

treatment options, and possibility that temozolomide might still provide clinical benefit to patients with tumors that have unmethylated *MGMT* promoters, temozolomide is still administered to every GBM patient as part of the standard treatment [152]. This alkylating treatment which damages DNA thus leads to 20-30% of cases recurring as hypermutated tumors for the reasons described above [153, 154].

The relationship between mutational burden and responsiveness to checkpoint blockade is not entirely straightforward. Indeed, a landmark phase II trial by Le and colleagues demonstrated that patients with mismatch repair-deficient colorectal cancer, which has a higher mutational burden than most tumors, had more favorable survival when treated with anti PD-1 therapy when compared to the mismatch repair-proficient patient cohort [159]. In a follow up second landmark study, Le and colleagues extended their findings to other tumor types and demonstrated that mismatch repair-deficiency (which would result in higher mutational burden than the same tumor with intact mismatch repair machinery) increased likelihood of response to and PD-1 therapy across twelve solid tumor types [160].

Additionally, GBM patients with hypermutated tumors have experienced some benefit after checkpoint blockade treatment in isolated cases. One such documented case was a patient with a germline DNA polymerase epsilon (POLε) mutation (L424V) which conferred loss of function of the proofreading exonuclease region in POLε, which replicates and proofreads the leading strand of DNA. This patient presented with multifocal brain tumors and had a germline POLε L424V mutation. His tumors harbored roughly 10000 non-synonymous mutations. He was treated with checkpoint blockade and experienced a robust T cell infiltrate into the tumor post-treatment as well as an objective radiographic response [109]. The second report of benefit from checkpoint blockade in the

setting of GBM occurred in a sibling pair who presented with pediatric recurrent hypermutated GBM (over 20000 mutations in each tumor) and biallelic mutations in the mismatch repair gene *PMS2*. They were treated with anti PD-1 therapy and experienced demonstrable benefit as well, well outliving the median survival of children with their condition [110].

Preclinical models have also demonstrated increased responsiveness to checkpoint blockade as a function of mutational burden. In a clever study, Germano and colleagues recently reported that deletion of the mismatch repair protein MLH1 followed by temozolomide treatment conferred hypermutation, increased abundance of neoantigens, and conferred checkpoint sensitivity in the in the normally checkpoint-insensitive CT26 colorectal cancer preclinical mouse model [161]. Although this finding is promising, this study would be unrealistic for CNS tumors—the parental CT26 line contained 152 mutations per megabase, whereas basally, GBM presents with 1 to 4 mutations per megabase [6]. An appropriate model should account for the low mutational burden of the primary tumor.

Moreover, although these findings might give reason for hope regarding the potential for checkpoint blockade to effectively treat hypermutated GBM, there is reason for some doubt that this treatment strategy will perform as a silver bullet. In a recent pivotal study, Wolf and colleagues reported that patients with melanoma that harbored greater intratumoral heterogeneity (defined as number of subclones clones comprising the tumor) had worse survival compared to patients with melanoma that harbored less intratumoral heterogeneity [95]. They devised a clever mechanism to increase the intratumoral heterogeneity in a preclinical model of melanoma—they subjected the B2905 mouse

melanoma cell line to UVB irradiation to increase both mutational burden and intratumoral heterogeneity. The UVB-irradiated cells had more subclones by their analysis and formed more aggressive tumors than un-irradiated less heterogenous controls. Notably, single cell clones isolated from the UVB-irradiated B2905 cell line grew less aggressively or were rejected altogether when transplanted into mice compared to either the un-irradiated tumors or the UVB-irradiated tumors. Interestingly, they determined that growth differences were eliminated between the parental line, the UVB-irradiated line, and single-cells clones derived from the UVB-irradiated line when these lines were transplanted into immune-deficient NSG mice instead of wild-type mice used for prior experiments. This demonstrated that the growth differences were immune-mediated. They also determined that responsiveness to checkpoint blockade could be predicted in patient cohorts by overlaying the intratumoral heterogeneity score over the response data: patients with high intratumoral heterogeneity were less likely to respond to checkpoint blockade, and patients with low intratumor heterogeneity were more likely to respond to checkpoint blockade.

Unfortunately, most patients with GBM have remarkably heterogeneous tumors [92, 93, 162]. Mutations are often not shared between different tumor regions. For instance, EGFRvIII, a common oncogene within GBM, has been shown to be expressed only by a fraction of the tumor cells within EGFRvIII-positive GBM [93, 94]. Additionally, there is evidence that patients with hypermutated GBM also harbor heterogeneous tumors. This was demonstrated by a landmark study conducted by our lab in collaboration with the Malachi Griffith lab, in which MD/PhD student Max Schaettler and PhD student Megan Richters sequenced different tumor regions of GBM tumors and compared the mutations between

different tumor regions originating from the same tumor. They found that similar to GBM tumors with a normal mutational burden across all regions, high mutational burden GBM tumors harbored mostly private mutations in the disparate tumor regions that were not shared with other regions originating from the same tumor [162].

However, given the isolated case reports demonstrating success of checkpoint blockade in treating hypermutated GBM, as well as the positive correlation between mutational burden and checkpoint blockade responsiveness in other tumor types, we strongly felt that studying the relationship between tumor mutational burden and responsiveness to checkpoint blockade in GBM using preclinical models was warranted. We set out to develop an isogenic preclinical model of GBM to investigate the relationship between mutational burden, intratumoral heterogeneity, and checkpoint blockade sensitivity in malignant glioma so that the 20%-30% of patients with hypermutated GBM might be afforded more effective treatment options.

To generate a model of recurrent, hypermutated GBM, we isolated astrocytes from the *INK4a/ARF*$^{-/-}$ x *PTEN*$^{-/-}$ mice and transformed them with Lenti-PDGFβ lentivirus to both delete *INK4a/ARF* and *PTEN* and to overexpress murine PDGFβ. We next used CRISPR to bi-allelically delete *MSH6*, a commonly lost or mutated mismatch repair gene in hypermutated GBM [155]. We treated these cell lines with temozolomide to simulate the standard therapy and induce increased tumor mutational burden in the MSH6$^{-/-}$ parental transformed Lenti-PDGFβ-*INK4a/ARF*$^{-/-}$ x *PTEN*$^{-/-}$ astrocyte line. We additionally modeled DNA polymerase epsilon mutations as drivers of hypermutation.

3.2 Results

3.2.1 Lenti-PDGFβ transforms INK4a/ARFfl/fl x PTENfl/fl mouse astrocytes

Before developing our isogenic model of hypermutation, we first set out to develop a parental isogenic transformed astrocyte-derived malignant glioma cell line with a low baseline mutational burden. We utilized both the mice and the lentiviral constructs from our autochthonous glioma GEMM. We began by isolating astrocytes from *INK4a/ARF*$^{fl/fl}$ x *PTEN*$^{fl/fl}$ P0 pups, grouped them into male or female cohorts, and transduced them with Cre +/- mPDGFβ expressing lentivirus constructs (Figure 3-1A). We generated three different *INK4a/ARF*$^{-/-}$ x *PTEN*$^{-/-}$ astrocyte lines: Lenti-Cre empty, to solely delete the loxP-flanked tumor suppressors, Lenti-PDGFβ to do the same plus additionally enforce murine PDGFβ overexpression, or Lenti-PDGFβ-OS to do the aforementioned plus additionally overexpress the OS cassette, which contains the MHCI/H-2K^{b}-restricted antigens SIINFEKL (from ovalbumin) and SIY, as well as the MHCII/I-A^{d} antigen from ovalbumin. We had previously verified that the lentivirus constructs expressed functional Cre and drove PDGFβ overexpression measured by qPCR and protein expression (see Chapter 2). To determine if the transformed *INK4a/ARF*$^{-/-}$ x *PTEN*$^{-/-}$ astrocytes retained characteristics of astrocytes, we performed immunofluorescence for GFAP, a commonly used astrocyte marker. Compared to either 3T3 mouse fibroblasts, or the GL261 mouse glioma line, *INK4a/ARF*$^{-/-}$ x *PTEN*$^{-/-}$ astrocytes that had been transduced with Lenti-PDGFβ lentivirus expressed GFAP by immunofluorescence (Figure 3-1B), which suggests we both successfully isolated astrocytes, and that they retained characteristics of their astrocyte lineage following tumor suppressor deletion and oncogene overexpression.

To determine if the transduced astrocytes were transformed into malignant cells, and whether they possessed the intrinsic ability to spontaneously generate an immune response, we transplanted them subcutaneously into flanks of immune competent wild-type C57BL/6 mice. We tested three different *INK4a/ARF*$^{-/-}$ x *PTEN*$^{-/-}$ astrocyte lines: first, a negative control which lacked oncogene overexpression (and was presumably untransformed), which was transduced with Lenti-Cre empty. Second: Lenti-PDGFβ-transduced, and third, Lenti-PDGFβ-OS-transduced. After transplantation, we monitored for tumor growth. As expected, the Lenti-Cre empty line did not form tumors. The Lenti-PDGFβ-OS ovalbumin/SIY antigen-expressing line formed small tumors, which soon after regressed. The Lenti-PDGFβ line grew progressively (Figure 3-1C). Collectively, these data show that to be transformed into malignant cells, *INK4a/ARF*$^{fl/fl}$ *x PTEN*$^{fl/fl}$ astrocytes required both (a) deletion of tumor suppressors and (b) oncogene overexpression, and additionally, that expression of the immunogenic OS cassette was sufficient to drive tumor rejection.

We next examined for evidence of a CD8^{+} T cell response in mice that had been transplanted with the astrocyte lines. With lines that formed tumors and grew progressively, we carried the growth curve until a later timepoint to fully measure tumor growth potential, and thus we did not include the progressively growing Lenti-PDGFβ cohort in this experiment. We isolated the lymph nodes adjacent to the injection site as well as the spleens from mice that had been transplanted with either the Lenti-Cre empty line (which never formed tumors), or the Lenti-PDGFβ-OS line, which formed small tumors that regressed. We performed an interferon-γ release assay (ELISPOT) on CD8^{+} T cells isolated from either the draining lymph node or the spleen.

Figure 3-1

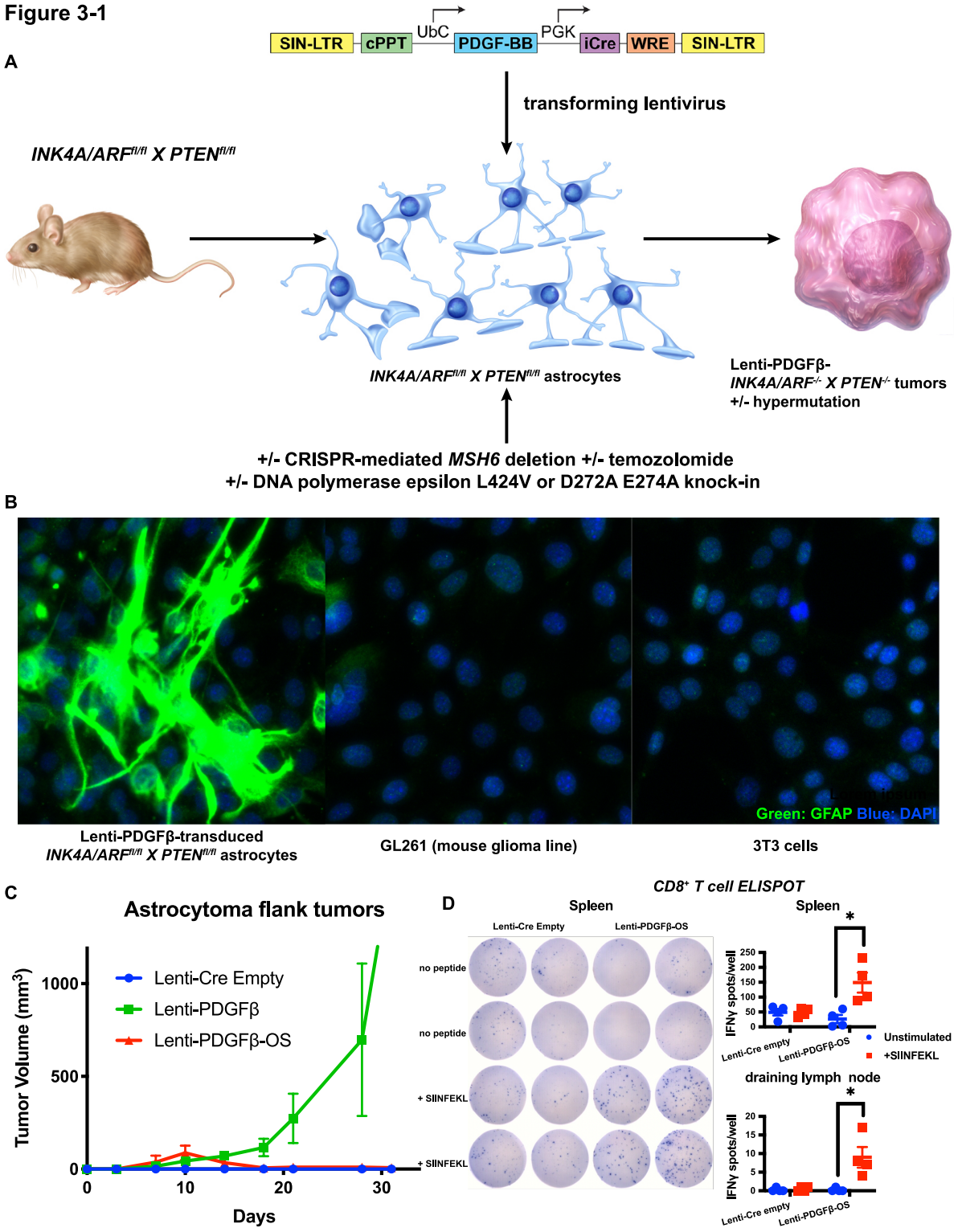

Figure 3-1. Astrocytes are transformed and conditionally immunogenic. A. Schematic of *INK4a/ARF*$^{fl/fl}$ x *PTEN*$^{fl/fl}$ astrocyte isolation and experimental design. B. Immunofluorescence of GFAP and DAPI in transformed astrocytes, GL261 glioma cells, and 3T3 mouse fibroblast cells. C. Growth curves of flank tumors from transplantation of transformed astrocytes. D. ELISPOT IFNγ release assay of CD8$^+$ T cells isolated from spleens or dLNs of Lenti-Cre Empty astrocyte line injected mice, or Lenti-PDGFβ-OS astrocyte line injected mice that had rejected tumors. Statistics by student's t-test. * p <0.05.

In contrast to both splenic and lymph node $CD8^+$ T cells which were isolated from mice subcutaneously transplanted with Lenti-Cre astrocytes, $CD8^+$ T cells isolated from the same organs of mice transplanted with Lenti-PDGFβ-OS astrocytes released IFNγ above background in response to stimulation with SIINFEKL peptide and naïve antigen presenting cells (Figure 3-1D).

Collectively, these data show that when transformed *INK4a/ARF*$^{-/-}$ x *PTEN*$^{-/-}$ astrocytes expressed the immunogenic antigens carried by the OS cassette, that mice transplanted with such astrocytes spontaneously generate a $CD8^+$ T cell response against those antigens.

3.2.2 CRISPR disrupts MSH6 gene to confer loss of MSH6 protein expression

To generate hypermutated tumors from Lenti-PDGFβ *INK4a/ARF*$^{-/-}$ x *PTEN*$^{-/-}$ transformed astrocytes, we targeted two different pathways: first, MSH6 of the mismatch repair pathway, and second, the exonuclease region of DNA polymerase epsilon, which proofreads as DNA polymerase epsilon performs replication of the leading strand. To target *MSH6*, we used CRISPR to disrupt the first exon of *MSH6* in Lenti-PDGFβ-transduced *INK4a/ARF*$^{-/-}$ x *PTEN*$^{-/-}$ astrocytes. We isolated single cell clones, and used Sanger sequencing combined with the TIDE computer program to deconvolute the Sanger sequence and assess for biallelic *MSH6* disruptions [163]. We screened single cell clones that grew well in culture and selected three clones which were predicted by TIDE to have biallelic disruption of *MSH6*. We performed a western blot for MSH6 and determined that compared to 293T cells which overexpressed murine MSH6, or to Cas9-empty transfected transformed astrocytes, that the three single-cell clones targeted with Cas9-*MSH6* did not express detectable protein levels of MSH6 (Figure 3-2A).

3.2.3 Lenti-PDGFβ transformed astrocytes resist temozolomide at baseline

We hypothesized that deletion of *MSH6* from the transformed astrocytes would confer resistance to temozolomide, which has been well documented in GBM [158]. We utilized a propidium iodide assay to assess cell cycle, and from the information gleaned, to identify cell populations which harbored temozolomide resistance. Cell cycle can be quantitatively analyzed by propidium iodide [164], which intercalates into DNA and fluoresces [165]. Temozolomide treatment methylates the O_6 atom on guanine bases, which causes the now-methylated guanine to be mis-paired with thiamine instead of its normal partner, cytosine [166]. In attempting to reverse this mis-pairing, cells upregulate mismatch repair machinery, and in doing so, can be trapped in a futile state of repair if MGMT is not present to repair and reverse the guanine methylation originally caused by temozolomide [166]. The result is that many cells are unable to complete cell division following their G2 phase. This leads to greater numbers of cells trapped in the 4N (and even 8N) state as their DNA continues to double without successful completion of cell division. This is quantifiable by flow cytometry as 4N and 8N cells will uptake either twice as much or four times as much PI because of the increased amount of DNA in each cell, and as a result, will fluoresce more brightly in a quantitatively detectable manner [164].

We treated GL261 murine glioma cells with escalating doses of temozolomide and determined that cells treated with increased levels of temozolomide harbored more cells in the 4N and 8N state in a dose-dependent manner (Figure 3-2B). In contrast, Lenti-PDGFβ *INK4a/ARF*$^{-/-}$ x *PTEN*$^{-/-}$ transformed astrocytes treated with temozolomide did not have more cells attributed to the 4N or 8N peaks (Figure 3-2C). Collectively, these data show that while GL261 murine glioma cells demonstrated sensitivity to temozolomide,

that the transformed astrocytes we generated were temozolomide resistant, despite having intact *MSH6*, which should permit temozolomide sensitivity when functional.

3.2.4 MGMT expression confers temozolomide resistance in transformed astrocytes

Temozolomide resistance is conferred by a variety of factors, including high MGMT expression in patient tumors [152]. When expressed by cells, MGMT reverses the guanine methylation damage caused by temozolomide [6]. Thus, we hypothesized that the transformed astrocytes might express high levels of MGMT at baseline, and hence would be resistant to temozolomide treatment. We performed a western blot on parental *MSH6*-WT transformed astrocytes, as well as on the three *MSH6*$^{-/-}$ clones, along with GL261, which we hypothesized would have low MGMT expression due to baseline temozolomide sensitivity. All transformed astrocytes, including the MSH6$^{-/-}$ clones, expressed detectable levels of MGMT (Figure 3-2D). In contrast, GL261 did not express detectable levels MGMT (Figure 3-2D). Notably, the three *MSH6*$^{-/-}$ clones expressed lower levels of MGMT than the parental MSH6-WT transformed astrocytes. Collectively, these data indicate MGMT expression as a potential mechanism that the transformed astrocytes might employ to resist temozolomide treatment as measured by propidium iodide nuclear analysis.

MGMT expression can be inhibited by the small molecule O_6 benzyl guanine (O_6BG) [167]. Because of this, treatment of cell lines with O_6BG can sensitize them to temozolomide. We subjected the *MSH6*-WT as well as the *MSH6*$^{-/-}$ astrocytes to dual treatment with both temozolomide and O_6BG and performed the propidium iodide nuclear analysis assay. The results were indeterminate and did not allow us to confirm that *MSH6* deletion conferred temozolomide resistance with proper MGMT inhibition. Thus, we performed an

orthogonal growth curve experiment to assess temozolomide sensitivity. From previous experiments in our lab, we had determined that treatment of GL261 glioma cells with 500μM temozolomide completely arrested growth of GL261 *in vitro*. We subjected the transformed astrocytes to the same concentration of temozolomide, with or without O_6BG, along with O_6BG alone. At baseline, either temozolomide or O_6BG treatments alone slightly restrained growth of *MSH6*-WT transformed astrocytes. However, both inhibitors combined restrained growth considerably in this cell line, leading to a 6.25-fold decrease in cell count at the end of the experiment (Figure 3-2E). In contrast, the three *MSH6*$^{-/-}$ clones displayed varying levels of decreased temozolomide sensitivity. Clone 1 was slightly sensitive to temozolomide, whereas clones 2 and 3 were not (Figure 3-2E). Treatment with O_6BG alone restrained growth slightly in clones 1 and 3. When treated with both temozolomide and O_6BG, all 3 clones grew more slowly. However, in contrast to the parental *MSH6*-WT line, which was growth-restricted over 6-fold from O_6BG + temozolomide treatment, the three *MSH6*$^{-/-}$ lines were growth-restricted by 2 to 4-fold from O_6BG + temozolomide treatment (Figure 3-2E). Collectively, these data show that *MSH6* deletion confers some amount of resistance to temozolomide/O_6BG-indued growth inhibition when compared to their MSH6-WT counterpart but suggests that high concentrations of temozolomide and MGMT inhibition can still somewhat restrain growth even in MSH6-deficient cells.

Given our previous findings that the Lenti-PDGFβ *INK4a/ARF*$^{-/-}$ x *PTEN*$^{-/-}$ transformed astrocytes expressed GFAP and formed tumors when transplanted into the flanks of wild-type mice, we hypothesized that they would also form brain tumors. When transplanted into the brain, the only tumors that resulted were extracranial, subcutaneous masses

outside of the skull (Figure 3-2F), with no tumor within the brain parenchyma. This observation suggests that the transformed cells, which originated from astrocytes, harbored growth traits that engendered them with tropism for subcutaneous, rather than intracranial anatomic locations. A possible explanation for the possibility of tumors forming extracranially despite being transplanted intracranially is that in addition to harboring tropism for subcutaneous regions, some malignant cells might have refluxed from the stab wound or were left behind by the needle upon withdrawal, leaving malignant cells outside of the skull to form tumors in subcutaneous spaces.

3.2.5 MSH6 deletion or DNA polymerase epsilon disruption confers hypermutation

Although the Lenti-PDGFβ *INK4a/ARF*$^{-/-}$ x *PTEN*$^{-/-}$ transformed astrocytes did not form intracranial tumors, and instead formed extracranial subcutaneous tumors, we still subjected them to conditions in an attempt to induce a hypermutated state and performed genomic analysis of the cells as a proof of concept.

To induce a hypermutated state in the *MSH6*$^{-/-}$*-INK4a/ARF*$^{-/-}$ x *PTEN*$^{-/-}$ transformed astrocytes, we treated them, plus their *MSH6*-WT counterparts with either vehicle or O_6BG + temozolomide for two months with continuous passaging. This treatment was to mimic what happens in the GBM patients who recur with hypermutated GBM after temozolomide treatment. During treatment, growth of the MSH6$^{-/-}$ transformed astrocytes as well as their wild-type counter parts completely arrested in the extended presence O_6BG + temozolomide. For one additional month, treatments were removed, and the cells were allowed to recover until they grew continuously and once again needed regular passaging. We hypothesized that the *MSH6*$^{-/-}$ astrocyte lines would harbor a hypermutated state, but only when treated with O_6BG and temozolomide. We extracted

DNA and RNA and performed whole exome sequencing. In addition to the exome sequencing data, we input the RNA-expression and variant calls into the pVAC-seq algorithm to assess for neoantigen burden [168].

We also generated DNA polymerase epsilon mutants with the assistance of the Genomic Engineering and iPSC Center (GEiC) at Washington University. We modeled a mutation after a GBM patient with a germline DNA polymerase epsilon (*POLε*) L424V mutation whose tumor was hypermutated. This particular patient was treated by Drs. Dunn and Johanns with checkpoint blockade, which conferred objective radiographic response [109]. Additionally, there was histologic evidence of increased numbers of $CD4^+$ and $CD8^+$ T cells infiltrating the tumor following treatment with pembrolizumab [109]. The patient's *POLε L424V* mutation occurred in DNA polymerase epsilon's proofreading exonuclease region, which caused this patient's primary tumor to have over 10000 mutations. This mutation is also associated with a high penetrance of colorectal cancer is families who carry the mutation [169]. We generated a second mutant: *POLε D272A E274A*, which has been used before to generate spontaneous tumors, as well as to cause defects in DNA proofreading in mice with the germline mutation [170]. We hypothesized that in contrast to the *MSH6*$^{-/-}$ mutants, the *POLε* mutants would become hypermutated simply through the act of cell division and continuous passaging, and that they would not require additional treatment from temozolomide or another such agent to cause DNA damage, in contrast to the *MSH6*$^{-/-}$ mutants. After the GEiC had provided single cell clones that were homozygous for either *POLε L424V* or *POLε D272A E274A*, we extracted DNA and RNA from low-passage cells, continuously passaged these cell lines for two months and then extracted DNA and RNA from high-passage cells for comparison.

Using the exome sequencing data, we generated a list of variants (total as well as non-synonymous) and used the pVAC-seq algorithm to identify potential neoantigens in both the *POLε* and *MSH6*$^{-/-}$ mutants. We determined that high passage polymerase epsilon mutants harbored more total mutations, more non-synonymous mutations, and more predicted neoantigens than parental transformed astrocytes (which were also continuously passaged), or the matched low passage *POLε* mutants (Figure 3-2G, 3-2H). Furthermore, *MSH6*$^{-/-}$ mutants which were treated with O_6BG + temozolomide harbored more total mutations, more non-synonymous mutations, and more predicted neoantigens than the untreated *MSH6*$^{-/-}$ mutants, or their *MSH6*-WT O_6BG + temozolomide-treated counter parts (Figure 3-2G, 3-2H). Notably, the *MSH6*$^{-/-}$ untreated mutants harbored considerably more mutations and non-synonymous variants than either the treated or untreated *MSH6*-WT counterparts, and more predicted neoantigens than any of the cell lines analyzed (Figure 3-2G, 3-2H). We had hypothesized that MSH6 would not be required to maintain DNA fidelity during normal cell culture passaging in the absence of O_6BG + temozolomide induced DNA damage, which stood in contrast to our findings.

Figure 3-2

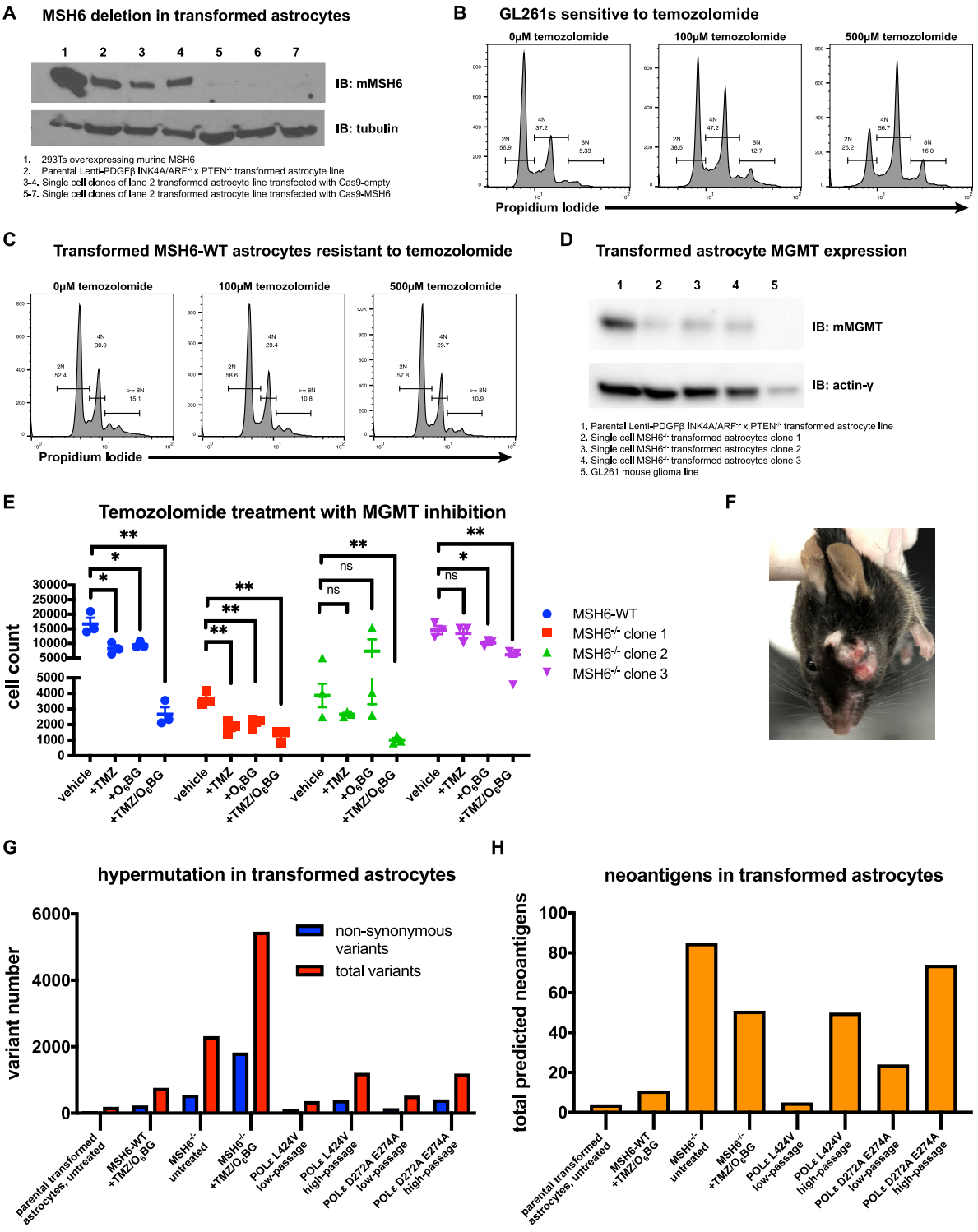

Figure 3-2. MSH6/POLε disruption leads to hypermutation. A. MSH6-deletion western blot. B and C. GL261 or transformed astrocytes sensitivity/resistance to temozolomide, measured by cell-cycle PI assay. D. MGMT western blot in various cell lines. E. Temozolomide/O_6BG growth arrest in transformed astrocytes as a function of MSH6 status. F. Extracranial tumor formation following intracranial astrocyte injection. G and H. Tumor mutational burden or predicted neoantigens in transformed astrocytes subject to various genetic permutations, treatments, and passage durations. Statistics by student's t-test. *p <.05, **p<.01.

3.3 Conclusion and Discussion

To generate an isogenic model of recurrent, hypermutated GBM, we isolated astrocytes from C57BL/6 *INK4a/ARF*$^{fl/fl}$ *x PTEN*$^{fl/fl}$ P0 pups. We transduced them with Cre/mPDGFβ expressing lentivirus and validated that they retained astrocyte characteristics, were transformed into malignant cells, and possessed the intrinsic ability to provoke an immune response. We demonstrated evidence of this immune response by observing growth and subsequent regression of OS-bearing tumors, as well as by isolating SIINFEKL-specific $CD8^+$ T cells from the spleens and draining lymph nodes of mice that had been challenged with OS-bearing tumors.

We disrupted *MSH6* and generated DNA polymerase epsilon mutants to induce a state of hypermutation in the transformed astrocytes. We demonstrated that *MSH6* disruption conferred additional resistance to temozolomide, but we found that the transformed astrocytes were temozolomide resistant at baseline, likely due to MGMT expression. This stood in contrast to the GL261 murine glioma line, which was temozolomide sensitive and did not express MGMT at baseline. When we inhibited MGMT in the transformed astrocytes by treating them with O_6 benzylguanine, they became sensitive to temozolomide treatment as assessed by growth curves. Furthermore, O_6BG + temozolomide treatment induced a state of hypermutation in the transformed astrocytes, as did continuous passaging (without temozolomide treatment) in the *POLε* mutants. The hypermutated cell lines harbored more mutations, more non-synonymous mutations, and had more predicted neoantigens than the control cell lines, which were untreated *MSH6*-WT or *POLε*-WT cells. Collectively, these data indicate that we successfully modeled

particular aspects of recurrent-hypermutated GBM, including temozolomide-induced hypermutation after *MSH6* disruption.

Although the *MSH6*$^{-/-}$ mutants harbored more mutations following treatment with temozolomide and the MGMT inhibitor O_6 benzylguanine, it was notable that even the treatment-naïve *MSH6*$^{-/-}$ mutants harbored more mutations than both the high-passage and low passage *POLε* mutants. We had originally hypothesized that the activity of the mismatch repair pathway would be low at baseline due to the absence of a DNA-damaging agent. However, our data suggest that normal passaging of our cell lines requires intact mismatch repair machinery to maintain genome fidelity. MSH6 is canonically understood to be part of the mismatch repair pathway and required to detect and correct mispairings between DNA bases, which would ordinarily be caused by a DNA-damaging agent. Our data suggest that in our particular case normal passaging without temozolomide and O_6 benzylguanine treatment was sufficient to cause the mispairings that mismatch repair machinery would ordinarily correct.

Although we generated an isogenic transformed astrocyte line and successfully induced hypermutation in the cells by multiple approaches, unfortunately the transformed cells did not appear to have tropism for the brain parenchyma when transplanted there. They instead grew in extracranial subcutaneous regions, even after intracranial transplantation. We believe this resulted from a combination of subcutaneous tropism and either reflux of malignant cells outside the burr hole in the skull or deposition of malignant cells as we withdrew the needle following transplantation of tumor cells into the brain parenchyma. While this same process likely happens during the transplantation of other established glioma cell lines into the mouse brain, the tropism of those malignant cells is for brain

parenchyma, which makes their growth more favorable in the brain. This permits brain tumors, rather than subcutaneous tumors, to form.

We transformed astrocytes and disrupted either the mismatch repair pathway or the DNA proofreading machinery and identified that either mutation was sufficient to induce hypermutation; however, our model is limited in that transplantation of transformed astrocytes into the brain did not result in brain tumor formation. Further work is needed to address whether using different oncogenes such as EGFRvIII would be sufficient to confer brain-specific tropism upon the transformed astrocytes. Alternatively, other tumor suppressors could be targeted. Additionally, other cell types could be used as the originating cell for the tumor model, such as neural stem cells, which we have begun isolating and transforming. Nevertheless, once we do identify factors that confer our model with brain-tumor forming capacity, we can correctly address the original hypothesis that higher tumor mutational burden leads to greater immunogenicity and higher likelihood of response to checkpoint blockade in the brain. We can also assess heterogeneity of the tumors and determine whether greater heterogeneity would portend for lower immunogenicity, as Wolf and colleagues identified in the B2905 melanoma model [95].

CHAPTER FOUR

cDC1 are required for CNS antitumor immunity

4.1 Introduction

Numerous studies have established that the conventional dendritic cell 1 subset (cDC1) is essential for antitumor immunity across a range of types [20-23, 27, 28, 30, 31], however their role in the CNS remains undefined. The lack of studies defining the role of cDC1 in CNS antitumor immunity could be for several reasons, among them that cDC1 (as well as other dendritic cell subsets) are absent in the steady state brain parenchyma [49], or that the CNS lacks conventional lymphatics [171] which would presumably be required for cDC to traffic from the periphery (or brain in this case) to a lymph node to prime a T cell response. In addition to the ostensible lack of cDC infiltrating the steady state brain and lack of conventional lymphatics, glioblastoma is associated with a range of immunologic defects, including GBM-induced lymphopenia [71, 72], a multitude of immunosuppressive factors secreted by the tumor itself or by infiltrating immune cells [77, 80-82, 172, 173], overexpression of checkpoint molecules such as PD-L1 [86, 87, 174], an immunosuppressive microenvironment with abundant tumor associated MDSCs [89], as well as high levels of circulating levels of MDSCs compared to healthy controls [90]. The combination of these immunosuppressive elements associated with GBM have led many to describe GBM as an immunologically “cold” tumor. The premise of GBM being an “immunologically cold” tumor, when combined with the absence of steady state dendritic cells in the brain parenchyma, has perhaps led many investigators to focus instead on the innate cell types

that are present in the brain parenchyma, or on the immunosuppressive aspects of GBM in the context of innate immunity and antigen presentation, rather than on the anatomic and cellular basis for endogenous antigen presentation and T cell priming in CNS antitumor immunity.

The anatomic location of dendritic cells in the steady state brain is restricted to the meninges and the choroid plexus [49, 51]. The only leukocytes in the steady state brain parenchyma are microglia, a specialized phagocytic cell unique to the brain and derived from the embryonic yolk sac [49]. Microglia are involved in maintenance of homeostasis, elimination of microbes, removal of dead cells and debris, and are a source of pro-inflammatory cytokines during inflammation [49, 175]. A second phagocytic cell type that has received some attention is the border associated macrophage (BAM), a specialized macrophage that exists along the basement membranes of blood vessels throughout the brain parenchyma [49]. Given their abundance in the steady state brain, these two cell types have garnered interest as the putative T cell-priming antigen presenting cell in the brain. However, even though they can phagocytize and present antigen, they are not known to be able to migrate outside the CNS to draining lymph nodes. In contrast, cDC have been demonstrated to possess the machinery required to cross the network of specialized endothelial cells which comprise the blood brain barrier in an *in vitro* system [53] as well as the capability of migrating to cervical lymph nodes in the neck under certain experimental conditions [23, 176]. However, cDC are largely absent from the steady state brain [51]. Despite these observations, an abundance of dendritic cells have been demonstrated to infiltrate the brain parenchyma during certain inflammatory conditions [51], and it is further conceivable that the inflammation and dysregulated blood-brain barrier present in GBM

would permit additional opportunity for entry of circulating dendritic cells from the blood. Needless to say, it remains an open question whether cDC, microglia, or BAM perform immune surveillance to prime T cell responses against CNS tumors.

Some of the most compelling experiments implicating the role of dendritic cells in CNS immune surveillance and T cell priming are those which involve CNS autoimmunity. A clever study by Mundt and colleagues measured the effect of temporal and conditional deletion of MHCII from different APC subsets in the brain during EAE [55]. They used a microglial specific Cre strain and crossed it to a *MHCII*$^{fl/fl}$ mouse to hinder antigen presenting capability of microglia. They determined that they could still induce EAE in these mice, which suggests that microglia were dispensable. They also crossed the *MHCII*$^{fl/fl}$ mouse to a Cx3cr1 Cre-ER strain in order to target all three APC subsets in the brain. This cross also allowed for temporal deletion of MHCII so that APC with different developmental origins and lifespans could be differentially targeted. Whereas chronic tamoxifen treatment deleted MHCII from all APC subsets, acute tamoxifen treatment followed by a recovery period completely deleted MHCII from slowly cycling microglia and BAMs but allowed nascent MHCII-intact cDC which had developed after tamoxifen clearance, to repopulate the CNS during inflammatory conditions. In contrast to acute treatment, which permitted cDC but not microglia or BAMs to express MHCII, only chronic treatment, which deleted MHCII from all APC subsets, ameliorated EAE. MHCII on cDC was sufficient for EAE progression. This set of experiments demonstrated that cDC are the critical APC required for disease progression in the EAE model.

A second compelling study by Giles and colleagues showed in an EAE model that during the inflammatory conditions of EAE, CNS cDC accumulated in considerably greater

numbers compared to during the steady state. Additionally, cDC possessed superior ability to prime MOG-specific CD4 T cells compared to endogenously arising monocyte-derived dendritic cells (moDC) and were additionally more pro-inflammatory than moDC. Furthermore, they showed that depletion of cDC using a ZBTB46-DTR mouse resulted in attenuated disease compared to non-depleted control mice [56].

While the steady state brain is relatively devoid of conventional dendritic cells, these studies highlight the importance of cDC for disease progression in EAE models. Notably, these studies did not distinguish between cDC1 and cDC2 subsets (their Cre strains and diphtheria-toxin cDC-depletion model targeted all cDC), and they additionally did not address the role of cDC in antitumor immunity of the CNS.

Given the open questions regarding identity of the antigen presenting cell responsible for T cell priming in the brain, the lack of studies regarding endogenous T cell priming for CNS tumors, the implication of cDC in other immunologic responses in the brain, and the established role of cDC1 in antitumor immunity of other tumor types, we set out to define the role of cDC1 in CNS antitumor immunity. Herein we demonstrate that while cDC1 are absent in the steady state brain, that cDC1 infiltrate the brain parenchyma when a brain tumor is present. We also demonstrate that cDC1 are required both to mount neoantigen-specific $CD8^+$ T cell responses and to confer benefit from checkpoint blockade in a preclinical model of GBM. Together, our findings demonstrate the critical role that cDC1 play in mounting antitumor immunity in the brain.

4.2 Results

4.2.1 cDC1 infiltrate brain tumors and mediate checkpoint blockade-conferred protection

During steady state conditions, the primary locations for dendritic cells in the CNS are the choroid plexus and the surrounding meninges (consisting of the dura, arachnoid, and pia mater) [49, 51, 177]. The parenchyma itself is largely devoid of conventional dendritic cells, including cDC1. Despite the low amount of apparent surveillance by cDC in the steady state brain parenchyma, cDC play pivotal roles for a variety of immunologic responses in the CNS [53, 55, 56, 178-181]. Therefore, we investigated their role in CNS antitumor immunity.

We first determined whether dendritic cells infiltrate the brain tumor microenvironment in two different murine orthotopic glioma lines derived from the C57BL/6 mouse strain: GL261, and CT2A. We transplanted GL261 or CT2A tumor cells into the striata of wild-type mice and analyzed the immune infiltrate two weeks following transplantation. Using flow cytometry, we identified that all dendritic cell subsets (defined as $CD45^+$, $F4/80^-$, $I\text{-}A^{b+}$, $CD11c^+$), including cDC1 (defined as dendritic cells which are $XCR1^+$, $SIRP\alpha^-$, $Ly\text{-}6C^-$), infiltrated brain tumors and accumulated in numbers that were orders of magnitude greater than the number present in the cerebral hemisphere of sham-injected mice (Figure 4-1A). In order to validate the presence of cDC1 in tumors, we used a novel cDC1 reporter mouse to examine this population using 2-photon microscopy as well as by flow cytometry. In this mouse strain, GFP is knocked into one allele of the sorting nexin 22 locus ($SNX22^{GFP/GFP}$), and the $XCR1^+$ cDC1 specifically and constitutively express GFP [182]. For experiments, we used heterozygotes ($Snx22^{GFP/+}$), which have normally functioning cDC1 that still express GFP [182].

Figure 4-1

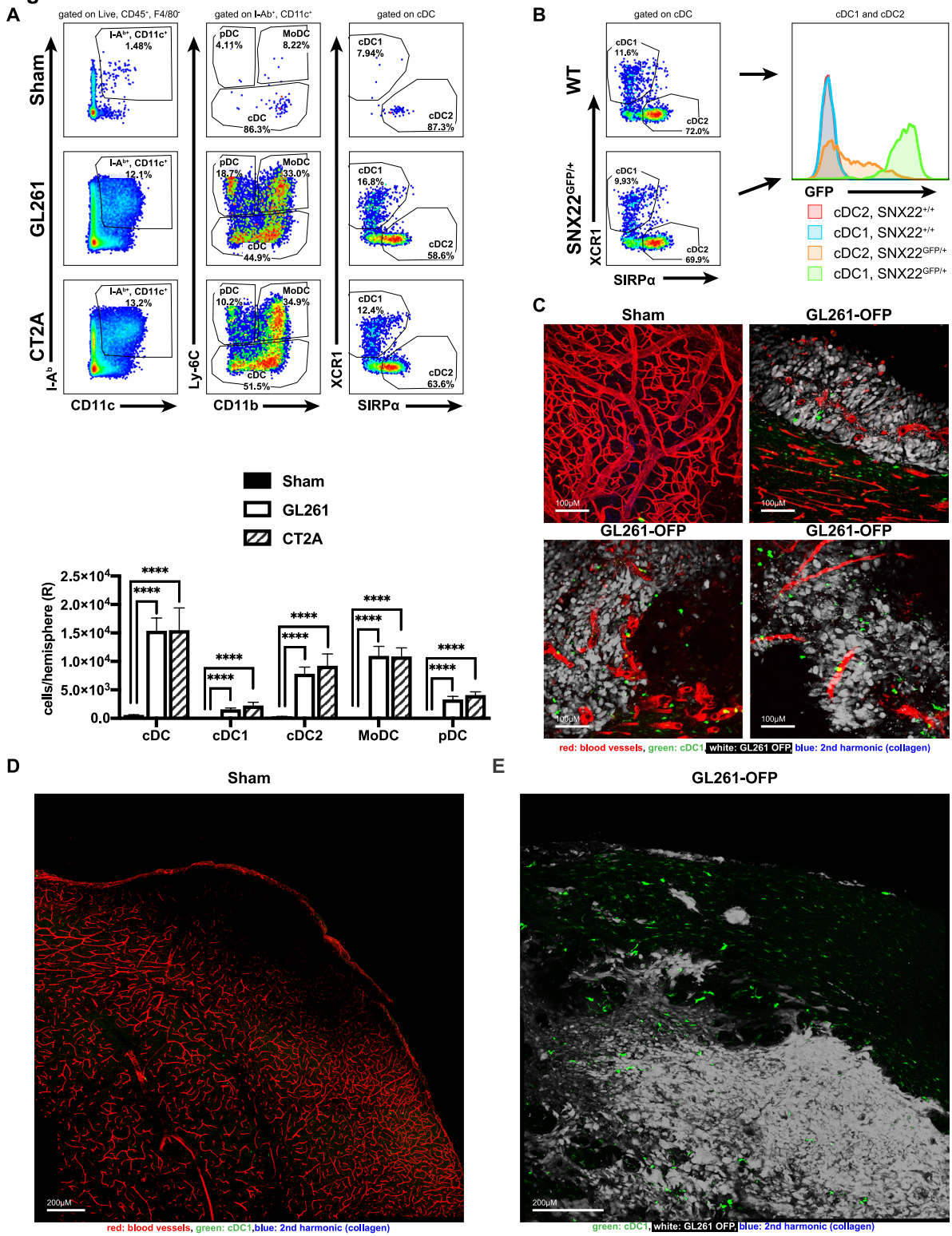

Figure 4-1. cDC1 infiltrate mouse glioma. A. cDC1, cDC2, MoDC and pDC quantification in brains of sham treated vs. GL261 or CT2A injected mice analyzed by flow cytometry at day 14 following tumor transplantation. B. cDC1/cDC2 profile and GFP expression of *SNX22*$^{GFP/+}$ mice. C-E. 2-photon microscopy of sham injected brain, or GL261-OFP injected brain at various regions in tumor. Data are represented as mean +/- SEM of at least three independent experiments. Statistics by student's t-test. **** p <.0001.

We transplanted GL261 tumors into the brains of *Snx22*$^{GFP/+}$ mice. Using flow cytometry, we identified that both cDC1 and cDC2 subsets infiltrated the brain tumors of both wild-type (WT) and *Snx22*$^{GFP/+}$ mice, but that GFP-expression was restricted to the cDC1 subset of the *Snx22*$^{GFP/+}$ mice (Figure 4-1B). To determine the localization of cDC1 in brain tumors, we used 2-photon microscopy to image OFP-transduced GL261 tumors that had been transplanted into the brains of *Snx22*$^{GFP/+}$ mice. In sham injected *Snx22*$^{GFP/+}$ mice, cDC1 were completely absent from the brain parenchyma (Figure 4-1C, 4-1D). In contrast, cDC1 infiltrated extravascular spaces of tumors and peri-tumor regions of *Snx22*$^{GFP/+}$ mice which bore GL261-OFP brain tumors (Figure 4-1C, 4-1E). Collectively, these data show that despite a scarcity in the steady state brain, dendritic cells, including the cDC1, abundantly infiltrate brain tumors in multiple orthotopic preclinical models of GBM.

Having identified that cDC1 are recruited to the brain tumor microenvironment, we investigated the immunologic consequences that result from their deficiency. To address this question, we used the *IRF8+32kb*$^{-/-}$ mouse, which harbors a 0.5kB deletion at *IRF8*/*BATF3* binding site within the *IRF8* super-enhancer, which falls 32kb downstream of the transcription start site. This mutation results in IRF8 levels in pre-cDC1 that are insufficient for cDC1 development [183]. We transplanted GL261 cells into the brains of wild-type or *IRF8+32kb*$^{-/-}$ mice and investigated the immune infiltrate by flow cytometry. Whereas wild-type mice with intracranial GL261 harbored abundant cDC1 in their brain tumors, *IRF8+32kb*$^{-/-}$ mice completely lacked cDC1 in their brain tumors (Figure 4-2A). Having confirmed that cDC1 were selectively deficient in *IRF8+32kb*$^{-/-}$ mice, we investigated the immunologic consequences of their deficiency. Although GL261 grows

progressively in immune competent mice, PD-1/PD-L1 blockade improves survival [124, 126]. We determined whether cDC1 are required to mediate this benefit. Whereas WT mice experienced improved median and overall survival following intracranial implantation of GL261 followed by αPD-L1 treatment, cDC1-deficient *IRF8+32kb*$^{-/-}$ mice subjected to the same treatment experienced no benefit (Figure 4-2B). Notably, we observed no survival difference between WT and *IRF8+32kb*$^{-/-}$ in vehicle-only treated mice which bore GL261 brain tumors (Figure 4-2B). Collectively, these data demonstrate that dendritic cells (including the cDC1) are recruited to brain tumors in numbers much greater than found in the steady state brain parenchyma, and that cDC1 in particular are required to mediate survival benefit from αPD-L1 in the setting of orthotopic GL261 brain tumors.

4.2.2 cDC1 prime CD8$^+$ T cell responses against glioblastoma

Because cDC1 can cross present antigen to prime CD8 T cell responses [25], we investigated the effect of cDC1-deficiency on brain tumor T cell composition. We transplanted GL261 into the brains of wild-type or *IRF8+32kb*$^{-/-}$ mice and examined the infiltrating immune cells by flow cytometry. Compared to wild-type mice, *IRF8+32kb*$^{-/-}$ mice had fewer infiltrating T cells, non-T_{reg} CD4$^+$ T cells, and CD8$^+$ T cells as a percentage of total CD45$^+$ cells infiltrating their brain tumors. In contrast, both wild-type mice and *IRF8+32kb*$^{-/-}$ had equal numbers of T_{regs} infiltrating their brain tumors (Figure 4-2C). Both mouse strains had equal numbers of CD45$^+$ cells infiltrating brain tumors (data not shown). In addition to *IRF8+32kb*$^{-/-}$ mice having fewer brain-tumor infiltrating CD8$^+$ T cells compared to wild-type mice, a smaller fraction of the infiltrating CD8$^+$ T cells present expressed granzyme B or PD-1 compared to wild-type mice (Figure 4-2D). These data demonstrate that in brain tumors, the T cell defect resulting from cDC1-deficiency spans

$CD4^+$ T cells and $CD8^+$ T cells, that cDC1-deficiency results in a smaller number of $CD8^+$ T cells infiltrating the tumor, and that of the $CD8^+$ T cells that do manage to infiltrate the tumor when cDC1 are absent, a smaller fraction of them possess effector function.

Although numerous studies have demonstrated that cDC1 cross present antigen to prime $CD8^+$ T cells in a variety of tumor types [20-23, 27, 28, 30, 31], it remains unclear whether they prime $CD8^+$ T cell responses in CNS tumors. Therefore, we tested the hypothesis that cDC1 are required to prime neoantigen-specific $CD8^+$ T cells in the GL261 preclinical model. We previously used a cancer immunogenomics approach to identify mutant Imp3 (mImp3) as a GL261-specific, H-$2D^b$ restricted neoantigen [123]. Mice that harbor either intracranial or subcutaneous GL261 spontaneously prime a $CD8^+$ T cell response against mImp3. To test the hypothesis that cDC1 are required to prime neoantigen-specific T cells in CNS tumors, we transplanted GL261 into the brains of wild-type or *IRF8+32kb*$^{-/-}$ mice and performed assays to assess presence and function of mImp3-specific $CD8^+$ T cells. We determined that tumor infiltrating lymphocytes (TIL) isolated from WT mice contained mImp3-specific $CD8^+$ T cells, whereas TIL isolated from *IRF8+32kb*$^{-/-}$ did not as measured by tetramer (Figure 4-2E). We performed an orthogonal approach to assess neoantigen-specific $CD8^+$ T cell function. Whereas $CD8^+$ TIL isolated from wild-type mice produced interferon gamma in response to stimulation with mImp3 peptide, equal numbers of $CD8^+$ TIL isolated from *IRF8+32kb*$^{-/-}$ mice did not as measured by ELISPOT (Figure 4-2F). These data demonstrate that cDC1 are required to prime functional neoantigen-specific $CD8^+$ T cells which can produce interferon gamma. More broadly, these data suggest that cDC1 are required for effector T cell function in CNS tumors.

Figure 4-2

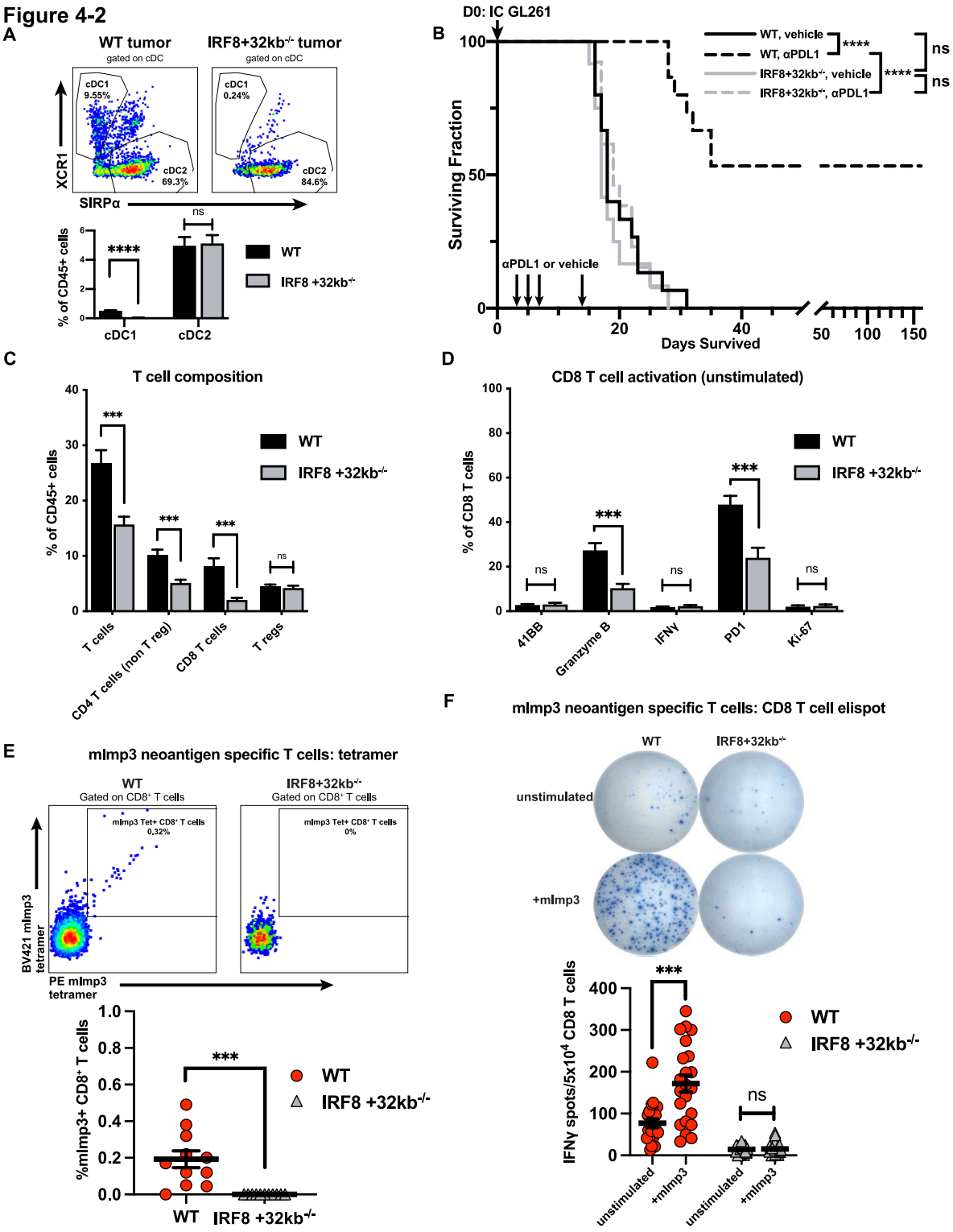

Figure 4-2. cDC1 prime effector CD8⁺ T cell responses against mouse glioma. A. cDC1-quantification in WT vs. *IRF8+32*$^{-/-}$ brain tumors. B. Survival fractions of vehicle or αPD-L1 treated WT or *IRF8+32*$^{-/-}$ mice. C-D Average T cell composition/activation status of WT vs. *IRF8+32*$^{-/-}$ GL261 brain tumors as assessed by flow cytometry. E-F. mImp3 neoantigen-specific CD8⁺ T cell response analyzed with mImp3 tetramer (E) or IFNγ ELISPOT (F). Data are represented as mean +/- SEM of at least three independent experiments. Survival differences in A assessed by log-rank test, C-F: student's t-test. *** p <.001, **** p <.0001.

4.3 Conclusion and Discussion

Here we demonstrated that cDC1 are required for CNS antitumor immunity in a preclinical model of glioblastoma. We identified that cDC, including cDC1 are recruited to the brain tumor microenvironment in numbers significantly greater than in the steady state. We determined that cDC1 are required for benefit from αPD-L1 checkpoint blockade, to prime functional $CD8^+$ T cells, and to prime neoantigen-specific $CD8^+$ T cell responses in GBM.

Notably, although cDC1 are essential for shaping the antitumor immune response in the brain, the steady state brain parenchyma is largely devoid of cDC1 (and all other dendritic cell subsets). cDC1 and other DC subsets are recruited in vast numbers into the tumor microenvironment when mice harbor a brain tumor. It is not presently known how exactly dendritic cells are recruited to the tumor microenvironment in the brain. Previous studies have shown that dendritic cells are recruited to the brain during inflammation [51, 55, 56, 178-181], but these studies fall short of describing the precise mechanism by which dendritic cells are attracted to and enter the inflamed parenchyma. Microglia are known to be a source of pro-inflammatory cytokines [175], however it is not clear whether they function as the sentinel immune cells responsible for instigating inflammation and secreting chemokines to trigger recruitment dendritic cells into the tumor microenvironment, or whether dendritic cells are able to detect the disturbance caused from brain tumors by some other means to initiate their extravasation from the blood into the tumor parenchyma. Future studies should distinguish if microglia are required to recruit dendritic cells into the tumor microenvironment and should additionally identify intrinsic factors harbored by dendritic cells required for their recruitment to the tumor microenvironment in the CNS.

In a clever and interesting study, Harris and colleagues showed that antigen sampling still takes place in the steady state brain using Cre driven expression of oligodendrocyte specific OVA, which restricted the antigen's expression to the CNS [52]. In this mouse, they observed OVA-driven proliferation of adoptively transferred OTI T cells in the periphery, despite OVA-expression being restricted to the CNS and despite there being no detectable inflammation in the brain. Notably these adoptively transferred OTI T cells did not enter the CNS in the steady state, nor did they cause disease progression when inflammatory conditions were triggered. Although this clever study showed steady state CNS antigen sampling takes place, these researchers did not show that dendritic cells are required for this process to occur. Given the previous studies showing the requirement of dendritic cells for EAE progression, and our work describing the pivotal role of cDC1 in the CNS antitumor immune response, future experiments should determine if dendritic cells are required for steady state antigen sampling. It is certainly conceivable that dendritic cells still may infiltrate the parenchyma and perform immune surveillance in the CNS in numbers too small to be appreciated by conventional experimental techniques.

Numerous studies have demonstrated that cDC1 cross present antigen to prime $CD8^+$ T cells in a variety of tumor types, in addition to performing other essential functions in antitumor immunity [20-23, 27, 28, 30, 31]. Herein we demonstrate the importance of cDC1 and show that they are absolutely required to mediate checkpoint blockade benefit and are additionally required to prime neoantigen-specific $CD8^+$ T cells (and effector T cells more broadly) against CNS tumors in a preclinical model of glioma. Importantly, our studies did not address the role of cDC2 in CNS antitumor immunity, nor did they determine if cDC1 were required for priming neoantigen-specific $CD4^+$ T cells. Our lab is currently screening

candidates for $CD4^+$ T cell specific neoantigens in GL261, and we are eager to test whether dendritic cells are required to prime neoantigen-specific $CD4^+$ T cell cells in this setting. Our data does suggest that cDC1 might be important for $CD4^+$ function in brain tumors. Although the majority of our studies focused on $CD8^+$ T cell function given the available tools to study neoantigen-specific T cell responses in $CD8^+$ T cells, it was notable that there were also fewer non-T_{reg} $CD4^+$ T cells infiltrating the brain tumors of cDC1-defecient mice. It is not clear whether there were fewer $CD4^+$ T cells as a downstream effect of fewer $CD8^+$ T cells having been primed by cDC1, or whether cDC1 were directly priming $CD4^+$ T cells. A potential experiment to address this would be to deplete $CD8^+$ T cells in cDC1-deficient mice, and to determine whether there were still non-T_{reg} $CD4^+$ T cell deficiencies. Important studies by Ferris and colleagues have recently demonstrated that cDC1 prime $CD4^+$ T cells when the tumor antigen is membrane associated [26]. Thus, whether cDC1 prime $CD4^+$ T cells in brain tumors may depend on the origin of the antigen. Indeed, cDC2 infiltrated brain tumors in numbers that were orders of magnitude greater than in the steady brain, however it is not clear whether they are bystanders, merely recruited because of the increased inflammation, or whether they additionally performed important functions there. No clean cDC2-deficient mouse exists—the $IRF4^{-/-}$ mouse has additional defects beyond cDC2 deficiency, and thus the hypothesis regarding whether cDC2 are important in CNS antitumor immunity (or antitumor immunity more broadly) is difficult to test. Studies have shown that cDC2 can help prime effector $CD4^+$ T cells in antitumor immunity [24], although it was notable that the ovalbumin antigen they used in their experiments was cytosolic, rather than membrane-associated. Furthermore, the most robust survival effects that they observed in their

model resulted from T_{reg} depletion. They showed that the survival benefits from T_{reg} depletion were reversed when they depleted $CD4^+$ but not $CD8^+$ T cells. They suggested this process was cDC2-mediated given that cDC2 have been shown to prime $CD4^+$ T cells, and that cDC2 associated with the ovalbumin-expressing tumor could exogenously drive OTII proliferation in their model. However, they did not actually show that cDC2 were required to mediate survival benefit following T_{reg} depletion. Nevertheless, important work remains to discern the role of cDC1 in priming $CD4^+$ T cells in brain tumors, as well as the potential role of cDC2 in mounting CNS antitumor immunity.

Important work also remains to establish the role of cDC1 in antitumor immunity in humans. GBM is an immune-suppressive tumor which employs a variety of mechanisms to suppress the immune system. It is certainly conceivable that if cDC1 ordinarily bolster CNS antitumor immunity in humans, and additionally that immune-suppressive mechanisms of the tumor might include driving cDC1 dysregulation, exclusion, or subversion. Nevertheless, important studies remain to answer these questions.

CHAPTER FIVE

Lymphatic drainage, T cell priming, and dura-involvement in CNS antitumor immunity

5.1 Introduction

The cellular basis for mounting a CNS antitumor immune response is incompletely understood. In chapter 4 we demonstrated that cDC1 play a key role in mounting CNS antitumor immunity, however there exists a dearth of knowledge regarding the intersection between the cellular and the anatomic basis of antitumor immunity in the brain. The CNS does not harbor conventional lymphatics, nor does it harbor secondary lymphoid structures [33, 49, 177, 184, 185]. This unique anatomic feature might lead one to conclude that the CNS is therefore hermetically sealed from the immune system that surveils the rest of the body; however, this conclusion would be incorrect. Although the CNS does not contain conventional lymphatics, investigators have known for quite some time that there exist mechanisms to clear debris and solutes from the brain [57, 59, 60]. Furthermore, experiments have demonstrated that the superficial and deep cervical lymph nodes in the neck play a supportive role both in the lymphatic drainage process and in priming CNS immune responses (primarily in EAE models) [61-63]. However, the complete anatomic basis for the connection between the CNS and the deep cervical lymph nodes remained incompletely described until recently.

Two landmark studies published in 2015 (from Louveau and colleagues in Kipnis' lab and Aspleund and colleagues in Alitalo's lab) described the existence bona fide lymphatic vessels harbored by the dura and which drain the CNS in mice [64, 65]. They identified that

these lymphatic vessels traverse along the superior sagittal sinus and the venous sinuses as they exit the skull and converge along the deep cervical lymph nodes in the neck which rest along the internal jugular vein. Louveau and colleagues described that intraventricular injection of liquid tracer (in the form of Evans Blue dye) led to accumulation of tracer in both the deep cervical lymph nodes, as well as in a second lymph node chain which lies more superficially in the neck, known as the superficial cervical lymph nodes, but that the route to the latter lymph node chain was unclear. They also stated that tracer reached the superficial cervical lymph nodes at later time points compared to the deep cervical lymph nodes. Complimenting these findings, Aspleund described that brain parenchyma-injected fluorescently labeled ovalbumin drained to the deep, but not the superficial cervical lymph nodes, that this process required intact dura lymphatics, and furthermore, that ligation of the lymphatic vessels along the internal jugular vein upstream of the deep cervical lymph nodes prevented drainage of tracer to the lymph node.

In 2018 Da Mesquita and colleagues (also from Kipnis's group) extended these findings. They demonstrated that dura lymphatic ablation diminished solute clearance and accelerated Alzheimer's disease progression in a preclinical mouse model. They also showed that conversely, administering VEGF-C to expand dura lymphatics and improve drainage function caused greater antigen clearance from the CNS and ameliorated cognitive deficits compared to control mice [66]. A second study by Louveau and colleagues demonstrated that ablation of dura lymphatics blunted disease severity in EAE and prevented chemokine receptor 7 (CCR7)-dependent trafficking of CNS-originating T cells to cervical lymph nodes. They showed this was the case when T cells had either been injected into the cisterna magma or had originated from the dura. They also demonstrated

that ablation of lymphatics along the cribriform plate prevented T cells from migrating from the CNS specifically to the superficial cervical lymph nodes [67].

A clever study by Absinta and colleagues in 2017 underscored the relevance of the 2015 mouse dura studies by demonstrating the existence of dura lymphatics in primates and humans using advanced MRI techniques. They verified the presence of lymphatic vessels by discerning differential MRI signals in blood vessels and lymphatic vessels by administering two different contrast agents: one that freely extravasated across permeable endothelial barriers within capillaries, and one that did not and was confined to the blood [68]. This allowed them to discern between blood vessels and lymphatic vessels, which function to collect waste products that have extravasated from the blood. They demonstrated that similar to their anatomic basis in mice, lymphatic vessels harbored by the dura in both humans and marmosets traverse along the superior sagittal sinus and lie in close proximity to the cribriform plate.

Relevant to our work in CNS cancer immunology, a landmark study by Song and colleagues (of Akiko Iwasaki's lab) published recently in 2020 described the relevance of dura lymphatics in CNS antitumor immunity. They demonstrated that VEGF-C agonism could expand the dura lymphatics to strengthen the CNS antitumor immune response, and that in this scenario the $CD8^+$ T cell response against the tumor was more potent than in control mice with unexpanded dura lymphatics. Additionally, they demonstrated that VEGF-C agonism could improve survival following orthotopic transplantation of glioma cells compared to control mice that had normal unexpanded dura lymphatics. Importantly, they determined that ligating the lymphatic vessels that drained to the deep

cervical lymph nodes could abrogate the antitumor immunity benefit conferred by VEGF-C agonism [69].

Adjacent to the studies describing the anatomic basis and immunologic importance of CNS lymphatic drainage, important studies by Fabry's group have demonstrated evidence for antigen presenting cell migration from the CNS to cervical lymph nodes. They made the important discovery that under certain conditions dendritic cells injected into the brain parenchyma migrate to the cervical lymph nodes in a CCR7-dependent manner [54, 179, 186]. These findings hinted at the cellular basis for lymphatic drainage of the CNS, however they were limited in that they introduced exogenously cultured monocyte-derived dendritic cells into the brain parenchyma and fell short of describing process as it occurs endogenously. Moreover, these studies did not implicate any particular dendritic cell subset known to arise naturally in mice—they used GM-CSF/IL-4 cultured monocyte-derived dendritic cells rather than Flt3L cultured dendritic cells, which much more closely approximate conventional dendritic cells as they occur *in vivo* [25, 187-190].

Taken together, these fundamental discoveries highlight the critical role of dura lymphatics in priming immunity in the CNS, and thus provide a framework for our understanding of the anatomic basis for lymphatic drainage of the CNS. The studies originating from Fabry's lab, which provide the strongest evidence for a possible cellular mechanism of priming immunity in the CNS, fall short of describing the endogenous cellular basis for the connection that exists between the brain, the dura lymphatic system, and the cervical lymph nodes. Thus, there remains an incomplete understanding of the cellular basis for lymphatic drainage in the context of CNS-antitumor immunity, and how dendritic cells might or might not be involved.

Given the incomplete understanding regarding the cellular basis for lymphatic drainage of the CNS, we set out to determine the relevance of endogenously arising dendritic cells in lymphatic drainage in the setting of CNS tumors. Herein we demonstrate that endogenously arising tumor antigen-containing dendritic cells can be isolated from the tumor, the dura, and the cervical lymph nodes. Moreover, we show that dendritic cells in the dura undergo dynamic changes in responses to CNS tumors, and that cDC1 specifically appear in the dura lymphatic vessels in both the tumor-bearing and the steady state settings. Finally, we describe that $CD8^+$ T cell priming and clonal expansion for CNS antitumor immune responses occurs in the cervical lymph nodes, rather than in the dura or any other secondary or tertiary lymphoid organ, which takes place before terminally divided effector $CD8^+$ T cells home to the brain tumor. Together, our findings unravel clues about the mechanism of lymphatic drainage and T cell priming in antitumor immunity of the brain.

5.2 Results

5.2.1 Endogenously arising tumor antigen-containing cDC1 appear in the tumor and cervical lymph nodes

Our current model of cDC1 function is that they phagocytize antigen at the periphery, activate, upregulate chemokine receptor 7 (CCR7) as well as MHCII, migrate to secondary lymphoid tissues, and present phagocytosed and processed antigen to prime naïve T cells. While the brain parenchyma lacks secondary lymphoid tissue and conventional lymphatics, compelling data have strongly suggested that the extracranial cervical lymph nodes are critical to prime CNS antigen-specific T cells [54, 65, 69, 178-180]. To determine if tumor antigen-containing cDC1 appeared in the brain or in these secondary

lymphoid structures, we exploited the property that conventional dendritic cells phagocytize target material, activate, and migrate to draining lymph nodes. To this end, we hypothesized (a) that fluorescent protein overexpressed by the tumor would be ingested by infiltrating dendritic cells as phagocytized tumor cells or tumor-associated debris, and (b) that this transferred tumor-derived fluorescent protein could be retained by and detected within dendritic cells using a flow cytometer, similar to the techniques used by Merad and Krummel in preclinical melanoma models [22-24].

We generated two fluorescent orthotopic glioma lines: GL261-zsGreen and CT2A-zsGreen. The premise of the experiment relies on the principle that when transplanted into mice, the tumor-derived zsGreen is ingested by infiltrating antigen presenting cells and can be used as a detectable surrogate for tumor antigen phagocytosis (Figure 5-1A). Because CT2A-zsGreen tumors most consistently and robustly retained zsGreen expression at the time of harvest, we used this model for most of the dendritic cell/tumor antigen tracking experiments we performed. To test the hypothesis that cDC1 which infiltrate the brain tumor uptake tumor-derived antigen, we transplanted CT2A-zsGreen tumor cells into the brains of mice and monitored for the presence of zsGreen-containing cDC1 (and other endogenously arising dendritic cell subsets) by flow cytometry at two weeks post-transplantation. In CT2A-zsGreen tumors, we identified zsGreen not only within tumor-infiltrating cDC1, but additionally within cDC2, monocyte-derived dendritic cells (MoDC), and plasmacytoid dendritic cells (pDC) (Figure 5-1B). These data suggest that all of these dendritic cell populations share the ability to ingest tumor-derived antigen *in vivo*. Importantly, we did not detect zsGreen-containing dendritic cells within the non-transduced, non-fluorescent CT2A control mice, which suggests that the phenomenon

we observed was specific to the presence of tumor-derived zsGreen protein. In addition to the tumor itself, we examined the ipsilateral superficial and deep cervical lymph nodes (cLN) to determine whether tumor antigen containing dendritic cells could be observed extracranially. We identified zsGreen$^+$ cDC1 (both migratory CD103$^+$CD8α$^-$ and resident CD8a$^+$CD103$^-$ subsets) in the superficial cLN, and zsGreen$^+$ migratory cDC1 in the deep cLN (Figure 5-1C, 5-1D). Notably a larger percentage of migratory cDC1, which presumably migrated from the tumor itself, were zsGreen$^+$ compared to resident cDC1 in both lymph node sets. We also identified zsGreen$^+$ cDC2, MoDC and pDC in the superficial cLNs, and zsGreen$^+$ MoDC in the deep cLNs (Figure 5-1C, 5-1D). Notably, the presence of zsGreen within dendritic cells was not restricted to the cDC1 subset, which suggests that while cDC1 are essential to prime an effective CNS antitumor immune response, other dendritic cell subsets are capable of ingesting and trafficking tumor-associated protein to cervical lymph nodes.

5.2.2 CCR7 is required for dendritic cells to traffic tumor antigen from the brain to cervical lymph nodes

Having determined that tumor antigen containing cDC1, cDC2, MoDC and pDC infiltrated the tumor and appeared in the cervical lymph nodes within the neck, we considered the possibilities by which tumor antigen containing cDC might appear within the cervical lymph nodes. We envisaged two potential mechanisms for trafficking tumor antigen to draining lymph nodes. As the first possibility, we considered that dendritic cells might infiltrate the tumor, activate, upregulate CCR7, and migrate down a chemokine ligand 19/21 gradient to carry the antigen that they had ingested to a draining lymph node via CCR7-mediated chemotaxis [176] (in short, active migration). Second, we that considered

the alternative possibility that tumor antigen would be expelled or lost from the tumor as debris, make its way into a lymphatic vessel, and flow down a pressure gradient toward an awaiting dendritic cell native to the lymph node, without being carried there by a migrating dendritic cell trafficking from tumor to the draining lymph node (in short, passive migration). Moreover, we considered that both processes could take place simultaneously. Because there was a predominance of zsGreen within migratory rather than resident cDC1 subsets, we hypothesized that active, cell-mediated antigen trafficking is the predominant mechanism by which zsGreen$^+$ tumor antigen containing dendritic cells appear within draining cervical lymph nodes.

To address this question, we tested the hypothesis that CCR7 is required for zsGreen$^+$ dendritic cells to appear within the cervical lymph nodes. *CCR7*$^{-/-}$ mice lack migratory dendritic cell subsets, therefore we did not distinguish between migratory cDC1 and resident cDC1 in our analysis of lymph nodes, and instead included all cDC1 together as XCR1$^+$ cDC in our analysis. To test our hypothesis, we transplanted CT2A zsGreen glioma cells into the brains of wild-type (WT) or *CCR7*$^{-/-}$ mice and monitored the zsGreen signal within dendritic cells isolated from the tumors and from the cervical lymph nodes. We first investigated the tumor microenvironment itself. Importantly, we identified equal proportions of tumor-infiltrating zsGreen$^+$ cDC1 (as well as other DC subsets) in both WT and *CCR7*$^{-/-}$ mice (Figure 5-1E). This suggested that dendritic cells which arose in either WT or *CCR7*$^{-/-}$ mice were capable of infiltrating the tumor and ingesting tumor antigen, and that any potential defect we might observe in *CCR7*$^{-/-}$ mice was downstream (in terms of lymphatic drainage) from the tumor microenvironment itself. We next investigated the CNS-draining cervical lymph nodes. In contrast to WT mice, *CCR7*$^{-/-}$ mice which bore

CT2A-zsGreen brain tumors had a significantly diminished zsGreen signal in cDC1 isolated from both the superficial and the deep cervical lymph nodes (Figure 5-1E). This observation of a diminished zsGreen signal in *CCR7*$^{-/-}$ mice compared to WT mice also held true for pDC from both the deep and superficial cLN, as well as MoDC from the superficial cLN (Figure 5-1E). Importantly, small but equal fractions of B cells isolated from cervical lymph nodes from WT or *CCR7*$^{-/-}$ mice were zsGreen^{+} (Figure 5-1E), which suggests that passive migration from the periphery still took place independent of CCR7 expression since B cells are not known to migrate from the periphery to draining lymph nodes in contrast to dendritic cells.

Notably, the zsGreen signal was incompletely extinguished from dendritic cells isolated from lymph nodes of *CCR7*$^{-/-}$ mice. This phenomenon was not uniform across replicates—most of the *CCR7*$^{-/-}$ mice with a zsGreen signal had only a small percentage of dendritic cells which were zsGreen^{+} within the cLN. However, a select few *CCR7*$^{-/-}$ mice harbored cLN zsGreen^{+} dendritic cell percentages comparable to WT counterparts. This suggests that under certain conditions, there exist cell-migration independent mechanisms to traffic tumor antigen from the brain to cLN, but that active, cell-mediated trafficking predominates. Together with our observation that cDC1 are required to mount effective antitumor immune responses in the CNS, these data collectively suggest that cDC1 do so in part by infiltrating the brain tumor, phagocytizing tumor antigen, and migrating with that phagocytosed tumor antigen to the cervical lymph nodes in a CCR7/cell migration-dependent fashion.

Figure 5-1

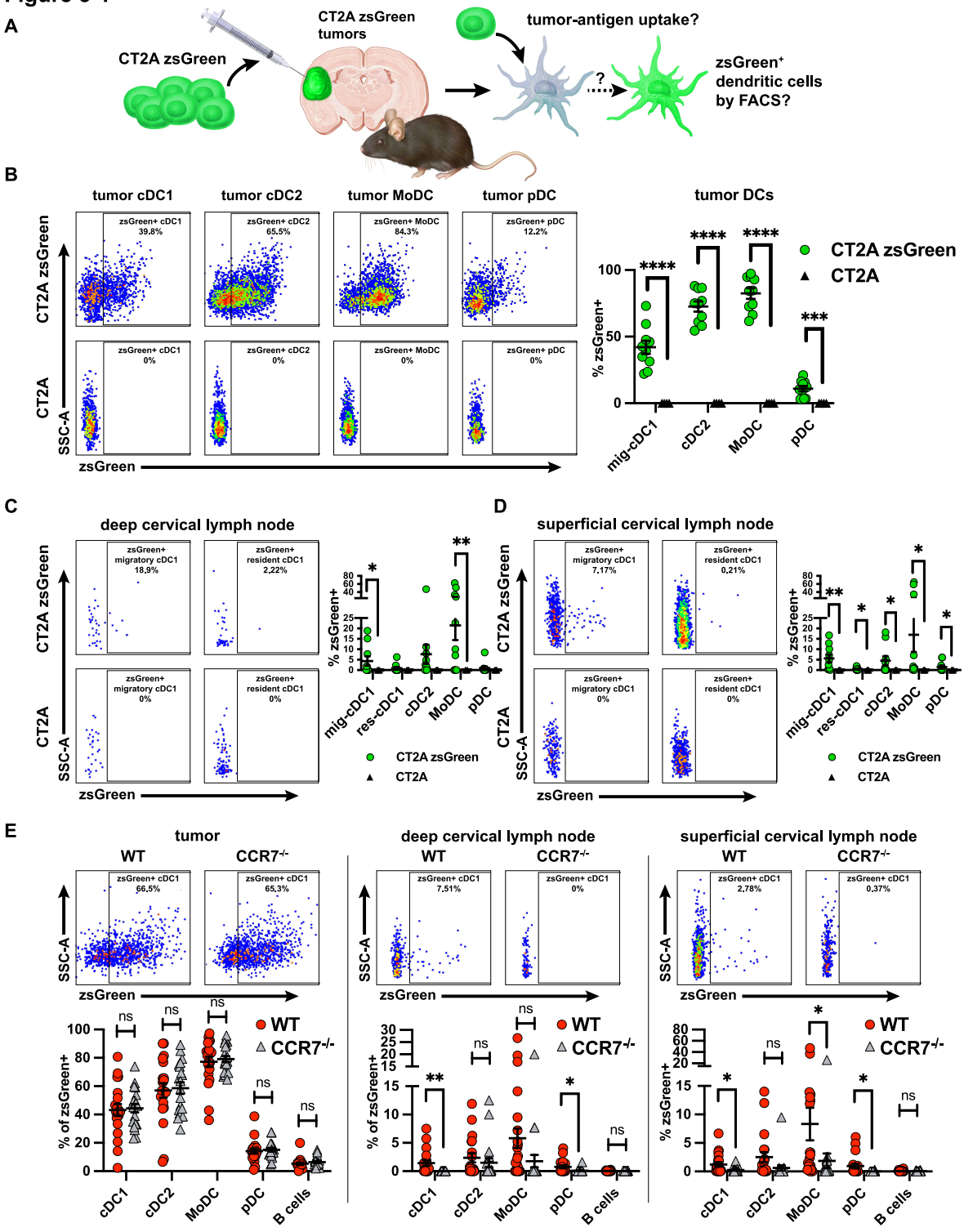

Figure 5-1. cDC1 isolated from TIL and CNS-draining cervical lymph nodes retain tumor antigen. A. Fluorescence transfer conceptual outline. B. zsGreen retention by DC infiltrating the tumor. C. zsGreen retention in deep cLN and D. superficial cLN dendritic cells. E. zsGreen retention by DC harbored by the tumor, the deep cLN, and the superficial cLN of WT vs. CCR7$^{-/-}$ mice. Data are represented as mean +/- SEM of at least three independent experiments, student's t-test to determine significance. * p<0.05, **p<0.01, ****p<0.0001. Grubbs outlier test was used to eliminate both a WT and a *CCR7*$^{-/-}$ outlier in E.

5.2.3 Dura-associated cDC1 undergo dynamic changes in response to GBM

Having determined that cDC1 are critical for mounting neoantigen-specific $CD8^+$ T cell responses against brain tumors as well as for priming CNS antitumor immunity more broadly, and also having determined that cDC1 perform their role in part by ingesting tumor antigen at the site of the tumor and trafficking that antigen to the cervical lymph nodes, we next investigated their function in the dura, which consists of the fibrous sheath covering the brain and lies just beneath the periosteum on the inner surface of the skull. The dura has been increasingly recognized as an immunologically dynamic location that in the steady state harbors a diverse composition of leukocytes, including all dendritic cell subsets, as well as macrophages, T cells, and B cells among other cell types. In contrast, the only steady state brain parenchymal leukocytes are microglia [49, 55]. In addition to harboring immune cells in the steady state, the dura also contains lymphatic vessels which traverse alongside the venous sinuses and drain to the deep cervical lymph nodes [64, 65, 69, 191]. More recently, studies have demonstrated that VEGF-C induced hyperplasia of dura lymphatics strengthened the CNS antitumor immune response [69]. Given these features, and the growing recognition of the importance of the dura for immune responses in the CNS, we investigated if there were any immunologic changes in the dura which were associated with the CNS antitumor immune response.

We determined the presence and location of dura-associated cDC1 using 2-photon microscopy and the same *SNX22*$^{GFP/+}$ mouse we had used previously. We first began by examining the dura with 2-photon microscopy in both the tumor-bearing and sham-treated control state. In both mice that harbored GL261-OFP brain tumors or were sham-injected, the dura harbored extravascular cDC1 near the superior sagittal sinus (Figure 5-2A). We

hypothesized that the number of cDC1 harbored by the dura would increase in mice that harbored intracranial GL261. To address this question, we used flow cytometry due to its capability regarding quantifying the total number of a particular cell type within a tissue. Compared to sham-injected control mice, mice bearing GL261 brain tumors harbored increased numbers of cDC, cDC1, cDC2, MoDC and pDC within their dura when measured quantitatively by flow cytometry (Figure 5-2B).

We next examined whether the growth factor responsible for dendritic cell development, Flt3L, could also expand the population of dura-associated cDC1. Previous work identified that Flt3L could drive expansion of $CD11c^{+}$, $I\text{-}A^{b+}$ cells within the dura [177], and a second study identified that Flt3L administration could specifically expand both cDC1 and cDC2 subsets harbored by the whole brain and surrounding meninges, which includes the dura [49]. We expanded on these findings and included specifically in our analysis measurement of the effects of Flt3L on dura-associated cDC1. Compared to control-treated mice, mice treated by Flt3L had a significantly expanded cDC1 population (as well as other DC subsets) within their dura as measured by flow cytometry (Figure 5-2C). Consistent with our observations using flow cytometry, we also observed expanded dura-associated cDC1 in the *SNX22*$^{GFP/+}$ mouse using 2-photon microscopy. Compared to control-treated mice, Flt3L-treated mice harbored dramatically more cDC1 within their dura near the lambda region of the skull (Figure 5-2D), which primarily localized to the dura adjacent to the superior sagittal sinus when we examined a larger field (Figure 5-2E). Notably, although both brain tumors and systemic Flt3L administration were both sufficient to drive expansion of dura-associated cDC1 (as well as all other DC subsets we examined), the magnitude of expansion was much greater from Flt3L administration.

Figure 5-2

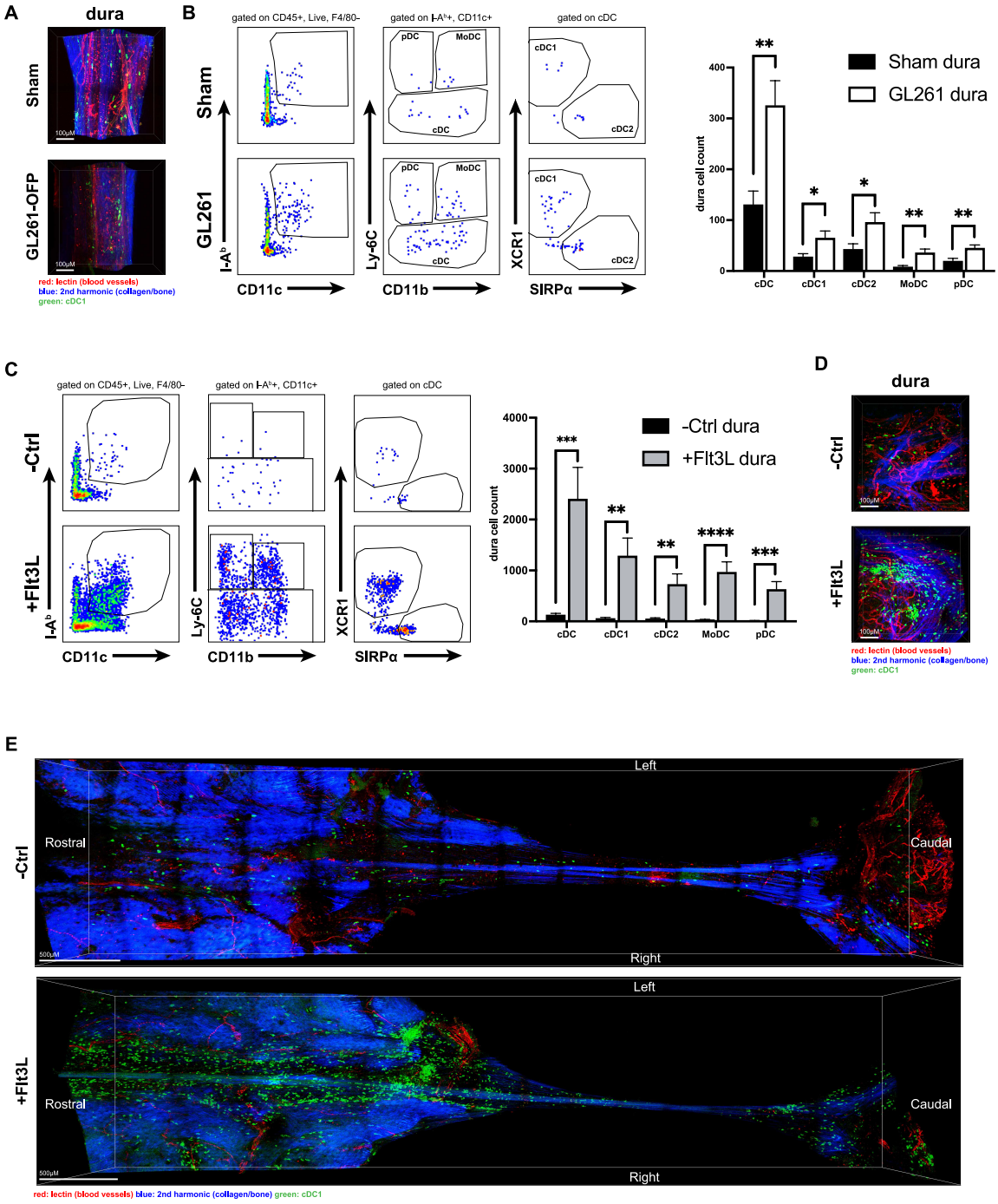

Figure 5-2. Mouse dura harbors Flt3L-sensitive tumor-responsive dendritic cells. A. 2-photon microscopy of *SNX22*$^{GFP/+}$ mouse dura along the superior sagittal sinus depicting sham vs. GL261 OFP intracranially injected mice. B. Dura DC quantified by flow cytometry from sham vs. GL261 injected brains at d14 post-tumor injection, and C. Dura DC quantified by flow cytometry from -Ctrl vs. Flt3L treated mice. D. Near Lambda or E. Full view 2-photon microscopy of SNX22$^{GFP/+}$ mouse dura of -Ctrl vs. Flt3L treated mice. For both samples in E, superior sagittal sinus runs horizontally from rostral to caudal in the middle of each image. Data are represented as mean +/- SEM of at least three independent experiments. Student's t-test used to determine significance, * p<0.05, **p<0.01, ***p<0.001, ****p<0.0001.

These data suggest that while both stimuli (brain tumors an Flt3L overexpression) expanded the dendritic cell populations harbored within the dura, that the mechanism of and precise factors driving expansion may have differed between each stimulus.

5.2.4 Dura-associated cDC1 reside in lymphatic vessels and contain tumor antigen

In addition to harboring a diverse population of immune cells, the dura is vested with lymphatic vessels which traverse parallel and immediately adjacent to the superior sagittal sinus, and which deliver lymph to the deep cervical lymph nodes in the neck [64, 65, 69, 191]. Lymphatic vessels associated with the dura also drain to the superficial lymph nodes via a separate route that traverses through the cribriform plate, parallel to the olfactory nerve roots [67], although the complete pathway for this route is less well characterized. To examine the spatial relationship between dura and cDC1, we crossed the *SNX22*$^{GFP/GFP}$ cDC1 reporter mouse with the *Prox1-Cre-tdTomato*$^{+/+}$ lymphatic vessel reporter mouse, which expresses the tdTomato fluorophore in lymphatic vessels after tamoxifen administration [192]. The resultant F1 mice have both GFP^{+} cDC1 and tdTomato^{+} lymphatic vessels post-tamoxifen administration. Using these mice and 2-photon microscopy, we confirmed that the dura harbors lymphatic vessels which run parallel to the superior sagittal sinuses and along venous sinuses as they diverge from the superior sagittal sinus (Figure 5-3A), consistent with previous reports [64, 65, 69, 191]. Within the dura, we also identified several instances of tomato/GFP signal overlap in all 3 dimensions, indicative of cDC1-lymphatic vessel spatial overlap. This suggests that the dura lymphatic vessels contained cDC1. This was true both when mice harbored intracranial GL261-OFP (Figure 5-3B) or were instead sham injected (Figure 5-3C). These data suggest that dura-

associated lymphatic vessels support cDC1 migration from the CNS to draining lymph nodes both in the tumor-bearing state as well as in the steady state.

Given our observations that the dura harbors cDC1, some of which can be localized to within lymphatic vessels, and given our observations that tumor antigen-retaining dendritic cells appeared in cervical lymph nodes in a CCR7/cell migration-dependent manner, we hypothesized that a small fraction of dura-associated cDC1 might also harbor tumor antigen in the setting of brain tumors. Because CT2A-zsGreen retained highest levels of zsGreen expression at the time of harvest compared to GL261-zsGreen, we used the CT2A-zsGreen model to assess for presence of tumor antigen within dura-associated cDC1. To test the hypothesis that a subset of dura-associated cDC1 contain tumor antigen in the brain tumor setting, we transplanted CT2A-zsGreen tumor cells intracranially and monitored for zsGreen within cDC1, as well as other DC subsets, by flow cytometry. We selected an early time point to ensure that tumors were small and confined to within the brain parenchyma. We also resected the dura that surrounded the injection site to avoid potential contamination of the dura samples by tumor which may have engrafted near the cerebral surface apposed to the dura. This phenomenon sometimes happens because of reflux or from leaving behind trace amounts of tumor cells along the needle trajectory during tumor cell transplantation. Using flow cytometry, we simultaneously observed zsGreen^{+} migratory cDC1 in the tumor itself, the dura, the superficial cervical lymph nodes, and the deep cervical lymph nodes (Figure 5-3D). Importantly, we did not observe CD45^{-}/zsGreen^{+} cells within the dura, which indicates that our dura samples were not contaminated by tumor infiltrate, and that the zsGreen^{+} cDC1 observed in dura samples were truly dura-associated rather than tumor-infiltrating.

Figure 5-3

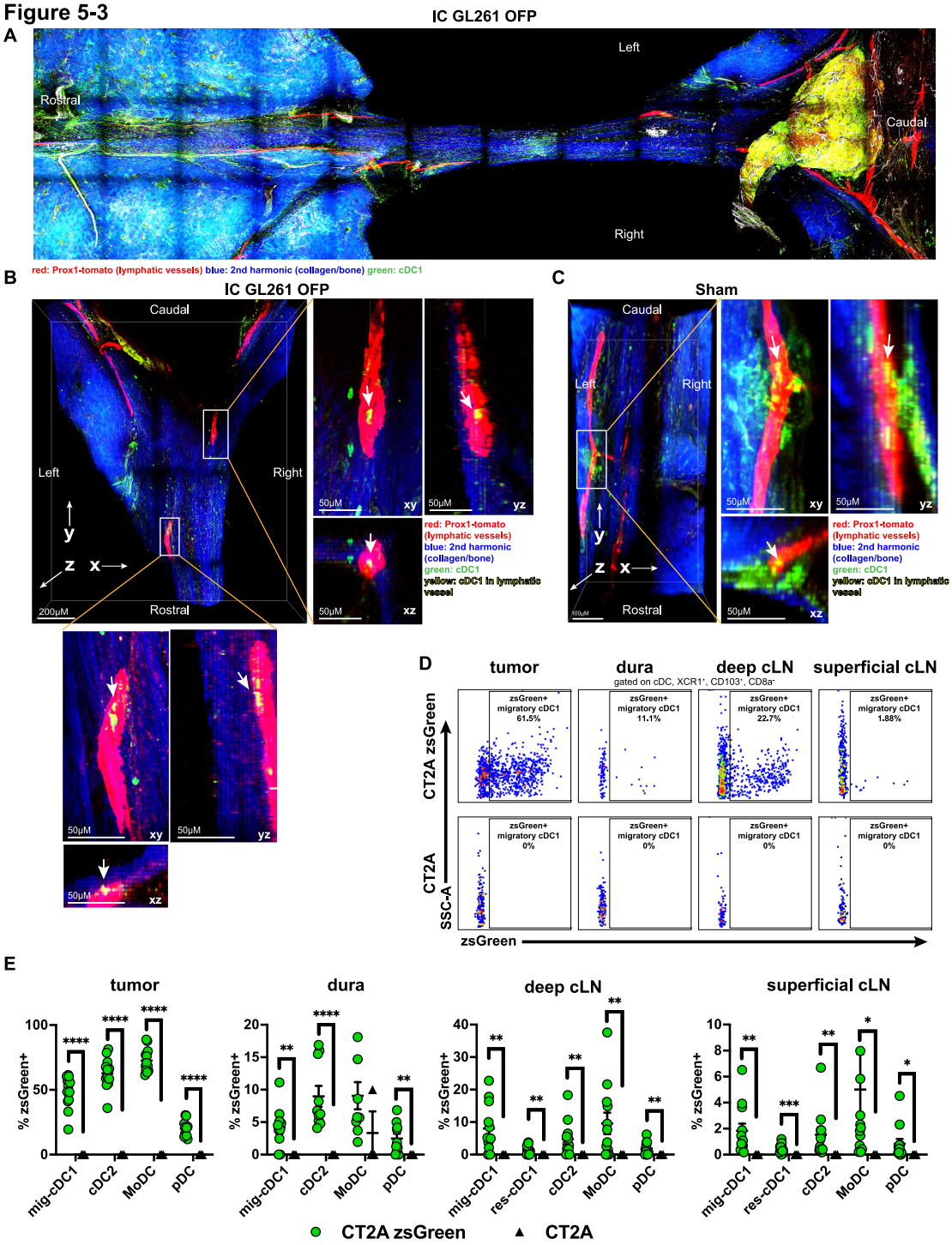

Figure 5-3. Mouse dura lymphatic vessels harbor cDC1 and dura-associated cDC1 retain tumor antigen. A. Dura from intracranial GL261 OFP-bearing, tamoxifen treated *SNX22*$^{GFP/+}$ x *Prox1-Cre-tdTomato*$^{+/-}$ mice. Superior sagittal sinus running horizontally across the page from rostral to caudal. B. Same sample as in A rotated 90º counterclockwise, near lambda: cDC1 visualized in lymphatic vessels. C. cDC1 visualized in a lymphatic vessel in Sham-injected mice with dura in same orientation in B. D. Tumor, dura, deep and superficial cLN-associated migratory cDC1 zsGreen retention. E. zsGreen retention quantified across all dendritic cell subsets. Dura samples with CD45^{-}/zsGreen^{+} cells were excluded from analysis. Data represent as mean +/- SEM of at least three independent experiments, student's t-test to determine significance, * p<0.05, **p<0.01, ***p<0.001, ****p<0.0001.

While our work has demonstrated the importance of cDC1 specifically in priming the CNS antitumor immune response, notably the phenomenon of tumor antigen retention by dendritic cells was not restricted to cDC1; we observed detectable levels of zsGreen within cDC2, MoDC and pDC that had been isolated from the tumor, the dura, the deep cervical lymph nodes, and the superficial cervical lymph nodes (Figure 5-3E). The dynamic changes of the dura when mice have brain tumors, including the expanded population of Flt3L-sensitive cDC1, the presence of cDC1 within lymphatic vessels, and the evidence for cell-mediated tumor antigen trafficking collectively suggest that the dura plays a supportive role in mounting CNS antitumor immune responses.

5.2.5 $CD8^+$ T cell priming and clonal expansion occurs in cervical lymph nodes

Where in the body a CNS antitumor immune response is primed remains an open question. We have demonstrated evidence for the essential role of cDC1 in this process, as well as evidence for cell-mediated tumor antigen trafficking by cDC1 from the tumor to the superficial and deep cervical lymph nodes, with the dura likely playing a supportive role in this process. However, these observations do not address the nature of T cell priming and clonal expansion, which lie downstream of antigen uptake and trafficking by dendritic cells. Multiple previous observations implicate the role of cervical lymph nodes in CNS immune responses. First, lymphadenectomy of cervical lymph nodes decreased EAE disease burden in rodents [61-63]. Second, ablation of dura lymphatics lessened disease incidence in an EAE model and was shown in the same set of experiments to decrease the CD11c+-T cell interactions in cervical lymph nodes compared to control mice [67]. Third, expansion of dura lymphatics using VEGF-C agonism has been shown to

bolster CNS-antitumor immunity and could be reversed by ligating the lymphatic vessels which drain to the deep cervical lymph nodes [69].

Because we identified tumor antigen-harboring dendritic cells in the tumor, the dura, and the CNS-draining cervical lymph nodes, we considered the possibilities of where $CD8^+$ T cell priming might occur in the setting of CNS antitumor immunity, and included in our analyses the tumor itself, the dura, the cervical lymph nodes, and the spleen. We also included in our analysis the presumably non-CNS-draining inguinal lymph node as an additional control. To address the question of where $CD8^+$ T cell priming occurs in this setting, we tracked the cell division of adoptively transferred OT-I $CD8^+$ T cells *in vivo* in mice that harbored intracranial GL261 transduced with full length cytosolic ovalbumin (GL261-OVA). In addition to an I-A^d/MHCII-restricted antigen, ovalbumin also contains in its amino acid sequence the H-2K^b/MHCI-restricted antigen SIINFEKL, which engages the OT-I T cell receptor of an adoptively transferred (or endogenously arising) OT-I T cell receptor when presented on the H-2K^b/MHCI protein [193]. Engagement of this T cell receptor and priming by a dendritic cell can cause the OT-I T cells to activate, divide, and clonally expand. The adoptively transferred OT-I T cells can themselves be tracked by congenic expression of unique CD45 alleles whose identity differ between the host and the adoptively transferred cells. Division can be measured by labeling the adoptively transferred OT-I T cells with the protein-binding fluorophore carboxyfluorescin succinimidyl ester (CFSE). CFSE cannot be expelled from the OT-I T cells and can only be proportionally divided between daughter cells. This dilution, which results only from cell division, can be detected on a flow cytometer as a weaker fluorescent signal compared to parental un-divided adoptively transferred CFSE-high OT-I T cells. The

CFSE dilution can be treated as a surrogate for antigen presentation to OT-I T cells. We crossed a C57BL/6 *CD45.1*$^{+/+}$ mouse with a C57BL/6 *CD45.2*$^{+/+}$*OT-I* mouse and used the resultant F1 mouse to purify CD45.1^{+}CD45.2^{+} OT-I CD8^{+} T cells for adoptive transfer experiments.

We transplanted GL261-OVA tumor cells into the brains of *CD45.2*$^{+/+}$ C57BL/6 WT mice and adoptively transferred CFSE labeled CD45.1^{+}CD45.2^{+} OT-I T cells 4 days after tumor transplantation. At both 3 and 6 days after the adoptive transfer (days 7 and 10 post-tumor transplantation), we harvested the region of brain where the tumor cells had been transplanted, the dura, the ipsilateral superficial and deep cervical lymph nodes, the spleen, and the non-CNS-draining contralateral inguinal lymph node. In each of these tissues we determined the degree of OT-I cell division with flow cytometry by measuring CFSE dilution in the congenically labeled OT-I T cells (Figure 5-4A).

We envisaged the different concentrations of CFSE (low, mid, and high) harbored by OT-I T cells to reflect how much cell division a parent cell had undergone as a result of being activated by cognate antigen presentation. We imagined CFSE-high to reflect un-divided naïve OT-I T cells, CFSE-mid to reflect early primed OT-I T cells (which might preferentially localize to a draining lymph node), and CFSE-low to reflect terminally divided OT-I T cells (which might preferentially localize to the effector site).

At 3 days post-adoptive transfer of OT-I T cells (seven days total after tumor implantation), we observed the greatest fraction (as a percentage of CD45^{+}/live cells) of undivided/naïve CFSE-high OT-I T cells in the lymph nodes, with no difference between any of the lymph nodes taken from different regions in the body. We observed the next highest fraction in the spleen, but there were significantly fewer than in the lymph nodes We observed a

near complete absence of CFSE-high OT-I T cells in both the dura and the tumor region, when compared to the spleen or the lymph nodes (Figure 5-4B). CFSE-mid, initially divided OT-I T cells occupied the greatest percentage of the $CD45^+$/live compartment in the CNS-draining superficial and deep cervical lymph nodes, with significantly more there than in any of the other organs (Figure 5-4B). CFSE-low terminally divided OT-I T cells were rare but occurred in greatest frequency in the deep cervical lymph node compared to the dura or the inguinal lymph node, with no differences between any of the other organs (Figure 5-4B). Collectively, this demonstrated that OT-I T cell priming and clonal expansion preferentially took place in the CNS-draining cervical lymph nodes when compared to other lymphoid organs, the dura, or the tumor itself. This early time point captured the first stages of clonal expansion, which was also reflected by a paucity of terminally divided OT-I cells within the tumor, the presumed effector site.

At 6 days post-adoptive transfer, we observed a similar pattern as at 3 days post-adoptive transfer with a few notable distinctions. CFSE-high naïve OT-I T cells persisted in the lymph nodes and spleen when compared to other organs similar to 3 days post-adoptive transfer. (Figure 5-4C). We also observed a similar pattern compared to 3 days post-adoptive transfer with CFSE-mid early divided OT-I T cells: predominance in the CNS-draining superficial and deep cervical lymph nodes, although the fraction of CFSE-mid OT-I T cells in the cervical lymph nodes had decreased when compared to day 3 post-adoptive transfer. The notable contrast between day 3 and day 6 post-adoptive transfer occurred in the CFSE-low terminally divided OT-I T cells. In contrast to day 3 post-adoptive transfer, when CFSE-low terminally divided OT-I T cells were not prevalent in any of the tissues analyzed, they predominated in the tumor region and in the dura at day

6 post-adoptive transfer. They occupied a significantly greater fraction of $CD45^+$/live cells in the tumor than in any of the lymph nodes (Figure 5-4C). Interestingly by day 6 post-adoptive transfer, CFSE low cells had also expanded systemically (beyond just the tumor region). They also appeared in the spleen and in the non-draining inguinal lymph node (Figure 5-4A). Interestingly, we did not observe OT-I cells of any CFSE dilution in the majority of dura samples in our experiments. However, in the isolated samples in which we did, they were always terminally divided, CFSE-low OT-I cells. The absence of early-divided CFSE-mid OT-I T cells in the dura indicates that the dura was not a site of T cell priming, despite being vested with lymphatic vessels and being considered an anatomic location of dynamic immunologic activity. We also never observed CFSE-mid, early primed, OT-I cells in organs other than the superficial and deep cervical lymph nodes, which suggests that the cervical lymph nodes are where T cell priming takes place in the setting of CNS antitumor immunity. This comports with our understanding that the cervical lymph nodes form the terminus of lymphatic vessels which drain the CNS. These data collectively suggest that in this setting, $CD8^+$ T cells are primed in the cervical lymph nodes to mount a CNS antitumor immune response, and that the dura or the tumor itself are sites of effector function rather than of $CD8^+$ T cell priming.

Figure 5-4

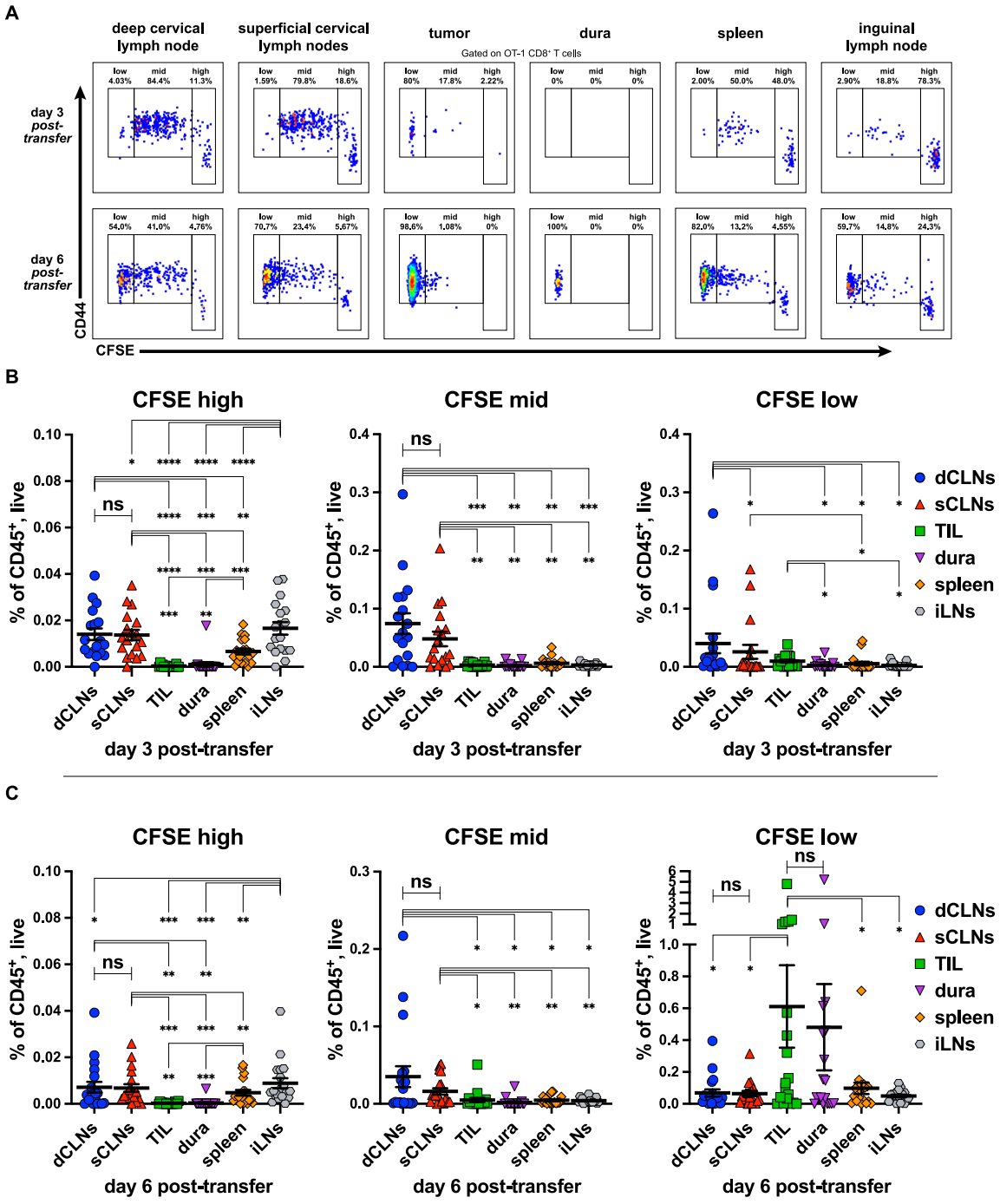

Figure 5-4. Clonal expansion of OT-I CD8⁺ T cells occurs in CNS-draining cervical lymph nodes. A. CD44 expression and CFSE dilution of OT-I CD8⁺ T cells assessed by flow cytometry at day 3 and day 6 post-adoptive transfer of ipsilateral superficial cLN, ipsilateral deep cLN, cerebral hemisphere region encompassing tumor, dura (with tumor abutting region resected), spleen, and non-draining contralateral inguinal LN. Cells gated on Live, CD45.1⁺, CD45.2⁺, CD4⁻, Dump⁻ (CD19, CD11b, CD11c, F4/80, Nk1.1), CD3ε⁺, CD8α⁺, TCR-Vα2⁺/Vβ5⁺. B-C. Quantitation of CFSE-high, mid, and low OT-I CD8⁺ T cells at 3 (B) and 6 (C) days post-adoptive transfer. Data represented as mean +/- SEM of at least three independent experiments, single comparisons using students t-test, * p<0.05, **p<0.01, ***p<0.001, ****p<0.0001.

5.2.6 cDC1 and CCR7 are required for early CD8$^+$ T cell clonal expansion

Given our observations that cDC1 are required to endogenously prime neoantigen-specific CD8$^+$ T cell responses against CNS tumors, and that CCR7 is required to traffic tumor antigen from brain tumors to CNS-draining cervical lymph nodes, we investigated whether absence of cDC1 or deletion of CCR7 affected clonal expansion of adoptively transferred OT-I T cells in mice that harbored GL261-OVA brain tumors. We used the same method as in the previous experiment described and harvested tissues at the same time points as previous adoptive transfer experiments, but did the experiment in WT, *CCR7$^{-/-}$*, or *IRF8+32kb$^{-/-}$* mice. However, we did not discern between CFSE-low, CFSE-mid, and CFSE-high OT-I CD8$^+$ T cells, we simply characterized OT-I CD8$^+$ T cells as "divided" if they had diminished CFSE expression due to cell division.

We hypothesized that absence of CCR7 or cDC1-deficiency would lead to defective clonal expansion of OT-I CD8$^+$ T cells, given the requirement of CCR7 for trafficking tumor antigen from brain tumor to cervical lymph nodes, and also given the requirement of cDC1 in priming neoantigen-specific CD8$^+$ T cell responses as demonstrated by our previous experiments. We transplanted GL261-OVA into brains of WT, *CCR7$^{-/-}$*, or *IRF8+32kb$^{-/-}$* mice, adoptively transferred OT-I T cells 4 days after tumor induction, and measured CFSE dilution of OT-I CD8$^+$ T cells at days 3 and 6 post-adoptive transfer of the OT-I CD8$^+$ cells. Compared to WT mice, *CCR7$^{-/-}$* and *IRF8+32kb$^{-/-}$* mice had decreased clonal expansion of OT-I CD8$^+$ T cells in the superficial cervical lymph nodes, the deep cervical lymph nodes, and the spleen, but not the tumor, the dura, or the inguinal lymph node at 3 days post-adoptive transfer (Figure 5-5A).

Notably, in contrast to day 3, we observed minimal differences in clonal expansion between WT, *CCR7*$^{-/-}$, and *IRF8+32kb*$^{-/-}$ mice in the organs examined at 6 days post-adoptive transfer (Figure 5-5B). Interestingly there were more congenically marked, expanded OT-I CD8^{+} T cells in the superficial cervical LNs of *CCR7*$^{-/-}$ compared to WT mice at day 6 post-transfer. At the same timepoint in the spleen, there were modestly but not significantly fewer expanded OT-I CD8^{+} T cells in CCR7$^{-/-}$ compared to WT mice. Moreover, at day 6 post-adoptive transfer there significantly fewer expanded OT-I CD8^{+} T cells in the spleens of *IRF8+32kb*$^{-/-}$ compared to WT mice.

These data collectively demonstrate that absence of intact cell migration to lymph nodes (reflected in *CCR7*$^{-/-}$ mice), and deficiency of cDC1 (reflected in *IRF8+32kb*$^{-/-}$ mice) both lead to delayed clonal expansion of adoptively transferred OT-I CD8^{+} T cells against tumor-specific antigens expressed by brain tumors. However, it was notable that clonal expansion of OT-I CD8^{+} T cells still occurred with varying degrees at the later day 6 post-adoptive transfer time point in mice with these defects. This suggests two things: first, if given enough time in *CCR7*$^{-/-}$ mice, tumor antigen can still passively drain to the cervical lymph nodes in amounts great enough to drive clonal expansion of adoptively transferred OT-I CD8^{+} T cells without being carried there by dendritic cells. Second, that cell types other the cDC1 can drive clonal expansion of adoptively transferred CD8^{+} T cells, albeit they carry out this task less efficiently as evidenced by clonal expansion being delayed in most organs until day 6 post-adoptive transfer our experiments. However, these data still underscore the importance of cell migration and the cDC1 subset in priming an effective CD8^{+} T cell response against CNS tumors that develops and expands with normal kinetics.

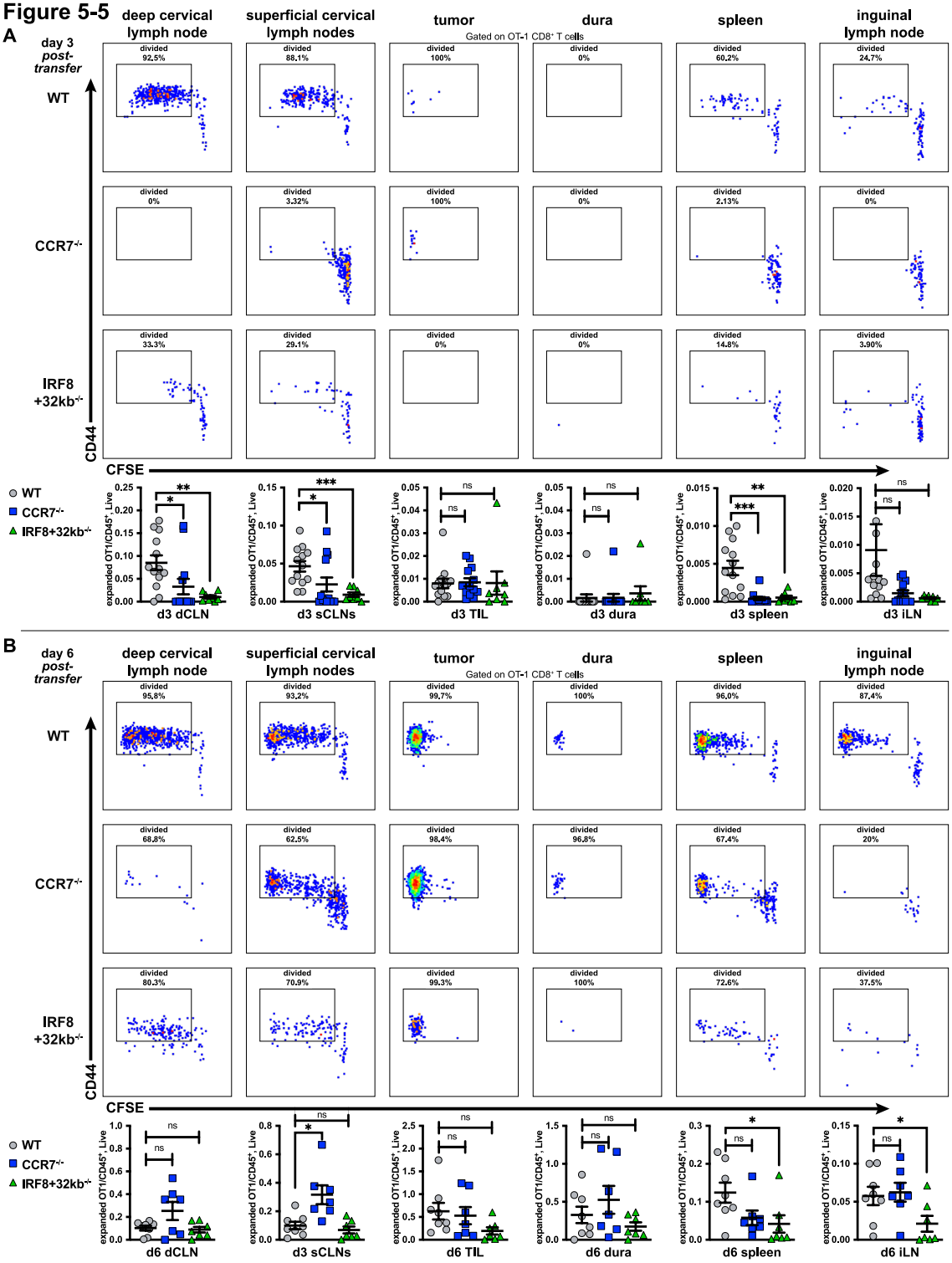

Figure 5-5. cDC1 and CCR7 are required for early clonal expansion of adoptively transferred OT-I CD8$^+$ T cells. A-B. CD44 x CFSE of OT-I CD8$^+$ T cells analyzed by flow cytometry at day 3 (A) and day 6 (B) post-adoptive transfer, in ipsilateral superficial cLN, ipsilateral deep cLN, cerebral hemisphere region encompassing tumor, dura (with tumor abutting region resected), spleen, and non-draining contralateral inguinal LN. Cells gated on Live, CD45.1$^+$,CD45.2$^+$, CD4$^-$, Dump$^-$ (CD19, CD11b, CD11c, F4/80, Nk1.1), CD3ε$^+$, CD8α$^+$, TCR-Vα2$^+$/Vβ5$^+$. Data represented as mean +/- SEM of at least three independent experiments, single comparisons using students t-test, * p<0.05, **p<0.01, ***p<0.001.

5.3 Conclusion and Discussion

Here we show that cDC1 (along with other dendritic cell subsets) infiltrate the tumor and acquire tumor antigen there. We also show that tumor antigen bearing dendritic cells can be isolated from the dura, and that they traffic tumor antigen to the lymph nodes in a CCR7-dependent manner. We determined that dura-associated Flt3L-sensitive cDC1 (along with other dendritic cell subsets) additionally expand their population in response to the stimulus of an intraparenchymal tumor within the brain, and that some cDC1 harbored by the dura specifically localize to the dura lymphatic vessels. Further, we show that $CD8^+$ T cell priming and clonal expansion of adoptively transferred $CD8^+$ T cells that recognize CNS tumors takes place in the CNS-draining cervical lymph nodes rather than in the spleen, non-draining lymph nodes, the tumor, or the dura. Moreover, we show that clonal expansion of adoptively transferred OT-I $CD8^+$ T cells requires CCR7 expression and intact cDC1 in order to take place with normal kinetics.

Previous work in EAE models demonstrated that the cervical lymph nodes play a role in CNS immune responses: resection of cervical lymph nodes was shown to dampen severity of EAE disease in mice and rats [61-63]. Studies by Kipnis and Alitalo also highlighted the role of the cervical lymph nodes in lymphatic drainage of the CNS [64, 65]. Moreover, studies by the Iwasaki lab showed that VEGF-C administration in the brain tumor setting expanded dura lymphatics, which both drove expansion of the neoantigen-specific $CD8^+$ T population in the deep cervical lymph nodes and improved survival compared to control mice with brain tumors [69]. Importantly, they also identified that ligation of the CNS draining lymphatic vessels in the neck could reverse the beneficial effect of VEGF-C on CNS antitumor immunity [69]. Given the importance of cervical lymph nodes in

lymphatic drainage of the CNS, and given our experiments demonstrating the importance of cDC1 in priming CNS antitumor immunity, we investigated how endogenously arising cDC1 might play a role in lymphatic drainage and tumor antigen trafficking from the CNS.

We utilized the traceable fluorophore zsGreen in our experiments as a surrogate for tumor antigen uptake, trafficking, and presentation. A similar approach was used by Krummel's and Merad's labs: each group determined that dendritic cells in draining lymph nodes contained tumor-derived fluorescent protein [21-24]. This experiment is only possible with fluorophores which fluoresce brightly, fluoresce at a low pH, and resist degradation in lysosomes. Conventional fluorophores like GFP do not meet those criteria and are degraded too rapidly to be observed in draining lymph node dendritic cells, although GFP^+ dendritic cells could be observed within the tumor in our preliminary experiments with GL261-GFP tumors. zsGreen fulfills those criteria and fluoresces extremely brightly, fluoresces at low pH, and resists degradation in lysosomes. These features make it an ideal candidate for study of antigen trafficking.

Interestingly, Krummel's group determined that the cDC1 was the primary dendritic cell subset in the lymph nodes which contained tumor-associated fluorophore when they used mCherry to label their tumors; however, when they instead used zsGreen, they found that zsGreen was distributed across both cDC1 and cDC2 subsets, as well as monocytes and macrophages in the lymph node [23]. They reasoned that this was because zsGreen was a more robust fluorophore and persisted for long enough to be "handed off" from the cDC1 to other dendritic cell subsets. In a more recent report, Krummel's group underscored the importance of cDC2 of priming the $CD4^+$ T cell response against soluble ovalbumin-expressing B16 melanoma tumors. In that report, they identified highest levels of

trafficking of zsGreen to lymph nodes by cDC2 and monocyte-derived DC, although significant zsGreen trafficking by cDC1 occurred as well [24]. In our experiments, zsGreen-containing antigen presenting cells across all subsets: cDC1 (predominantly migratory), cDC2, MoDC, and pDC appeared in both the superficial and deep cervical lymph nodes at multiple time points following tumor induction. It was impossible in our experiments to discern whether the surrogate tumor antigen was carried to the lymph node by cDC1 and then passed off to other dendritic cell subsets, or whether that antigen was carried to the lymph node by a non-cDC1 dendritic cell in the first place. Our results as well as the results described by Krummel's group suggest that multiple dendritic cell subsets within draining lymph nodes harbor tumor antigen and potentially carry tumor antigen there. However, our experiments showed that the cDC1 are absolutely required to prime an endogenous neoantigen-specific $CD8^+$ T cell response in mice, and further, that mice harboring intracranial checkpoint-responsive GL261 glioblastoma require cDC1 to derive benefit from αPD-L1 therapy.

An important caveat of the transfer of fluorescence observations is that they still leave open the question regarding the precise behavior of dendritic cells when they phagocytize target material. When a dendritic cell phagocytizes tumor-associated zsGreen, it is possible that (a) the dendritic cell phagocytizes an apoptotic or necrotic tumor cell, (b) that it phagocytizes debris that was leached by a dead or dying tumor cell, or (c) that it ingests a zsGreen containing exosome expelled by the tumor. The zsGreen we employed in our model was cytosolic and could presumably be phagocytized by a dendritic cell in any one of those three scenarios. One approach to determining the mechanism of antigen transfer would be to engineer a tumor that transgenically expressed different fluorophores

engineered to be anchored in different organelles within the cell. By examining the potentially multiple and disparate colors of tumor-associated fluorophores individually or simultaneously present within tumor-infiltrating dendritic cells, one could determine if the dendritic cells had phagocytized cytosolic contents commonly found in exosomes or debris, in a fraction of a cell, or in a whole cell. If the predominant fluorescing dendritic cell population simultaneously fluoresced brightly for all tumor-associated fluorophores that had been anchored to different organelles within the tumor cell, one could conclude that the dendritic cells primarily functioned by engulfing entire tumor cells instead of leached debris. Moreover, additional investigation of this question using high resolution imaging such as electron microscopy could help resolve what parts of the cancer cell a dendritic cell phagocytizes when it captures antigen to prime a T cell response.

We consistently observed that both the superficial and the deep cervical lymph nodes harbored zsGreen-positive conventional dendritic cells following intracranial transplantation with CT2A-zsGreen. Important studies by Kipnis's group found that when Evan's Blue Dye was injected into the ventricles of mice, the deep cervical lymph nodes contained Evan's Blue within 30 minutes of injection. They also remarked that the superficial cervical lymph nodes contained Evan's Blue at later time points [64]. In contrast to those findings, Alitalo's group reported that molecular tracers injected into the brain parenchyma drained only to the deep cervical lymph nodes [65]. In our experiments, we observed that 7 days post-injection of zsGreen-expressing tumors, a relatively larger fraction of cDC1 (and other dendritic cell subsets) were zsGreen$^+$ when isolated from the deep cervical lymph nodes compared to those isolated matched subsets isolated from the superficial cervical lymph nodes at the same time point, although all dendritic cell

subsets still were zsGreen^{+} in both superficial and deep cervical lymph nodes at the early 7 day timepoint (Figure 5-3D, Figure 5-3E). In contrast, at 14 days post-induction, there were percentages of zsGreen^{+} migratory cDC1 that were roughly equivalent between superficial and deep cervical lymph nodes. Additionally, at the day 14 harvest timepoint, all of the dendritic cell subsets were positive for zsGreen compared to control mice in the superficial cervical lymph nodes, whereas at this time point in the deep cervical lymph nodes, only the migratory cDC1 and MoDC were positive for zsGreen. This suggested to us that the deep cervical lymph nodes might be the predominant (but not exclusive) site of tumor antigen trafficking earlier in the CNS antitumor immune response, whereas the superficial cervical lymph nodes might be the predominant (but not exclusive) site of tumor antigen trafficking later in the CNS antitumor immune response.

Although the kinetics of the process of trafficking Evan's Blue dye from the ventricles to cervical lymph nodes in Kipnis' experiments differ greatly from the process of trafficking tumor antigen from brain parenchyma to cervical lymph node (they observed solute drainage to cervical lymph nodes within minutes to hours following intraventricular injection of dye; we observed tumor antigen trafficking to lymph nodes within days to weeks following intraparenchymal injection of tumor cells), our findings somewhat mirror Kipnis' findings in which the deep cervical lymph nodes are the predominant site of early lymphatic drainage, and that the superficial cervical lymph nodes also drain the CNS at later timepoints [64, 194]. Furthermore, the apparent absence of drainage of molecular tracers from brain parenchyma to superficial cervical lymph nodes in Alitalo's studies could be due to the inherent acellular nature of these substrates, or perhaps the location of the injection site [65]. In contrast, we transplanted into the brain parenchyma an expansile

and rapidly growing tumor that created increasingly more traceable fluorophore with each passing day. It is also important to note that the drainage route to the deep cervical lymph nodes compared to the superficial cervical lymph nodes is much better characterized. The drainage pathway to the former consists of lymphatic vessels that traverse along the venous sinuses and converge upon the deep cervical lymph nodes resting upon the internal jugular vein deep in the neck. In contrast, less is known about the drainage route to the superficial cervical lymph nodes.

The CNS drainage pathway to the superficial cervical lymph nodes is known to involve the cribriform plate. Work by Kipnis's group clarified the drainage route when they ablated lymphatics that traverse the cribriform plate using a clever visudyne system to destroy lymphatic vessels in specific anatomic locations around the CNS—they identified that ablation of cribriform lymphatics prevented trafficking of T cells originating from the dura or from the ventricles to the superficial cervical lymph nodes [67]. However, they did not examine dendritic cell trafficking, nor did they comment on the specifics of the drainage route between the cribriform plate and the superficial cervical lymph nodes. Notably, they did identify that this drainage route occurred independently of drainage route to the deep cervical lymph nodes.

Additionally, experiments involving the superficial cervical lymph nodes are further cofounded by the fact that these lymph nodes are also known to perform lymphatic drainage of superficial non-CNS structures on the face. Given all these observations, our experiments with zsGreen strongly suggest that both the deep cervical lymph nodes and the superficial cervical lymph nodes are involved in CNS lymphatic drainage in the context of brain tumors. In the context of experiments regarding dura and antitumor immunity by

other groups, Iwasaki's group identified that expansion of dura lymphatics improved CNS antitumor immunity, and that ligation of the lymphatic vessels which enter the deep cervical lymph node negated that effect [69]. This suggests that the deep cervical lymph nodes are indispensable for CNS antitumor immunity. Our observations of tumor antigen trafficking to and $CD8^+$ T cell clonal expansion within both sets of cervical lymph nodes suggest that both locations might play a role. Future experiments should specifically abrogate either superficial cervical lymph node function or deep cervical lymph node function and compare the possible disparate resulting defects in CNS antitumor immunity.

Lymphatic drainage consists of both migrating cells and bulk solute flow from periphery to lymph node, via lymphatic vessels. The Evan's blue findings by Kipnis underlie the importance of bulk-solute flow in the context of lymphatic drainage of the CNS. In contrast, cellular trafficking requires CCR7. In this process, activated dendritic cells from the periphery use CCR7 to chemotactically migrate into a lymphatic vessel and down a CCL19/CCL21 gradient toward a draining lymph node where the highest concentrations of CCL19 and CCL21 exist [176]. We used the *CCR7*$^{-/-}$ mouse to discern the predominant mechanism of lymphatic drainage in the context of CNS antitumor immunity: active, cell-mediated drainage, or passive, bulk-solute flow. We consistently observed that a much larger fraction of cDC1 isolated from cervical lymph nodes were $zsGreen^+$ in the wild-type compared to the *CCR7*$^{-/-}$ mice. This suggests that tumor antigen trafficking by dendritic cells is predominantly an active process in which dendritic cells phagocytize tumor antigen from within the tumor and carry that tumor antigen to draining lymph nodes, rather than a passive process in which dendritic cells residing in the lymph node "catch" tumor

antigen that wasn't carried to the lymph node by a migrating cell and instead passively flowed there through the draining lymphatic vessel down a pressure gradient.

We used B cells as a control to examine for passive drainage—they are not known to migrate from the periphery to lymph nodes and instead enter lymph nodes via high endothelial venules originating from blood vessels [195]. Our thoughts were that if tumor-derived zsGreen drains passively, B cells in the lymph node would hypothetically phagocytize and retain zsGreen, which we could detect with a flow cytometer. Both the wild-type and *CCR7*$^{-/-}$ mice had small but equal fractions of zsGreen^{+} B cells within the cervical lymph nodes, which suggests that passive drainage is also a potential, albeit minor mechanism of trafficking tumor-associated material to lymph nodes. In the same vein, the dendritic cell zsGreen signal was diminished, but not completely extinguished in the *CCR7*$^{-/-}$ mice, (and was particularly strong in a few of the *CCR7*$^{-/-}$ replicates, which suggests that passive flow can still be sufficient to traffic at least some tumor antigen from CNS to dendritic cells residing in the draining lymph node). Given our observations of intact passive drainage of tumor antigen to draining lymph nodes in various capacities when CCR7 was deficient, it is important underscore that the zsGreen signal was significantly amplified and considerably more robust when active cell migration was intact. Similar to our findings, previous work by Krummel identified that *CCR7* deletion led to a diminished, but not extinguished zsGreen signal in draining lymph nodes in a preclinical melanoma model [23].

An important caveat of using lymph node zsGreen^{+} B cells as a control to measure passive lymphatic drainage is that we additionally observed zsGreen^{+} B cells within the brain tumors of both wild-type and *CCR7*$^{-/-}$ mice. These B cells may have extravasated

from the blood into the brain tumor via leaky capillaries, which are known to permeate a brain tumor's parenchyma. We do not know the function of B cells in the tumor—whether they were bystanders or performing an important function remains unknown. Nor can we completely exclude the possibility that B cells migrated from the brain tumor to cervical lymph nodes. However, migration from the periphery to lymph nodes in this setting is not a known B cell function. Additionally, if B cells did migrate from the brain tumor to cervical lymph nodes, we presume that this process would require CCR7, as is the case with dendritic cells and T cells. Our observation was that small but equal fractions of zsGreen$^+$ B cells could be isolated from the cervical lymph nodes of both wild-type and *CCR7*$^{-/-}$ mice. If B cells phagocytized tumor antigen in the tumor and migrated from the brain tumor to cervical lymph nodes (presumably in a CCR7 dependent fashion), we would expect wild-type mice to have much larger fractions of lymph node zsGreen$^+$ B cells compared to *CCR7*$^{-/-}$ mice. The fractions of zsGreen$^+$ cervical lymph node B cells were both small but also equal between wild-type and *CCR7*$^{-/-}$ mice, which suggests that zsGreen$^+$ B cells are an appropriate control for passive drainage in our experiments.

Previous work has identified the meninges as an immunologically dynamic structure that harbors cDC1, cDC2, and pDC [49, 55], and furthermore, that conventional dendritic cells within the dura could expand in response to Flt3L as a stimulus [177]. In addition to harboring these dendritic cell subsets, the dura is vested with lymphatic vessels [64, 65, 191] which drain CSF and as well as antigens from the CNS to the deep cervical lymph nodes in the neck. The dura lymphatic vessels have been shown to expand in response to VEGF-C stimulation to bolster the CNS antitumor immune response [69]. Our work extends these findings—we identified that all dendritic cell subsets within the dura expanded in response

to the stimulus of a brain tumor, and that we could additionally expand all dendritic cell subsets, including the cDC1 subset, by systemic administration of Flt3L. Furthermore, we observed cDC1 in dura lymphatic vessels by 2-photon microscopy, and additionally observed tumor-derived zsGreen within dendritic cells harbored by the dura when mice bore zsGreen-expressing brain tumors. Our collective observations could represent dendritic cells phagocytizing tumor antigen from within the tumor and trafficking the tumor antigen to the deep cervical lymph node, via dura-lymphatics. The transit point and the mechanism by which antigen enters the dura-lymphatic vessels remains an open question, and further work is needed to investigate this phenomenon.

After characterizing the dynamics of lymphatic drainage, tumor antigen trafficking, and dura involvement in the CNS antitumor immune response, we next investigated the downstream steps of this process, in particular the location of T cell priming in CNS antitumor immunity. Given our observations that zsGreen-containing dendritic cells could be isolated from both groups of cervical lymph nodes, from the tumor, and from the dura, we considered the possibility that any of those anatomic locations could be a potential site for a tumor antigen-containing dendritic cell to encounter a cognate T cell and initiate T cell priming. We also considered other locations, such as the spleen, as a location of priming the CNS antitumor immune response. To investigate this phenomenon, we employed an ovalbumin-expressing tumor and monitored for expansion of adoptively transferred CFSE-labeled OT-I $CD8^+$ T cells in the different previously mentioned anatomic locations. We envisaged that locations of naïve T cell priming in the setting of the CNS antitumor immune response would display the earliest evidence of clonal expansion of OT-I T cells, and thus would harbor the bulk of early-primed CFSE-mid, OT-

I CD8$^+$ T cells. Accordingly, we observed earliest expansion of OT-I CD8$^+$ T cells in both the superficial and deep cervical lymph nodes. They consistently harbored the bulk of CFSE-mid, early primed, OT-I CD8$^+$ T cells among the organs we examined. Moreover, we primarily observed the CFSE-low, terminally divided OT-I CD8$^+$ T cells at the later day 6 post-transfer timepoint, and the majority of them localized to the tumor. While expanded OT-I cells sometimes appeared in the tumor and dura by the early time point, they were always terminally expanded, CFSE low, which suggests that they had been primed elsewhere, in particular the cervical lymph nodes, as suggested by our observations. Notably, neither the spleen, the dura, nor the non-CNS draining inguinal lymph node appeared to be the site of clonal expansion of adoptively transferred OT-I cells. Our observations extend previous work done with EAE models in which investigators showed that cervical lymph node resection dampened disease burden [61-63], and expand the known role of cervical lymph nodes to include priming a CNS antitumor immune response. Additional experiments should include abrogating cervical lymph node function and monitoring for T cell response, and alternatively preventing T cell egress from lymph nodes with a sphingosine-1-phosphate receptor antagonist and examining for down-stream effects on CNS antitumor immunity.

We expanded our findings to define the role of cDC1 and CCR7 in this process of T cell priming in antitumor immunity. In CCR7-deficient and cDC1-deficient mice, we determined that both of these defects led to delayed, but not completely defective clonal expansion of adoptively transferred OT-I T cells. This could be for a variety of reasons. We know from our previous experiments that cDC1 are required for endogenous priming of neoantigen-specific CD8$^+$ T cells, and that cDC1 are additionally required to mediate

survival benefit conferred by checkpoint blockade in a preclinical model of glioblastoma. However, these two different scenarios of T cell expansion are quite different. The ovalbumin brain tumor/OT-I adoptive transfer experiments involved initiating a T cell response with several hundred thousand adoptively transferred naïve T cells against a tumor that overexpresses a particular antigen recognized by those T cells. In contrast, the unmodified GL261 brain tumor experiments involved allowing 1-100 naïve T cells comprising the precursor population of a particular T cell clone to be spontaneously primed and to clonally expand on their own. The former scenario in which both tumor antigen expression and precursor T cell frequency are artificially high might be a sufficient catalyst to overcome some of the defect created by absence of cDC1. Moreover, the ovalbumin construct we used is not entirely cell-associated—there is no sequence or structure anchoring it to the cell membrane. In addition to specializing in cross presentation, cDC1 are specifically equipped to handle cell membrane-associated antigen [26]. Soluble ovalbumin, which these tumors make, could potentially be cross-presented by other dendritic cell subsets in small but non-zero amounts sufficient drive OT-I $CD8^+$ T cell expansion (albeit less efficiently), even in the absence of cDC1 [26, 29]. This was reflected by our observations: given enough time in cDC1-deficient mice, OT-I $CD8^+$ T cells still expanded when mice harbored GL261-OVA brain tumors.

Interestingly, we also observed delayed but not absent OT-I $CD8^+$ T cell expansion in *CCR7*$^{-/-}$ mice compared to wild-type mice. At day 3 post-adoptive transfer, OT-I $CD8^+$ T cells had failed to expand in *CCR7*$^{-/-}$ mice whereas at the same time point they had expanded robustly in cervical lymph nodes of wild-type mice. In contrast, at day 6 post-adoptive transfer, OT-I $CD8^+$ T cells expanded in proportions comparable between both

CCR7$^{-/-}$ and wild-type mice in all the tissues we analyzed. This suggests that there exist cell migration-independent mechanisms of trafficking tumor antigen from the CNS to draining lymph nodes. An important caveat that warrants mention is that we could not determine where initial priming and OT-I CD8^{+} T cell expansion initially commenced in *CCR7*$^{-/-}$ mice—it was as if in these mice there was negligible OT-I clonal expansion in the cervical lymph nodes by day 3 post-adoptive transfer, and by day 6 post-adoptive transfer we observed expanded OT-I CD8^{+} T cells in every anatomic location we examined. Additional experiments should examine the nature of expansion at different time points that fall between days 3 and 6 post-adoptive transfer, and specifically, to determine where the first site of clonal expansion of adoptively transferred OT-I cells occurs in *CCR7*$^{-/-}$ mice.

One additional caveat of our observations regarding the relationship between host CCR7-deficiency and clonal expansion of adoptively transferred T cells is that we used an artificial system of T cell priming by performing experiments that involved adoptive transfer of large numbers of T cells and overexpression by the tumor of the cognate antigen that the T cells recognized. Moreover, CCR7-deficiency in mice leads to broad immunologic defects. We know from our experiments that that precise deficiency of a single cell type, the cDC1, leads to defective neoantigen-specific T cell priming and incompetent immune responses against CNS tumors. The same precise experiment which isolates and implicates a single cell type is not possible in *CCR7*$^{-/-}$ mice. The goal of our experiments with the *CCR7*$^{-/-}$ mice was to determine the immunologic defects caused by deficient dendritic cell trafficking of tumor antigen from brain tumors to draining lymph nodes. However, *CCR7*$^{-/-}$ mice harbor additional defects in the immune response:

they have defective T cells in addition to all dendritic cell subsets. This is because both T cells and dendritic cells require CCR7 to migrate to the proper location in a lymph node's paracortex to commence T cell priming and clonal expansion through antigen presentation and co-stimulation by activated dendritic cells. We attempted to circumvent this problem by adoptively transferring *CCR7*$^{WT/WT}$ OT-I CD8^{+} T cells into *CCR7*$^{-/-}$ hosts, however our adoptive transfer experiments involved a precursor frequency of several hundred thousand adoptively transferred T cells clonally expanding in response to an overexpressed tumor-associated antigen, which is somewhat unrealistic. The proper way to address the requirement of cell migration from periphery to lymph nodes by cDC1 in mounting CNS antitumor immunity would be to selectively restrict CCR7-deficiency to the cDC1 subset and monitor for endogenous T cell priming in that setting. This could be achieved by using a *CCR7*$^{-/-}$ + *IRF8+32kb*$^{-/-}$ mixed bone marrow chimera, or by crossing an *XCR1-Cre* mouse (cDC1-specific Cre) to a *CCR7*$^{fl/fl}$ mouse.

Important work remains to establish the role and importance (or lack thereof) of cDC1 migration in antitumor immunity of the CNS, and to further characterize the complete pathway of cDC1 migration from tumor parenchyma in the CNS to the dura lymphatic vessel, and from the dura lymphatic vessel to the cervical lymph nodes, in particular, superficial cervical lymph nodes given their less well-characterized drainage route compared to deep cervical lymph nodes.

CHAPTER SIX

Dendritic cells and antigen presentation in human GBM

6.1 Introduction

In mouse preclinical models of GBM we demonstrated that cDC1 play a critical role in mounting an effective antitumor immune response in the CNS—they are required to both prime neoantigen-specific $CD8^+$ T cell responses as well as to mediate survival benefit conferred by checkpoint blockade in the setting of malignant glioma. We also demonstrated evidence which suggests that cDC1 carry out their role in part by phagocytizing tumor antigen from within the tumor, migrating via dura lymphatics, and appearing with phagocytized tumor antigen in the deep and the superficial cervical lymph nodes, where they prime $CD8^+$ T cells to drive clonal expansion to mount antitumor immunity against the tumor residing in the CNS. We also showed that these processes of brain tumor antigen trafficking and clonal expansion of adoptively transferred $CD8^+$ T cells depend on both presence of cDC1 and intact CCR7-mediated cell migration to occur with normal kinetics. Despite the results from these experiments, as well as other rodent studies which clarified the role of dendritic cells in the progression of the CNS immune response in other disease processes or which demonstrated the importance of dura lymphatics in CNS immunity (including CNS anti-tumor immunity), little is known about whether or how dendritic cells play a role in human brain tumors, or in the human central nervous system more broadly.

To date there have been a few isolated reports regarding dendritic cells in the human brain. Researchers have identified dendritic cells in human choroid plexus by cellular expression of HLA-DR [196]. A second report described in greater detail dendritic cells embedded among epithelial cells in the choroid plexus. Observers described cells in the choroid plexus which both expressed HLA-DR, possessed long dendrites extending in all directions, and lacked tight junction proteins expressed by their epithelial cell neighbors [197]. Dendritic cells have also been isolated from human CSF and characterized as cDC by their expression of HLA-DR, CD11c and variable expression of CD123 to discern pDC from cDC (human pDC are $CD123^+$, human cDC are $CD123^-$) [198]. Investigators have also identified CD209-expressing cells (an established human dendritic cell marker) in extravascular spaces in the brain that lie beyond the glia-limitans and well into the brain parenchyma [199]. An interesting study of human stroke patients identified transient decreases in circulating dendritic cells and increased infiltrate of dendritic cells over background into the diseased area in both ischemic and hemorrhagic strokes, which reflected a potential recruitment of dendritic cells into the brain from the blood into injured tissue [200]. In another stroke study, researchers identified that APC (including $CD1c^+$ dendritic cells) in the cervical lymph nodes and palatine tonsils harbored neuronal-derived and oligodendrocyte-derived antigens in levels greater than in healthy control patients [201]. They did not explore cDC in the brain directly, but this study's implications hint toward the relationship between the brain and extracranial immune responses in humans, which would be consistent with similar observations from mice. Despite these discoveries, little is known about the potential role of dendritic cells in antitumor immunity of human brain tumors.

Most studies that have examined innate immunity in human GBM have not focused on dendritic cells and instead have investigated the immune-suppressive mechanisms of the tumor itself, as well as how the infiltrating innate immune cells engage in immune-suppressive behavior. Previous work has identified that the microenvironment of human GBM tumors could induce PD-L1 expression on monocytes/macrophages isolated from healthy donors [88]. Studies have also shown that human GBMs are infiltrated by MDSCs [89], and that GBM patients tend to have high levels of circulating MDSCs compared to healthy controls [90]. Moreover, experiments have shown that tumor associated macrophages and microglia express high levels of the immune-suppressive cytokine IL-10 [83, 84]. Although these researchers demonstrated the immune-suppressive functions which APC and innate immune cells can perform within the tumor microenvironment, they fall short of explaining whether or how cDC infiltrate the tumor and perform their function of antigen presentation to prime T cell responses. Perhaps similar to in mice, human cDC have been underappreciated and understudied in brain tumors due to their low background prevalence in the brain parenchyma.

Most of the work on dendritic cells in human brain tumors has centered around developing dendritic cell vaccines for glioma. These efforts originate from rodent studies performed in the late 1990s/early 2000s, in which researchers identified that pulsing exogenously cultured monocyte-derived dendritic cells with peptides derived from glioma tumors followed by subsequent vaccination with those antigen-loaded monocyte-derived dendritic cells led to greater infiltration of $CD4^+$ and $CD8^+$ T cells into the rodent brain tumors compared to control mice [202]. These researchers also determined that the monocyte-derived dendritic cell vaccination strategy led to improved survival in these

rodent models as well [203]. The findings spurred investigators in 2001 to design a phase 1 clinical trial in which peptide derived from the patient's brain tumor was combined with autologous cultured monocyte-derived dendritic cells to create a personalized vaccine. Vaccination was demonstrated to lead to increased $CD8^+$ T cell and memory T cell infiltrate into the tumors in 2/7 of the vaccinated patients, with evidence of systemic response in 4/7 vaccinated patients [204]. More recently, Northwest Biotherapeutics has enrolled patients in a phase III clinical trial called DCVax, which uses a similar formulation of dendritic cell vaccines. To administer this dendritic cell vaccine, researchers expose a patient's own autologous monocyte-derived DC to their brain tumor lysate and inject these tumor lysate-exposed DC intradermally [121]. This trial is currently underway and reports a median survival of 23.1 months and a subset of long-term survivors in their intent-to-treat cohort compared to the placebo group [122]. Despite early promise, the trial is ongoing and DCVax has not proven to change the standard of care for GBM.

Although there might be some early hints of benefit from these vaccines, they have not radically changed GBM treatment strategies at present. Notably (and perhaps for apparent historical reasons), these DC-vaccine studies and trials have employed exogenously derived cultured dendritic cells known as monocyte-derived dendritic cells, which were first developed in 1992 in mice, and which require culturing hematopoietic stem cells (HSCs) with GM-CSF and IL-4 [205, 206]. Just two years after the rodent studies, researchers successfully differentiated human HSCs into equivalent monocyte-derived dendritic cells using a similar technique [207]. Monocyte-derived dendritic cells may have been selected for cancer vaccines for a variety of reasons. First, researchers have how to differentiate them successfully since the mid 1990s. Second, they can present soluble

antigen efficiently *in vitro*. Third, additional characterization suggests they are a functional dendritic cell beyond sheer antigen presentation capability: they lack expression of the monocyte marker CD14, they express costimulatory molecules required for priming T cells, and can actually stimulate naïve T cell proliferation *in vitro* [207]. Researchers have also demonstrated that monocyte-derived dendritic cells can induce demonstrable benefit with respect to antitumor immune responses—dendritic cell vaccines were demonstrated to broaden the neoantigen-specific T cell repertoire in melanoma patients [208]. Despite these potential benefits from vaccination with monocyte-derived dendritic cells, these cells are not true dendritic cells that arise endogenously *in vivo*.

In contrast to exogenously cultured monocyte-derived dendritic cells, endogenously arising conventional dendritic cells require Flt3L for development, and have been demonstrated to expand in both mice [209] and in humans [210] following systemic administration of Flt3L. Conversely, experiments in mice have demonstrated that administration of GM-CSF and IL-4, the same factors used to generate monocyte-derived dendritic cells *in vitro*, causes no such expansion conventional dendritic cell populations or monocyte-derived dendritic cell populations *in vivo* [209]. Moreover, conventional dendritic cells are transcriptionally distinct from exogenously cultured monocyte-derived dendritic cells [190]. Additionally, monocyte-derived dendritic cells and are comprised of a heterogeneous population of monocyte-derived macrophages and cDC-like cells with unique and disparate functions [211]. Researchers have sorted the cell populations comprising cultured monocyte-derived the dendritic cells and identified that the cDC-like fraction is much more capable of stimulating $CD4^+$ and $CD8^+$ T cell proliferation compared to macrophage-like population *in vitro* [211].

Beyond *in vitro* differences demonstrated between conventional dendritic cells and monocyte-derived dendritic cells, of the conventional dendritic cell subsets, true cDC1 are the only dendritic cells that arise endogenously and cross present antigen *in vivo* [25, 212]. Critically, cDC1 are the only cell type that has been repeatedly demonstrated to elicit potent $CD8^+$ T cell responses and to be required for antitumor immunity *in vivo* [20-23, 25-31]. cDC1 are also the only dendritic cells that can process cell-associated antigen *in vivo* [26], as is the case for many neoantigens derived from tumor cells. Despite these potential advantages of using true dendritic cells for a vaccine, GM-CSF/IL-4 cultured monocyte-derived dendritic cells have had such a strong foothold in vaccine studies of GBM and other tumors likely because researchers did not know how to culture human HSCs into bona fide cDC until recently, and the issue still stands regarding how to generate sufficient numbers of human cDC to generate a vaccine from exogenously cultured dendritic cells. Flt3L exposure alone is sufficient to culture dendritic cells from mouse bone marrow-originating HSCs [213, 214]. In contrast, human dendritic cells are much more difficult to generate exogenously. Culturing human HSCs with Flt3L results in few dendritic cells, unlike with mice. Only recently in 2018 did researchers develop a method to generate somewhat appreciable numbers of functional human cDC1 and cDC2 from HSCs [215]. This technique requires co-culturing HSCs with adherent OP9-DL1 feeder cells to induce notch signaling, and requires adding to the media Flt3L, stem cell factor, and GM-CSF in order to differentiate a large fraction of HSCs into cDC [215]. This complex protocol still might fall short of generating a sufficient number of cDC for a dendritic cell vaccine. The delay of the development of this protocol until much more recently, combined with the lingering issue of insufficient dendritic cell numbers resulting from this culture method, have

contributed to the significant delay in using conventional dendritic cells instead of monocyte-derived dendritic cells for dendritic cell vaccines.

In addition to the difficulty regarding culturing human dendritic cells, studies to determine which dendritic cell subsets in mice correlate to their human counter parts have not been published since the last decade or so. Poulin and colleagues identified a subpopulation of human blood dendritic cells analogous to the mouse cDC1 which also express the mouse cDC1-specific cell surface marker Clec9A, express high levels of IRF8 and BATF3 transcription factors (required for mouse cDC1 development), respond to TLR agonists, produce IL-12 (also mouse cDC1-spefic), and which have been shown to present exogenous proteins derived from internalized dead cells to prime $CD8^+$ T cells *in vitro* (in which mouse cDC1 specialize) [216]. Notably, this study also showed that $CD8\alpha^+$ human DC possessed superior ability to phagocytize dead cells, and to cross present antigen, when compared to monocyte-derived dendritic cells *in vitro* [216]. This equivalence between the mouse and human cDC1 counterparts was further underscored by a case report of a patient with biallelic *IRF8* mutations, which caused severe immunodeficiency [217]. *IRF8*$^{-/-}$ mice have completely defective cDC1 development [183]. The patient with the biallelic *IRF8* mutations had a complete loss of circulating pDC ($CD123^+$ DC) and cDC1 ($CD141^+$ cDC), as well as a monocyte deficiency, underscoring the parallel between the human $CD141^+Clec9A^+$ cDC and the mouse cDC1 subset.

Given the dearth of knowledge regarding the role of dendritic cells in human brain tumors, the lack of understanding regarding endogenously arising CNS antitumor immunity, and the focus on monocyte-derived dendritic cell vaccines as a form of immunotherapy to treat brain tumors (which for reasons described above may not be the most appropriate cell

type), we set out to determine the role of endogenously arising dendritic cells in human brain tumors and to describe the characteristics of cDC1 within anatomic locations inside and adjacent to the tumor. We also devised an assay that like our mouse models, leverages a tumor-specific fluorophore as a surrogate for tumor antigen. We again leveraged the transfer of fluorescence principle to measure tumor-antigen uptake by tumor-infiltrating dendritic cells, including the human cDC1 equivalent $CD141^+$ cDC.

6.2 Results

6.2.1 The human equivalent of the cDC1 is detectable in dura and brain tumors

Having demonstrated that mouse dura and brain tumors harbored orders of magnitude more dendritic cells than the same anatomic locations in the steady state, and also having demonstrated the important role of the cDC1 in mounting CNS antitumor immunity in mice, we investigated the infiltrate of human dura and brain tumors for the presence of the human cDC1-equivalent: the $CD141^+$ cDC. In both mice and humans, the cDC1 can produce IL-12 [216], cross present exogenous proteins derived from internalized dead cells to $CD8^+$ T cells [216], and expresses high levels of IRF8 [188], a critical regulatory factor required for cDC1 development in mice [183] and in humans [217].

We explored the immune cell populations comprising the cellular infiltrate of tumor and matched dura specimens from patients undergoing craniotomies for tumor resection for whom there was, in addition to an indication to resect the tumor, a clinical indication to resect the tumor-adjacent dura as well (Figure 6-1A). We disaggregated several patients' tumor and matched dura specimens from five meningiomas and a GBM. We analyzed an additional twelve GBM tumor specimens in which no dura was resected. We performed flow cytometry to characterize the immune infiltrate of these samples, with particular focus

on dendritic cells. In both GBM tumors as well as meningiomas, we detected the presence multiple human dendritic cell equivalents, in addition to other APC subsets, within the cellular infiltrate of the patients' respective tumor and dura specimens. We observed the cDC1 ($CD141^+$ cDC) and cDC2 ($CD1c^+$ cDC) subsets, $CD14^+$ classical monocytes, as well as $CD16^+$ non-classical monocytes, in dura and tumor samples (Figure 6-1B, 6-1C, 6-1D). Additionally, we also observed $CD4^+$ T cells as well as $CD8^+$ T cells in most of the thirteen total GBM specimens that we analyzed (Figure 6-1C). Moreover, between the GBM and meningioma dura specimens, the tissue harbored similar fractions of $CD141^+$ cDC, $CD1c^+$ cDC, $CD14^+$ classical monocytes, and $CD16^+$ non-classical monocytes (Figure 6-1E), although our analysis was limited to a single GBM sample in which dura was additionally resected. These findings collectively demonstrate that human conventional dendritic cell subsets are abundant in dura and tumors and across different brain tumor types, which suggests they play a role in human CNS antitumor immunity.

Figure 6-1

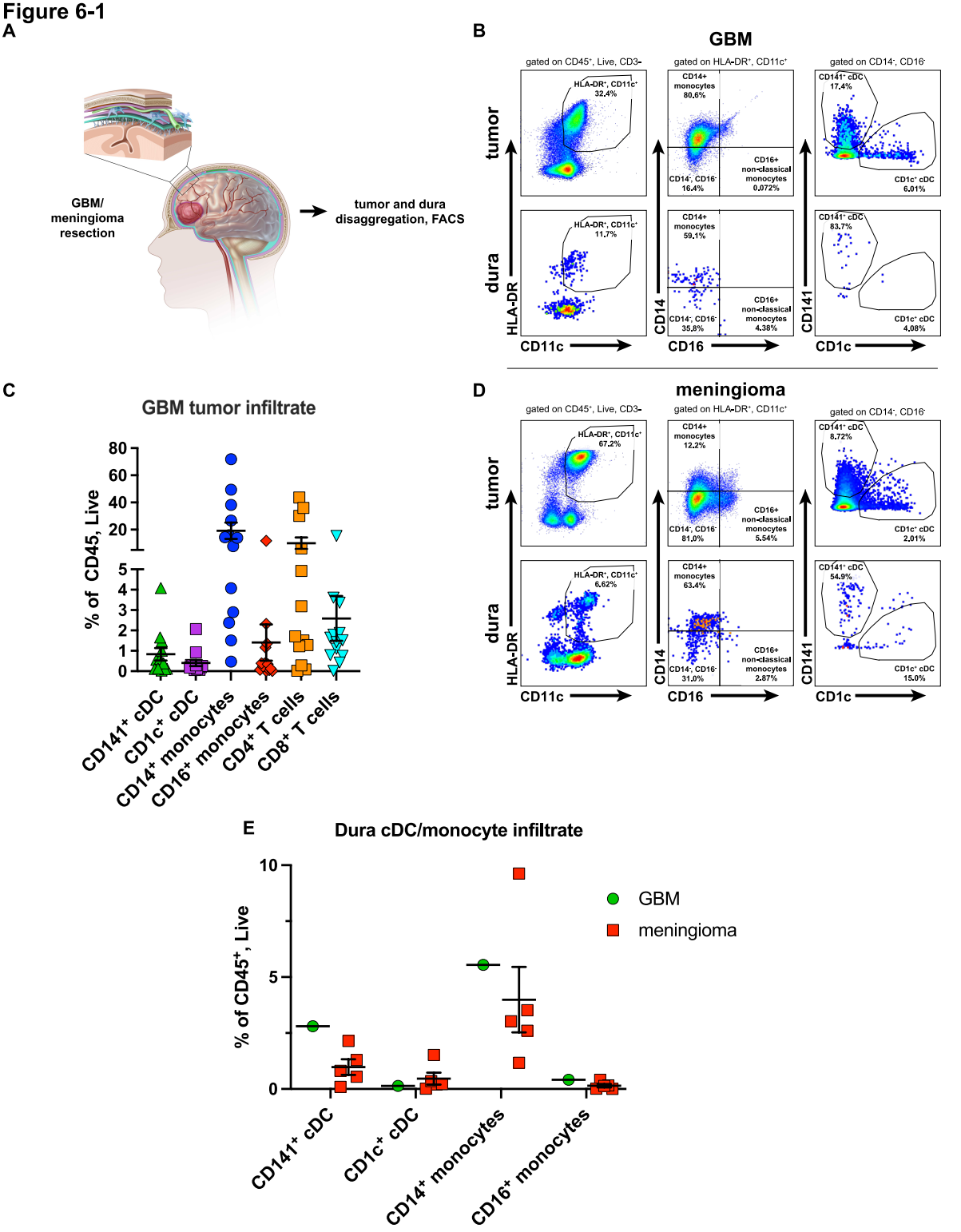

Figure 6-1. Dendritic cells infiltrate human dura and brain tumors. Representative sketch of meningioma/associated dura or GBM/associated dura. B. Flow cytometry of immune infiltrate of GBM tumor and dura. C. GBM immune infiltrate quantified as a fraction of $CD45^+$/live cells from twelve GBM specimens (ten primary and two recurrent). D. Flow cytometry of immune infiltrate of meningioma tumor and dura. E. Quantification of APC subsets from one GBM and five meningioma dura samples.

6.2.2 The CD141+ cDC phagocytizes a tumor specific marker in GBM

Having identified in mice that a fluorophore transgenically expressed by the brain tumor could be detected within cDC1 (and other dendritic cell subsets) isolated from the tumor, the dura, and the cervical lymph nodes, we next investigated whether this phenomenon of tumor antigen transfer occurred in dendritic cells isolated from human GBM. During GBM resection, the FDA-approved drug 5-aminolevulinic acid (5-ALA) can be used to fluorescently label the tumor to distinguish it from normal brain [218-221]. 5-ALA is administered systemically during the preoperative period, extravasates from the leaky blood vessels that permeate the tumor, and is imported and converted by target tumor cells to the fluorescent metabolite, protoporphyrin IX (PPIX) [222]. PPIX is selectively retained by, and highly specific to tumor cells [222, 223]. During resection, the neurosurgeon can illuminate the tumor with blue light, and the PPIX harbored by the tumor selectively fluoresces pink, which allows the surgeon to discern fluorescent pink tumor-tissue from dark blue normal brain to safely and maximally resect the tumor without disturbing normal brain (Figure 6-2A). We leveraged the same principle we had employed previously with fluorescent mouse GBM tumors to investigate human GBM. This principle relies on the premise that fluorescent material specific to the tumor could potentially be transferred to, and detectable within tumor-infiltrating dendritic cell subsets (Figure 6-2B).

When incorporated into cells, PPIX fluoresces across the wavelengths that span the brilliant violet channels on a conventional flow cytometer. To test whether we could detect $PPIX^+$ cells by FACS, we first disaggregated a GBM tumor which was resected using 5-ALA and subjected the resulting purified single cell suspension to flow cytometry. We determined that the PPIX signal was strongest in the BV650 channel and were able to

observe clearly defined $PPIX^-$ and $PPIX^+$ populations within the sample (Figure 6-2C, left). In an orthogonal approach we additionally exposed the U343 GBM cell line to 5-ALA *in vitro*. Compared to untreated U343 cells, 5-ALA-exposed U343 cells fluoresced brightly in the BV650 channel (Figure 6-2C, right).

We designed a panel that could stain for conventional dendritic cell subsets, monocytes, and T cells, while leaving open the brilliant violet channels that span the PPIX fluorescence spectrum, including BV650, to avoid potential compensation conflicts. Whereas with preclinical models, we could use a non-fluorescent brain tumor as a negative control for a fluorescing brain tumor to determine that a fluorescent signal in dendritic cells was specific to the transgenic expression of a tumor-specific fluorophore, and to additionally discern the fluorescence intensity cutoff between positive and negative fluorophore expression, no such control exists for human brain tumors resected using 5-ALA/PPIX. To try to identify a $PPIX^+/PPIX^-$ fluorescence intensity, we devised two internal controls with two questions in mind. First would PPIX fluorescence depend on immune cell identity, with only phagocytic cells acquiring PPIX? Second, would PPIX fluorescence depend on cell location, with only tumor-infiltrating immune cells acquiring PPIX?

We surmised that a brightly fluorescing $PPIX^+$ tumor would harbor high levels of PPIX in the microenvironment, and that any cells that had infiltrated the environment would be universally exposed to PPIX. However, if a unique cell population, such as $CD3^-$ cells (which includes phagocytic cells) was the only $PPIX^+$ cell population, PPIX fluorescence could be attributed to the specific identity of the infiltrating immune cell rather than solely because that cell had been exposed to a high concentration of PPIX. This was the basis for our first control to identify a $PPIX^+/PPIX^-$ fluorescence cutoff.

As our second control, we harvested, stained with the same antibody panel, and performed flow cytometry on patients' intraoperative peripheral blood mononuclear cells. This controlled for systemic exposure of APC to 5-ALA and allowed us to identify a $PPIX^-$ cutoff through a second means by analyzing matched peripheral cells, which were presumably exposed to lower concentrations of 5-ALA/PPIX, against tumor-infiltrating cells where PPIX was most concentrated. If circulating dendritic cells systemically exposed to 5-ALA did not fluoresce with PPIX, any potential PPIX signal observed in dendritic cells infiltrating the tumor would be attributable to them having infiltrated the tumor, rather than having been systemically exposed to 5-ALA. By using these controls and identifying a range of cellular PPIX fluorescence intensities, we were able to discern a fluorescence intensity cutoff $PPIX^+$ vs. $PPIX^-$ cell populations, akin to the fluorescence intensity cutoff we identified between $zsGreen^+$ and $zsGreen^-$ populations by comparing a zsGreen-transduced tumor against a non-transduced control.

We hypothesized that PPIX would be detectable specifically in tumor-infiltrating rather than peripheral immune cells, and further, that only phagocytic cells would fluoresce with PPIX. To test these hypotheses, we performed flow cytometry on intraoperatively taken PBMC along with a patient's disaggregated GBM tumor which had been resected using 5-ALA/PPIX. Of a patient's $CD45^+$/Live PBMCs, neither the $CD3\varepsilon^+$ fraction, nor the $CD3\varepsilon^-$ fraction fluoresced with PPIX (Figure 6-2D, left, figure 6-2E). In contrast, of a patient's $CD45^+$/Live tumor-infiltrating immune cells, only a miniscule fraction of $CD3\varepsilon^+$ cells were PPIX-positive, whereas a significantly larger fraction of the $CD3\varepsilon^-$ cells were PPIX-positive (Figure 6-2D, right, Figure 6-2E). These observations demonstrate that the phenomenon of PPIX-fluorescence within $CD45^+$ cells was attributable to their cell identity (tumor

infiltrating CD3ε$^-$ cells, but not CD3ε$^+$ cells were PPIX-positive), and specific to a cell's anatomic localization to the tumor (Peripheral CD3ε$^-$ cells where largely PPIX-negative, whereas a significant fraction tumor infiltrating CD3ε$^-$ cells were PPIX-positive).

We next investigated whether different tumor infiltrating APC subsets had detectable levels of PPIX in six primary and two recurrent GBM specimens that had been resected using 5-ALA. We used peripheral intraoperative PBMCs to determine where to set the negative/positive threshold for PPIX-positivity by comparing PPIX-fluorescence between corresponding antigen presenting cell populations isolated from the tumor against matched cells from the periphery. We identified that compared to their matched controls, majorities of tumor-infiltrating CD141$^+$ cDC1, CD1c$^+$ cDC2, CD14$^+$ classical monocytes, and CD16$^+$ non-classical monocytes contained PPIX (Figure 6-2F, Figure 6-2G). Moreover, across all tumor samples the PPIX-signal was absent from T cells and instead specific to antigen presenting cells that had infiltrated the tumor (Figure 6-2H).

The fraction of a particular APC population that was PPIX-positive varied between APC identities as well as patients, similar to our observations in mice with zsGreen. However, our observations suggest that multiple distinct APC subsets infiltrating the tumor possessed the required machinery to home to the tumor and to phagocytize tumor-derived material after arriving, similar to our observations in mice. Collectively, these data demonstrate that the phenomenon of acquiring tumor-derived material by immune cells was specific to cell identity (phagocytic but not CD3ε$^+$ immune cells within the tumor were PPIX$^+$) as well as cell location (tumor-infiltrating but not peripheral phagocytic cells of the same identity were PPIX$^+$). These data also underscore the similar behavior shared between mouse and human phagocytic cells in the setting of brain tumors.

Figure 6-2

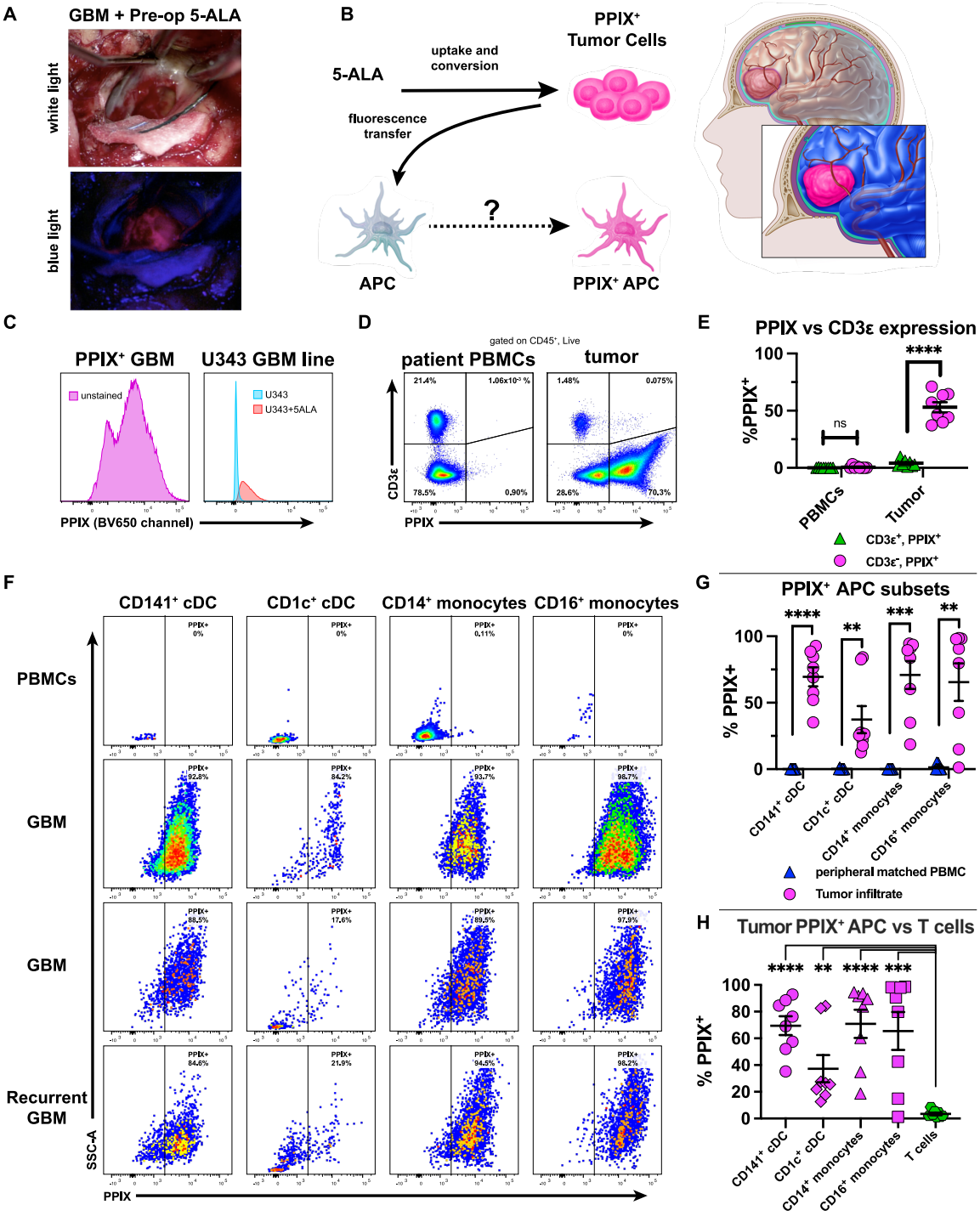

Figure 6-2. Dendritic cells infiltrate human GBM and retain the tumor-specific reporter PPIX. A. Photograph of GBM after 5-ALA administration illuminated by white (top) or blue (bottom) light. B. Schematic describing experimental concepts. C. 5-ALA/PPIX$^+$ tumor single cell suspension without antibodies (left) or PPIX$^+$ U343 cells on the BV650 channel (right). D. CD3ε expression by PPIX fluorescence gated on CD45$^+$/Live PBMC (left) or CD45$^+$/Live tumor (right) cells. E. PPIX fluorescence quantified in CD3ε$^+$ vs. CD3ε$^-$ fractions in either PBMC or tumor. F. PPIX expression in APC subsets across 3 representative tumors compared to peripheral PBMCs harvested at the time of surgery, quantified in G across 8 specimens. H. PPIX fluorescence quantification in tumor APC vs. tumor T cells.

6.3 Conclusion and Discussion

Here we demonstrate that human brain tumors and adjacent matched dura harbor conventional dendritic cells in meningiomas and GBM. Furthermore, in a surrogate assay for tumor antigen uptake and presentation, we also demonstrate that GBM infiltrating cDC1, cDC2, and monocytes are positive for the tumor antigen-surrogate PPIX, which is used to in 5-ALA fluorescence-guided surgery to resect GBM. We determined that this signal was specific to cells that had infiltrated the tumor, and was unique to non-T cells (i.e., phagocytic cells) within the tumor. The PPIX fluorescence intensities which varied between cell type and were dependent on cell location comport with our understanding that the highest concentration of PPIX lies within the tumor and that phagocytic cells within the tumor preferentially acquire tumor-derived material compared to non-phagocytic cells within the tumor. These observations fit with our understanding regarding the mechanisms of fluorescence transfer. They suggest that the results from our experiments designed to observe a surrogate for antigen uptake represent a naturally occurring biologic phenomenon that arises endogenously in the tumor. Moreover, we observed similar findings in 8 different GBM specimens, which further corroborates the conclusions we drew from the data. These experiments demonstrate that across multiple patients, dendritic cells and monocytes infiltrate GBM and phagocytize tumor-associated material once they arrive, a function that dendritic cells were known to perform, but which has yet to be directly observed in human tumors to our knowledge.

The majority of studies regarding dendritic cells in the CNS have focused on preclinical models in rodents, and for obvious reasons—acquiring human brain tissue is only possible in unique cases. Most human dendritic cell studies have been restricted to the

study of blood, due to the limited availability of donors and the limited ability to collect tissue without compromising patients' health. With the advancement of cancer immunology as a field, human brain tumor specimens have been probed for neoantigen-specific T cells, which have been observed in the vaccine setting [224-226]. In the non-tumor setting, lymphatic vessels have been observed with non-invasive techniques in human and non-human primates using clever MRI imaging sequences [68]. However, to date there are a paucity of studies which describe the role or presence of dendritic cells in human brain tumors. Most previous work has identified dendritic cells in isolated locations, like the choroid plexus [196, 197], the CSF[198], just beyond the glia limitans, [199], or as having relevance in stroke [200, 201]. Despite these discoveries, little is known about dendritic cells in human brain tumors.

Most studies that have examined innate immunity in human brain tumors have instead focused on the immune-suppressive mechanisms in GBM, or on dendritic cell vaccines, instead of on the endogenously arising conventional dendritic cells that home to the tumor without an exogenous stimulus. While the immune suppression mechanisms of GBM are extensive [83, 84, 88-90], we set out to instead study endogenously arising dendritic cells as well as their potential role in antigen capture within the tumor, with a focus on conventional dendritic cells. We identified the $CD141^+$ cDC1 human equivalent, along the $CD1c^+$ cDC2 human equivalent in human dura and tumor samples across different tumor types, including GBM specimens as well as meningiomas. We analyzed both meningiomas and a GBM tumor in which associated matched dura was also resected. We additionally analyzed eleven GBM tumor specimens (nine primary, two recurrent) which did not have matched dura. These findings extend our observations in mice, in which we observed that

brain tumors are infiltrated with dendritic cells far above the normal background for steady state brain. Additional studies remain to characterize more samples and to delve into dendritic cell subsets with increased granularity and characterization of their specific migration patterns and additional functions.

Finally, to our knowledge, the phenomenon of direct tumor antigen uptake by dendritic cells has yet to be observed in human cancer. The use of 5-ALA (and the associated fluorescent tumor-specific PPIX metabolite) allows the neurosurgeon to discern fluorescing malignant glioma tissue from normal brain more easily than otherwise, and accordingly, to achieve better safe and total resection of the tumor [218-222]. Systemically administered 5-ALA is selectively imported, metabolized, and retained by the GBM tumor cells [222, 223]. We leveraged this phenomenon of tumor-specific fluorescence and integrated it with conventional flow cytometry to probe for the fluorescent 5-ALA metabolite PPIX in various dendritic cell and antigen presenting cell subsets that infiltrated the tumor. According to our model, a fluorescent dendritic cell would indicate that the dendritic cell had phagocytized part of or a whole tumor cell, or debris leached or expelled from a tumor cell. Importantly we observed this phenomenon uniquely in antigen presenting cells (T cells in the tumor were $PPIX^-$) which were specifically isolated from the tumor (the same dendritic cell subsets isolated from intraoperatively collected patient PBMCs were $PPIX^-$). These were important controls to establish first, that PPIX retention was dependent on immune cell identity, and second to establish that any PPIX signal in a tumor-infiltrating APC was due to presence within the tumor, rather than systemic exposure to 5-ALA/PPIX. As with mice, transfer of fluorescence from tumor to infiltrating APC could have occurred because the infiltrating APC phagocytized a whole tumor cell,

phagocytized debris leached from a dead or dying tumor cell, or phagocytized exosomes expelled by the tumor. Our observational techniques preclude us from discerning the means by which a dendritic cell phagocytosed tumor-derived material. Determining this would require a technique such as high-resolution electron microscopy to discern what takes place at the cellular and sub-cellular levels. Nevertheless, these findings extend our observations of tumor antigen uptake by dendritic cells from mice to humans.

Our work also has important implications for the field of dendritic cell vaccines. Dendritic cell vaccines were based on a few studies that showed more robust T cell responses and survival benefit from exogenously cultured monocyte-derived dendritic cell vaccines in rodent GBM models [202, 203] in the late 1990s. These observations led to a phase I trial that showed some efficacy and demonstrated safety with this vaccination strategy in GBM [204]. More recently, an ongoing phase III trial by Northwest Biotherapeutics has enrolled patients to determine whether there is benefit from exogenously cultured monocyte-derived dendritic cell vaccines in GBM [121]. Although trial is currently underway and reports a median survival of 23.1 months as well as a subset of long term survivors in their intent-to-treat cohort compared to the placebo group [122], DC-Vax has not proven to be a silver bullet and probably won't change the standard of care.

There are a few reasons that the investigators might not be conducting a trial destined for success. Notably these DC-vaccine studies and trials have employed exogenously cultured monocyte-derived dendritic cells, which were first developed in 1992 in mice, and in 1994 in humans. These vaccines require culturing hematopoietic stem cells (HSCs) with GM-CSF and IL-4, along with different additional cytokines such as TNF-α depending on the formulation [205-207]. Monocyte-derived dendritic cells may have been selected for

cancer vaccines because researchers have known how to differentiate them for nearly 30 years, and because these cells share some characteristics with conventional dendritic cells such as the capacity to uptake antigen and present it to T cells to stimulate their proliferation *in vitro* [207]. Exogenously cultured monocyte-derived dendritic cells have also induced demonstrable antitumor immune responses by expanding the neoantigen-specific T cell repertoire in melanoma patients [208]. These results notwithstanding, monocyte-derived dendritic cell vaccines have not changed the standard of care appreciably. It could be because T cell priming by monocyte-derived dendritic cells isn't optimal. It could additionally be because monocyte-derived dendritic cells don't have the same capability (beyond T cell priming) as true dendritic cells that arise endogenously *in vivo*. Exogenously cultured monocyte-derived dendritic cells are comprised of a heterogeneous population of monocyte-derived macrophages and dendritic cell-like cells that each have unique functions and differential ability to stimulate T cells [211]. True conventional dendritic cells require Flt3L rather than GM-CSF for development [209, 210]. Moreover, of the conventional dendritic cell subsets, true cDC1 are the only dendritic cells that arise endogenously and perform the functions of $CD8^+$ T cell-priming through cross-presentation, cell-associated antigen processing/presentation, and T_H1 polarization *in vivo* [20-23, 25-31, 212], all functions which have been demonstrated to be important in eliciting potent antitumor immunity in countless experiments.

In addition to work demonstrating that exogenously monocyte-derived dendritic cells differ in function and potential utility from true cDC1, a recent report by Maier and colleagues of the Merad lab also calls into question the utility of IL-4, which is used to culture monocyte-derived dendritic cells from human or mouse HSCs. Maier and colleagues used

a GFP-expressing non-small cell lung cancer (NSCLC) preclinical model to examine the function of tumor antigen-containing dendritic cells under various perturbations [227, 228]. They demonstrated that IL-4 negatively impacted the ability of GFP^+ dendritic cells, which had acquired tumor antigen, to produce IL-12. IL-12 is normally required to polarize naïve $CD4^+$ T cells into IFNγ-secreting T_H1 $CD4^+$ T cells [229, 230]. They further demonstrated that tumor-infiltrating GFP^+ dendritic cells isolated from mice treated with anti-IL-4 antibodies to globally restrain IL-4 signaling had greater capacity to stimulate tumor antigen-specific T cell division, as well as greater T cell production of IFNγ and TNFα, when compared to the same GFP^+ dendritic cells isolated from untreated tumor-bearing mice. Importantly, they also showed that IL-4 inhibition led to greater tumor control compared with untreated mice. Collectively, this study demonstrated that IL-4 signaling negatively impacted dendritic cell function in a manner that had negative downstream consequences for T cell activation and tumor control. While this study did not investigate potential deleterious effects of IL-4 signaling on anti-tumor immunity in humans, its implications should be cause for further investigation regarding human monocyte-derived dendritic cell vaccination, which require culturing in IL-4 for their derivation. It is conceivable that monocyte-derived dendritic cells arise from the beginning with functional impairments and less capacity to stimulate potent T_H1 $CD4^+$ or cytotoxic $CD8^+$ T cell responses when compared to true cDC1 which are not differentiated using IL-4. Nevertheless, the potential deleterious effects of IL-4 signaling on a dendritic cell's capacity (whether endogenously arising or exogenously cultured monocyte-derived) to stimulate antitumor immunity should be further investigated in human tumors.

In addition to the reasons discussed above, the limited use of true cDC1 in vaccines might be because suitable techniques to differentiate appreciable numbers of *bona fide* human cDC1 were not developed until just recently in 2018, and even so, the number of dendritic cells which result from that culturing method may still be insufficient to make an effective dendritic cell vaccine [215]. Future work should include developing techniques to efficiently culture large numbers of *bona fide* human cDC1 so that they can be used instead of monocyte-derived dendritic cells, in order to give dendritic cell-based vaccines the greatest chance of bolstering strong antitumor immunity and improving patient outcomes. From previous experiments by our lab and others, we know that cDC1-deficient mice have severe deficits with respect to antitumor immunity. These defects cannot be rescued by adoptive transfer of exogenously cultured monocyte-derived dendritic cells.

The Northwest Biotherapeutics DC-Vax in phase III trials involves injecting tumor lysate-exposed exogenously cultured monocyte-derived dendritic cells *intradermally* [121]. Our data demonstrates that endogenously arising cDC1 appear in the tumor and uptake antigen upon arrival in both mice and humans. In mice we show that tumor antigen-containing cDC1 can be additionally isolated from the dura and the CNS-draining cervical lymph nodes. Dendritic cell vaccines should introduce true cDC1 instead of monocyte-derived dendritic cells (for reasons enumerated above) and would take care to consider where CNS immune responses are normally primed in order to stimulate the most potent response and introduce them there instead of intradermally. There exists an axiom in vaccinology which holds that vaccines generate the most effective immunity when the vaccine itself is administered at the same anatomic location as the portal of entry of the pathogen against which they vaccinate [231]. The reason for this is that T cells are more

likely to be polarized correctly and to more efficiently home back to the site where antigen was first introduced, and furthermore, antibody of the most effective isotype is more likely to be generated. Moreover, given the demonstrated clinical benefit of neoadjuvant checkpoint blockade in GBM, which derives its clinical benefit from pre-operative rather than post-operative administration [112], perhaps a similar approach should be employed with cDC1 vaccination, in which cDC1 are introduced pre-operatively into the tumor mass so that they have a chance to phagocytose tumor antigen, activate, and prime neoantigen-specific T cell responses.

Nevertheless, many additional experiments are required to elucidate human dendritic cell function, and to develop more effective dendritic cell-based therapies. Our experiments revealed the presence of dendritic cells in GBM, which upon entry into the tumor acquire tumor-derived material in both mice in humans. Our additional experiments in mice demonstrated that dendritic cells additionally traffic the tumor-derived antigen from the brain tumor itself to the cervical lymph nodes, likely via the dura lymphatics, to prime CNS antitumor immunity. We also showed in mice that cDC1 in particular are indispensable for CNS antitumor immunity. Our findings collectively portend that correctly designed dendritic cell-based therapies have the potential to improve the standard of care and extend survival in GBM patients. We hope that our work in describing the importance and function of dendritic cells in human and mouse brain tumors demonstrates the need to study them further.

CHAPTER SEVEN

Conclusion, discussion, and future directions

In summary, while there are certainly unique traits of immune surveillance in the central nervous system, our data suggest that the antitumor immune response in the CNS shares many commonalities with the immune response elsewhere in the body: in both settings the cDC1 is required to mount an effective antitumor immune response, the consequences of cDC1-deficiency are distinct and severe, and the cDC1 subset (along with other dendritic cell subsets) traffics tumor antigen from the tumor to draining lymph nodes, where cDC1 prime neoantigen-specific $CD8^+$ T cells. Importantly, many questions remain. The mechanism by which dendritic cells extravasate from the blood to infiltrate the tumor remains unknown, particularly regarding whether the tumor somehow serves as a stimulus for dendritic cell entry, or whether their entry is merely a stochastic event made all the more likely by the leaky vasculature that permeates the tumor. Furthermore, it remains unknown whether additional cell types already present in the steady state brain parenchyma (such as microglia) act as sentinels and by some means detect the disturbance caused by a growing tumor, secrete chemokines, and recruit dendritic cells from the blood into the tumor to trigger an adaptive immune response.

The exact migration path of dendritic cells from the brain tumor parenchyma to the cervical lymph nodes (particularly to the superficial cervical lymph nodes) also requires further investigation in mice. In both mice and humans, the transit path by which dendritic cells exit the tumor parenchyma and enter the dura lymphatic vessels is also unknown. The

dura lymphatic vessels in mice and humans follow the venous sinuses as they traverse out of the skull and become internal jugular veins, where experiments (only in mice thus far) have demonstrated that the lymphatic vessels converge upon the deep cervical lymph nodes. This pathway is well characterized in mice (at least regarding drainage to the deep cervical lymph nodes), however the complete pathway of CNS lymphatic drainage in humans remains unknown.

Moreover, the question regarding whether human cDC even migrate extracranially remains incompletely understood. There have been a few limited experiments in humans which have demonstrated supportive evidence for extracranial dendritic cell migration. Investigators demonstrated that APC (including that $CD1c^+$ cDC2 equivalent) isolated from the cervical lymph nodes and palatine tonsils harbored CNS-derived antigens in the setting of stroke at levels greater than in healthy control patients [201]. While this clever study suggested that cervical lymph nodes perform CNS lymphatic drainage functions in humans, their evidence was indirectly supportive. Their experiments fell short of tracing the migration path of a dendritic cell which arose in the CNS to an extracranial location such as a cervical lymph node. Moreover, an additional confounding factor complicating future studies is that human CNS lymphatic drainage is much more complex than in mice. Humans typically have hundreds of cervical lymph nodes instead of 5 per side, as is the case in mice.

We are currently engaging in experiments to determine whether extracranial dendritic cell migration occurs in the setting of human GBM. To investigate this phenomenon, we are using LYMPHOSEEK®, which consists of a mannose analogue conjugated with Techetium-99m isotope. This γ-emitting macromolecule binds CD206 (also known as

mannose receptor), which is expressed by macrophages and immature dendritic cells [232-234], and is ordinarily used by surgeons resecting tumors with metastatic potential to trace dendritic cell migration from the tumor to lymph nodes to determine which lymph nodes might harbor metastases [235, 236]. We have just been granted IRB approval for a protocol in which Dr. Dunn and his colleagues will administer LYMPHOSEEK® to the GBM tumor cavity following resection. After administration, we will use a gamma camera to determine whether the γ-radiation signal localizes preferentially to the neck, which harbors cervical lymph nodes in humans (as well as mice). A detectable γ-signal that localized to the neck and not to other anatomic locations would suggest that CD206-expressing cells had migrated extracranially to cervical lymph nodes.

Despite our discoveries underscoring the importance of dendritic cells in CNS antitumor immunity, GBM itself is an immune-suppressive tumor that employs multifaceted tactics of immune escape. It is conceivable that one of the immune-suppressive mechanisms employed by GBM is to subvert antigen presentation and dendritic cell function either within the tumor, or at downstream steps. Important work by Gajewski has shown that excessive WNT signaling by the tumor excluded dendritic cells from the tumor environment in a melanoma model [30, 31]. While we have detected cDC in most human brain tumors, there have been isolated GBM specimens in which we observed a paucity of conventional dendritic cells infiltrating the tumor. Notably, we analyzed one GBM specimen in which we observed that the dendritic cell infiltrate was polarized toward $CD1c^+$ cDC, which are presumably less capable of priming potent $CD8^+$ and/or $CD4^+$ T_H1 antitumor immune responses. Moreover, there are additional steps downstream of

dendritic cells infiltrating the tumor and phagocytizing tumor antigen that could be subject to subversion by the tumor.

Incidentally, we identified possible evidence of suppression of antigen presentation and/or T cell activation downstream of tumor antigen trafficking to lymph nodes in preliminary studies which were not discussed in this thesis. Among murine preclinical models of GBM, CT2A is a less immunogenic brain tumor that cannot be treated successfully with checkpoint blockade alone unlike its GL261 counterpart. CT2A instead requires combination adjuvant checkpoint blockade and neoantigen-specific therapeutic vaccination [126]. This is despite the two models harboring thousands of mutations and having neoantigen burdens of roughly the same magnitude [126]. These differences regarding immunogenicity between the two models were notable considering experiments that we additionally performed comparing GL261-zsGreen to CT2A-zsGreen tumor antigen trafficking. Our preliminary data demonstrated that despite CT2A being less immunogenic than GL261, and despite CT2A-zsGreen being an objectively less brightly fluorescent tumor than GL261-zsGreen when measured by both fluorescence microscopy and flow cytometry, CT2A-zsGreen showed a stronger signal than GL261-zsGreen did of tumor antigen trafficking by dendritic cells to the CNS-draining cervical lymph nodes, which suggests that the immune suppression resulting from CT2A falls downstream of tumor antigen trafficking to draining lymph nodes.

Moreover, we performed additional preliminary experiments pertinent to this line of inquiry (also not discussed in this thesis) in which we transduced CT2A with a lentivirus that enforced expression of the same mImp3 antigen which when natively expressed by GL261, causes a neoantigen-specific $CD8^+$ T cell response to be spontaneously primed

against GL261 brain tumors. Compared to the CT2A-WT-Imp3-transduced control tumors, we detected no mImp3-specific $CD8^+$ T cell responses above background in mice that had been transplanted with CT2A-mImp3-transduced tumors despite multiple attempts using multiple screening platforms and investigating multiple organs. These results showed us that despite evidence of more robust tumor antigen trafficking from the CNS in CT2A brain tumors compared to GL261 brain tumors, neoantigen-specific $CD8^+$ T cell responses don't typically arise spontaneously in CT2A, even if the tumor itself over-expresses a neoantigen capable of priming neoantigen-specific $CD8^+$ T cell responses in different settings. To have detectable neoantigen-specific $CD8^+$ T cell responses in the setting of CT2A brain tumors requires bolstering the immune response with therapeutic vaccination in combination with adjuvant checkpoint blockade therapy [126].

This set of preliminary experiments suggests that in the setting of CT2A brain tumors, subversion of antitumor immunity occurred at some point downstream of the step of tumor antigen trafficking by dendritic cells from the CNS to the draining lymph nodes. Several mechanisms could be responsible for this, including (a) subversion by the CT2A brain tumor of dendritic cells in their T cell priming function, or alternatively (b) suppression of T cell activation and clonal expansion, or otherwise (c) enforced sequestration of T cells at an anatomic location distant from the tumor, such as the bone marrow, as has been suggested by work performed by Fecci's group [71, 72]. Our preliminary experiments could not determine at which step downstream of tumor antigen trafficking to lymph nodes that immune suppression occurred in the setting of CT2A brain tumors. Nevertheless, future studies should examine all potential mechanisms that GBM might employ to blunt antigen presentation and dendritic cell function, and additionally should compare the unique and

disparate methods by which individual GBM tumors differentially suppress immune responses against the tumor.

In course of developing this thesis, we generated a GEMM preclinical model of glioma, which for unknown reasons, resulted in tumors that were histologically distinct from GBM; their histologic characteristics were instead those of gliosarcoma, which is a considerably less common form of malignant glioma. Moreover, the isogenic recurrent hypermutator model also had characteristics that made it unsuitable for testing the relationship between checkpoint blockade and mutational burden: the transformed astrocytes, also for unknown reasons, did not form brain tumors and instead had a predilection to form extracranial tumors, despite being transplanted directly into the brain parenchyma. The easiest next step in both models would be to try a different oncogene. Our model used murine rather than human PDGFβ as the oncogene to drive transformation. We selected murine PDGFβ to avoid the potential pitfall of creating artificial neoantigens under the assumption that murine immune systems are not tolerant to human PDGFβ. To our knowledge, our model is one of the first such models to use mouse rather than human PDGFβ. Other GEMM GBM models have used human PDGFβ expression to drive transformation, which has resulted in successful transformation and tumors with the correct GBM histology [129, 135, 140]. However, we set out to generate a model in which potential neoantigens harbored by the tumor resulted from mutations that spontaneously arose through the act of cell division, rather than from mutations engendered from the transforming factors themselves. The next rational oncogene to employ is EGFRvIII, which incidentally, is more commonly a driver than aberrant PDGFβ signaling [6], and which

has been used in combination with *PTEN* and *INK4a/ARF* gene deletion in autochthonous GEMMs before to generate tumors with GBM histology [237].

We originally set out to generate a GEMM that could simulate the entire evolution of GBM from near-spontaneous nascence, in which the malignant cells arose from cells already present in the host. We did so in part to avoid the issues with orthotopic models, in which thousands of cells syngeneic to the host, but still a foreign entity, are transplanted into the brain to initiate tumor formation. This initiating event does not recapitulate GBM as it occurs in humans where one or a few cells become mutated and transform into malignant cells, all while under constant selective pressure from the immune system. Moreover, the GL261 and CT2A preclinical orthotopic glioma lines we used each harbor thousands of mutations [123], whereas human GBM harbors 50-100 mutations [6].

The pinnacle of convergence of the disparate aims in this thesis would be to combine the dendritic cell and GEMM projects. A combination of these projects could result if future work optimized the GEMM model to result in GBM with the correct histology. The GEMM could be combined with either a genetic model of cDC1-deficiency or with zsGreen expression by the tumor. By generating these tools, one could determine the role of cDC1 in a model that more closely aligns with both the immunologic, genomic, and evolutionary characteristics of human GBM.

Despite having fallen short regarding some of the aims in this thesis, we did make interesting and important discoveries about cDC1 in preclinical brain tumor models—first, that they are indispensable for CNS antitumor immunity. Second, that they capture antigen in the tumor and traffic it to cervical lymph nodes in a CCR7/cell-migration-dependent manner to drive clonal expansion of $CD8^+$ T cells that recognize the tumor.

Third, that the dura plays a supportive role in CNS-antitumor immunity, including likely functioning as a transit point by which dendritic cells traffic tumor antigen from the tumor parenchyma to draining lymph nodes via dura lymphatic vessels. Fourth, and perhaps most importantly, we extended our observations from preclinical models to human disease. We identified cDC1 as well as other APC subsets within human GBM and meningioma tumor and dura specimens. We also identified that GBM-infiltrating antigen presenting cells (including the cDC1) uniquely phagocytize tumor-associated material.

Future work on this project should employ single cell RNA sequencing to examine the granular characteristics of antigen presenting cells in human GBM that have acquired tumor antigen. Tumor antigen-harboring cDC could be compared against cDC that lacked tumor antigen to determine whether changes in gene-expression were attributable to dendritic cell antigen acquisition and activation. Similar experiments have been performed in mouse tumors by the Merad lab, which revealed that both cDC1 and cDC2 dendritic cell subsets harbored a gene signature associated with convergence of identity upon acquiring tumor antigen that was associated with upregulation of both common activation genes, as well as immunoregulatory genes [227, 228]. We need to study the same question in human dendritic cells.

Here we report several important novel findings which underscore the role and significance of antigen presentation and cDC1 (as well as other dendritic cell subsets) in CNS antitumor immunity in mice and humans. Our hope is that better understanding how the antitumor immune response is endogenously primed against brain tumors could ultimately lead to therapeutic advances which improve disease outcomes for the patients who have the misfortune of being diagnosed with glioblastoma.

CHAPTER EIGHT

Methods

Mice

All animal experiments were approved by the Washington University Animal Studies Committee. For survival studies, mice were euthanized upon first sign of neurologic deficit and/or neurologic deficits. Male and female mice 6-16 weeks of age were used for all experiments. Wild-type C57BL/6 mice were purchased from Taconic Biosciences (Hudson, NY).

For autochthonous tumor model experiments, *INK4a/ARF*$^{fl/fl}$ mice were maintained on a C57BL/6 background. These mice harbor a loxP insertions upstream of exon 2 and downstream of exon 3 (common to *INK4a/ARF* alternative splice products), and are susceptible to both *p19ARF* and *p16INK4a* deletion in any Cre-expressing cell [238]. *PTEN*$^{fl/fl}$ mice, which harbor loxP sites flanking exon 5 [239], were obtained on a BALB/cAnNTac background. They were backcrossed to C57BL/6 using speed congenics to obtain a pure C57BL/6 *PTEN*$^{fl/fl}$ mouse line. *INK4a/ARF*$^{fl/fl}$ mice were crossed with *PTEN*$^{fl/fl}$ mice and F1s were intercrossed until mice were homozygous for loxP insertions at both alleles in both respective loci.

Unless otherwise specified, mice on C57BL/6 backgrounds were used for all experiments concerning dendritic cells. *IRF8+32kb*$^{-/-}$ were used for experiments regarding cDC1-deficiency, shared generously by Kenneth Murphy. For experiments in which cDC1 were GFP-expressing, *SNX22*$^{GFP/WT}$ mice were used, shared generously by Kenneth Murphy

as well. We bred these mice by crossing a *SNX22*$^{GFP/GFP}$ mouse on either a 129/SvEv background, or a C57BL/6 background to a wild-type C57BL/6 mouse and used the resultant *SNX22*$^{GFP/WT}$ F1 mice for experiments. For experiments with GFP-expressing cDC1 and Tomato-labeled lymphatics, we crossed *SNX22*$^{GFP/GFP}$ mice with Prox1Cre-ER-tdTomato$^{+/+}$ mice, which were generously shared with us by Gwendalyn Randolph. We used resulting F1 mice for experiments. After genotyping, we injected mice 3x/week for two weeks (six total doses) of tamoxifen (10mg/mL) in corn oil (Sigma) at a dose of 50mg/kg intraperitoneally. We allowed two subsequent weeks to elapse before experiments, so that lymphatic vessels would be sufficiently labeled with tomato fluorophore. *CCR7*$^{-/-}$ mice [240], OT-I mice [193], and CD45.1 mice [241] were purchased from Jackson. All mice were housed and handled humanely in accordance with IACUC standards.

Cell lines

Astrocytes were isolated with the assistance of Najla Kfoury of the Josh Rubin Lab as described [242]. *INK4a/ARF*$^{fl/fl}$ x *PTEN*$^{fl/fl}$ P0 pups were decapitated, and brains were dissected from the encasing skull. Under a stereomicroscope (all Najla's hands), the meninges was removed and mouse cortices were separated from the rest of the brain. Isolated brain cortices were mechanically disaggregated and incubated with trypsin until the mixture had become a single cell suspension. Cells were spun, the trypsin supernatant was decanted, and the remaining pellet was resuspended in media (DMEM, high glucose + 10% heat-inactivated fetal bovine serum + 1% Penicillin/Streptomycin). Resuspended cells were plated on a poly-D-Lysine coated flask and allowed to adhere. After cells (including astrocytes) had adhered, flasks were topped off with media, and

placed on an orbital shaker at max speed at 37ºC overnight to disrupt less adherent cells, which left behind only the strongly-adhering astrocytes after 24-hours. Astrocytes were cultured in Corning® Primaria™ Culture Plates or poly-D-lysine coated plates subsequently.

CT2A (generous gift of Peter Fecci), GL261, 293T, and 3T3 cells were maintained in culture at 37ºC, 5% CO_2 in a culture medium comprised of DMEM with 10% heat-inactivated FBS, 1% Penicillin/Streptomycin, 1% minimum essential amino acids, 1% L-glutamine, and 1% Sodium Pyruvate (D10). Cells were harvested at 90% confluency to inject intracranially.

Lentivirus and retrovirus, stable cell lines

Lentivirus/Retrovirus production for *in vitro* transductions. For lentivirus production, 293Ts were transfected with 1µg of lentiviral backbone, 100ng of VSV-G envelope protein plasmid, 900ng of Δ8.9 transfer plasmid. One day before transfection, 293Ts were plated at a density of $1x10^6$ cells per T25. Transfections were performed with the FuGENE® HD Transfection reagent according to the manufacturers protocol. On days 2 and 3 post-transfection, lentiviral supernatant was collected, filtered through a 0.45µM filter, and combined with polybrene (final concentration of 8µg/mL). Target cells were transduced by completely removing target cell growth media and exchanging with the filtered lentivirus-containing polybrene infused supernatant. For retrovirus production, we used the same protocol, except used the pCL-Eco transfer plasmid along with the retroviral backbone to transfect 293Ts. For cloning purposes, all lentivirus backbones were grown by transforming One Shot™ Stbl3™ Chemically Competent (ThermoFisher catalog #C737303) or NEB® Stable Competent (NEB catalog #C3040H) *E. coli* strains, and

retroviral backbones were grown by transforming DH5α (ThermoFisher catalog #EC0112) or NEB® 5-alpha Competent (NEB catalog #C2987H) *E. coli* strains.

Lenti PDGFβ, Lenti-PDGFβ-OS, Lenti-Cre-Empty lentiviral backbones: Lenti-PDGFβ and Lenti-PDGFβ-OS was derived from cloning the murine PDGFβ coding sequence into Lenti-LucOS (gift from Tyler Jacks, Addgene plasmid # 22777; http://n2t.net/addgene:22777; RRID:Addgene_22777) at the NheI and XhoI restriction sites, just upstream of the OS cassette. The OS cassette encodes for the ovalbumin H-2K^{b}-restricted antigen SIINFEKL, the ovalbumin I-A^{d}-restricted antigen ISQAVHAAHAEINEAGR, and the H-2K^{b}-restricted antigen SIYRYYGL. For Lenti-PDGFβ, a stop codon was inserted at the end of the mPDGFβ coding sequence just upstream of the OS cassette to prevent protein expression of the OS antigens. For Lenti-PDGFβ, the stop codon was removed to allow for translation into the OS cassette. For experiments in which Cre but neither oncogene nor OS cassette was used to transduce cells or inject mice, the Luc.Cre empty (termed Lenti-Cre-Empty in figures) was used (gift from Tyler Jacks, Addgene plasmid # 20905; http://n2t.net/addgene:20905; RRID:Addgene_20905).

CMV/GFAP/MBP promoter-driven lentiviral constructs. The following plasmids were obtained from the Washington University Hope Center Viral Vectors Core: pRRLsinCMV-GFP (CMV promoter), pRRLsinGFAP-GFP (GFAP promoter), and pRRL-MBP-GFP (MBP promoter). GFP was removed from each of the plasmids using the BamHI and EcoRI restriction enzymes and replaced with either Cre (as a single fragment) or Cre-P2A-mPDGFβ (as two separate but overlapping fragments) using the Gibson Assembly® cloning system (NEB catalog #E2611S) according to the manufacturer's protocol.

INK4a/ARF$^{fl/fl}$ x *PTEN*$^{fl/fl}$ astrocytes were transformed with either *Luc.cre Empty*, *Lenti PDGFβ*, or *Lenti-PDGFβ-OS* lentiviruses for experiments.

3T3 dsRed Cre reporter. The pMSCV-loxP-dsRed-loxP-eGFP-Puro-WPRE retroviral plasmid was a gift from Hans Clevers (Addgene plasmid # 32702; http://n2t.net/addgene:32702; RRID:Addgene_32702), which we used to transduce 3T3 cells in order to generate the Cre reporter cell line.

GL261-OFP. OFP designated our abbreviation for the mOrange2 fluorophore, which was a gift from Bob Schreiber. We inserted the mOrange2 gene into the pLX304 lentiviral backbone using the Gateway Cloning protocol according to manufacturer's instructions (Invitrogen™ Gateway™ BP Clonase™ II Enzyme mix, catalog #11789020; Invitrogen™ Gateway™ LR Clonase™ II Enzyme mix, catalog #11791020) as described [243, 244].

GL261-zsGreen and CT2A-zsGreen. zsGreen was a gift from David DeNardo. The gene for zsGreen was inserted into the pLX304 lentiviral backbone using the gateway cloning protocol as described above.

CT2A-mFlt3L. The coding sequence for murine Flt3L was obtained (SinoBiological catalog #MG51113-UT) and inserted into the pLX304 lentiviral backbone using the gateway cloning protocol as described above.

GL261-OVA. Full length cytoplasmic ovalbumin was cloned from pcDNA3-OVA (gift from Sandra Diebold & Martin Zenke, Addgene plasmid # 64599; http://n2t.net/addgene:64599; RRID:Addgene_64599), and inserted into pBabe-puro retroviral backbone (gift from Hartmut Land & Jay Morgenstern & Bob Weinberg,

Addgene plasmid # 1764; http://n2t.net/addgene:1764 ; RRID:Addgene_1764), using EcoRI and SalI restriction enzymes at the multiple cloning site.

Intracranial Injections

Orthotopic lines: cells for injection were trypsinized at 70-90% confluency, trypsin was neutralized with D10, and cells were washed 1X in PBS before suspending cells in PBS for injection. Before surgery, mice were anesthetized with ketamine/xylazine mouse cocktail and administered Buprenorphine SR (1mg/kg) in the nape of the neck for analgesic. For intracranial injections, 50,000 cells were injected 2mm to the right and 2mm posterior of bregma, at a depth of 3.5mm using a Stoelting stereotactic headframe that fixed the mouse head in place and allowed for precise injections at a slow and controlled rate. For most experiments mice were euthanized and tissues were analyzed two weeks post-injection, except for dura experiments with intracranial CT2A-zsGreen brain tumors, in which case mice were euthanized one-week post-injection. For *CCR7*$^{-/-}$ intracranial CT2A-zsGreen brain tumor experiments, mice were euthanized 12 days post-injection.

Lentivirus for *in vivo* injections: Concentrated Lenti-PDGFβ, Lenti-PDGFβ-OS and Lenti-Empty (Luc.cre Empty) lentiviruses were obtained from the University of Iowa Lentivirus core. Concentrated CMV/GFAP/MBP promoter-driven lentiviral constructs were obtained from the Washington University Hope Center Viral Vectors Core. For experiments, $1x10^5$-$1.5x10^6$ titered units were injected at the same coordinates as with orthotopic injections into the striatum using a Stoelting headframe with mice anesthetized as described above. Health of mice was monitored by weighing weekly, until mice lost weight and became cachectic, at which point they were euthanized.

mPDGFβ qPCR

RNA was extracted from 3T3s transduced with *Lenti PDGFβ*, *Lenti-PDGFβ-OS*, *Lenti-Cre-Empty* using an RNA-easy extraction kit (Qiagen), cDNA was amplified using an Applied Biosystems™ High-Capacity cDNA Reverse Transcription kit and a murine PDGFβ TaqMan® gene expression assay, with GAPDH as a reference control, according to manufacturer instructions.

PDGF-BB ELISA

In supernatants and total cell lysates, murine PDGFβ concentration was measured using Mouse/Rat PDGF-BB Quantikine ELISA Kit (R&D Biosystems) according to manufacturer's instructions.

CRISPR-mediated gene disruption

Genetic mutations were made in Lenti-PDGFβ *INK4a/ARF*$^{fl/fl}$ x *PTEN*$^{fl/fl}$ astrocytes.

MSH6: the first exon of murine *MSH6* was targeted using the following guide sequence: GGCGGTATCCGCCTCGTCGC, and cloned into the pSpCas9(BB)-2A-Puro plasmid (PX459) (gift from Feng Zhang, Addgene plasmid # 62988; http://n2t.net/addgene:62988; RRID:Addgene_62988). MSH6 was genetically disrupted as described [245]. Briefly, cells were transfected with the MSH6-pSpCas9(BB)-2A-Puro plasmid, subjected to puromycin selection, allowed to recover, and plated in limiting dilution to derive single cell clones. Clones were screened for genomic biallelic disruption of MSH6, and clones with disruption were screened for protein loss.

POLε: L424V and D272A E274A mutants were generated by Washington University GEiC. Single cell clones were screened for biallelic mutant knock-in.

Long term passage of hypermutated lines

POLε INK4a/ARF$^{fl/fl}$ x *PTEN*$^{fl/fl}$ astrocytes were immediately frozen at low passage, and subsequent splits were passaged continuously for three months to derive high passage cells.

MSH6-WT and *MSH6*$^{-/-}$ Lenti-mPDGFβ-transduced *INK4a/ARF*$^{-/-}$ x *PTEN*$^{-/-}$ astrocytes were subjected to no treatment or treatment with 500μM temozolomide/40μM O_6Benzyl Guanine for two months with passaging as needed. Growth had completely arrested in all cell lines treated with 500μM temozolomide/40μM O_6Benzyl Guanine, regardless of MSH6 status. At the end of the two months of treatment, cells were allowed to recover in growth media with no treatment for an additional month, until cell growth had restored to normal and regular passaging was required.

DNA and RNA were extracted using an AllPrep DNA/RNA Mini Kit (Qiagen). RNA sequencing and whole exome sequencing was performed by Novagene. Variants were called and subjected to pVAC-Seq to identify neoantigens [168].

Propidium iodide nuclear analysis

For analysis of temozolomide sensitivity, nuclei were analyzed as described [164], including cold ethanol fixation of the cells whose nuclei were analyzed.

Survival studies

For survival studies, age matched, sex matched WT or *IRF8+32kb*$^{-/-}$ C57BL/6 mice were intracranially injected with 50,000 GL261 cells as described above. At days 3, 5, 7, and 14, mice were administered intraperitoneal injections of either PBS vehicle or αPD-L1 (Clone 10F.9G2, Leinco Technologies, Inc) at a dose of 200μg/mouse in a volume of

100µL. Mice were euthanized before they became moribund. The day of euthanasia was considered the day of death for purposes of this study.

ELISPOT

For ELISPOT studies, age matched sex matched WT or *IRF8+32kb*$^{-/-}$ C57BL/6 mice were intracranially injected with 50,000 GL261 cells as described above. Mice were euthanized at two weeks post-injection and tumors were mechanically dissociated between frosted slides, and further dissociated by incubating in a collagenase A solution (1mg/mL Collagenase A (Millipore Sigma catalog#11088793001) and 2% heat inactivated FBS in RPMI) at 37ºC for 20 minutes, with intermittent pipetting. Tumor single cell suspensions were separated from myelin using a 22.5% Percoll® (GE/Cytivia product #17089101) solution and subjected to ACK buffer to lyse red blood cells. $CD8^+$ T cells were isolated with an EasySep™ Mouse CD8a Positive Selection Kit II (Stem Cell), counted and plated with naïve splenocytes that were isolated that day using a Ficoll® (GE/Cytivia product #17144003) centrifugation gradient from a naïve sex-matched C57BL/6 mouse. The ELISPOT antigen presentation assay was performed as follows: 50,000 $CD8^+$ T cells isolated from the tumor were cultured with 125,000 naïve splenocytes with or without mImp3 peptide overnight at 37ºC/5% CO_2 on a pre-coated murine IFNγ detection plate according to manufacturer's instructions (Cellular Technologies Limited). Plates were developed the following day and analyzed with an Immunospot Plate Reader (Cellular Technologies Limited).

mImp3 Tetramer

For mImp3 tetramer studies, age matched sex matched WT and *IRF8+32kb*$^{-/-}$ C57BL/6 mice were intracranially injected with 50,000 GL261 cells as described above. Mice were

euthanized at two weeks post-injection. Tumors were removed from the brain, cut into small chunks, and cultured in R10βME media (RPMI, 10% heat inactivated FBS, 1% sodium bicarbonate, 1% L-glutamine, 1% minimum essential amino acids, 1% sodium pyruvate, 1% Penicillin/Streptomycin, 55μM β-mercaptoethanol) overnight. The following morning, the cultures were assessed for lymphocyte egress from tumor chunks. Tumor chunks were removed, and the remnants containing the remaining lymphocytes were filtered and separated from myelin using a 22.5% Percoll solution and subjected to ACK buffer to lyse red blood cells. mImp3 (AALLNKLYA)/H-2D^b tetramer stock solutions were generated by the Washington University Immune Monitoring Lab. Briefly, tetramer was conjugated with the PE or BV421 fluorophore bound to streptavidin, incubated for 15 mins at 37ºC. Subsequently, the remaining surface antibodies were added, suspensions were incubated on ice for 20 additional minutes, washed, and subjected to flow cytometry.

Tissue Harvest

Mice with intracranial tumors were harvested 7-14 days after injection, depending on the experiment. The brain/tumor, superficial cervical lymph nodes, deep cervical lymph nodes, inguinal lymph node, dura, and/or spleen were harvested depending on the experiment. Lymph nodes, dura, and tumor were mechanically dissociated between two frosted slides and digested in 1mg/mL Collagenase A (Roche), 2%FBS, in RMPI for 20 minutes at 37ºC/5% CO_2. Suspensions were washed and red blood cells were lysed with ACK as necessary. Tumors were separated from myelin using a 22.5% Percoll™ solution and centrifuged at room temperature for 15 minutes at 500g, (acceleration 9, deceleration 5). Mononuclear cells were separated from spleens by first mechanically dissociating the

spleens between two frosted slides, and then using a Ficoll™ gradient (GE) to generate a buffy coat. We retained the cells in the buffy coat for experiments.

OT-I cell division assay

CD45.1 mice were mated to OT-I mice. CD45.1 and CD45.2, as well as $CD8^+$ T cell TCR-Vα2Vβ5 expression was verified in F1 mice before experiments. For adoptive transfer experiments, $5x10^5$ GL261-OVA cells were injected intracranially. Four days later, a spleen from a CD45.1xOT1 F1 mouse >6 weeks of age was subjected to Ficoll gradient, and $CD8^+$ T cells were isolated using an EasySep™ Mouse CD8a Positive Selection Kit II (Stem Cell). Immediately after isolation, OT-1 $CD8^+$ T cells were CFSE labeled in PBS (10 mins at RT, 5μM), and adoptively transferred via tail vein into recipient mice. At days 3 and 6 post-adoptive transfer, mice were harvested, and tissues were dissociated as described above.

Human dura preparation

Human dura was macerated and incubated in 2mg/mL Collagenase A (Roche) and 2mg/mL Collagenase D (Roche), 10% FBS and IMDM overnight at 37ºC, with pipetting every few hours throughout the evening before leaving for the night. The next morning, the single cell suspension was filtered through progressively smaller strainers (100μM first, then 70μM, then 40μM) and red blood cells were lysed with ACK buffer as needed to prepare cells for flow cytometry.

Human tumor preparation

Human tumors were macerated and incubated in 2mg/mL Collagenase A (Roche) and 2mg/mL Collagenase D (Roche), 10% FBS and IMDM overnight at 37ºC. The next

morning, the single cell suspension was filtered through a 100μM filter into a 22.5% Percoll™ solution and centrifuged as described above. After centrifugation, pellets were subjected to ACK lysis as necessary, and then filtered through progressively smaller strainers (70μM then 40μM) to prepare cells for flow cytometry.

Flow cytometry and tissue preparation

Before flow cytometry, single cell suspensions were filtered at least 3 times over the course of the preparation (usually progressively smaller strainers: 100μM, then 70μM, then 40μM), subjected to 1/200 Fc block, and then stained with surface antibodies for >20 minutes on ice. Cells were washed once and suspended in MACS buffer (10g/L BSA, 4mM EDTA in PBS). Flow cytometry was performed on a BD LSR Fortessa™ X- 20 flow cytometer.

2photon images

For harvest, mice were anesthetized and perfused with cold PBS until the liver blanched and became pale. The skull cap was removed (dura still attached to skull) and skull cap and brain were fixed in ice cold 4%PFA, with gentle shaking overnight. If blood vessels were to be labeled, 5 minutes prior to perfusion, mice were injected IV with 100μL of 1:2 PBS-diluted 594-lectin (Lycopersicon Esculentum (Tomato) Lectin (LEL, TL), DyLight® 594, Vector Laboratories). For brain sections, brain was cut with a vibrotome after fixation. Fixed tissues were glued to a cover slip with superglue and immersed in PBS for imaging.

Images were collected using a custom Leica SP8 two-photon microscope (Leica Microsystems, Wetzlar, Germany) equipped with a 25x 0.95 NA water immersion

objective, and two Femtosecond pulsing tunable Ti:Sapphir lasers (Mai Tai HP DeepSee and InSight DS+), both Spectra-Physics (Mountain View, CA, USA).

GFP, mOrange2/OFP and TdTomato were excited using a wavelength of 925nm whereas Dylight 594 and Dylight 649 were excited using a wavelength of 830nm.

Fluorescence emission was guided directly to 4 external detectors in dendritic arrangement (two hybrid and two classical PMTs). For signal separation, three dichroic beam splitters (Semrock, Rochester, NY, USA) were used. To separate GFP, mOrange2/OFP, Dylight 594 and the SHG (Second-harmonic generation), the three cutoff wavelengths were 358nm ,538nm and 593nm. The separation of GFP, tdTomato, DyLight 649 and the SHG was obtained with cutoff wavelengths of 458nm, 560nm, and 652nm.

Flt3L treatment

To administer Flt3L to mice, mice were injected subcutaneously in the flanks with $1x10^6$ cells of CT2A transduced with Flt3L, such that the tumor drove overexpression of Flt3L similar to as described [177]. As a negative control, mice were injected in the same manner with untransduced CT2A. Mice were harvested 2-3 weeks post-transplant of tumor cells into the flank, when tumors had reached 1-2cm in diameter.

Table 1. Mouse Antibodies

Antigen	Color	Vendor	Product no.	Clone
4-1BB	APC	BioLegend	106109	17B5
B220	BV510	BioLegend	103248	RA3-6B2
CCR7	PE-Cy7	BioLegend	120123	4B12
CD103	BV421	BioLegend	121421	2E7
CD11b	PE-Cy7	BioLegend	101216	M1/70
CD11b	BV650	BioLegend	101239	M1/70
CD11c	PE-Cy7	BioLegend	117318	N418
CD11c	APC	BioLegend	117310	N418
CD19	PE-Cy7	BioLegend	123113	6D5
CD3	PE-Cy5	BioLegend	100310	145-2C11
CD4	PerCP Cy5.5	BioLegend	100433	GK1.5
CD4	APC	BioLegend	100412	GK1.5
CD44	BV785	BioLegend	103041	IM7
CD44	BV785	BioLegend	103041	IM7
CD45	AF700	BioLegend	103128	30-F11
CD45	APC-Cy7	BioLegend	103116	30-F11
CD45.1	BV421	BioLegend	110731	A20
CD45.2	AF700	BioLegend	109822	104
CD62L	BV605	BioLegend	104441	MEL-14
CD62L	BV510	BioLegend	104441	MEL-14
CD8a	PE-Dazzle	BioLegend	100762	53-6.7
CD8a	BV711	BioLegend	100747	53-6.7
CD8α	FITC	BioLegend	100706	53-6.7
CD8α	PE-Cy7	BioLegend	100722	53-6.7
CTLA-4	BV605	BioLegend	106323	UC10-4B9
F4/80	PE-Cy7	BioLegend	115519	BM8
F4/80	BV711	BioLegend	123147	BM8
FoxP3	PE	BioLegend	126403	MF-14
granzyme B	AF700	BioLegend	372221	QA16A02
I-A^b	AF700	BioLegend	107622	M4/114.15.2
Ki-67	FITC	BioLegend	652409	16A8
Ly-6C	BV785	BioLegend	128041	HK1.4
mIFNγ	BV421	BioLegend	505830	XMG1.2
NK1.1	PE-Cy7	BioLegend	108713	PK136
NK1.1	BV650	BioLegend	108735	PK136
OX-40	PE-CF594	BioLegend	119417	OX-86
PD-1	PE-Cy7	BioLegend	135215	29F.1A12
PE tetramer	PE	BioLegend	405204	streptavidin
SIRPα	PE-CF594	BioLegend	144016	P84
TCR Vα2	APC	BioLegend	127809	B20.1
TCR Vβ5	PE	BioLegend	139503	MR9-4
XCR1	PE	BioLegend	148204	ZET
Zombie	APC-Cy7	BioLegend	423106	n/a
BV421 streptavidin	BV421	BioLegend	405225	n/a
PE streptavidin	PE	BioLegend	405204	n/a

Table 2. Human Antibodies

Antigen	Color	Vendor	Product no.	Clone
CD11c	PE-Cy5	BioLegend	301609	3.9
CD11c	BV421	BioLegend	301627	3.9
CD14	APC-Cy7	BioLegend	367107	63D3
CD14	BV650	BioLegend	301835	M5E2
CD141	APC	BioLegend	344105	M80
CD16	PerCP-Cy5.5	BioLegend	302027	3G8
CD1c	PE-CF594	BioLegend	331531	L161
CD3	PE-Cy7	BioLegend	371333	OKT3
CD3	BV510	BioLegend	371331	OKT3
CD4	FITC	BioLegend	357405	A161A1
CD45	AF700	BioLegend	368513	2D1
CD8α	BV711	BioLegend	301043	RPA-T8
HLA-DR	BV785	BioLegend	307641	L243
UV Zombie	UV	BioLegend	423107	n/a

Table 3. Gating Definitions

Mouse

Cell type	Definition
cDC	$CD45^+$, $F4/80^-$, $CD11c^+$, $I\text{-}A^{b+}$, $Ly\text{-}6C^-$
cDC1	cDC plus $XCR1^+$, $SIRP\alpha^-$
migratory cDC1	cDC1 plus $CD103^+$, $CD8\alpha^-$
resident cDC1	cDC1 plus $CD103^-$, $CD8\alpha^+$
cDC2	cDC plus, $XCR1^-$, $SIRP\alpha^+$
pDC	$CD45^+$, $F4/80^-$, $CD11c^+$, $I\text{-}A^{b+}$, $Ly\text{-}6C^+$, $CD11b^-$
MoDC	$CD45^+$, $F4/80^-$, $CD11c^+$, $I\text{-}A^{b+}$, $Ly\text{-}6C^+$, $CD11b^+$
T cells	$CD45^+$, $CD3^+$, $NK1.1^-$
$CD8^+$ T cells	T cell plus $CD8\alpha^+$, $CD4^-$
$CD4^+$ T cells	T cell plus $CD8\alpha^-$, $CD4^+$; plus FOXP3 for T regulatory cells
OT-I $CD8^+$ T cells	$CD45.1^+$, $CD45.2^+$, $Dump^-$ (NK1.1, CD19, CD11b, CD11c, F4/80), $CD3^+$, $CD8\alpha^+$, $CD4^-$, $TCRV\alpha2^+$, $TCRV\beta5^+$, CFSE variable.

Human

Cell type	Definition
cDC	$CD45^+$, $CD11c^+$, $HLA\text{-}DR^+$, $CD14^-$, $CD16^-$
cDC1/$CD141^+$ cDC	cDC plus $CD141^+$, $CD1c^-$
cDC1/$CD1c^+$ cDC	cDC plus $CD141^-$, $CD1c^+$
$CD14^+$ monocytes	$CD45^+$, $CD11c^+$, $HLA\text{-}DR^+$, $CD14^+$, $CD16^-$
$CD16^+$ monocytes	$CD45^+$, $CD11c^+$, $HLA\text{-}DR^+$, $CD14^-$, $CD16^+$
T cells	$CD45^+$, $CD3^+$
$CD8^+$ T cells	$CD45^+$, $CD3^+$, $CD8\alpha^+$, $CD4^-$
$CD4^+$ T cells	$CD45^+$, $CD3^+$, $CD8\alpha^-$, $CD4^+$

References

1. Ostrom QT, Cioffi G, Gittleman H, Patil N, Waite K, Kruchko C, Barnholtz-Sloan JS. CBTRUS Statistical Report: Primary Brain and Other Central Nervous System Tumors Diagnosed in the United States in 2012-2016. Neuro Oncol. 2019;21(Suppl 5):v1-v100. Epub 2019/11/02. doi: 10.1093/neuonc/noz150. PubMed PMID: 31675094; PMCID: PMC6823730.

2. Stupp R, Mason WP, van den Bent MJ, Weller M, Fisher B, Taphoorn MJ, Belanger K, Brandes AA, Marosi C, Bogdahn U, Curschmann J, Janzer RC, Ludwin SK, Gorlia T, Allgeier A, Lacombe D, Cairncross JG, Eisenhauer E, Mirimanoff RO, European Organisation for R, Treatment of Cancer Brain T, Radiotherapy G, National Cancer Institute of Canada Clinical Trials G. Radiotherapy plus concomitant and adjuvant temozolomide for glioblastoma. N Engl J Med. 2005;352(10):987-96. Epub 2005/03/11. doi: 10.1056/NEJMoa043330. PubMed PMID: 15758009.

3. Gilbert MR, Wang M, Aldape KD, Stupp R, Hegi ME, Jaeckle KA, Armstrong TS, Wefel JS, Won M, Blumenthal DT, Mahajan A, Schultz CJ, Erridge S, Baumert B, Hopkins KI, Tzuk-Shina T, Brown PD, Chakravarti A, Curran WJ, Jr., Mehta MP. Dose-dense temozolomide for newly diagnosed glioblastoma: a randomized phase III clinical trial. J Clin Oncol. 2013;31(32):4085-91. Epub 2013/10/09. doi: 10.1200/JCO.2013.49.6968. PubMed PMID: 24101040; PMCID: PMC3816958.

4. Binabaj MM, Bahrami A, ShahidSales S, Joodi M, Joudi Mashhad M, Hassanian SM, Anvari K, Avan A. The prognostic value of MGMT promoter methylation in glioblastoma: A meta-analysis of clinical trials. J Cell Physiol. 2018;233(1):378-86. Epub 2017/03/08. doi: 10.1002/jcp.25896. PubMed PMID: 28266716.

5. Kessler T, Sahm F, Sadik A, Stichel D, Hertenstein A, Reifenberger G, Zacher A, Sabel M, Tabatabai G, Steinbach J, Sure U, Krex D, Grosu AL, Bewerunge-Hudler M, Jones D, Pfister SM, Weller M, Opitz C, Bendszus M, von Deimling A, Platten M, Wick W. Molecular differences in IDH wildtype glioblastoma according to MGMT promoter methylation. Neuro Oncol. 2018;20(3):367-79. Epub 2017/10/11. doi: 10.1093/neuonc/nox160. PubMed PMID: 29016808; PMCID: PMC5817966.

6. Brennan CW, Verhaak RG, McKenna A, Campos B, Noushmehr H, Salama SR, Zheng S, Chakravarty D, Sanborn JZ, Berman SH, Beroukhim R, Bernard B, Wu CJ, Genovese G, Shmulevich I, Barnholtz-Sloan J, Zou L, Vegesna R, Shukla SA, Ciriello G, Yung WK, Zhang W, Sougnez C, Mikkelsen T, Aldape K, Bigner DD, Van Meir EG, Prados M, Sloan A, Black KL, Eschbacher J, Finocchiaro G, Friedman W, Andrews DW, Guha A, Iacocca M, O'Neill BP, Foltz G, Myers J, Weisenberger DJ, Penny R, Kucherlapati R, Perou CM, Hayes DN, Gibbs R, Marra M, Mills GB, Lander E, Spellman P, Wilson R, Sander C, Weinstein J, Meyerson M, Gabriel S, Laird PW, Haussler D, Getz G, Chin L, Network TR. The somatic genomic landscape of glioblastoma. Cell. 2013;155(2):462-77. Epub 2013/10/15. doi: 10.1016/j.cell.2013.09.034. PubMed PMID: 24120142; PMCID: PMC3910500.

7. DANDY WE. REMOVAL OF RIGHT CEREBRAL HEMISPHERE FOR CERTAIN TUMORS WITH HEMIPLEGIA: PRELIMINARY REPORT. Journal of the American Medical Association. 1928;90(11):823-5. doi: 10.1001/jama.1928.02690380007003.

8. Shankaran V, Ikeda H, Bruce AT, White JM, Swanson PE, Old LJ, Schreiber RD. IFNgamma and lymphocytes prevent primary tumour development and shape tumour immunogenicity. Nature. 2001;410(6832):1107-11. Epub 2001/04/27. doi: 10.1038/35074122. PubMed PMID: 11323675.

9. Schreiber RD, Old LJ, Smyth MJ. Cancer immunoediting: integrating immunity's roles in cancer suppression and promotion. Science. 2011;331(6024):1565-70. Epub 2011/03/26. doi: 10.1126/science.1203486. PubMed PMID: 21436444.

10. Dunn GP, Bruce AT, Ikeda H, Old LJ, Schreiber RD. Cancer immunoediting: from immunosurveillance to tumor escape. Nat Immunol. 2002;3(11):991-8. Epub 2002/10/31. doi: 10.1038/ni1102-991. PubMed PMID: 12407406.

11. Dunn GP, Old LJ, Schreiber RD. The immunobiology of cancer immunosurveillance and immunoediting. Immunity. 2004;21(2):137-48. Epub 2004/08/17. doi: 10.1016/j.immuni.2004.07.017. PubMed PMID: 15308095.

12. Dunn GP, Old LJ, Schreiber RD. The three Es of cancer immunoediting. Annu Rev Immunol. 2004;22:329-60. Epub 2004/03/23. doi: 10.1146/annurev.immunol.22.012703.104803. PubMed PMID: 15032581.

13. Coley WB. II. Contribution to the Knowledge of Sarcoma. Ann Surg. 1891;14(3):199-220. Epub 1891/09/01. doi: 10.1097/00000658-189112000-00015. PubMed PMID: 17859590; PMCID: PMC1428624.

14. Old LJ, Clarke DA, Benacerraf B. Effect of Bacillus Calmette-Guerin infection on transplanted tumours in the mouse. Nature. 1959;184(Suppl 5):291-2. Epub 1959/07/25. doi: 10.1038/184291a0. PubMed PMID: 14428599.

15. Old LJ, Boyse EA, Clarke DA, Carswell EA. Antigenic properties of chemically induced tumors. Annals of the New York Academy of Sciences. 1962;101(1):80-106.

16. Thomas L, Lawrence H. Cellular and humoral aspects of the hypersensitive states. New York: Hoeber-Harper. 1959:529-32.

17. Burnet M. Cancer: a biological approach. III. Viruses associated with neoplastic conditions. IV. Practical applications. Br Med J. 1957;1(5023):841-7. Epub 1957/04/13. doi: 10.1136/bmj.1.5023.841. PubMed PMID: 13413231; PMCID: PMC1973618.

18. Steinman RM, Cohn ZA. Identification of a novel cell type in peripheral lymphoid organs of mice. I. Morphology, quantitation, tissue distribution. J Exp Med. 1973;137(5):1142-62. Epub 1973/05/01. doi: 10.1084/jem.137.5.1142. PubMed PMID: 4573839; PMCID: PMC2139237.

19. Nussenzweig MC, Steinman RM, Gutchinov B, Cohn ZA. Dendritic cells are accessory cells for the development of anti-trinitrophenyl cytotoxic T lymphocytes. J Exp Med. 1980;152(4):1070-84. Epub 1980/10/01. doi: 10.1084/jem.152.4.1070. PubMed PMID: 6968335; PMCID: PMC2185968.

20. Hildner K, Edelson BT, Purtha WE, Diamond M, Matsushita H, Kohyama M, Calderon B, Schraml BU, Unanue ER, Diamond MS, Schreiber RD, Murphy TL, Murphy KM. Batf3 deficiency reveals a critical role for CD8alpha+ dendritic cells in cytotoxic T cell immunity. Science. 2008;322(5904):1097-100. Epub 2008/11/15. doi: 10.1126/science.1164206. PubMed PMID: 19008445; PMCID: PMC2756611.

21. Broz ML, Binnewies M, Boldajipour B, Nelson AE, Pollack JL, Erle DJ, Barczak A, Rosenblum MD, Daud A, Barber DL, Amigorena S, Van't Veer LJ, Sperling AI, Wolf DM, Krummel MF. Dissecting the Tumor Myeloid Compartment Reveals Rare Activating Antigen-Presenting Cells Critical for T Cell Immunity. Cancer Cell. 2014;26(6):938. Epub 2014/12/08. doi: 10.1016/j.ccell.2014.11.010. PubMed PMID: 28898680.

22. Salmon H, Idoyaga J, Rahman A, Leboeuf M, Remark R, Jordan S, Casanova-Acebes M, Khudoynazarova M, Agudo J, Tung N, Chakarov S, Rivera C, Hogstad B, Bosenberg M, Hashimoto D, Gnjatic S, Bhardwaj N, Palucka AK, Brown BD, Brody J, Ginhoux F, Merad M. Expansion and Activation of CD103(+) Dendritic Cell Progenitors at the Tumor Site Enhances Tumor Responses to Therapeutic PD-L1 and BRAF Inhibition. Immunity. 2016;44(4):924-38. Epub 2016/04/21. doi: 10.1016/j.immuni.2016.03.012. PubMed PMID: 27096321; PMCID: PMC4980762.

23. Roberts EW, Broz ML, Binnewies M, Headley MB, Nelson AE, Wolf DM, Kaisho T, Bogunovic D, Bhardwaj N, Krummel MF. Critical Role for CD103(+)/CD141(+) Dendritic Cells Bearing CCR7 for Tumor Antigen Trafficking and Priming of T Cell Immunity in Melanoma. Cancer Cell. 2016;30(2):324-36. Epub 2016/07/19. doi: 10.1016/j.ccell.2016.06.003. PubMed PMID: 27424807; PMCID: PMC5374862.

24. Binnewies M, Mujal AM, Pollack JL, Combes AJ, Hardison EA, Barry KC, Tsui J, Ruhland MK, Kersten K, Abushawish MA, Spasic M, Giurintano JP, Chan V, Daud AI, Ha P, Ye CJ, Roberts EW, Krummel MF. Unleashing Type-2 Dendritic Cells to Drive Protective Antitumor CD4(+) T Cell Immunity. Cell. 2019;177(3):556-71 e16. Epub 2019/04/09. doi: 10.1016/j.cell.2019.02.005. PubMed PMID: 30955881; PMCID: PMC6954108.

25. Theisen DJ, Davidson JTt, Briseno CG, Gargaro M, Lauron EJ, Wang Q, Desai P, Durai V, Bagadia P, Brickner JR, Beatty WL, Virgin HW, Gillanders WE, Mosammaparast N, Diamond MS, Sibley LD, Yokoyama W, Schreiber RD, Murphy TL, Murphy KM. WDFY4 is required for cross-presentation in response to viral and tumor antigens. Science. 2018;362(6415):694-9. Epub 2018/11/10. doi: 10.1126/science.aat5030. PubMed PMID: 30409884; PMCID: PMC6655551.

26. Ferris ST, Durai V, Wu R, Theisen DJ, Ward JP, Bern MD, Davidson JTt, Bagadia P, Liu T, Briseno CG, Li L, Gillanders WE, Wu GF, Yokoyama WM, Murphy TL,

Schreiber RD, Murphy KM. cDC1 prime and are licensed by CD4(+) T cells to induce anti-tumour immunity. Nature. 2020;584(7822):624-9. Epub 2020/08/14. doi: 10.1038/s41586-020-2611-3. PubMed PMID: 32788723; PMCID: PMC7469755.

27. Diamond MS, Kinder M, Matsushita H, Mashayekhi M, Dunn GP, Archambault JM, Lee H, Arthur CD, White JM, Kalinke U, Murphy KM, Schreiber RD. Type I interferon is selectively required by dendritic cells for immune rejection of tumors. J Exp Med. 2011;208(10):1989-2003. Epub 2011/09/21. doi: 10.1084/jem.20101158. PubMed PMID: 21930769; PMCID: PMC3182061.

28. Fuertes MB, Kacha AK, Kline J, Woo SR, Kranz DM, Murphy KM, Gajewski TF. Host type I IFN signals are required for antitumor CD8+ T cell responses through CD8{alpha}+ dendritic cells. J Exp Med. 2011;208(10):2005-16. Epub 2011/09/21. doi: 10.1084/jem.20101159. PubMed PMID: 21930765; PMCID: PMC3182064.

29. Theisen DJ, Ferris ST, Briseno CG, Kretzer N, Iwata A, Murphy KM, Murphy TL. Batf3-Dependent Genes Control Tumor Rejection Induced by Dendritic Cells Independently of Cross-Presentation. Cancer Immunol Res. 2019;7(1):29-39. Epub 2018/11/30. doi: 10.1158/2326-6066.CIR-18-0138. PubMed PMID: 30482745.

30. Spranger S, Dai D, Horton B, Gajewski TF. Tumor-Residing Batf3 Dendritic Cells Are Required for Effector T Cell Trafficking and Adoptive T Cell Therapy. Cancer Cell. 2017;31(5):711-23 e4. Epub 2017/05/10. doi: 10.1016/j.ccell.2017.04.003. PubMed PMID: 28486109; PMCID: PMC5650691.

31. Spranger S, Bao R, Gajewski TF. Melanoma-intrinsic beta-catenin signalling prevents anti-tumour immunity. Nature. 2015;523(7559):231-5. Epub 2015/05/15. doi: 10.1038/nature14404. PubMed PMID: 25970248.

32. Shirai Y. On the transplantation of the rat sarcoma in adult heterogenous animals. Jap Med World. 1921;1:14-5.

33. Murphy JB, Sturm E. Conditions Determining the Transplantability of Tissues in the Brain. J Exp Med. 1923;38(2):183-97. Epub 1923/07/31. doi: 10.1084/jem.38.2.183. PubMed PMID: 19868782; PMCID: PMC2128434.

34. Medawar PB. Immunity to homologous grafted skin; the fate of skin homografts transplanted to the brain, to subcutaneous tissue, and to the anterior chamber of the eye. Br J Exp Pathol. 1948;29(1):58-69. Epub 1948/02/01. PubMed PMID: 18865105; PMCID: PMC2073079.

35. Matyszak MK, Perry VH. Demyelination in the central nervous system following a delayed-type hypersensitivity response to bacillus Calmette-Guerin. Neuroscience. 1995;64(4):967-77. Epub 1995/02/01. doi: 10.1016/0306-4522(94)00448-e. PubMed PMID: 7753389.

36. Stevenson PG, Hawke S, Sloan DJ, Bangham CR. The immunogenicity of intracerebral virus infection depends on anatomical site. J Virol. 1997;71(1):145-51.

Epub 1997/01/01. doi: 10.1128/JVI.71.1.145-151.1997. PubMed PMID: 8985333; PMCID: PMC191034.

37. Byrnes AP, MacLaren RE, Charlton HM. Immunological instability of persistent adenovirus vectors in the brain: peripheral exposure to vector leads to renewed inflammation, reduced gene expression, and demyelination. J Neurosci. 1996;16(9):3045-55. Epub 1996/05/01. PubMed PMID: 8622134; PMCID: PMC6579058.

38. Galea I, Bechmann I, Perry VH. What is immune privilege (not)? Trends Immunol. 2007;28(1):12-8. doi: 10.1016/j.it.2006.11.004. PubMed PMID: WOS:000243707900003.

39. Nicholas MK, Antel JP, Stefansson K, Arnason BG. Rejection of fetal neocortical neural transplants by H-2 incompatible mice. J Immunol. 1987;139(7):2275-83. Epub 1987/10/01. PubMed PMID: 3309054.

40. Mason DW, Charlton HM, Jones AJ, Lavy CB, Puklavec M, Simmonds SJ. The fate of allogeneic and xenogeneic neuronal tissue transplanted into the third ventricle of rodents. Neuroscience. 1986;19(3):685-94. Epub 1986/11/01. doi: 10.1016/0306-4522(86)90292-7. PubMed PMID: 3796814.

41. Finsen BR, Sorensen T, Castellano B, Pedersen EB, Zimmer J. Leukocyte infiltration and glial reactions in xenografts of mouse brain tissue undergoing rejection in the adult rat brain. A light and electron microscopical immunocytochemical study. J Neuroimmunol. 1991;32(2):159-83. Epub 1991/05/01. doi: 10.1016/0165-5728(91)90008-u. PubMed PMID: 1849517.

42. Engelhardt B, Vajkoczy P, Weller RO. The movers and shapers in immune privilege of the CNS. Nature Immunology. 2017;18(2):123-31. doi: 10.1038/ni.3666. PubMed PMID: WOS:000392360900003.

43. Huber JD, Egleton RD, Davis TP. Molecular physiology and pathophysiology of tight junctions in the blood-brain barrier. Trends Neurosci. 2001;24(12):719-25. Epub 2001/11/24. doi: 10.1016/s0166-2236(00)02004-x. PubMed PMID: 11718877.

44. Tietz S, Engelhardt B. Brain barriers: Crosstalk between complex tight junctions and adherens junctions. J Cell Biol. 2015;209(4):493-506. doi: 10.1083/jcb.201412147. PubMed PMID: WOS:000355643900007.

45. Abbott NJ, Ronnback L, Hansson E. Astrocyte-endothelial interactions at the blood-brain barrier. Nat Rev Neurosci. 2006;7(1):41-53. doi: 10.1038/nrn1824. PubMed PMID: WOS:000234139600015.

46. Dunn GP, Okada H. Principles of immunology and its nuances in the central nervous system. Neuro Oncol. 2015;17 Suppl 7:vii3-vii8. Epub 2015/10/31. doi: 10.1093/neuonc/nov175. PubMed PMID: 26516224; PMCID: PMC4625893.

47. Long DM. Capillary ultrastructure and the blood-brain barrier in human malignant brain tumors. J Neurosurg. 1970;32(2):127-44. Epub 1970/02/01. doi: 10.3171/jns.1970.32.2.0127. PubMed PMID: 5411991.

48. Wang R, Chadalavada K, Wilshire J, Kowalik U, Hovinga KE, Geber A, Fligelman B, Leversha M, Brennan C, Tabar V. Glioblastoma stem-like cells give rise to tumour endothelium. Nature. 2010;468(7325):829-33. Epub 2010/11/26. doi: 10.1038/nature09624. PubMed PMID: 21102433.

49. Mrdjen D, Pavlovic A, Hartmann FJ, Schreiner B, Utz SG, Leung BP, Lelios I, Heppner FL, Kipnis J, Merkler D, Greter M, Becher B. High-Dimensional Single-Cell Mapping of Central Nervous System Immune Cells Reveals Distinct Myeloid Subsets in Health, Aging, and Disease. Immunity. 2018;48(3):599. Epub 2018/03/22. doi: 10.1016/j.immuni.2018.02.014. PubMed PMID: 29562204.

50. Hart DN, Fabre JW. Demonstration and characterization of Ia-positive dendritic cells in the interstitial connective tissues of rat heart and other tissues, but not brain. J Exp Med. 1981;154(2):347-61. doi: 10.1084/jem.154.2.347. PubMed PMID: 6943285; PMCID: PMC2186417.

51. Matyszak MK, Perry VH. The potential role of dendritic cells in immune-mediated inflammatory diseases in the central nervous system. Neuroscience. 1996;74(2):599-608. Epub 1996/09/01. doi: 10.1016/0306-4522(96)00160-1. PubMed PMID: 8865208.

52. Harris MG, Hulseberg P, Ling C, Karman J, Clarkson BD, Harding JS, Zhang M, Sandor A, Christensen K, Nagy A, Sandor M, Fabry Z. Immune privilege of the CNS is not the consequence of limited antigen sampling. Sci Rep. 2014;4:4422. Epub 2014/03/22. doi: 10.1038/srep04422. PubMed PMID: 24651727; PMCID: PMC3961746.

53. Zozulya AL, Reinke E, Baiu DC, Karman J, Sandor M, Fabry Z. Dendritic cell transmigration through brain microvessel endothelium is regulated by MIP-1alpha chemokine and matrix metalloproteinases. J Immunol. 2007;178(1):520-9. Epub 2006/12/22. doi: 10.4049/jimmunol.178.1.520. PubMed PMID: 17182592; PMCID: PMC1950722.

54. Karman J, Ling C, Sandor M, Fabry Z. Initiation of immune responses in brain is promoted by local dendritic cells. J Immunol. 2004;173(4):2353-61. Epub 2004/08/06. doi: 10.4049/jimmunol.173.4.2353. PubMed PMID: 15294948.

55. Mundt S, Mrdjen D, Utz SG, Greter M, Schreiner B, Becher B. Conventional DCs sample and present myelin antigens in the healthy CNS and allow parenchymal T cell entry to initiate neuroinflammation. Sci Immunol. 2019;4(31). Epub 2019/01/27. doi: 10.1126/sciimmunol.aau8380. PubMed PMID: 30679199.

56. Giles DA, Duncker PC, Wilkinson NM, Washnock-Schmid JM, Segal BM. CNS-resident classical DCs play a critical role in CNS autoimmune disease. J Clin Invest. 2018;128(12):5322-34. Epub 2018/09/19. doi: 10.1172/JCI123708. PubMed PMID: 30226829; PMCID: PMC6264723.

57. Sandrone S, Moreno-Zambrano D, Kipnis J, van Gijn J. A (delayed) history of the brain lymphatic system. Nat Med. 2019;25(4):538-40. Epub 2019/04/06. doi: 10.1038/s41591-019-0417-3. PubMed PMID: 30948855.

58. Lukic IK, Gluncic V, Ivkic G, Hubenstorf M, Marusic A. Virtual dissection: a lesson from the 18th century. Lancet. 2003;362(9401):2110-3. Epub 2003/12/31. doi: 10.1016/S0140-6736(03)15114-8. PubMed PMID: 14697818.

59. Zhang ET, Richards HK, Kida S, Weller RO. Directional and compartmentalised drainage of interstitial fluid and cerebrospinal fluid from the rat brain. Acta Neuropathol. 1992;83(3):233-9. Epub 1992/01/01. doi: 10.1007/BF00296784. PubMed PMID: 1373020.

60. Kida S, Pantazis A, Weller RO. CSF drains directly from the subarachnoid space into nasal lymphatics in the rat. Anatomy, histology and immunological significance. Neuropathol Appl Neurobiol. 1993;19(6):480-8. Epub 1993/12/01. doi: 10.1111/j.1365-2990.1993.tb00476.x. PubMed PMID: 7510047.

61. Phillips MJ, Needham M, Weller RO. Role of cervical lymph nodes in autoimmune encephalomyelitis in the Lewis rat. J Pathol. 1997;182(4):457-64. Epub 1997/08/01. doi: 10.1002/(SICI)1096-9896(199708)182:4<457::AID-PATH870>3.0.CO;2-Y. PubMed PMID: 9306968.

62. Furtado GC, Marcondes MC, Latkowski JA, Tsai J, Wensky A, Lafaille JJ. Swift entry of myelin-specific T lymphocytes into the central nervous system in spontaneous autoimmune encephalomyelitis. J Immunol. 2008;181(7):4648-55. Epub 2008/09/20. doi: 10.4049/jimmunol.181.7.4648. PubMed PMID: 18802067; PMCID: PMC3973185.

63. van Zwam M, Huizinga R, Heijmans N, van Meurs M, Wierenga-Wolf AF, Melief MJ, Hintzen RQ, t Hart BA, Amor S, Boven LA, Laman JD. Surgical excision of CNS-draining lymph nodes reduces relapse severity in chronic-relapsing experimental autoimmune encephalomyelitis. J Pathol. 2009;217(4):543-51. Epub 2008/11/22. doi: 10.1002/path.2476. PubMed PMID: 19023878.

64. Louveau A, Smirnov I, Keyes TJ, Eccles JD, Rouhani SJ, Peske JD, Derecki NC, Castle D, Mandell JW, Lee KS, Harris TH, Kipnis J. Structural and functional features of central nervous system lymphatic vessels. Nature. 2015;523(7560):337-41. Epub 2015/06/02. doi: 10.1038/nature14432. PubMed PMID: 26030524; PMCID: PMC4506234.

65. Aspelund A, Antila S, Proulx ST, Karlsen TV, Karaman S, Detmar M, Wiig H, Alitalo K. A dural lymphatic vascular system that drains brain interstitial fluid and macromolecules. J Exp Med. 2015;212(7):991-9. Epub 2015/06/17. doi: 10.1084/jem.20142290. PubMed PMID: 26077718; PMCID: PMC4493418.

66. Da Mesquita S, Louveau A, Vaccari A, Smirnov I, Cornelison RC, Kingsmore KM, Contarino C, Onengut-Gumuscu S, Farber E, Raper D, Viar KE, Powell RD, Baker W, Dabhi N, Bai R, Cao R, Hu S, Rich SS, Munson JM, Lopes MB, Overall CC, Acton ST,

Kipnis J. Functional aspects of meningeal lymphatics in ageing and Alzheimer's disease. Nature. 2018;560(7717):185-91. Epub 2018/07/27. doi: 10.1038/s41586-018-0368-8. PubMed PMID: 30046111; PMCID: PMC6085146.

67. Louveau A, Herz J, Alme MN, Salvador AF, Dong MQ, Viar KE, Herod SG, Knopp J, Setliff JC, Lupi AL, Da Mesquita S, Frost EL, Gaultier A, Harris TH, Cao R, Hu S, Lukens JR, Smirnov I, Overall CC, Oliver G, Kipnis J. CNS lymphatic drainage and neuroinflammation are regulated by meningeal lymphatic vasculature. Nat Neurosci. 2018;21(10):1380-91. Epub 2018/09/19. doi: 10.1038/s41593-018-0227-9. PubMed PMID: 30224810; PMCID: PMC6214619.

68. Absinta M, Ha SK, Nair G, Sati P, Luciano NJ, Palisoc M, Louveau A, Zaghloul KA, Pittaluga S, Kipnis J, Reich DS. Human and nonhuman primate meninges harbor lymphatic vessels that can be visualized noninvasively by MRI. Elife. 2017;6. Epub 2017/10/04. doi: 10.7554/eLife.29738. PubMed PMID: 28971799; PMCID: PMC5626482.

69. Song E, Mao T, Dong H, Boisserand LSB, Antila S, Bosenberg M, Alitalo K, Thomas JL, Iwasaki A. VEGF-C-driven lymphatic drainage enables immunosurveillance of brain tumours. Nature. 2020;577(7792):689-94. Epub 2020/01/17. doi: 10.1038/s41586-019-1912-x. PubMed PMID: 31942068; PMCID: PMC7100608.

70. Cyster JG, Schwab SR. Sphingosine-1-phosphate and lymphocyte egress from lymphoid organs. Annu Rev Immunol. 2012;30:69-94. Epub 2011/12/14. doi: 10.1146/annurev-immunol-020711-075011. PubMed PMID: 22149932.

71. Chongsathidkiet P, Jackson C, Koyama S, Loebel F, Cui X, Farber SH, Woroniecka K, Elsamadicy AA, Dechant CA, Kemeny HR, Sanchez-Perez L, Cheema TA, Souders NC, Herndon JE, Coumans JV, Everitt JI, Nahed BV, Sampson JH, Gunn MD, Martuza RL, Dranoff G, Curry WT, Fecci PE. Sequestration of T cells in bone marrow in the setting of glioblastoma and other intracranial tumors. Nat Med. 2018;24(9):1459-68. Epub 2018/08/15. doi: 10.1038/s41591-018-0135-2. PubMed PMID: 30104766; PMCID: PMC6129206.

72. Chongsathidkiet P, Jackson C, Koyama S, Loebel F, Cui X, Farber SH, Woroniecka K, Elsamadicy AA, Dechant CA, Kemeny HR, Sanchez-Perez L, Cheema TA, Souders NC, Herndon JE, Coumans JV, Everitt JI, Nahed BV, Sampson JH, Gunn MD, Martuza RL, Dranoff G, Curry WT, Fecci PE. Author Correction: Sequestration of T cells in bone marrow in the setting of glioblastoma and other intracranial tumors. Nat Med. 2019;25(3):529. Epub 2019/01/24. doi: 10.1038/s41591-019-0355-0. PubMed PMID: 30670876; PMCID: PMC6825406.

73. O'Connor JC, Lawson MA, Andre C, Briley EM, Szegedi SS, Lestage J, Castanon N, Herkenham M, Dantzer R, Kelley KW. Induction of IDO by bacille Calmette-Guerin is responsible for development of murine depressive-like behavior. J Immunol. 2009;182(5):3202-12. Epub 2009/02/24. doi: 10.4049/jimmunol.0802722. PubMed PMID: 19234218; PMCID: PMC2664258.

74. Zhai L, Bell A, Ladomersky E, Lauing KL, Bollu L, Sosman JA, Zhang B, Wu JD, Miller SD, Meeks JJ, Lukas RV, Wyatt E, Doglio L, Schiltz GE, McCusker RH, Wainwright DA. Immunosuppressive IDO in Cancer: Mechanisms of Action, Animal Models, and Targeting Strategies. Front Immunol. 2020;11:1185. Epub 2020/07/03. doi: 10.3389/fimmu.2020.01185. PubMed PMID: 32612606; PMCID: PMC7308527.

75. Fallarino F, Grohmann U, Vacca C, Bianchi R, Orabona C, Spreca A, Fioretti MC, Puccetti P. T cell apoptosis by tryptophan catabolism. Cell Death Differ. 2002;9(10):1069-77. Epub 2002/09/17. doi: 10.1038/sj.cdd.4401073. PubMed PMID: 12232795.

76. Mezrich JD, Fechner JH, Zhang X, Johnson BP, Burlingham WJ, Bradfield CA. An interaction between kynurenine and the aryl hydrocarbon receptor can generate regulatory T cells. J Immunol. 2010;185(6):3190-8. Epub 2010/08/20. doi: 10.4049/jimmunol.0903670. PubMed PMID: 20720200; PMCID: PMC2952546.

77. Wainwright DA, Balyasnikova IV, Chang AL, Ahmed AU, Moon KS, Auffinger B, Tobias AL, Han Y, Lesniak MS. IDO expression in brain tumors increases the recruitment of regulatory T cells and negatively impacts survival. Clin Cancer Res. 2012;18(22):6110-21. Epub 2012/08/31. doi: 10.1158/1078-0432.CCR-12-2130. PubMed PMID: 22932670; PMCID: PMC3500434.

78. Wainwright DA, Chang AL, Dey M, Balyasnikova IV, Kim CK, Tobias A, Cheng Y, Kim JW, Qiao J, Zhang LJ, Han Y, Lesniak MS. Durable Therapeutic Efficacy Utilizing Combinatorial Blockade against IDO, CTLA-4, and PD-L1 in Mice with Brain Tumors. Clinical Cancer Research. 2014;20(20):5290-301. doi: 10.1158/1078-0432.Ccr-14-0514. PubMed PMID: WOS:000343873100016.

79. Zhai L, Ladomersky E, Dostal CR, Lauing KL, Swoap K, Billingham LK, Gritsina G, Wu M, McCusker RH, Binder DC, Wainwright DA. Non-tumor cell IDO1 predominantly contributes to enzyme activity and response to CTLA-4/PD-L1 inhibition in mouse glioblastoma. Brain Behav Immun. 2017;62:24-9. Epub 2017/02/10. doi: 10.1016/j.bbi.2017.01.022. PubMed PMID: 28179106; PMCID: PMC5514839.

80. de Martin R, Haendler B, Hofer-Warbinek R, Gaugitsch H, Wrann M, Schlusener H, Seifert JM, Bodmer S, Fontana A, Hofer E. Complementary DNA for human glioblastoma-derived T cell suppressor factor, a novel member of the transforming growth factor-beta gene family. Embo J. 1987;6(12):3673-7. Epub 1987/12/01. PubMed PMID: 3322813; PMCID: PMC553836.

81. Yamada N, Kato M, Yamashita H, Nister M, Miyazono K, Heldin CH, Funa K. Enhanced expression of transforming growth factor-beta and its type-I and type-II receptors in human glioblastoma. Int J Cancer. 1995;62(4):386-92. Epub 1995/08/09. doi: 10.1002/ijc.2910620405. PubMed PMID: 7635563.

82. Hao C, Parney IF, Roa WH, Turner J, Petruk KC, Ramsay DA. Cytokine and cytokine receptor mRNA expression in human glioblastomas: evidence of Th1, Th2 and

Th3 cytokine dysregulation. Acta Neuropathol. 2002;103(2):171-8. Epub 2002/01/26. doi: 10.1007/s004010100448. PubMed PMID: 11810184.

83. Wagner S, Czub S, Greif M, Vince GH, Suss N, Kerkau S, Rieckmann P, Roggendorf W, Roosen K, Tonn JC. Microglial/macrophage expression of interleukin 10 in human glioblastomas. Int J Cancer. 1999;82(1):12-6. Epub 1999/06/09. doi: 10.1002/(sici)1097-0215(19990702)82:1<12::aid-ijc3>3.0.co;2-o. PubMed PMID: 10360813.

84. Huettner C, Czub S, Kerkau S, Roggendorf W, Tonn JC. Interleukin 10 is expressed in human gliomas in vivo and increases glioma cell proliferation and motility in vitro. Anticancer Research. 1997;17(5a):3217-24. PubMed PMID: WOS:A1997YK65700005.

85. Taylor A, Verhagen J, Blaser K, Akdis M, Akdis CA. Mechanisms of immune suppression by interleukin-10 and transforming growth factor-beta: the role of T regulatory cells. Immunology. 2006;117(4):433-42. Epub 2006/03/25. doi: 10.1111/j.1365-2567.2006.02321.x. PubMed PMID: 16556256; PMCID: PMC1782242.

86. Berghoff AS, Kiesel B, Widhalm G, Rajky O, Ricken G, Wohrer A, Dieckmann K, Filipits M, Brandstetter A, Weller M, Kurscheid S, Hegi ME, Zielinski CC, Marosi C, Hainfellner JA, Preusser M, Wick W. Programmed death ligand 1 expression and tumor-infiltrating lymphocytes in glioblastoma. Neuro Oncol. 2015;17(8):1064-75. Epub 2014/10/31. doi: 10.1093/neuonc/nou307. PubMed PMID: 25355681; PMCID: PMC4490866.

87. Parsa AT, Waldron JS, Panner A, Crane CA, Parney IF, Barry JJ, Cachola KE, Murray JC, Tihan T, Jensen MC, Mischel PS, Stokoe D, Pieper RO. Loss of tumor suppressor PTEN function increases B7-H1 expression and immunoresistance in glioma. Nature Medicine. 2007;13(1):84-8. doi: 10.1038/nm1517. PubMed PMID: WOS:000243301800040.

88. Bloch O, Crane CA, Kaur R, Safaee M, Rutkowski MJ, Parsa AT. Gliomas Promote Immunosuppression through Induction of B7-H1 Expression in Tumor-Associated Macrophages. Clinical Cancer Research. 2013;19(12):3165-75. doi: 10.1158/1078-0432.Ccr-12-3314. PubMed PMID: WOS:000320381000007.

89. Bayik D, Zhou Y, Park C, Hong C, Vail D, Silver DJ, Lauko A, Roversi G, Watson DC, Lo A, Alban TJ, McGraw M, Sorensen M, Grabowski MM, Otvos B, Vogelbaum MA, Horbinski C, Kristensen BW, Khalil AM, Hwang TH, Ahluwalia MS, Cheng F, Lathia JD. Myeloid-Derived Suppressor Cell Subsets Drive Glioblastoma Growth in a Sex-Specific Manner. Cancer Discov. 2020;10(8):1210-25. Epub 2020/04/18. doi: 10.1158/2159-8290.CD-19-1355. PubMed PMID: 32300059; PMCID: PMC7415660.

90. Gielen PR, Schulte BM, Kers-Rebel ED, Verrijp K, Bossman SAJFH, ter Laan M, Wesseling P, Adema GJ. Elevated levels of polymorphonuclear myeloid-derived suppressor cells in patients with glioblastoma highly express S100A8/9 and arginase

and suppress T cell function. Neuro-Oncology. 2016;18(9):1253-64. doi: 10.1093/neuonc/now034. PubMed PMID: WOS:000384005900013.

91. Gabrilovich DI, Nagaraj S. Myeloid-derived suppressor cells as regulators of the immune system. Nat Rev Immunol. 2009;9(3):162-74. doi: 10.1038/nri2506. PubMed PMID: WOS:000263677400011.

92. Aum DJ, Kim DH, Beaumont TL, Leuthardt EC, Dunn GP, Kim AH. Molecular and cellular heterogeneity: the hallmark of glioblastoma. Neurosurg Focus. 2014;37(6):E11. Epub 2014/12/02. doi: 10.3171/2014.9.FOCUS14521. PubMed PMID: 25434380.

93. Dunn GP, Rinne ML, Wykosky J, Genovese G, Quayle SN, Dunn IF, Agarwalla PK, Chheda MG, Campos B, Wang A, Brennan C, Ligon KL, Furnari F, Cavenee WK, Depinho RA, Chin L, Hahn WC. Emerging insights into the molecular and cellular basis of glioblastoma. Gene Dev. 2012;26(8):756-84. doi: 10.1101/gad.187922.112. PubMed PMID: WOS:000302909600004.

94. Nishikawa R, Sugiyama T, Narita Y, Furnari F, Cavenee WK, Matsutani M. Immunohistochemical analysis of the mutant epidermal growth factor, deltaEGFR, in glioblastoma. Brain Tumor Pathol. 2004;21(2):53-6. Epub 2005/02/11. doi: 10.1007/BF02484510. PubMed PMID: 15700833.

95. Wolf Y, Bartok O, Patkar S, Bar Eli G, Cohen S, Litchfield K, Levy R, Jimenez-Sanchez A, Trabish S, Lee JS, Karathia H, Barnea E, Day CP, Cinnamon E, Stein I, Solomon A, Bitton L, Perez-Guijarro E, Dubovik T, Shen-Orr SS, Miller ML, Merlino G, Levin Y, Pikarsky E, Eisenbach L, Admon A, Swanton C, Ruppin E, Samuels Y. UVB-Induced Tumor Heterogeneity Diminishes Immune Response in Melanoma. Cell. 2019;179(1):219-+. doi: 10.1016/j.cell.2019.08.032. PubMed PMID: WOS:000486618500025.

96. Rosenberg SA. IL-2: the first effective immunotherapy for human cancer. J Immunol. 2014;192(12):5451-8. Epub 2014/06/08. doi: 10.4049/jimmunol.1490019. PubMed PMID: 24907378; PMCID: PMC6293462.

97. Krummel MF, Allison JP. CD28 and CTLA-4 have opposing effects on the response of T cells to stimulation. J Exp Med. 1995;182(2):459-65. Epub 1995/08/01. doi: 10.1084/jem.182.2.459. PubMed PMID: 7543139; PMCID: PMC2192127.

98. Tivol EA, Borriello F, Schweitzer AN, Lynch WP, Bluestone JA, Sharpe AH. Loss of Ctla-4 Leads to Massive Lymphoproliferation and Fatal Multiorgan Tissue Destruction, Revealing a Critical Negative Regulatory Role of Ctla-4. Immunity. 1995;3(5):541-7. doi: Doi 10.1016/1074-7613(95)90125-6. PubMed PMID: WOS:A1995TG28100002.

99. Leach DR, Krummel MF, Allison JP. Enhancement of antitumor immunity by CTLA-4 blockade. Science. 1996;271(5256):1734-6. Epub 1996/03/22. doi: 10.1126/science.271.5256.1734. PubMed PMID: 8596936.

100. Ishida Y, Agata Y, Shibahara K, Honjo T. Induced Expression of Pd-1, a Novel Member of the Immunoglobulin Gene Superfamily, Upon Programmed Cell-Death. Embo J. 1992;11(11):3887-95. doi: DOI 10.1002/j.1460-2075.1992.tb05481.x. PubMed PMID: WOS:A1992JT32800010.

101. Agata Y, Kawasaki A, Nishimura H, Ishida Y, Tsubata T, Yagita H, Honjo T. Expression of the PD-1 antigen on the surface of stimulated mouse T and B lymphocytes. Int Immunol. 1996;8(5):765-72. Epub 1996/05/01. doi: 10.1093/intimm/8.5.765. PubMed PMID: 8671665.

102. Nishimura H, Okazaki T, Tanaka Y, Nakatani K, Hara M, Matsumori A, Sasayama S, Mizoguchi A, Hiai H, Minato N, Honjo T. Autoimmune dilated cardiomyopathy in PD-1 receptor-deficient mice. Science. 2001;291(5502):319-22. doi: DOI 10.1126/science.291.5502.319. PubMed PMID: WOS:000166352900050.

103. Iwai Y, Ishida M, Tanaka Y, Okazaki T, Honjo T, Minato N. Involvement of PD-L1 on tumor cells in the escape from host immune system and tumor immunotherapy by PD-L1 blockade. P Natl Acad Sci USA. 2002;99(19):12293-7. doi: 10.1073/pnas.192461099. PubMed PMID: WOS:000178187000055.

104. Bersanelli M, Buti S. From targeting the tumor to targeting the immune system: Transversal challenges in oncology with the inhibition of the PD-1/PD-L1 axis. World J Clin Oncol. 2017;8(1):37-53. Epub 2017/03/02. doi: 10.5306/wjco.v8.i1.37. PubMed PMID: 28246584; PMCID: PMC5309713.

105. Johanns T, Waqar SN, Morgensztern D. Immune checkpoint inhibition in patients with brain metastases. Ann Transl Med. 2016;4(Suppl 1):S9. Epub 2016/11/22. doi: 10.21037/atm.2016.09.40. PubMed PMID: 27867977; PMCID: PMC5104596 other authors have no conflicts of interest to declare.

106. Goldberg SB, Gettinger SN, Mahajan A, Chiang AC, Herbst RS, Sznol M, Tsiouris AJ, Cohen J, Vortmeyer A, Jilaveanu L, Yu J, Hegde U, Speaker S, Madura M, Ralabate A, Rivera A, Rowen E, Gerrish H, Yao X, Chiang V, Kluger HM. Pembrolizumab for patients with melanoma or non-small-cell lung cancer and untreated brain metastases: early analysis of a non-randomised, open-label, phase 2 trial. Lancet Oncol. 2016;17(7):976-83. Epub 2016/06/09. doi: 10.1016/S1470-2045(16)30053-5. PubMed PMID: 27267608; PMCID: PMC5526047.

107. Martins F, Schiappacasse L, Levivier M, Tuleasca C, Cuendet MA, Aedo-Lopez V, Gautron Moura B, Homicsko K, Bettini A, Berthod G, Gerard CL, Wicky A, Bourhis J, Michielin O. The combination of stereotactic radiosurgery with immune checkpoint inhibition or targeted therapy in melanoma patients with brain metastases: a retrospective study. J Neurooncol. 2020;146(1):181-93. Epub 2019/12/15. doi: 10.1007/s11060-019-03363-0. PubMed PMID: 31836957.

108. Margolin K, Ernstoff MS, Hamid O, Lawrence D, McDermott D, Puzanov I, Wolchok JD, Clark JI, Sznol M, Logan TF, Richards J, Michener T, Balogh A, Heller KN, Hodi FS. Ipilimumab in patients with melanoma and brain metastases: an open-label,

phase 2 trial. Lancet Oncol. 2012;13(5):459-65. Epub 2012/03/30. doi: 10.1016/S1470-2045(12)70090-6. PubMed PMID: 22456429.

109. Johanns TM, Miller CA, Dorward IG, Tsien C, Chang E, Perry A, Uppaluri R, Ferguson C, Schmidt RE, Dahiya S, Ansstas G, Mardis ER, Dunn GP. Immunogenomics of Hypermutated Glioblastoma: A Patient with Germline POLE Deficiency Treated with Checkpoint Blockade Immunotherapy. Cancer Discov. 2016;6(11):1230-6. Epub 2016/11/04. doi: 10.1158/2159-8290.CD-16-0575. PubMed PMID: 27683556; PMCID: PMC5140283.

110. Bouffet E, Larouche V, Campbell BB, Merico D, de Borja R, Aronson M, Durno C, Krueger J, Cabric V, Ramaswamy V, Zhukova N, Mason G, Farah R, Afzal S, Yalon M, Rechavi G, Magimairajan V, Walsh MF, Constantini S, Dvir R, Elhasid R, Reddy A, Osborn M, Sullivan M, Hansford J, Dodgshun A, Klauber-Demore N, Peterson L, Patel S, Lindhorst S, Atkinson J, Cohen Z, Laframboise R, Dirks P, Taylor M, Malkin D, Albrecht S, Dudley RW, Jabado N, Hawkins CE, Shlien A, Tabori U. Immune Checkpoint Inhibition for Hypermutant Glioblastoma Multiforme Resulting From Germline Biallelic Mismatch Repair Deficiency. J Clin Oncol. 2016;34(19):2206-11. Epub 2016/03/24. doi: 10.1200/JCO.2016.66.6552. PubMed PMID: 27001570.

111. Coxon AT, Johanns TM, Dunn GP. An Innovative Immunotherapy Vaccine with Combination Checkpoint Blockade as a First Line Treatment for Glioblastoma in the Context of Current Treatments. Mo Med. 2020;117(1):45-9. Epub 2020/03/12. PubMed PMID: 32158049; PMCID: PMC7023938.

112. Cloughesy TF, Mochizuki AY, Orpilla JR, Hugo W, Lee AH, Davidson TB, Wang AC, Ellingson BM, Rytlewski JA, Sanders CM, Kawaguchi ES, Du L, Li G, Yong WH, Gaffey SC, Cohen AL, Mellinghoff IK, Lee EQ, Reardon DA, O'Brien BJ, Butowski NA, Nghiemphu PL, Clarke JL, Arrillaga-Romany IC, Colman H, Kaley TJ, de Groot JF, Liau LM, Wen PY, Prins RM. Neoadjuvant anti-PD-1 immunotherapy promotes a survival benefit with intratumoral and systemic immune responses in recurrent glioblastoma. Nat Med. 2019;25(3):477-86. Epub 2019/02/12. doi: 10.1038/s41591-018-0337-7. PubMed PMID: 30742122; PMCID: PMC6408961.

113. Wikstrand CJ, Hale LP, Batra SK, Hill ML, Humphrey PA, Kurpad SN, McLendon RE, Moscatello D, Pegram CN, Reist CJ, et al. Monoclonal antibodies against EGFRvIII are tumor specific and react with breast and lung carcinomas and malignant gliomas. Cancer Res. 1995;55(14):3140-8. Epub 1995/07/15. PubMed PMID: 7606735.

114. Wu AH, Xiao J, Anker L, Hall WA, Gregerson DS, Cavenee WK, Chen W, Low WC. Identification of EGFRvIII-derived CTL epitopes restricted by HLA A0201 for dendritic cell based immunotherapy of gliomas. J Neurooncol. 2006;76(1):23-30. Epub 2005/09/13. doi: 10.1007/s11060-005-3280-7. PubMed PMID: 16155724.

115. Purev E, Cai D, Miller E, Swoboda R, Mayer T, Klein-Szanto A, Marincola FM, Mick R, Otvos L, Wunner W, Birebent B, Somasundaram R, Wikstrand CJ, Bigner D, DeMichele A, Acs G, Berlin JA, Herlyn D. Immune responses of breast cancer patients

to mutated epidermal growth factor receptor (EGF-RvIII, Delta EGF-R, and de2-7 EGF-R). J Immunol. 2004;173(10):6472-80. Epub 2004/11/06. doi: 10.4049/jimmunol.173.10.6472. PubMed PMID: 15528389.

116. Schuster J, Lai RK, Recht LD, Reardon DA, Paleologos NA, Groves MD, Mrugala MM, Jensen R, Baehring JM, Sloan A, Archer GE, Bigner DD, Cruickshank S, Green JA, Keler T, Davis TA, Heimberger AB, Sampson JH. A phase II, multicenter trial of rindopepimut (CDX-110) in newly diagnosed glioblastoma: the ACT III study. Neuro Oncol. 2015;17(6):854-61. Epub 2015/01/15. doi: 10.1093/neuonc/nou348. PubMed PMID: 25586468; PMCID: PMC4483122.

117. Weller M, Butowski N, Tran DD, Recht LD, Lim M, Hirte H, Ashby L, Mechtler L, Goldlust SA, Iwamoto F, Drappatz J, O'Rourke DM, Wong M, Hamilton MG, Finocchiaro G, Perry J, Wick W, Green J, He Y, Turner CD, Yellin MJ, Keler T, Davis TA, Stupp R, Sampson JH, investigators AIt. Rindopepimut with temozolomide for patients with newly diagnosed, EGFRvIII-expressing glioblastoma (ACT IV): a randomised, double-blind, international phase 3 trial. Lancet Oncol. 2017;18(10):1373-85. Epub 2017/08/29. doi: 10.1016/S1470-2045(17)30517-X. PubMed PMID: 28844499.

118. Morgan RA, Johnson LA, Davis JL, Zheng Z, Woolard KD, Reap EA, Feldman SA, Chinnasamy N, Kuan CT, Song H, Zhang W, Fine HA, Rosenberg SA. Recognition of glioma stem cells by genetically modified T cells targeting EGFRvIII and development of adoptive cell therapy for glioma. Hum Gene Ther. 2012;23(10):1043-53. Epub 2012/07/12. doi: 10.1089/hum.2012.041. PubMed PMID: 22780919; PMCID: PMC3472555.

119. O'Rourke DM, Nasrallah MP, Desai A, Melenhorst JJ, Mansfield K, Morrissette JJD, Martinez-Lage M, Brem S, Maloney E, Shen A, Isaacs R, Mohan S, Plesa G, Lacey SF, Navenot JM, Zheng Z, Levine BL, Okada H, June CH, Brogdon JL, Maus MV. A single dose of peripherally infused EGFRvIII-directed CAR T cells mediates antigen loss and induces adaptive resistance in patients with recurrent glioblastoma. Sci Transl Med. 2017;9(399). Epub 2017/07/21. doi: 10.1126/scitranslmed.aaa0984. PubMed PMID: 28724573; PMCID: PMC5762203.

120. Bagley SJ, Desai AS, Linette GP, June CH, O'Rourke DM. CAR T-cell therapy for glioblastoma: recent clinical advances and future challenges. Neuro Oncol. 2018;20(11):1429-38. Epub 2018/03/07. doi: 10.1093/neuonc/noy032. PubMed PMID: 29509936; PMCID: PMC6176794.

121. Eagles ME, Nassiri F, Badhiwala JH, Suppiah S, Almenawer SA, Zadeh G, Aldape KD. Dendritic cell vaccines for high-grade gliomas. Ther Clin Risk Manag. 2018;14:1299-313. Epub 2018/08/14. doi: 10.2147/TCRM.S135865. PubMed PMID: 30100728; PMCID: PMC6067774.

122. Liau LM, Ashkan K, Tran DD, Campian JL, Trusheim JE, Cobbs CS, Heth JA, Salacz M, Taylor S, D'Andre SD, Iwamoto FM, Dropcho EJ, Moshel YA, Walter KA, Pillainayagam CP, Aiken R, Chaudhary R, Goldlust SA, Bota DA, Duic P, Grewal J,

Elinzano H, Toms SA, Lillehei KO, Mikkelsen T, Walbert T, Abram SR, Brenner AJ, Brem S, Ewend MG, Khagi S, Portnow J, Kim LJ, Loudon WG, Thompson RC, Avigan DE, Fink KL, Geoffroy FJ, Lindhorst S, Lutzky J, Sloan AE, Schackert G, Krex D, Meisel HJ, Wu J, Davis RP, Duma C, Etame AB, Mathieu D, Kesari S, Piccioni D, Westphal M, Baskin DS, New PZ, Lacroix M, May SA, Pluard TJ, Tse V, Green RM, Villano JL, Pearlman M, Petrecca K, Schulder M, Taylor LP, Maida AE, Prins RM, Cloughesy TF, Mulholland P, Bosch ML. First results on survival from a large Phase 3 clinical trial of an autologous dendritic cell vaccine in newly diagnosed glioblastoma. J Transl Med. 2018;16(1):142. Epub 2018/05/31. doi: 10.1186/s12967-018-1507-6. PubMed PMID: 29843811; PMCID: PMC5975654.

123. Johanns TM, Ward JP, Miller CA, Wilson C, Kobayashi DK, Bender D, Fu Y, Alexandrov A, Mardis ER, Artyomov MN, Schreiber RD, Dunn GP. Endogenous Neoantigen-Specific CD8 T Cells Identified in Two Glioblastoma Models Using a Cancer Immunogenomics Approach. Cancer Immunol Res. 2016;4(12):1007-15. Epub 2016/11/02. doi: 10.1158/2326-6066.CIR-16-0156. PubMed PMID: 27799140; PMCID: PMC5215735.

124. Reardon DA, Gokhale PC, Klein SR, Ligon KL, Rodig SJ, Ramkissoon SH, Jones KL, Conway AS, Liao X, Zhou J, Wen PY, Van Den Abbeele AD, Hodi FS, Qin L, Kohl NE, Sharpe AH, Dranoff G, Freeman GJ. Glioblastoma Eradication Following Immune Checkpoint Blockade in an Orthotopic, Immunocompetent Model. Cancer Immunol Res. 2016;4(2):124-35. Epub 2015/11/08. doi: 10.1158/2326-6066.CIR-15-0151. PubMed PMID: 26546453.

125. Fecci PE, Ochiai H, Mitchell DA, Grossi PM, Sweeney AE, Archer GE, Cummings T, Allison JP, Bigner DD, Sampson JH. Systemic CTLA-4 blockade ameliorates glioma-induced changes to the CD4+ T cell compartment without affecting regulatory T-cell function. Clin Cancer Res. 2007;13(7):2158-67. doi: 10.1158/1078-0432.CCR-06-2070. PubMed PMID: 17404100.

126. Liu CJ, Schaettler M, Blaha DT, Bowman-Kirigin JA, Kobayashi DK, Livingstone AJ, Bender D, Miller CA, Kranz DM, Johanns TM, Dunn GP. Treatment of an Aggressive Orthotopic Murine Glioblastoma Model with Combination Checkpoint Blockade and a Multivalent Neoantigen Vaccine. Neuro Oncol. 2020. Epub 2020/03/07. doi: 10.1093/neuonc/noaa050. PubMed PMID: 32133512.

127. Hanahan D, Weinberg RA. Hallmarks of cancer: the next generation. Cell. 2011;144(5):646-74. Epub 2011/03/08. doi: 10.1016/j.cell.2011.02.013. PubMed PMID: 21376230.

128. Roe T, Reynolds TC, Yu G, Brown PO. Integration of murine leukemia virus DNA depends on mitosis. Embo J. 1993;12(5):2099-108. Epub 1993/05/01. PubMed PMID: 8491198; PMCID: PMC413431.

129. Lei L, Sonabend AM, Guarnieri P, Soderquist C, Ludwig T, Rosenfeld S, Bruce JN, Canoll P. Glioblastoma Models Reveal the Connection between Adult Glial Progenitors and the Proneural Phenotype. Plos One. 2011;6(5). doi: ARTN e20041

10.1371/journal.pone.0020041. PubMed PMID: WOS:000291005200027.

130. Yao M, Li S, Wu X, Diao S, Zhang G, He H, Bian L, Lu Y. Cellular origin of glioblastoma and its implication in precision therapy. Cell Mol Immunol. 2018;15(8):737-9. Epub 2018/03/20. doi: 10.1038/cmi.2017.159. PubMed PMID: 29553137; PMCID: PMC6141605.

131. Cook PJ, Thomas R, Kannan R, de Leon ES, Drilon A, Rosenblum MK, Scaltriti M, Benezra R, Ventura A. Somatic chromosomal engineering identifies BCAN-NTRK1 as a potent glioma driver and therapeutic target. Nat Commun. 2017;8:15987. Epub 2017/07/12. doi: 10.1038/ncomms15987. PubMed PMID: 28695888; PMCID: PMC5508201.

132. Xiao X, Li J, Samulski RJ. Production of high-titer recombinant adeno-associated virus vectors in the absence of helper adenovirus. Journal of Virology. 1998;72(3):2224-32. doi: Doi 10.1128/Jvi.72.3.2224-2232.1998. PubMed PMID: WOS:000071997600062.

133. Gardner JP, Zhu H, Colosi PC, Kurtzman GJ, Scadden DT. Robust, but transient expression of adeno-associated virus-transduced genes during human T lymphopoiesis. Blood. 1997;90(12):4854-64. Epub 1998/01/07. PubMed PMID: 9389702.

134. Suzuki K, Mitsui K, Aizawa E, Hasegawa K, Kawase E, Yamagishi T, Shimizu Y, Suemori H, Nakatsuji N, Mitani K. Highly efficient transient gene expression and gene targeting in primate embryonic stem cells with helper-dependent adenoviral vectors. Proc Natl Acad Sci U S A. 2008;105(37):13781-6. Epub 2008/09/05. doi: 10.1073/pnas.0806976105. PubMed PMID: 18768795; PMCID: PMC2544531.

135. Hambardzumyan D, Parada LF, Holland EC, Charest A. Genetic modeling of gliomas in mice: new tools to tackle old problems. Glia. 2011;59(8):1155-68. Epub 2011/02/10. doi: 10.1002/glia.21142. PubMed PMID: 21305617; PMCID: PMC3619979.

136. Holland EC. A mouse model for glioma: biology, pathology, and therapeutic opportunities. Toxicol Pathol. 2000;28(1):171-7. Epub 2000/02/11. doi: 10.1177/019262330002800122. PubMed PMID: 10669005.

137. Lindberg N, Kastemar M, Olofsson T, Smits A, Uhrbom L. Oligodendrocyte progenitor cells can act as cell of origin for experimental glioma. Oncogene. 2009;28(23):2266-75. doi: 10.1038/onc.2009.76. PubMed PMID: WOS:000266886300003.

138. Marumoto T, Tashiro A, Friedmann-Morvinski D, Scadeng M, Soda Y, Gage FH, Verma IM. Development of a novel mouse glioma model using lentiviral vectors. Nat

Med. 2009;15(1):110-6. Epub 2009/01/06. doi: 10.1038/nm.1863. PubMed PMID: 19122659; PMCID: PMC2671237.

139. Rahme GJ, Luikart BW, Cheng C, Israel MA. A recombinant lentiviral PDGF-driven mouse model of proneural glioblastoma. Neuro Oncol. 2018;20(3):332-42. Epub 2017/10/11. doi: 10.1093/neuonc/nox129. PubMed PMID: 29016807; PMCID: PMC5817944.

140. Hambardzumyan D, Amankulor NM, Helmy KY, Becher OJ, Holland EC. Modeling Adult Gliomas Using RCAS/t-va Technology. Transl Oncol. 2009;2(2):89-95. Epub 2009/05/05. doi: 10.1593/tlo.09100. PubMed PMID: 19412424; PMCID: PMC2670576.

141. DuPage M, Mazumdar C, Schmidt LM, Cheung AF, Jacks T. Expression of tumour-specific antigens underlies cancer immunoediting. Nature. 2012;482(7385):405-9. Epub 2012/02/10. doi: 10.1038/nature10803. PubMed PMID: 22318517; PMCID: PMC3288744.

142. Koo BK, Stange DE, Sato T, Karthaus W, Farin HF, Huch M, van Es JH, Clevers H. Controlled gene expression in primary Lgr5 organoid cultures. Nat Methods. 2011;9(1):81-3. Epub 2011/12/06. doi: 10.1038/nmeth.1802. PubMed PMID: 22138822.

143. McIver SR, Lee CS, Lee JM, Green SH, Sands MS, Snider BJ, Goldberg MP. Lentiviral transduction of murine oligodendrocytes in vivo. J Neurosci Res. 2005;82(3):397-403. Epub 2005/09/15. doi: 10.1002/jnr.20626. PubMed PMID: 16158420.

144. Lacar B, Young SZ, Platel JC, Bordey A. Imaging and recording subventricular zone progenitor cells in live tissue of postnatal mice. Front Neurosci. 2010;4. Epub 2010/08/12. doi: 10.3389/fnins.2010.00043. PubMed PMID: 20700392; PMCID: PMC2918349.

145. Alcantara Llaguno S, Chen J, Kwon CH, Jackson EL, Li Y, Burns DK, Alvarez-Buylla A, Parada LF. Malignant astrocytomas originate from neural stem/progenitor cells in a somatic tumor suppressor mouse model. Cancer Cell. 2009;15(1):45-56. doi: 10.1016/j.ccr.2008.12.006. PubMed PMID: 19111880; PMCID: PMC2650425.

146. Alcantara Llaguno SR, Wang Z, Sun D, Chen J, Xu J, Kim E, Hatanpaa KJ, Raisanen JM, Burns DK, Johnson JE, Parada LF. Adult Lineage-Restricted CNS Progenitors Specify Distinct Glioblastoma Subtypes. Cancer Cell. 2015;28(4):429-40. doi: 10.1016/j.ccell.2015.09.007. PubMed PMID: 26461091; PMCID: PMC4607935.

147. Wang Z, Sun D, Chen YJ, Xie X, Shi Y, Tabar V, Brennan CW, Bale TA, Jayewickreme CD, Laks DR, Alcantara Llaguno S, Parada LF. Cell Lineage-Based Stratification for Glioblastoma. Cancer Cell. 2020;38(3):366-79 e8. Epub 20200709. doi: 10.1016/j.ccell.2020.06.003. PubMed PMID: 32649888; PMCID: PMC7494533.

148. Beaumont TL, Kupsky WJ, Barger GR, Sloan AE. Gliosarcoma with multiple extracranial metastases: case report and review of the literature. J Neurooncol. 2007;83(1):39-46. Epub 2006/12/16. doi: 10.1007/s11060-006-9295-x. PubMed PMID: 17171442.

149. Piguet AC, Saran U, Simillion C, Keller I, Terracciano L, Reeves HL, Dufour JF. Regular exercise decreases liver tumors development in hepatocyte-specific PTEN-deficient mice independently of steatosis. J Hepatol. 2015;62(6):1296-303. Epub 2015/01/28. doi: 10.1016/j.jhep.2015.01.017. PubMed PMID: 25623824.

150. Hegi ME, Liu L, Herman JG, Stupp R, Wick W, Weller M, Mehta MP, Gilbert MR. Correlation of O6-methylguanine methyltransferase (MGMT) promoter methylation with clinical outcomes in glioblastoma and clinical strategies to modulate MGMT activity. J Clin Oncol. 2008;26(25):4189-99. Epub 2008/09/02. doi: 10.1200/JCO.2007.11.5964. PubMed PMID: 18757334.

151. Sarkaria JN, Kitange GJ, James CD, Plummer R, Calvert H, Weller M, Wick W. Mechanisms of chemoresistance to alkylating agents in malignant glioma. Clin Cancer Res. 2008;14(10):2900-8. Epub 2008/05/17. doi: 10.1158/1078-0432.CCR-07-1719. PubMed PMID: 18483356; PMCID: PMC2430468.

152. Butler M, Pongor L, Su YT, Xi LQ, Raffeld M, Quezado M, Trepel J, Aldape K, Pommier Y, Wu J. MGMT Status as a Clinical Biomarker in Glioblastoma. Trends Cancer. 2020;6(5):380-91. doi: 10.1016/j.trecan.2020.02.010. PubMed PMID: WOS:000530165200006.

153. Johanns TM, Dunn GP. Applied Cancer Immunogenomics: Leveraging Neoantigen Discovery in Glioblastoma. Cancer J. 2017;23(2):125-30. Epub 2017/04/15. doi: 10.1097/PPO.0000000000000247. PubMed PMID: 28410300; PMCID: PMC5605294.

154. Cancer Genome Atlas Research N. Comprehensive genomic characterization defines human glioblastoma genes and core pathways. Nature. 2008;455(7216):1061-8. Epub 2008/09/06. doi: 10.1038/nature07385. PubMed PMID: 18772890; PMCID: PMC2671642.

155. Hunter C, Smith R, Cahill DP, Stephens P, Stevens C, Teague J, Greenman C, Edkins S, Bignell G, Davies H, O'Meara S, Parker A, Avis T, Barthorpe S, Brackenbury L, Buck G, Butler A, Clements J, Cole J, Dicks E, Forbes S, Gorton M, Gray K, Halliday K, Harrison R, Hills K, Hinton J, Jenkinson A, Jones D, Kosmidou V, Laman R, Lugg R, Menzies A, Perry J, Petty R, Raine K, Richardson D, Shepherd R, Small A, Solomon H, Tofts C, Varian J, West S, Widaa S, Yates A, Easton DF, Riggins G, Roy JE, Levine KK, Mueller W, Batchelor TT, Louis DN, Stratton MR, Futreal PA, Wooster R. A hypermutation phenotype and somatic MSH6 mutations in recurrent human malignant gliomas after alkylator chemotherapy. Cancer Res. 2006;66(8):3987-91. Epub 2006/04/19. doi: 10.1158/0008-5472.CAN-06-0127. PubMed PMID: 16618716.

156. Cahill DP, Levine KK, Betensky RA, Codd PJ, Romany CA, Reavie LB, Batchelor TT, Futreal PA, Stratton MR, Curry WT, Iafrate AJ, Louis DN. Loss of the mismatch repair protein MSH6 in human glioblastomas is associated with tumor progression during temozolomide treatment. Clin Cancer Res. 2007;13(7):2038-45. Epub 2007/04/04. doi: 10.1158/1078-0432.CCR-06-2149. PubMed PMID: 17404084; PMCID: PMC2873832.

157. Li GM. Mechanisms and functions of DNA mismatch repair. Cell Res. 2008;18(1):85-98. Epub 2007/12/25. doi: 10.1038/cr.2007.115. PubMed PMID: 18157157.

158. McFaline-Figueroa JL, Braun CJ, Stanciu M, Nagel ZD, Mazzucato P, Sangaraju D, Cerniauskas E, Barford K, Vargas A, Chen Y, Tretyakova N, Lees JA, Hemann MT, White FM, Samson LD. Minor Changes in Expression of the Mismatch Repair Protein MSH2 Exert a Major Impact on Glioblastoma Response to Temozolomide. Cancer Res. 2015;75(15):3127-38. Epub 2015/05/31. doi: 10.1158/0008-5472.CAN-14-3616. PubMed PMID: 26025730; PMCID: PMC4526337.

159. Le DT, Uram JN, Wang H, Bartlett BR, Kemberling H, Eyring AD, Skora AD, Luber BS, Azad NS, Laheru D, Biedrzycki B, Donehower RC, Zaheer A, Fisher GA, Crocenzi TS, Lee JJ, Duffy SM, Goldberg RM, de la Chapelle A, Koshiji M, Bhaijee F, Huebner T, Hruban RH, Wood LD, Cuka N, Pardoll DM, Papadopoulos N, Kinzler KW, Zhou S, Cornish TC, Taube JM, Anders RA, Eshleman JR, Vogelstein B, Diaz LA, Jr. PD-1 Blockade in Tumors with Mismatch-Repair Deficiency. N Engl J Med. 2015;372(26):2509-20. Epub 2015/06/02. doi: 10.1056/NEJMoa1500596. PubMed PMID: 26028255; PMCID: PMC4481136.

160. Le DT, Durham JN, Smith KN, Wang H, Bartlett BR, Aulakh LK, Lu S, Kemberling H, Wilt C, Luber BS, Wong F, Azad NS, Rucki AA, Laheru D, Donehower R, Zaheer A, Fisher GA, Crocenzi TS, Lee JJ, Greten TF, Duffy AG, Ciombor KK, Eyring AD, Lam BH, Joe A, Kang SP, Holdhoff M, Danilova L, Cope L, Meyer C, Zhou S, Goldberg RM, Armstrong DK, Bever KM, Fader AN, Taube J, Housseau F, Spetzler D, Xiao N, Pardoll DM, Papadopoulos N, Kinzler KW, Eshleman JR, Vogelstein B, Anders RA, Diaz LA, Jr. Mismatch repair deficiency predicts response of solid tumors to PD-1 blockade. Science. 2017;357(6349):409-13. Epub 2017/06/10. doi: 10.1126/science.aan6733. PubMed PMID: 28596308; PMCID: PMC5576142.

161. Germano G, Lamba S, Rospo G, Barault L, Magri A, Maione F, Russo M, Crisafulli G, Bartolini A, Lerda G, Siravegna G, Mussolin B, Frapolli R, Montone M, Morano F, de Braud F, Amirouchene-Angelozzi N, Marsoni S, D'Incalci M, Orlandi A, Giraudo E, Sartore-Bianchi A, Siena S, Pietrantonio F, Di Nicolantonio F, Bardelli A. Inactivation of DNA repair triggers neoantigen generation and impairs tumour growth. Nature. 2017;552(7683):116-20. Epub 2017/12/01. doi: 10.1038/nature24673. PubMed PMID: 29186113.

162. Schaettler MO, Richters MM, Wang AZ, Skidmore ZL, Fisk B, Miller KE, Vickery TL, Kim AH, Chicoine MR, Osbun JW, Leuthardt EC, Dowling JL, Zipfel GJ, Dacey RG,

Lu HC, Johanns TM, Griffith OL, Mardis ER, Griffith M, Dunn GP. Characterization of the Genomic and Immunologic Diversity of Malignant Brain Tumors through Multisector Analysis. Cancer Discov. 2022;12(1):154-71. Epub 2021/10/07. doi: 10.1158/2159-8290.CD-21-0291. PubMed PMID: 34610950.

163. Brinkman EK, Chen T, Amendola M, van Steensel B. Easy quantitative assessment of genome editing by sequence trace decomposition. Nucleic Acids Res. 2014;42(22):e168. Epub 2014/10/11. doi: 10.1093/nar/gku936. PubMed PMID: 25300484; PMCID: PMC4267669.

164. Krishan A. Rapid flow cytofluorometric analysis of mammalian cell cycle by propidium iodide staining. J Cell Biol. 1975;66(1):188-93. Epub 1975/07/01. doi: 10.1083/jcb.66.1.188. PubMed PMID: 49354; PMCID: PMC2109516.

165. Hudson B, Upholt WB, Devinny J, Vinograd J. The use of an ethidium analogue in the dye-buoyant density procedure for the isolation of closed circular DNA: the variation of the superhelix density of mitochondrial DNA. Proc Natl Acad Sci U S A. 1969;62(3):813-20. Epub 1969/03/01. doi: 10.1073/pnas.62.3.813. PubMed PMID: 4308095; PMCID: PMC223671.

166. Zhang J, Stevens MF, Bradshaw TD. Temozolomide: mechanisms of action, repair and resistance. Curr Mol Pharmacol. 2012;5(1):102-14. Epub 2011/11/30. doi: 10.2174/1874467211205010102. PubMed PMID: 22122467.

167. Bobola MS, Silber JR, Ellenbogen RG, Geyer JR, Blank A, Goff RD. O6-methylguanine-DNA methyltransferase, O6-benzylguanine, and resistance to clinical alkylators in pediatric primary brain tumor cell lines. Clin Cancer Res. 2005;11(7):2747-55. Epub 2005/04/09. doi: 10.1158/1078-0432.CCR-04-2045. PubMed PMID: 15814657.

168. Hundal J, Carreno BM, Petti AA, Linette GP, Griffith OL, Mardis ER, Griffith M. pVAC-Seq: A genome-guided in silico approach to identifying tumor neoantigens. Genome Med. 2016;8(1):11. Epub 2016/01/31. doi: 10.1186/s13073-016-0264-5. PubMed PMID: 26825632; PMCID: PMC4733280.

169. Palles C, Cazier JB, Howarth KM, Domingo E, Jones AM, Broderick P, Kemp Z, Spain SL, Guarino E, Salguero I, Sherborne A, Chubb D, Carvajal-Carmona LG, Ma Y, Kaur K, Dobbins S, Barclay E, Gorman M, Martin L, Kovac MB, Humphray S, Consortium C, Consortium WGS, Lucassen A, Holmes CC, Bentley D, Donnelly P, Taylor J, Petridis C, Roylance R, Sawyer EJ, Kerr DJ, Clark S, Grimes J, Kearsey SE, Thomas HJ, McVean G, Houlston RS, Tomlinson I. Germline mutations affecting the proofreading domains of POLE and POLD1 predispose to colorectal adenomas and carcinomas. Nat Genet. 2013;45(2):136-44. Epub 2012/12/25. doi: 10.1038/ng.2503. PubMed PMID: 23263490; PMCID: PMC3785128.

170. Albertson TM, Ogawa M, Bugni JM, Hays LE, Chen Y, Wang Y, Treuting PM, Heddle JA, Goldsby RE, Preston BD. DNA polymerase epsilon and delta proofreading suppress discrete mutator and cancer phenotypes in mice. Proc Natl Acad Sci U S A.

2009;106(40):17101-4. Epub 2009/10/07. doi: 10.1073/pnas.0907147106. PubMed PMID: 19805137; PMCID: PMC2761330.

171. Da Mesquita S, Fu Z, Kipnis J. The Meningeal Lymphatic System: A New Player in Neurophysiology. Neuron. 2018;100(2):375-88. Epub 2018/10/26. doi: 10.1016/j.neuron.2018.09.022. PubMed PMID: 30359603; PMCID: PMC6268162.

172. Zhai L, Ladomersky E, Lauing KL, Wu M, Genet M, Gritsina G, Gyorffy B, Brastianos PK, Binder DC, Sosman JA, Giles FJ, James CD, Horbinski C, Stupp R, Wainwright DA. Infiltrating T Cells Increase IDO1 Expression in Glioblastoma and Contribute to Decreased Patient Survival. Clin Cancer Res. 2017;23(21):6650-60. Epub 2017/07/29. doi: 10.1158/1078-0432.CCR-17-0120. PubMed PMID: 28751450; PMCID: PMC5850948.

173. Ladomersky E, Zhai L, Lenzen A, Lauing KL, Qian J, Scholtens DM, Gritsina G, Sun X, Liu Y, Yu F, Gong W, Liu Y, Jiang B, Tang T, Patel R, Platanias LC, James CD, Stupp R, Lukas RV, Binder DC, Wainwright DA. IDO1 Inhibition Synergizes with Radiation and PD-1 Blockade to Durably Increase Survival Against Advanced Glioblastoma. Clin Cancer Res. 2018;24(11):2559-73. Epub 2018/03/04. doi: 10.1158/1078-0432.CCR-17-3573. PubMed PMID: 29500275; PMCID: PMC5984675.

174. Nduom EK, Wei J, Yaghi NK, Huang N, Kong LY, Gabrusiewicz K, Ling X, Zhou S, Ivan C, Chen JQ, Burks JK, Fuller GN, Calin GA, Conrad CA, Creasy C, Ritthipichai K, Radvanyi L, Heimberger AB. PD-L1 expression and prognostic impact in glioblastoma. Neuro Oncol. 2016;18(2):195-205. Epub 2015/09/02. doi: 10.1093/neuonc/nov172. PubMed PMID: 26323609; PMCID: PMC4724183.

175. Colonna M, Butovsky O. Microglia Function in the Central Nervous System During Health and Neurodegeneration. Annu Rev Immunol. 2017;35:441-68. Epub 2017/02/23. doi: 10.1146/annurev-immunol-051116-052358. PubMed PMID: 28226226.

176. Forster R, Schubel A, Breitfeld D, Kremmer E, Renner-Muller I, Wolf E, Lipp M. CCR7 coordinates the primary immune response by establishing functional microenvironments in secondary lymphoid organs. Cell. 1999;99(1):23-33. Epub 1999/10/16. doi: 10.1016/s0092-8674(00)80059-8. PubMed PMID: 10520991.

177. Anandasabapathy N, Victora GD, Meredith M, Feder R, Dong B, Kluger C, Yao K, Dustin ML, Nussenzweig MC, Steinman RM, Liu K. Flt3L controls the development of radiosensitive dendritic cells in the meninges and choroid plexus of the steady-state mouse brain. J Exp Med. 2011;208(8):1695-705. Epub 2011/07/27. doi: 10.1084/jem.20102657. PubMed PMID: 21788405; PMCID: PMC3149213.

178. Karman J, Ling C, Sandor M, Fabry Z. Dendritic cells in the initiation of immune responses against central nervous system-derived antigens. Immunol Lett. 2004;92(1-2):107-15. Epub 2004/04/15. doi: 10.1016/j.imlet.2003.10.017. PubMed PMID: 15081534.

179. Karman J, Chu HH, Co DO, Seroogy CM, Sandor M, Fabry Z. Dendritic cells amplify T cell-mediated immune responses in the central nervous system. J Immunol. 2006;177(11):7750-60. Epub 2006/11/23. doi: 10.4049/jimmunol.177.11.7750. PubMed PMID: 17114446.

180. Zozulya AL, Ortler S, Lee J, Weidenfeller C, Sandor M, Wiendl H, Fabry Z. Intracerebral dendritic cells critically modulate encephalitogenic versus regulatory immune responses in the CNS. J Neurosci. 2009;29(1):140-52. Epub 2009/01/09. doi: 10.1523/JNEUROSCI.2199-08.2009. PubMed PMID: 19129392; PMCID: PMC2942091.

181. Clarkson BD, Heninger E, Harris MG, Lee J, Sandor M, Fabry Z. Innate-adaptive crosstalk: how dendritic cells shape immune responses in the CNS. Adv Exp Med Biol. 2012;946:309-33. Epub 2011/09/29. doi: 10.1007/978-1-4614-0106-3_18. PubMed PMID: 21948376; PMCID: PMC3666851.

182. Brahler S, Zinselmeyer BH, Raju S, Nitschke M, Suleiman H, Saunders BT, Johnson MW, Bohner AMC, Viehmann SF, Theisen DJ, Kretzer NM, Briseno CG, Zaitsev K, Ornatsky O, Chang Q, Carrero JA, Kopp JB, Artyomov MN, Kurts C, Murphy KM, Miner JH, Shaw AS. Opposing Roles of Dendritic Cell Subsets in Experimental GN. J Am Soc Nephrol. 2018;29(1):138-54. Epub 2017/12/09. doi: 10.1681/ASN.2017030270. PubMed PMID: 29217759; PMCID: PMC5748909.

183. Durai V, Bagadia P, Granja JM, Satpathy AT, Kulkarni DH, Davidson JTt, Wu R, Patel SJ, Iwata A, Liu TT, Huang X, Briseno CG, Grajales-Reyes GE, Wohner M, Tagoh H, Kee BL, Newberry RD, Busslinger M, Chang HY, Murphy TL, Murphy KM. Cryptic activation of an Irf8 enhancer governs cDC1 fate specification. Nat Immunol. 2019;20(9):1161-73. Epub 2019/08/14. doi: 10.1038/s41590-019-0450-x. PubMed PMID: 31406378; PMCID: PMC6707878.

184. Bailey SL, Carpentier PA, McMahon EJ, Begolka WS, Miller SD. Innate and adaptive immune responses of the central nervous system. Crit Rev Immunol. 2006;26(2):149-88. Epub 2006/05/17. doi: 10.1615/critrevimmunol.v26.i2.40. PubMed PMID: 16700651.

185. Waisman A, Liblau RS, Becher B. Innate and adaptive immune responses in the CNS. Lancet Neurol. 2015;14(9):945-55. Epub 2015/08/22. doi: 10.1016/S1474-4422(15)00141-6. PubMed PMID: 26293566.

186. Clarkson BD, Walker A, Harris MG, Rayasam A, Hsu M, Sandor M, Fabry Z. CCR7 deficient inflammatory Dendritic Cells are retained in the Central Nervous System. Sci Rep. 2017;7:42856. Epub 2017/02/22. doi: 10.1038/srep42856. PubMed PMID: 28216674; PMCID: PMC5316931.

187. Helft J, Bottcher J, Chakravarty P, Zelenay S, Huotari J, Schraml BU, Goubau D, Reis e Sousa C. GM-CSF Mouse Bone Marrow Cultures Comprise a Heterogeneous Population of CD11c(+)MHCII(+) Macrophages and Dendritic Cells. Immunity. 2015;42(6):1197-211. Epub 2015/06/18. doi: 10.1016/j.immuni.2015.05.018. PubMed PMID: 26084029.

188. Murphy TL, Grajales-Reyes GE, Wu X, Tussiwand R, Briseno CG, Iwata A, Kretzer NM, Durai V, Murphy KM. Transcriptional Control of Dendritic Cell Development. Annu Rev Immunol. 2016;34:93-119. Epub 2016/01/07. doi: 10.1146/annurev-immunol-032713-120204. PubMed PMID: 26735697; PMCID: PMC5135011.

189. Theisen D, Murphy K. The role of cDC1s in vivo: CD8 T cell priming through cross-presentation. F1000Res. 2017;6:98. Epub 2017/02/12. doi: 10.12688/f1000research.9997.1. PubMed PMID: 28184299; PMCID: PMC5288679.

190. Briseno CG, Haldar M, Kretzer NM, Wu X, Theisen DJ, Kc W, Durai V, Grajales-Reyes GE, Iwata A, Bagadia P, Murphy TL, Murphy KM. Distinct Transcriptional Programs Control Cross-Priming in Classical and Monocyte-Derived Dendritic Cells. Cell Rep. 2016;15(11):2462-74. Epub 2016/06/07. doi: 10.1016/j.celrep.2016.05.025. PubMed PMID: 27264183; PMCID: PMC4941620.

191. Ahn JH, Cho H, Kim JH, Kim SH, Ham JS, Park I, Suh SH, Hong SP, Song JH, Hong YK, Jeong Y, Park SH, Koh GY. Meningeal lymphatic vessels at the skull base drain cerebrospinal fluid. Nature. 2019;572(7767):62-6. Epub 2019/07/26. doi: 10.1038/s41586-019-1419-5. PubMed PMID: 31341278.

192. Bianchi R, Teijeira A, Proulx ST, Christiansen AJ, Seidel CD, Rulicke T, Makinen T, Hagerling R, Halin C, Detmar M. A transgenic Prox1-Cre-tdTomato reporter mouse for lymphatic vessel research. PLoS One. 2015;10(4):e0122976. Epub 2015/04/08. doi: 10.1371/journal.pone.0122976. PubMed PMID: 25849579; PMCID: PMC4388455.

193. Hogquist KA, Jameson SC, Heath WR, Howard JL, Bevan MJ, Carbone FR. T cell receptor antagonist peptides induce positive selection. Cell. 1994;76(1):17-27. Epub 1994/01/14. doi: 10.1016/0092-8674(94)90169-4. PubMed PMID: 8287475.

194. Louveau A, Smirnov I, Keyes TJ, Eccles JD, Rouhani SJ, Peske JD, Derecki NC, Castle D, Mandell JW, Lee KS, Harris TH, Kipnis J. Corrigendum: Structural and functional features of central nervous system lymphatic vessels. Nature. 2016;533(7602):278. Epub 2016/02/26. doi: 10.1038/nature16999. PubMed PMID: 26909581.

195. Picker LJ, Butcher EC. Physiological and molecular mechanisms of lymphocyte homing. Annu Rev Immunol. 1992;10:561-91. Epub 1992/01/01. doi: 10.1146/annurev.iy.10.040192.003021. PubMed PMID: 1590996.

196. Hanly A, Petito CK. HLA-DR-positive dendritic cells of the normal human choroid plexus: a potential reservoir of HIV in the central nervous system. Hum Pathol. 1998;29(1):88-93. Epub 1998/01/28. doi: 10.1016/s0046-8177(98)90395-1. PubMed PMID: 9445139.

197. Serot J-M, Foliguet B, Béné M-C, Faure G-C. Ultrastructural and immunohistological evidence for dendritic-like cells within human choroid plexus

epithelium. NeuroReport. 1997;8(8):1995-8. PubMed PMID: 00001756-199705260-00039.

198. Pashenkov M, Huang YM, Kostulas V, Haglund M, Soderstrom M, Link H. Two subsets of dendritic cells are present in human cerebrospinal fluid. Brain. 2001;124(Pt 3):480-92. Epub 2001/02/27. doi: 10.1093/brain/124.3.480. PubMed PMID: 11222448.

199. Prodinger C, Bunse J, Krüger M, Schiefenhövel F, Brandt C, Laman JD, Greter M, Immig K, Heppner F, Becher B, Bechmann I. CD11c-expressing cells reside in the juxtavascular parenchyma and extend processes into the glia limitans of the mouse nervous system. Acta Neuropathologica. 2011;121(4):445-58. doi: 10.1007/s00401-010-0774-y.

200. Yilmaz A, Fuchs T, Dietel B, Altendorf R, Cicha I, Stumpf C, Schellinger Peter D, Blümcke I, Schwab S, Daniel Werner G, Garlichs Christoph D, Kollmar R. Transient decrease in circulating dendritic cell precursors after acute stroke: potential recruitment into the brain. Clinical Science. 2009;118(2):147-57. doi: 10.1042/cs20090154.

201. Planas AM, Gomez-Choco M, Urra X, Gorina R, Caballero M, Chamorro A. Brain-derived antigens in lymphoid tissue of patients with acute stroke. J Immunol. 2012;188(5):2156-63. Epub 2012/01/31. doi: 10.4049/jimmunol.1102289. PubMed PMID: 22287710.

202. Liau LM, Black KL, Prins RM, Sykes SN, DiPatre PL, Cloughesy TF, Becker DP, Bronstein JM. Treatment of intracranial gliomas with bone marrow-derived dendritic cells pulsed with tumor antigens. J Neurosurg. 1999;90(6):1115-24. Epub 1999/06/01. doi: 10.3171/jns.1999.90.6.1115. PubMed PMID: 10350260.

203. Siesjo P, Visse E, Sjogren HO. Cure of established, intracerebral rat gliomas induced by therapeutic immunizations with tumor cells and purified APC or adjuvant IFN-gamma treatment. J Immunother Emphasis Tumor Immunol. 1996;19(5):334-45. Epub 1996/09/01. PubMed PMID: 8941873.

204. Yu JS, Wheeler CJ, Zeltzer PM, Ying H, Finger DN, Lee PK, Yong WH, Incardona F, Thompson RC, Riedinger MS, Zhang W, Prins RM, Black KL. Vaccination of malignant glioma patients with peptide-pulsed dendritic cells elicits systemic cytotoxicity and intracranial T-cell infiltration. Cancer Res. 2001;61(3):842-7. Epub 2001/02/28. PubMed PMID: 11221866.

205. Inaba K, Inaba M, Romani N, Aya H, Deguchi M, Ikehara S, Muramatsu S, Steinman RM. Generation of large numbers of dendritic cells from mouse bone marrow cultures supplemented with granulocyte/macrophage colony-stimulating factor. J Exp Med. 1992;176(6):1693-702. Epub 1992/12/01. doi: 10.1084/jem.176.6.1693. PubMed PMID: 1460426; PMCID: PMC2119469.

206. Caux C, Dezutter-Dambuyant C, Schmitt D, Banchereau J. GM-CSF and TNF-alpha cooperate in the generation of dendritic Langerhans cells. Nature.

1992;360(6401):258-61. Epub 1992/11/19. doi: 10.1038/360258a0. PubMed PMID: 1279441.

207. Sallusto F, Lanzavecchia A. Efficient Presentation of Soluble-Antigen by Cultured Human Dendritic Cells Is Maintained by Granulocyte-Macrophage Colony-Stimulating Factor Plus Interleukin-4 and down-Regulated by Tumor-Necrosis-Factor-Alpha. Journal of Experimental Medicine. 1994;179(4):1109-18. doi: DOI 10.1084/jem.179.4.1109. PubMed PMID: WOS:A1994NC77700004.

208. Carreno BM, Magrini V, Becker-Hapak M, Kaabinejadian S, Hundal J, Petti AA, Ly A, Lie WR, Hildebrand WH, Mardis ER, Linette GP. Cancer immunotherapy. A dendritic cell vaccine increases the breadth and diversity of melanoma neoantigen-specific T cells. Science. 2015;348(6236):803-8. Epub 2015/04/04. doi: 10.1126/science.aaa3828. PubMed PMID: 25837513; PMCID: PMC4549796.

209. Maraskovsky E, Brasel K, Teepe M, Roux ER, Lyman SD, Shortman K, McKenna HJ. Dramatic increase in the numbers of functionally mature dendritic cells in Flt3 ligand-treated mice: multiple dendritic cell subpopulations identified. J Exp Med. 1996;184(5):1953-62. Epub 1996/11/01. doi: 10.1084/jem.184.5.1953. PubMed PMID: 8920882; PMCID: PMC2192888.

210. Galibert L, Diemer GS, Liu Z, Johnson RS, Smith JL, Walzer T, Comeau MR, Rauch CT, Wolfson MF, Sorensen RA, de Vries ARV, Branstetter DG, Koelling RM, Scholler J, Fanslow WC, Baum PR, Derry JM, Yan W. Nectin-like protein 2 defines a subset of T-cell zone dendritic cells and is a ligand for class-I-restricted T-cell-associated molecule. J Biol Chem. 2005;280(23):21955-64. doi: 10.1074/jbc.M502095200. PubMed PMID: WOS:000229557900037.

211. Helft J, Bottcher J, Chakravarty P, Zelenay S, Huotari J, Schraml BU, Goubau D, Sousa CRE. GM-CSF Mouse Bone Marrow Cultures Comprise a Heterogeneous Population of CD11c(+)MHCII(+) Macrophages and Dendritic Cells. Immunity. 2015;42(6):1197-211. doi: 10.1016/j.immuni.2015.05.018. PubMed PMID: WOS:000356362800022.

212. den Haan JM, Lehar SM, Bevan MJ. CD8(+) but not CD8(-) dendritic cells cross-prime cytotoxic T cells in vivo. J Exp Med. 2000;192(12):1685-96. Epub 2000/12/20. doi: 10.1084/jem.192.12.1685. PubMed PMID: 11120766; PMCID: PMC2213493.

213. Naik SH, Proietto AI, Wilson NS, Dakic A, Schnorrer P, Fuchsberger M, Lahoud MH, O'Keeffe M, Shao QX, Chen WF, Villadangos JA, Shortman K, Wu L. Cutting edge: generation of splenic CD8+ and CD8- dendritic cell equivalents in Fms-like tyrosine kinase 3 ligand bone marrow cultures. J Immunol. 2005;174(11):6592-7. Epub 2005/05/21. doi: 10.4049/jimmunol.174.11.6592. PubMed PMID: 15905497.

214. Mayer CT, Ghorbani P, Nandan A, Dudek M, Arnold-Schrauf C, Hesse C, Berod L, Stuve P, Puttur F, Merad M, Sparwasser T. Selective and efficient generation of functional Batf3-dependent CD103+ dendritic cells from mouse bone marrow. Blood.

2014;124(20):3081-91. Epub 2014/08/08. doi: 10.1182/blood-2013-12-545772. PubMed PMID: 25100743; PMCID: PMC4260363.

215. Kirkling ME, Cytlak U, Lau CM, Lewis KL, Resteu A, Khodadadi-Jamayran A, Siebel CW, Salmon H, Merad M, Tsirigos A, Collin M, Bigley V, Reizis B. Notch Signaling Facilitates In Vitro Generation of Cross-Presenting Classical Dendritic Cells. Cell Rep. 2018;23(12):3658-72 e6. Epub 2018/06/21. doi: 10.1016/j.celrep.2018.05.068. PubMed PMID: 29925006; PMCID: PMC6063084.

216. Poulin LF, Salio M, Griessinger E, Anjos-Afonso F, Craciun L, Chen JL, Keller AM, Joffre O, Zelenay S, Nye E, Le Moine A, Faure F, Donckier V, Sancho D, Cerundolo V, Bonnet D, Reis e Sousa C. Characterization of human DNGR-1+ BDCA3+ leukocytes as putative equivalents of mouse CD8alpha+ dendritic cells. J Exp Med. 2010;207(6):1261-71. Epub 2010/05/19. doi: 10.1084/jem.20092618. PubMed PMID: 20479117; PMCID: PMC2882845.

217. Hambleton S, Salem S, Bustamante J, Bigley V, Boisson-Dupuis S, Azevedo J, Fortin A, Haniffa M, Ceron-Gutierrez L, Bacon CM, Menon G, Trouillet C, McDonald D, Carey P, Ginhoux F, Alsina L, Zumwalt TJ, Kong XF, Kumararatne D, Butler K, Hubeau M, Feinberg J, Al-Muhsen S, Cant A, Abel L, Chaussabel D, Doffinger R, Talesnik E, Grumach A, Duarte A, Abarca K, Moraes-Vasconcelos D, Burk D, Berghuis A, Geissmann F, Collin M, Casanova JL, Gros P. IRF8 mutations and human dendritic-cell immunodeficiency. N Engl J Med. 2011;365(2):127-38. Epub 2011/04/29. doi: 10.1056/NEJMoa1100066. PubMed PMID: 21524210; PMCID: PMC3136554.

218. Pastor J, Vega-Zelaya L, Pulido P, Garnes-Camarena O, Abreu A, Sola RG. Role of intraoperative neurophysiological monitoring during fluorescence-guided resection surgery. Acta Neurochir (Wien). 2013;155(12):2201-13. Epub 2013/09/28. doi: 10.1007/s00701-013-1864-0. PubMed PMID: 24072425.

219. Zhao S, Wu J, Wang C, Liu H, Dong X, Shi C, Shi C, Liu Y, Teng L, Han D, Chen X, Yang G, Wang L, Shen C, Li H. Intraoperative fluorescence-guided resection of high-grade malignant gliomas using 5-aminolevulinic acid-induced porphyrins: a systematic review and meta-analysis of prospective studies. PLoS One. 2013;8(5):e63682. Epub 2013/06/01. doi: 10.1371/journal.pone.0063682. PubMed PMID: 23723993; PMCID: PMC3665818.

220. Li Y, Rey-Dios R, Roberts DW, Valdes PA, Cohen-Gadol AA. Intraoperative fluorescence-guided resection of high-grade gliomas: a comparison of the present techniques and evolution of future strategies. World Neurosurg. 2014;82(1-2):175-85. Epub 2013/07/16. doi: 10.1016/j.wneu.2013.06.014. PubMed PMID: 23851210.

221. Huang Z, Shi S, Qiu H, Li D, Zou J, Hu S. Fluorescence-guided resection of brain tumor: review of the significance of intraoperative quantification of protoporphyrin IX fluorescence. Neurophotonics. 2017;4(1):011011. Epub 2017/01/18. doi: 10.1117/1.NPh.4.1.011011. PubMed PMID: 28097209; PMCID: PMC5227178.

222. Collaud S, Juzeniene A, Moan J, Lange N. On the selectivity of 5-aminolevulinic acid-induced protoporphyrin IX formation. Curr Med Chem Anticancer Agents. 2004;4(3):301-16. Epub 2004/05/12. doi: 10.2174/1568011043352984. PubMed PMID: 15134506.

223. Stummer W, Stocker S, Novotny A, Heimann A, Sauer O, Kempski O, Plesnila N, Wietzorrek J, Reulen HJ. In vitro and in vivo porphyrin accumulation by C6 glioma cells after exposure to 5-aminolevulinic acid. J Photochem Photobiol B. 1998;45(2-3):160-9. Epub 1998/12/30. doi: 10.1016/s1011-1344(98)00176-6. PubMed PMID: 9868806.

224. Johanns TM, Miller CA, Liu CJ, Perrin RJ, Bender D, Kobayashi DK, Campian JL, Chicoine MR, Dacey RG, Huang J, Fritsch EF, Gillanders WE, Artyomov MN, Mardis ER, Schreiber RD, Dunn GP. Detection of neoantigen-specific T cells following a personalized vaccine in a patient with glioblastoma. Oncoimmunology. 2019;8(4):e1561106. Epub 2019/03/25. doi: 10.1080/2162402X.2018.1561106. PubMed PMID: 30906654; PMCID: PMC6422384.

225. Keskin DB, Anandappa AJ, Sun J, Tirosh I, Mathewson ND, Li S, Oliveira G, Giobbie-Hurder A, Felt K, Gjini E, Shukla SA, Hu Z, Li L, Le PM, Allesoe RL, Richman AR, Kowalczyk MS, Abdelrahman S, Geduldig JE, Charbonneau S, Pelton K, Iorgulescu JB, Elagina L, Zhang W, Olive O, McCluskey C, Olsen LR, Stevens J, Lane WJ, Salazar AM, Daley H, Wen PY, Chiocca EA, Harden M, Lennon NJ, Gabriel S, Getz G, Lander ES, Regev A, Ritz J, Neuberg D, Rodig SJ, Ligon KL, Suva ML, Wucherpfennig KW, Hacohen N, Fritsch EF, Livak KJ, Ott PA, Wu CJ, Reardon DA. Neoantigen vaccine generates intratumoral T cell responses in phase Ib glioblastoma trial. Nature. 2019;565(7738):234-9. Epub 2018/12/21. doi: 10.1038/s41586-018-0792-9. PubMed PMID: 30568305; PMCID: PMC6546179.

226. Hilf N, Kuttruff-Coqui S, Frenzel K, Bukur V, Stevanovic S, Gouttefangeas C, Platten M, Tabatabai G, Dutoit V, van der Burg SH, Thor Straten P, Martinez-Ricarte F, Ponsati B, Okada H, Lassen U, Admon A, Ottensmeier CH, Ulges A, Kreiter S, von Deimling A, Skardelly M, Migliorini D, Kroep JR, Idorn M, Rodon J, Piro J, Poulsen HS, Shraibman B, McCann K, Mendrzyk R, Lower M, Stieglbauer M, Britten CM, Capper D, Welters MJP, Sahuquillo J, Kiesel K, Derhovanessian E, Rusch E, Bunse L, Song C, Heesch S, Wagner C, Kemmer-Bruck A, Ludwig J, Castle JC, Schoor O, Tadmor AD, Green E, Fritsche J, Meyer M, Pawlowski N, Dorner S, Hoffgaard F, Rossler B, Maurer D, Weinschenk T, Reinhardt C, Huber C, Rammensee HG, Singh-Jasuja H, Sahin U, Dietrich PY, Wick W. Actively personalized vaccination trial for newly diagnosed glioblastoma. Nature. 2019;565(7738):240-5. Epub 2018/12/21. doi: 10.1038/s41586-018-0810-y. PubMed PMID: 30568303.

227. Maier B, Leader AM, Chen ST, Tung N, Chang C, LeBerichel J, Chudnovskiy A, Maskey S, Walker L, Finnigan JP, Kirkling ME, Reizis B, Ghosh S, D'Amore NR, Bhardwaj N, Rothlin CV, Wolf A, Flores R, Marron T, Rahman AH, Kenigsberg E, Brown BD, Merad M. A conserved dendritic-cell regulatory program limits antitumour immunity. Nature. 2020;580(7802):257-62. Epub 2020/04/10. doi: 10.1038/s41586-020-2134-y. PubMed PMID: 32269339.

228. Maier B, Leader AM, Chen ST, Tung N, Chang C, LeBerichel J, Chudnovskiy A, Maskey S, Walker L, Finnigan JP, Kirkling ME, Reizis B, Ghosh S, D'Amore NR, Bhardwaj N, Rothlin CV, Wolf A, Flores R, Marron T, Rahman AH, Kenigsberg E, Brown BD, Merad M. Author Correction: A conserved dendritic-cell regulatory program limits antitumour immunity. Nature. 2020;582(7813):E17. Epub 2020/06/06. doi: 10.1038/s41586-020-2326-5. PubMed PMID: 32499658.

229. Mosmann TR, Cherwinski H, Bond MW, Giedlin MA, Coffman RL. Two types of murine helper T cell clone. I. Definition according to profiles of lymphokine activities and secreted proteins. J Immunol. 1986;136(7):2348-57. Epub 1986/04/01. PubMed PMID: 2419430.

230. Hsieh CS, Macatonia SE, Tripp CS, Wolf SF, Ogarra A, Murphy KM. Development of Th1 Cd4+ T-Cells through Il-12 Produced by Listeria-Induced Macrophages. Science. 1993;260(5107):547-9. doi: DOI 10.1126/science.8097338. PubMed PMID: WOS:A1993KY50400036.

231. Murphy K, Weaver C. Janeway's immunobiology. 9th edition. ed. New York, NY: Garland Science/Taylor & Francis Group, LLC; 2016. xx, 904 pages p.

232. Noorman F, Braat EAM, BarrettBergshoeff M, Barbe E, vanLeeuwen A, Lindeman J, Rijken DC. Monoclonal antibodies against the human mannose receptor as a specific marker in flow cytometry and immunohistochemistry for macrophages. J Leukocyte Biol. 1997;61(1):63-72. PubMed PMID: WOS:A1997WC77000009.

233. Engering AJ, Cella M, Fluitsma D, Brockhaus M, Hoefsmit ECM, Lanzavecchia A, Pieters J. The mannose receptor functions as a high capacity and broad specificity antigen receptor in human dendritic cells. European Journal of Immunology. 1997;27(9):2417-25. doi: DOI 10.1002/eji.1830270941. PubMed PMID: WOS:A1997YA32400040.

234. Wollenberg A, Mommaas M, Oppel T, Schottdorf EM, Gunther S, Moderer M. Expression and function of the mannose receptor CD206 on epidermal dendritic cells in inflammatory skin diseases. J Invest Dermatol. 2002;118(2):327-34. Epub 2002/02/14. doi: 10.1046/j.0022-202x.2001.01665.x. PubMed PMID: 11841552.

235. Sondak VK, King DW, Zager JS, Schneebaum S, Kim J, Leong SP, Faries MB, Averbook BJ, Martinez SR, Puleo CA, Messina JL, Christman L, Wallace AM. Combined analysis of phase III trials evaluating [(9)(9)mTc]tilmanocept and vital blue dye for identification of sentinel lymph nodes in clinically node-negative cutaneous melanoma. Ann Surg Oncol. 2013;20(2):680-8. Epub 2012/10/12. doi: 10.1245/s10434-012-2612-z. PubMed PMID: 23054107; PMCID: PMC3560941.

236. Wallace AM, Han LK, Povoski SP, Deck K, Schneebaum S, Hall NC, Hoh CK, Limmer KK, Krontiras H, Frazier TG, Cox C, Avisar E, Faries M, King DW, Christman L, Vera DR. Comparative evaluation of [(99m)tc]tilmanocept for sentinel lymph node mapping in breast cancer patients: results of two phase 3 trials. Ann Surg Oncol.

2013;20(8):2590-9. Epub 2013/03/19. doi: 10.1245/s10434-013-2887-8. PubMed PMID: 23504141; PMCID: PMC3705144.

237. Zhu H, Acquaviva J, Ramachandran P, Boskovitz A, Woolfenden S, Pfannl R, Bronson RT, Chen JW, Weissleder R, Housman DE, Charest A. Oncogenic EGFR signaling cooperates with loss of tumor suppressor gene functions in gliomagenesis. Proc Natl Acad Sci U S A. 2009;106(8):2712-6. Epub 2009/02/07. doi: 10.1073/pnas.0813314106. PubMed PMID: 19196966; PMCID: PMC2650331.

238. Krimpenfort P, Quon KC, Mooi WJ, Loonstra A, Berns A. Loss of p16Ink4a confers susceptibility to metastatic melanoma in mice. Nature. 2001;413(6851):83-6. Epub 2001/09/07. doi: 10.1038/35092584. PubMed PMID: 11544530.

239. Groszer M, Erickson R, Scripture-Adams DD, Lesche R, Trumpp A, Zack JA, Kornblum HI, Liu X, Wu H. Negative regulation of neural stem/progenitor cell proliferation by the Pten tumor suppressor gene in vivo. Science. 2001;294(5549):2186-9. Epub 2001/11/03. doi: 10.1126/science.1065518. PubMed PMID: 11691952.

240. Hopken UE, Droese J, Li JP, Joergensen J, Breitfeld D, Zerwes HG, Lipp M. The chemokine receptor CCR7 controls lymph node-dependent cytotoxic T cell priming in alloimmune responses. Eur J Immunol. 2004;34(2):461-70. Epub 2004/02/10. doi: 10.1002/eji.200324690. PubMed PMID: 14768051.

241. Janowska-Wieczorek A, Majka M, Kijowski J, Baj-Krzyworzeka M, Reca R, Turner AR, Ratajczak J, Emerson SG, Kowalska MA, Ratajczak MZ. Platelet-derived microparticles bind to hematopoietic stem/progenitor cells and enhance their engraftment. Blood. 2001;98(10):3143-9. Epub 2001/11/08. doi: 10.1182/blood.v98.10.3143. PubMed PMID: 11698303.

242. Schildge S, Bohrer C, Beck K, Schachtrup C. Isolation and culture of mouse cortical astrocytes. J Vis Exp. 2013(71). Epub 2013/02/06. doi: 10.3791/50079. PubMed PMID: 23380713; PMCID: PMC3582677.

243. Petersen LK, Stowers RS. A Gateway MultiSite recombination cloning toolkit. PLoS One. 2011;6(9):e24531. Epub 2011/09/21. doi: 10.1371/journal.pone.0024531. PubMed PMID: 21931740; PMCID: PMC3170369.

244. Hartley JL. Use of the gateway system for protein expression in multiple hosts. Curr Protoc Protein Sci. 2003;Chapter 5:Unit 5 17. Epub 2008/04/23. doi: 10.1002/0471140864.ps0517s30. PubMed PMID: 18429245.

245. Ran FA, Hsu PD, Wright J, Agarwala V, Scott DA, Zhang F. Genome engineering using the CRISPR-Cas9 system. Nat Protoc. 2013;8(11):2281-308. Epub 2013/10/26. doi: 10.1038/nprot.2013.143. PubMed PMID: 24157548; PMCID: PMC3969860.